Induction of anti-apoptotic factors by cutaneous Human Papillomaviruses

CHRISTINE TOMLINS

Linacre College

A Thesis submitted to the Medical Sciences Division of the University of Oxford in partial fulfilment of the requirements for the Degree of Doctor of Philosophy

Hilary Term 2010

Department of Molecular Oncology

Weatherall Institute of Molecular Medicine

University of Oxford

Abstract:

Induction of anti-apoptotic factors by cutaneous Human Papillomaviruses.

Christine Tomlins DPhil Thesis

Linacre College Hilary Term 2010

Human Papillomaviruses (HPVs) are small DNA viruses which specifically infect keratinocytes at different body sites. An association between cutaneous Squamous Cell Carcinoma (SCC) formation, UV irradiation and infection with a high-risk subset of cutaneous HPVs has been postulated although the underlying molecular mechanisms by which HPV may play a role in SCC development are not yet fully elucidated. Expression of the viral E6 oncoprotein has been shown to interfere with DNA damage responses and inhibit UV induced apoptosis, suggesting HPV can contribute to early stages in tumourigenesis. Here, expression of E6 from HPV types 5, 8, 10, 18 and 77 was shown to reduce UV- or Fas-induced apoptosis, and the changes in a range of intracellular apoptotic regulators were investigated. Additionally, the subject of cutaneous SCCs, in contrast to HPV-associated anogenital cancers, not harboring HPV DNA in every tumor cell was explored. Results herein show that expression of E6 from skin cancer-associated HPV types 5 and 8 induced the secretion of factors that were able to inhibit UV-induced apoptosis in non-HPV expressing cell lines and primary human keratinocytes. The anti-apoptotic effect of HPV E6 expression was found to be mediated in part by upregulation of Osteoprotegerin (OPG) and Interleukin 6 (IL6). Purified OPG and IL6, when added to cells together, but not individually, reduced apoptosis following UV irradiation. Evidence is shown that OPG and IL6 inhibit the extrinsic and intrinsic apoptotic pathways respectively. Furthermore immunohistochemistry of HPV-typed SCC sections shows that IL6 protein is up-regulated in HPV positive tumors compared to HPV-negative cancers. To further test the effects of HPV5E6 expression, in combination with UV irradiation, on primary human keratinocytes microarray studies were performed. These findings support the hypothesis that a small number of HPV infected cells influence UV induced apoptosis in the skin and contribute to tumourigenesis.

Table of Contents

List of Figures

List of Tables

Acknowledgements

I would like to thank my supervisor Dr Alan Storey for his guidance and support throughout the course of this work, and especially for the opportunity to attend, and present at, several conferences. I would also like to thank the members of the labs in both London and Oxford, for their helpful advice, and good company; Mark Simmonds, Ferina Ismail, Baki Akgul and James Cooke in London and Joanna Fox, Abul Azad and Amy Holloway in Oxford. I am also very grateful to all my colleagues in both departments, the Institute for Cell and Molecular Science, and the Weatherall Institute of Molecular Medicine, for their friendly assistance. Special thanks also go to Sally Lambert, Karin Purdie and Catherine Harwood (ICMS, Bart's and the London School of Medicine and Dentistry, University of London) for providing the HPV-typed SCC sections and help with IHC scoring; and to Gary Warnes (as above) for helping with FACS analysis.

I also owe many thanks to my family for their encouragement; and to my friends in London, for remembering me when I moved away, and my friends in Oxford for welcoming me. I would particularly like to thank my housemates in both cities for providing a good atmosphere at home and tolerating my quirks; and to thank Stuart Ingleby for being a great help, and distraction, as needed during the writing up.

Additionally I would like to gratefully acknowledge the financial support of Cancer Research UK who funded this studentship.

Presentations

Parts of the work in this thesis have been presented in oral communications at the following:

Society of General Microbiology; 160th AGM, Human Papillomavirus workshop, University of Manchester, UK, 26-29 March 2007

HPV and Skin Cancer International meeting, Besancon, France, 27-30 June 2007
"Cutaneous HPV E6 expression changes cytokine secretion patterns and protects non-E6 expressing cells from apoptosis."

DNA Tumour virus meeting, Madison, USA, 22-27 July 2008
"Anti-apoptotic bystander effect of cutaneous HPV E6 proteins."

DNA Tumour virus meeting, Oxford, UK, 14-18 July 2009
"Anti-apoptotic bystander effect of cutaneous HPV E6 proteins."

Abbreviations

AIF: Apoptosis inducing factor

Apaf1: Apoptosis activating factor 1

APS: Ammonium persulphate

BIR: Baculovirus IAP repeat

BCC: Basal cell carcinoma

CARD: Caspase active recruitment domain

CIN: Cervical intraepithelial neoplasia

CST: Cell Signalling Technology

CytC: Cytochrome C

DD: Death domain

DED: Death effector domain

DED: De-epidermalised dermis

DFCS: Dialysed foetal calf serum

DISC: Death inducing signalling complex

DMEM: Dulbecco's modified Eagle medium

DMSO: Dimethylsulphoxide

ECM: Extracellular matrix

ER: Endoplasmic reticulum

EV: Eidermodysplasia verruciformis

FCS: Foetal calf serum

FADD: Fas-associated death domain

FasL: Fas ligand

HPV: Human papillomavirus

HRP: Horseradish peroxidase

IAP: Inhibitor of apoptosis protein

IFN: Interferon

IL: Interleukin

JNK: c-Jun kinase

LCR: Long control region

MMP: Matrix metalloproteinase

MWCO: Molecular weight cut off

NFκB: Nuclear factor κ B

NMSC: Non-melanoma skin cancer

OMM: Outer mitochondrial membrane

OPG : Osteoprotegerin

ORF: Open reading frame

PARP: Poly(ADP- ribose) polymerase

PCD: Programmed cell death

PCR: Polymerase chain reaction

ROS: Reactive oxygen species

RT: Room temperature

SCC: Squamous cell cancer

SDS-PAGE: Sodium dodecyl sulphate polyacrylamide gel electrophoresis

TBST: Tris buffered saline 0.1% Tween

TEWL: Trans-epidermal water loss

TNF: Tumour necrosis factor

TNFR: TNF receptor

TRAIL: TNF-related apoptosis inducing ligand

URR: Upstream regulatory region

UV: Ultraviolet

VLP: Virus-like particle

1 Introduction

1.1 The Skin

1.1.1 Structure

The skin is a large organ, estimated to constitute 6% of the mass of an adult human. It consists of two layers, the outermost epidermis, and the underlying dermis, along with many accessory appendages including hair follicles and nails, secretory glands, including eccrine and apocrine sweat glands and sebaceous glands, and sensory nerve receptors (Tobin, 2006). The dermis mainly consists of fibroblasts and the elastic connective fibres known as the extracellular matrix (ECM), and it contains the skin's vascular, lymphatic, immune and neural components. Inwardly it is connected to deeper tissues by the fatty *sub-cutis* layer, and outwardly separated from the epidermis by the basement membrane. The epidermis is a non-vascularised stratified epithelium mainly consisting of keratinocytes, along with Langerhans cells (dendritic cells), Merkel cells (sensory cells) and melanocytes (melanin producing cells), and interspersed with pores and hair follicles at different densities according to body site. The keratinocytes undergo terminal differentiation allowing the continual renewal of the cornified outer layer, a hardened layer of non-viable keratinocytes. Terminal differentiation is a form of programmed cell death distinct from apoptosis, for example it does not lead to phagocytosis of dying cells, the morphological changes involved are not restricted to one cell but coordinated across the tissue, executioner caspase activation is not necessary, and it takes weeks rather than hours (Lippens et al., 2005). A summary of the structure and terminal differentiation of the epidermis is illustrated in Figure 1-1.

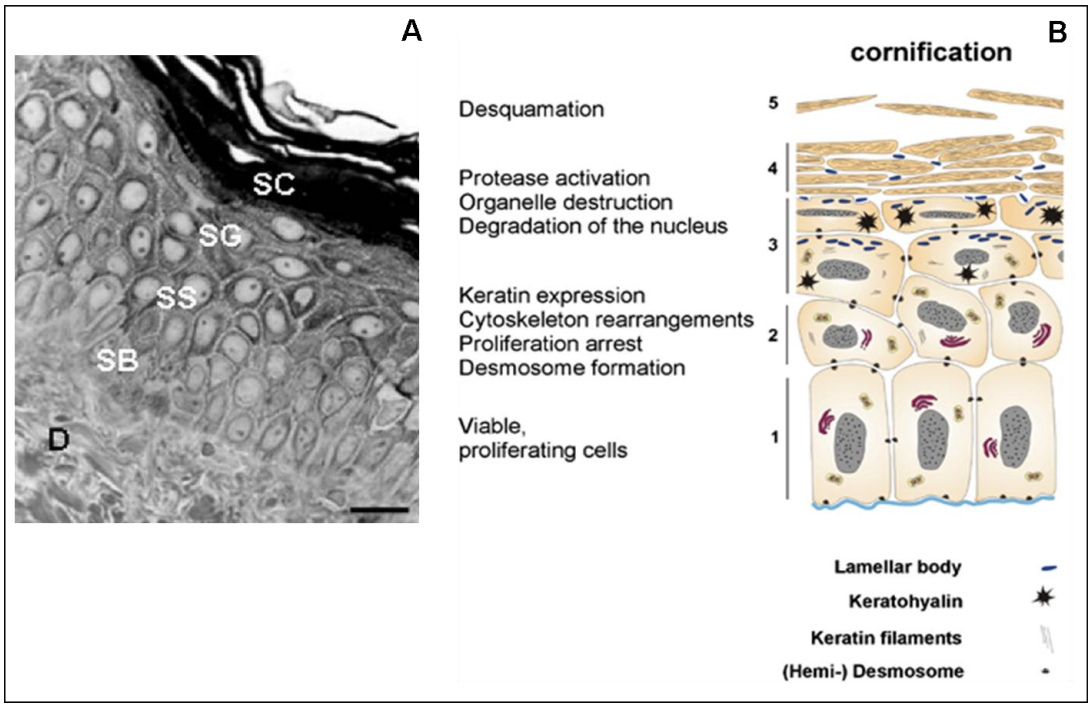

Figure 1-1 Structure of the epidermis.

A High-resolution microscopy view of a portion of normal human skin showing epidermis and dermis (D), scale bar = 30 μM, taken from (Tobin, 2006).

B Diagram depicting the layers of the epidermis including some of the morphological changes of keratinocytes undergoing terminal differentiation into corneocytes, taken from (Lippens et al., 2005).

1 = SB, *s.basale*; 2 = SS, *s.spinosum*; 3 = SG, *s.granulosum*; 4 = SC, *s.corneum*.

The deepest layer of the epidermis adjacent to the basement membrane is termed the *stratum basale* (basal layer), containing dividing keratinocytes with stem cell-like properties. Keratinocyte stem cells (KSCs) reside in clusters in the hair follicle bulge region, and can migrate to the epidermis where necessary, for example in wound healing (Ohyama et al., 2006). However the high proliferative capacity of the epidermis is maintained by the presence of slow-cycling long-lived stem cell-like keratinocytes, which are dispersed through the interfollicular epithelium and give rise to transit amplifying cells which form the columnar unit structure of the epidermis (Mackenzie, 1997). These basal stem cells are protected from apoptosis by the anti-apoptotic proteins survivin and Bcl2 family members (Marconi et al., 2007; Tiberio et al., 2002), and by anchorage to the basement membrane by

specific integrins, β1 and α6 (Webb et al., 2004). These markers, in combination with low expression of the differentiation marker CD71 (transferrin receptor), are used to identify highly-proliferative keratinocyte population enriched for stem cells (Terunuma et al., 2007). The transit amplifying keratinocytes produced move upwards into the *stratum spinosum* where they lose the capacity for cell division, until they reach the *stratum granulosum* (granular layer). Here the keratinocytes produce granules of keratohyalin protein, become more impermeable, their organelles and nuclei begin to break down, and the network of keratins produced by the cells, which alter as they progress through the epidermis, is cross-linked. Finally the cells reach the outer *stratum corneum* as non-viable, flattened corneocytes, which together with a lipid-rich extracellular matrix formed by secretion of lamellar bodies and cross-linkage by transglutaminases, form the 'bricks and mortar' model of the *s.corneum* (Elias, 1983) which is eventually shed into the environment as squames. As will be seen presently, this is important in the life cycle of human Papillomaviruses which release progeny not by cell lysis but by shedding with the squames.

The amount of keratin in the epidermis increases from 30% in the *s.basale* to 80% in the *s.corneum* over the 30 days taken for a keratinocyte to undergo terminal differentiation. Keratins are a very large family of intermediate filament proteins which have many functions including cellular stability and signalling regulation. They form heteropolymeric filaments through binding to specific keratin partners, which are expressed at specific times and places, for example K5 and K14 in the basal layer, and K1 and K2 in the granular layer (Moll et al., 2008). These filaments are linked to desmosomes, cell-cell adhesion structures that contribute to the mechanical strength and flexibility of the skin.

1.1.2 Function

The epidermis has many functions, including the prevention of water loss. The term barrier function is synonymous with the activity of the cornified layer in preventing desiccation through excessive trans-epidermal water loss (Elias, 2005). The lipid-rich cornified envelope consisting of ceramides, cholesterol and free fatty acids cross-linked to proteins of the corneocytes make the *s.corneum* essentially impervious to water loss.

In addition, studies on the neuroendocrine role of the skin show that it can produce several hormones, steroids and associated factors which have many roles (Slominski, 2005). An associated function is the production of Vitamin D following Ultraviolet (UV) irradiation of the skin (Webb, 2006). The eccrine glands are the primary producers of thermoregulatory sweat, making the skin the primary organ for maintaining the correct core temperature (Shibasaki et al., 2006).

The skin also protects from many insults of different types, including physical, chemical and microbial agents. For example, a large number of xenobiotics are absorbed by the skin at varying rates dependent on their chemical structure, and the skin expresses a number of cytochrome P450 enzymes that metabolise them, altering their activity (Ahmad and Mukhtar, 2004). The antimicrobial activity of the skin is mediated not only by the physical barrier formed but also by the antimicrobial peptides (AMPs), proteins and lipids produced by different cell types in the skin, for example cathelicidin, which not only has direct antimicrobial activity, disrupting the membranes of bacteria and enveloped viruses, but is also involved in initiating the innate immune response to infection (Schauber and Gallo, 2008). Part of the skin's protective mechanism against UV is the production by melanocytes of melanin, granules of which are transferred to keratinocytes and arranged around the nuclei to absorb UV radiation and protect the DNA (Park et al., 2009).

1.1.3 Immunology

As a major interface between the body and the environment, the skin is exposed to a number of immunological challenges by viruses, bacteria, fungi, and chemicals; however unless it is physically damaged by breaks or disease, or the individual is immuno-compromised, it is usually able to effectively repel these challenges. All of the cell types of the skin are involved in the immunology of the organ, in which both the innate and adaptive (early, relatively indiscriminate and specific antigen guided respectively) immune systems are important. Keratinocytes are poor antigen presenting cells due to terminal differentiation moving them away from immune cells and destining them for death without additional immune interactions. Dendritic cells (of which Langerhans cells are one cutaneous type) are the professional antigen-presenting cells which process foreign antigens, migrate to skin-draining lymph nodes and then initiate adaptive immune responses via T cell differentiation. They are also involved in the innate system through their production of cytokines such as Interleukin (IL)1β. Mast cells are the main mediators of cutaneous allergic reactions; however they are also involved in the innate response to bacteria, through activation of one of their many receptors which leads to secretion of inflammatory mediators (Metz and Maurer, 2009). Natural killer (NK) cells are the lymphocytes whose main innate immunity functions are cytotoxicity against tumour and virally-infected cells, and cytokine production. They also play a role in regulation of adaptive immunity, for example stimulating maturation of dendritic cells and activation of T cells, and have been associated with inflammatory skin diseases such as atopic dermatitis (von Bubnoff et al., 2010). T lymphocytes are the effectors of immunological memory, along with the production of antibodies by B lymphocytes, and also have their roles in the skin (Girardi, 2007). Normal skin is inhabited by a subset of 20 billion effector memory T cells, which provide quick responses to re-exposure to pathogens via production of

cytokines and specific cytotoxicity, and they may also be involved in inflammatory skin conditions such as psoriasis (Clark, 2010).

Keratinocytes themselves are important immune regulators. Their constitutive secretion of anti-microbial peptides (as described above) and cytokines is increased and modified upon detection of damage such as UV irradiation (Grone, 2002). Other molecules such as endothelin-1 peptide and a range of cytokines are important in keratinocyte mediated immune responses, which can influence for example the activation of immune effector cells and the behaviour of other keratinocytes, shown in Figure 1-2. The proinflammatory cytokines interleukin (IL) 1, 6 and 8 and tumour necrosis factor (TNF) α are produced by keratinocytes and mediate effects such as protection from TNF-related apoptosis inducing ligand (TRAIL), keratinocyte proliferation and neutrophil migration (for example Kothny-Wilkes et al., 1998). IL6 production by and effect on keratinocytes has been studied for more than 20 years (Yoshizaki et al., 1990), and its proliferative and inflammatory properties have been linked to psoriasis (Grossman et al., 1989). In addition to its role in the immune system it has been shown to be involved in regulation of epidermal barrier homeostasis (Wang et al., 2004b). In contrast the T cell-trophic cytokines IL 7 and 15 are downregulated after UV irradiation (Han et al., 1999; Wagner et al., 1999). The immuno-modulating cytokines IL10 and 12 have opposing effects by promoting or repressing UV-induced immune suppression respectively (Schmitt et al., 2000). IL4 and 13 receptors are present on keratinocytes and activation leads to increased production of IL6 (Derocq et al., 1994), whereas activation of IL17 receptor affects the keratinocyte response to IL4 and interferon (IFN) γ. As in other systems, disruption of the immunology of the skin can lead to numerous diseases, for example blistering diseases, atopic dermatitis and cutaneous T cell lymphomas. The specific modulation of the cutaneous immune response by UV is described in section 1.4.2.

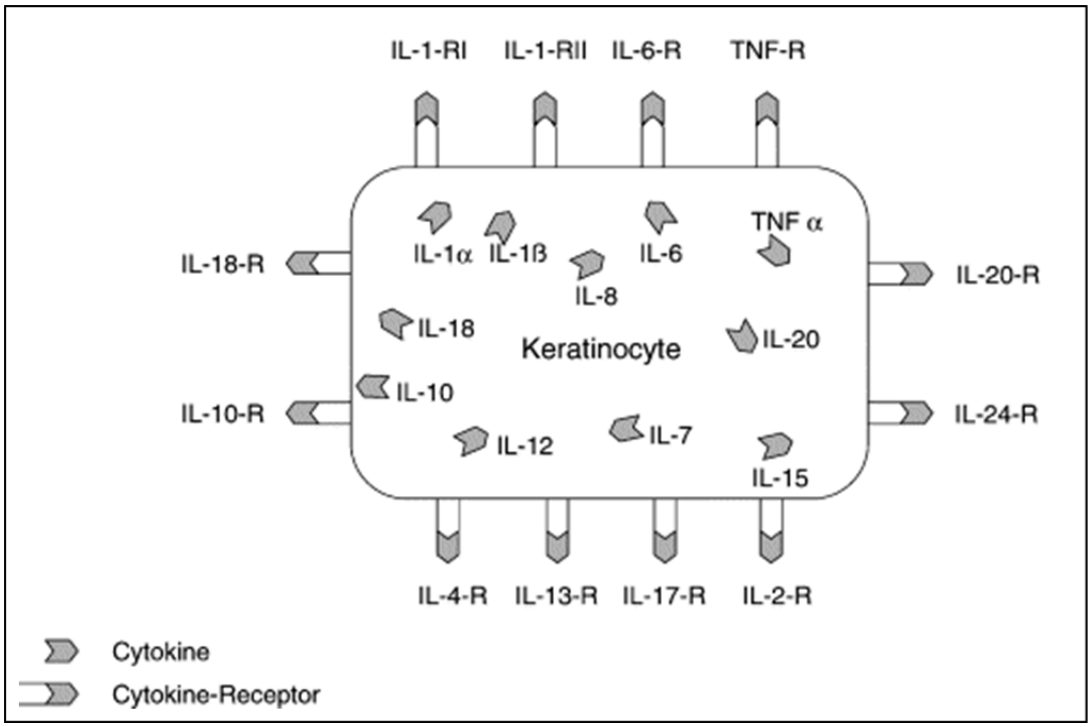

Figure 1-2 The keratinocyte as a source and target of cytokines.

Taken from (Grone, 2002).

1.2 Apoptosis

Apoptosis is a form of programmed cell death (PCD) that is evolutionarily conserved across eukaryotes with an increasingly complex regulatory programme, with the genes controlling apoptosis in *C.elegans* having human homologues (Yuan, 2006). The term apoptosis was first coined in 1972, and the morphological characteristics have been described in many cell types (Kerr et al., 1972). It is an essential process with several important roles. It is crucial in embryo development for the nervous system assembly and tissue sculpting, with apoptosis removing unwanted cells, for example those that form the web between embryonic fingers and toes (Meier et al., 2000; Zakeri and Lockshin, 2002). Apoptosis is also vital for the development and regulation of the immune system, with many lymphocytes being removed by apoptosis during generation of the T cell repertoire and during activation-induced cell death to prevent over-production of T cells; low-affinity or

auto-reactive B cells are also removed by apoptosis during development (Krammer, 2000). Apoptosis is essential for tissue homeostasis as well as development, as detachment of many cell types from their correct position linked to neighbouring cells or membranes triggers a form of apoptosis called anoikis which is important in construction of the organism, as well as maintaining cells in the correct microenvironment (Zahir and Weaver, 2004). In addition, the general activity of apoptosis in removing damaged or virally-infected cells is vital. As a consequence, deregulation of or faults in apoptosis are linked to many diseases including most types of cancer, autoimmune disorders and neurodegenerative syndromes (Fadeel and Orrenius, 2005).

Apoptosis involves activation of a number of processes described in the following sections, including activation of a cascade of cysteine-aspartic proteases called caspases, which results in the dismantling of the cell into apoptotic bodies which are then phagocytosed by macrophages and neighbouring cells. It is distinct from other forms of cell death for example necrosis, autophagy and terminal differentiation, for several reasons. Autophagy ('self-eating') is the process by which cells digest and utilise their own organelles and cytoplasmic components, and it can be a survival mechanism during times of cell starvation as well as a death mechanism. Necrosis is the uncontrolled cell death resulting from trauma to cells such as toxins or direct injury. In contrast to necrosis, where membrane rupturing spills the cellular contents into the micro-environment, cells which undergo apoptosis are packaged into vesicles before phagocytosis, thus avoiding a potentially harmful inflammatory response (Edinger and Thompson, 2004). Apoptosis is also an energy-dependent process which is tightly regulated at several stages, which are described below. For an overview of apoptosis please see Figure 1-3.

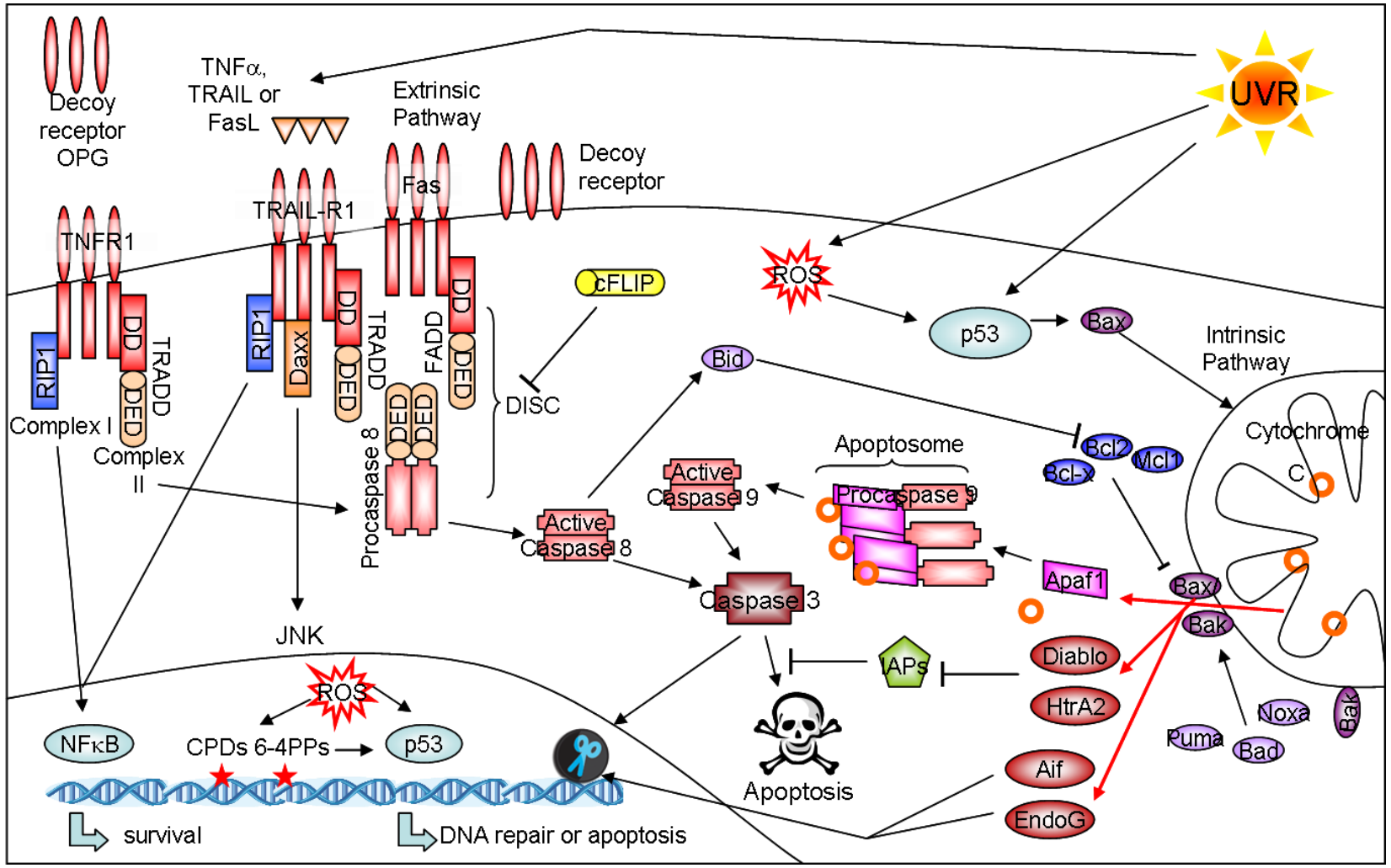

Figure 1-3 Overview of apoptotic pathways. See text for details.

1.2.1 Extrinsic pathway

The apoptotic caspase cascade can be activated in human cells by two main mechanisms, one of which is the extrinsic or death receptor pathway, which as the name suggests depends on the activation of cell surface 'death receptors' (Jin and El-Deiry, 2005). The tumour necrosis factor (TNF) receptor family are type I transmembrane proteins with an extracellular N-terminal domain containing the hallmark cysteine-rich domains (CRDs) which determine ligand specificity, a membrane spanning region and an intracellular C-terminal region which contains a conserved death domain (DD) which is essential for apoptosis induction (Itoh and Nagata, 1993). The receptors Fas (CD95/APO-1), TNF-receptor 1 (TNFR1), TNF-related apoptosis inducing ligand receptors 1 and 2 (TRAIL-R1/DR4, TRAIL-R2/DR5) are most studied, with the roles of DR3 and DR6 less well characterized. Decoy receptors may also be expressed, which lack functional DDs and so are unable to activate apoptotic signalling, but compete for ligand binding. These are the soluble DcR3 and OPG (against FasL and TRAIL respectively) and cellular DcR1 and DcR2 against TRAIL.

Activation of Fas and TRAIL-R1/2 usually leads to apoptosis whereas TNFR1 activation by TNF (a multifunctional proinflammatory cytokine) leads to the formation of two signalling complexes, Complex I signalling survival via the activation of NF-κB, and Complex II inducing apoptosis (Micheau and Tschopp, 2003), controlled by recruitment of different adaptor proteins and regulatory modifications such as phosphorylation and ubiquitination (Fujita and Srinivasula, 2009). Fas, TNFR1 and TRAIL-R1/R2 bind their cognate ligands (FasL, TNFα and TRAIL respectively) which are type II transmembrane proteins with an extracellular C-terminal domain. These ligands can be expressed as both membrane bound and soluble forms, the latter generally having lower apoptosis-inducing properties (Schneider et al., 1998) which can be increased by cross-linking. The receptors

form complexes on the cell surface (Chan et al., 2000) which aggregate and re-organize upon ligand binding leading to the recruitment of adaptor proteins, which in apoptosis signalling constitute FADD (Fas associated death domain) (Eberstadt et al., 1998) or TRADD (TNFR1 associated death domain) (Hsu et al., 1995) via association of the receptor and adaptor DDs. Aggregated receptors are also endocytosed as internalization facilitates further protein recruitment (Lee et al., 2006). The adaptor proteins also contain death effector domains (DED) that allow recruitment of effector molecules through interactions with corresponding DEDs on initiator caspases (8 and 10), leading to DISC (death-inducing signalling complex) formation (Kischkel et al., 1995). The caspase can then be activated as described presently.

Other regulatory molecules can also bind to the DISC, for example cFLIP (cellular FLICE-inhibitory protein; FLICE being an alternative name for caspase 8). The two isoforms of cFLIP $_{Long}$ and $_{Short}$ are catalytically inactive caspase 8 homologues (Peter, 2005). $cFLIP_S$ blocks caspase 8 binding and activation at the DISC (Irmler et al., 1997), and $cFLIP_L$ can either promote or inhibit caspase 8 activation depending on its expression levels (Chang et al., 2002). The protein DAXX can also bind to the Fas DD and contribute to apoptosis signalling, independently of FADD and caspase activation, via the activation of JNK (Jun N-terminal kinase) (Yang et al., 1997). JNK is a member of the mitogen-activated protein kinase (MAPK) family which can activate the c-Jun transcription factor. The serine-threonine kinase RIP1 (receptor-interacting protein) also contains a DD and so can bind to the death receptors and adaptor proteins, and mediates the switch between apoptotic and survival signalling (Meylan and Tschopp, 2005; Stanger et al., 1995). These opposing signalling pathways are regulated by the subcellular localization of the signalling complexes of which RIP1 can be a member, modification of RIP1 by phosphorylation or ubiquitination (O'Donnell et al., 2007), and its cleavage by

caspase 8 which inhibits NF-κB signalling and facilitates apoptosis (Lin et al., 1999).

The above example of RIP1 highlights the further roles of Fas and TRAIL-R1/2 in non-apoptotic signalling, in addition to the more well-studied survival signalling mediated by TNFR1 (Guicciardi and Gores, 2009). FasL and TRAIL can stimulate proliferation and anti-apoptotic signals via activation of signalling pathways such as NF-κB and MAP kinases (Falschlehner et al., 2007; Park et al., 2005) especially in cells where apoptosis in inhibited (Barnhart et al., 2004).

1.2.2 Intrinsic pathway

The other main mechanism by which the apoptotic caspase cascade can be activated is termed the intrinsic or mitochondrial pathway, as it is centred on the mitochondrial outer membrane permeabilization (MOMP). MOMP is chiefly induced by intracellular stress signals such as DNA damage, Reactive Oxygen Species (ROS), growth factor withdrawal, and chemotherapeutic agents, and is regulated by the Bcl2 family of proteins (Brenner and Mak, 2009). Members of the three subfamilies (Groups I-III) share different combinations of the four conserved BH (Bcl2 homology) domains, the combination of which mediates their interactions and subsequent pro- or anti-apoptotic activity. The prototypic member, B-cell lymphoma 2, contains all four BH domains (BH1-4), is over-expressed in follicular lymphoma and was found to promote cell survival (Vaux et al., 1988). The other anti-apoptotic Group I members containing BH1-4 in mammalian cells are Bcl-x, Mcl1, A1 and Bcl-w. These proteins bind to and sequester the apoptotic family members Bak and Bax. The Group II proteins Bak and Bax contain BH1-3 domains and are the family members that lead directly to MOMP, shown by the protection of Bax/Bak double knockout cells from a large variety of apoptotic stimuli that disrupt the integrity of mitochondria (Wei et al., 2001). An additional level of regulation is provided by the apoptotic Group III BH3-only subfamily, which in

mammalian cells consists of Bim, Bid, Puma, Noxa, Bad, Bmf, Hrk and Bik (Lessene et al., 2008).

Bax is located in the cytosol and Bak in the outer mitochondrial membrane, however upon apoptosis Bax translocates to the mitochondria (Wolter et al., 1997), and both undergo several conformational changes leading to their multimerization in the outer mitochondrial membrane and subsequent pore formation and MOMP (Mikhailov et al., 2003). The exact mechanism by which Bak and Bax are released by BH3-only proteins from their inhibition is still debated, with two models proposed. In the direct model, the 'activator' BH3-only proteins Bim and tBid bind and activate Bak/Bax, whereas 'sensitizer' BH3-only proteins Bad, Noxa and Puma bind to the anti-apoptotic Bcl2 family members, causing the release of the activator BH3-only proteins (Letai et al., 2002). In the indirect model, the binding of BH3-only proteins to the anti-apoptotic Bcl2 family members forces the release of Bak/Bax (Willis et al., 2007), with the different BH3-only proteins having different affinities for sub-groups of the anti-apoptotic Bcl2 family members (Chen et al., 2005).

The BH3-only protein Bid illustrates the cross-talk between the extrinsic and intrinsic pathways. After death receptor activation, Bid can be cleaved by activated caspase 8 and tBid then initiates intrinsic mitochondrial apoptosis (Li et al., 1998). The requirement for mitochondrial involvement for complete apoptosis after death receptor activation classifies cells as Type II, whereas Type I cells do not require such amplification.

MOMP releases several apoptotic factors from the mitochondria; the first to be identified was Cytochrome C (CytC), a key component of the mitochondrial electron transport chain (Liu et al., 1996). Upon its release, in the presence of ATP, CytC binds to Apaf1 (apoptotic protease activating factor 1), which undergoes conformational changes resulting in formation of a large complex called the apoptosome. Apaf1, as an adaptor protein, contains a caspase activation and

recruitment domain (CARD) which enables recruitment of the initiator caspases 9 and 2 via their own CARDs and triggers their activation (Li et al., 1997). Other proteins released during MOMP contribute to apoptosis by inhibiting the IAP (Inhibitor of apoptosis protein) family. Smac/DIABLO (Second mitochondrial activator of apoptosis/Direct IAP binding protein of low pI) competes with the caspases in binding to IAPs, therefore releasing caspases from their sequestration (Du et al., 2000; Verhagen et al., 2000). HtrA2/Omi (high temperature requirement protein A2) is a serine protease also released upon MOMP, and it binds to cIAP1/2 and XIAP, releasing caspases from inhibition. A different active site also proteolytically degrades the IAPs and also contributes to caspase-independent apoptosis through its protease activity (Verhagen et al., 2002). The release of EndonucleaseG, a DNase, from the mitochondria, also contributes to caspase-independent apoptosis by its cleavage of nuclear DNA (Li et al., 2001b). AIF (apoptosis inducing factor) is released from its tethering in the mitochondria during apoptosis, and translocates to the nucleus, where it condenses chromatin and degrades the DNA, resulting in large DNA fragments (~50kb) distinct from the apoptotic DNA ladder seen with caspase-dependent oligonucleosomal DNA degradation (Ye et al., 2002).

1.2.2.1 p53

Another important regulator of apoptosis is the p53 tumour suppressor, which is involved in the cellular response to DNA damage including decisions whether to exit the cell cycle to permit DNA repair, or to initiate apoptosis in cases of severe damage (Yoshida and Miki, 2010). Upon receipt of cellular stress signals p53 is stabilised via post-translational modifications including phosphorylation and accumulates in the cell, allowing it to perform its varied functions to maintain genome integrity. The N-terminal domain of p53 contains several phosphorylation sites which are important for its stabilization. For example upon DNA damage, the

ATM (ataxia telangiectasia mutated) kinase phosphorylates p53 at serine15, and Chk2 phosphorylates at serine20, blocking p53 binding to MDM2 and its subsequent targeting for degradation. The C-terminal domain also contains modification sites for phosphorylation, acetylation, methylation and sumoylation, which regulate p53's ability for sequence-specific DNA binding, oligomerization, and nuclear localisation (Lavin and Gueven, 2006). p53 can also regulate the cell cycle at the G1/S checkpoint through interaction with p21. One of p53's main functions is as a transcription factor, known to activate and repress over 100 genes (Menendez et al., 2009). Where cellular stress is sufficient to cause apoptosis, p53 upregulates apoptotic genes such as Puma, Bid, Noxa and Apaf1 (for example Nakano and Vousden, 2001), and also genes involved in the death receptor pathway such as TRAIL and Fas (Kuribayashi et al., 2008; Muller et al., 1998), facilitating cross-talk between the intrinsic and extrinsic pathways. p53 also has transcription-independent roles in apoptosis induction. For example its interaction with anti-apoptotic Bcl2 family members Bcl2, Bcl-x_L and Mcl1 can disrupt mitochondrial membrane integrity (Wolff et al., 2008), and direct binding of p53 to Bak can induce MOMP (Leu et al., 2004).

1.2.3 Effectors

As has been seen in the sections above, the caspase family are key apoptotic effectors with roles for initiator caspases in both the extrinsic and intrinsic pathways, which converge upon activation of executioner caspases. The CED3 gene responsible for cell death in *C. elegans* was found to share homology with the human interleukin-1β converting enzyme (ICE) (Miura et al., 1993), leading to the discovery of a family of ICE-like proteins named caspases (cysteine-aspartic proteases). The 14 mammalian caspases share features such as the ability to cleave XXX-Asp bonds, with the specificity determined by the XXX sequence. To prevent unwanted proteolytic activity procaspases are all produced as inactive

zymogens, consisting of large and small subunits connected by a linker region along with a prodomain that is removed upon activation (Degterev et al., 2003). The caspases can be classified according to their functions: the inflammatory caspases 1, 4, 5, 11, 12, 13 and 14 regulate innate immune responses via the inflammasome molecular platform (Schroder and Tschopp, 2010). The apoptotic caspases can be divided into initiator/apical and executioner/effector types. Initiator caspases contain long prodomains containing the adaptor domains used to mediate apoptotic signals from upstream adaptor molecules, DEDs in extrinsic caspases 8 and 10 and CARDs in intrinsic caspases 2 and 9. Executioner caspases contain a short prodomain, and are activated by initiator caspases, after which they cleave a large number of cellular proteins leading to the controlled dismantling of the cell characteristic of apoptosis.

Upon their aggregation by adaptor molecules (for example FADD and Apaf1) at the DISC or apoptosome initiator caspases are activated to form enzymatically active dimers. This was previously thought to be due to auto-proteolytic cleavage by adjacent monomers in the linker domain, the 'proximity-induced' model (Salvesen and Dixit, 1999), however this was modified when further evidence showed that dimerization is the essential step for activation, with subsequent cleavage stabilising the dimers, in the 'proximity-induced dimerization' model (Boatright et al., 2003; Renatus et al., 2001). In contrast, the executioner caspases 3, 6 and 7 are present as inactive dimers, and their activation is triggered by initiator caspase-mediated cleavage of the linker domain (Chai et al., 2001).

The executioner caspases specifically cleave many cellular substrates that lead to the characteristic morphological changes and degradation of the cell. For example cleavage of the cytoskeletal proteins fodrin and gelsolin leads to detachment and the loss of cell shape, and of nuclear lamins to nuclear shrinkage and budding (Kothakota et al., 1997; Rao et al., 1996). DNA repair enzymes are also key caspase substrates, as inactivation of energetically expensive DNA repair

mechanisms is important for ensuring ATP is available for apoptosis. One of the first caspase 3 substrates to be classified was PARP (poly(ADP-ribose) polymerase) which is inactivated upon cleavage, inhibiting its DNA repair activity (Lazebnik et al., 1994). In addition, caspase cleavage of DFF45/ICAD (DNA fragmentation factor 45/Inhibitor caspase-activated DNAse) removes its inhibitory subunit, leaving DFF40/CAD to cleave DNA, producing the typical apoptotic fragmentation (Widlak and Garrard, 2005). Also, cleavage of several pro-apoptotic kinases makes them constitutively active, including PAK2 (p21-activated kinase 2) which leads to membrane blebbing (Rudel and Bokoch, 1997). Anti-apoptotic kinases which are cleaved and inactivated by caspases include AKT, FAK, and RIP1 which has been described in section 1.2.1. FAK (focal adhesion kinase) transmission of survival signals induced by attachment to integrins is inactivated by caspase cleavage, contributing to apoptotic morphology (Wen et al., 1997).

The activity of caspases needs to be closely regulated, in which the IAP (Inhibitor of apoptosis) family of proteins have key roles, for example IAPs are inhibited to enable apoptosis to proceed, by caspase cleavage (Deveraux et al., 1999) and by factors released during MOMP as mentioned in section 1.2.1. The human IAPs include XIAP, cIAP1, cIAP2, survivin, livin/melanoma-associated IAP, NAIP and BRUCE. They contain one to three Baculovirus IAP repeat (BIR) domains and a Really interesting new gene (RING) domain. The BIR domain was named after a baculovirus protein was discovered to inhibit apoptosis (Clem and Miller, 1994) and homologues were found in species from nematodes to human. BIR domains mediate the binding to caspases and can inhibit their activity (Roy et al., 1997), for example the BIR3 of XIAP binds to caspase 9 while caspases 3 and 7 are bound by BIR2 (Takahashi et al., 1998). However, in contrast to XIAP, cIAPs1 and 2 do not directly inhibit the bound caspases (Eckelman and Salvesen, 2006). The IAPs can also inhibit caspase activation pathways by the E3 ubiquitin ligase activity of their RING domain, via targeting caspases themselves for degradation (Huang et

al., 2000) but also by modifying the TNFR signalling complex. Ubiquitination of RIP1 leads to NF-κB survival signalling, as described in section 1.2.1, and NIK (NF-κB inducing kinase) signalling is also regulated by cIAPs (Bertrand et al., 2008; Zarnegar et al., 2008).

1.2.4 Keratinocytes and Ultraviolet-induced apoptosis

Given their position in the body, ultraviolet (UV) radiation is a primary cause of apoptosis in keratinocytes, with 'sunburn cells' being used as an early example of apoptotic cells (Young, 1987). UV is divided into UVA (320-400nm), UVB (290-320nm) and UVC (200-290nm) however UVC does not penetrate the ozone layer. The effects of UVA and B on the epidermis vary according to the wavelength. As wavelength increases: depth of epidermal penetration increases, direct molecular absorption decreases, and indirect damage mediated by Reactive Oxygen Species (ROS) increases (Van Laethem et al., 2009). DNA is the main cellular chromophore of UVB, with damage causing p53-mediated cell cycle arrest to allow repair of the photoproducts (see section 1.4.1). ROS can also cause oxidative photodamage to DNA. If the damage is too great, apoptosis is induced as a protective mechanism to eliminate mutant, potentially tumourigenic cells from the epidermis. p53 is important in UV induced apoptosis but not essential, shown by the apoptotic response to UV of the keratinocyte cell line HaCaT, which contains transcriptionally silent p53 (Assefa et al., 2000). The role of apoptosis and p53 in skin cancer formation is further discussed in 1.4.1.

The extrinsic pathway is also activated in UV-irradiated keratinocytes, with signalling induced both directly by UV (Leverkus et al., 1997), and by ligand-independent receptor aggregation (Sheikh et al., 1998). However more studies indicate that the intrinsic pathway to caspase activation is the principle apoptotic response in keratinocytes, with the BH3-only protein Noxa identified as an important factor (Naik et al., 2007), and caspase 9 as the apical caspase (Daher et

al., 2006). The effect of UV on other signalling pathways also contributes to keratinocyte apoptosis (Rodust et al., 2009). For example, prolonged ROS production leads to activation of the p38 and JNK MAP kinase pathways in keratinocytes (Peus et al., 1999; Van Laethem et al., 2004), with JNK activation mediated by the extrinsic pathway adaptor protein Daxx, which is also involved in apoptosis (Wu et al., 2002).

1.3 Human Papillomaviruses

The Papillomaviruses are small (c. 55 nm diameter), non-enveloped, icosahedral, double-stranded DNA viruses with genomes of approximately 8 kbp. They are strictly epitheliotrophic, infecting mucosal and cutaneous stratified epithelia. Over 100 human types (HPVs) have been identified and are associated with a number of conditions, from asymptomatic carriage, to benign hyperproliferative lesions (warts), to cervical cancer (Bernard, 2005).

1.3.1 Phylogeny and classification

Papillomaviruses form their own family, the *Papillomaviridae*. A classification system based on the sequence homology of a conserved part of the viral genome, the L1 ORF, has been developed and is shown in Figure 1-4 (de Villiers et al., 2004). Viruses that share 71-89% sequence identity are of the same type, 60-70% the same species, with <60% indicating the genus. There are 16 genera, of which the alpha, beta, gamma, mu and nu infect humans. Different viral types show differences in genomic structure, life cycle, sites of infection, biological activity and therefore pathogenesis, with the species groups tending to contain viruses with similar properties. For example, viruses of genus-α species 4, which contains HPV2, typically form cutaneous warts.

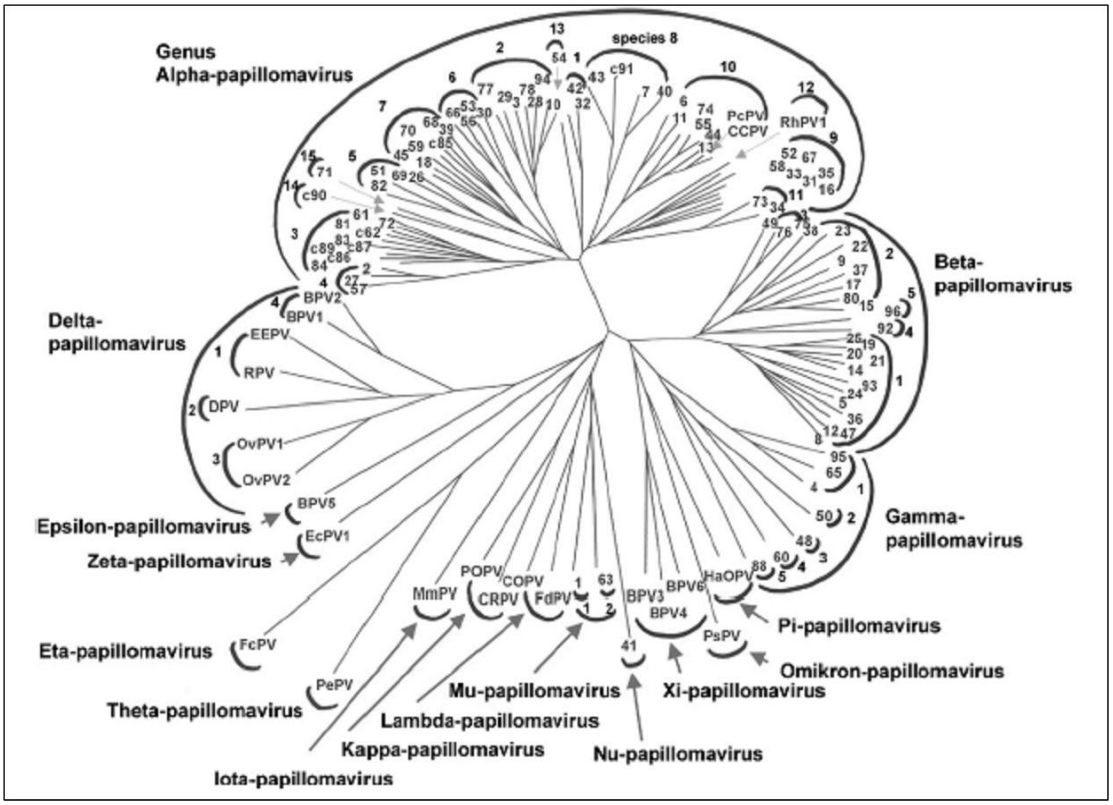

Figure 1-4 Phylogenetic tree of 118 papillomaviruses.

The numbers at the end of branches indicate human papillomavirus types (other abbreviations indicate animal types), the 'brackets' refer to species, and the outermost semicircles to genera. Taken from (de Villiers et al., 2004).

The largest genus, α, includes both mucosal and cutaneous types, which are also classified as low- or high-risk according to association with malignant progression. It contains species 10 (including HPV6 and 11) which are associated with low-risk mucosal lesions (condylomata, genital warts). Also in the genus-α, along with species 4 as mentioned above, species 2 (including HPV10 and 77) causes low-risk cutaneous infections, however, HPV77 has also been associated with lesions in renal transplant recipients. High-risk HPV DNA is found in >99.7% of cervical cancer, which mainly belongs to two high-risk mucosal species; species 7, which contains HPV18, along with HPV39 and 45, and species 9, containing HPV16 (which causes 50% of cervical cancers), along with HPV31, 33, 52 and 58 (Munoz, 2000; Walboomers et al., 1999).

The genus-β HPVs infect the cutaneous epithelium, most frequently forming benign lesions. However, HPVs from species 1 and 2 are also associated with non-melanoma skin cancer (NMSC) formation (including HPV types 5, 8, 9, 12, 14, 15, 17, 19-25, 36-38, 47, 49, 75, 76, 80, 92, 93 and 96). Due to the association between the rare inherited disorder Epidermodysplasia verruciformis (EV), skin cancer formation, and infection with certain β-HPVs, these types are also known as EV-types (Majewski and Jablonska, 1995). HPV5 and 8 from species 1 are described as high-risk types as they are frequently associated with NMSC in EV patients, as described in section 1.4.3.

1.3.2 Life cycle

Despite the association with cancer, and some differences based on infection site and virus type, most HPV infections result in productive 'normal' infections as a result of well-regulated gene expression, leading to shedding of progeny virus (Longworth and Laimins, 2004b). Such a lifecycle, as illustrated in Figure 1-5, begins with an HPV accessing a dividing basal keratinocyte through a micro-abrasion of the skin. The cellular receptor/s used for infection have not yet been fully elucidated but roles for heparin sulphate proteoglycans (Shafti-Keramat et al., 2003) and α6 integrin (Evander et al., 1997) have been suggested, with the extracellular component laminin 5 assisting with virion transfer (Culp et al., 2006). Once bound, the virions are thought to be taken up via endocytosis of clathrin-coated pits (Day et al., 2003), and trafficked to the nucleus where they will replicate, thought to be via an association with the endoplasmic reticulum Syntaxin 18 protein (Bossis et al., 2005).

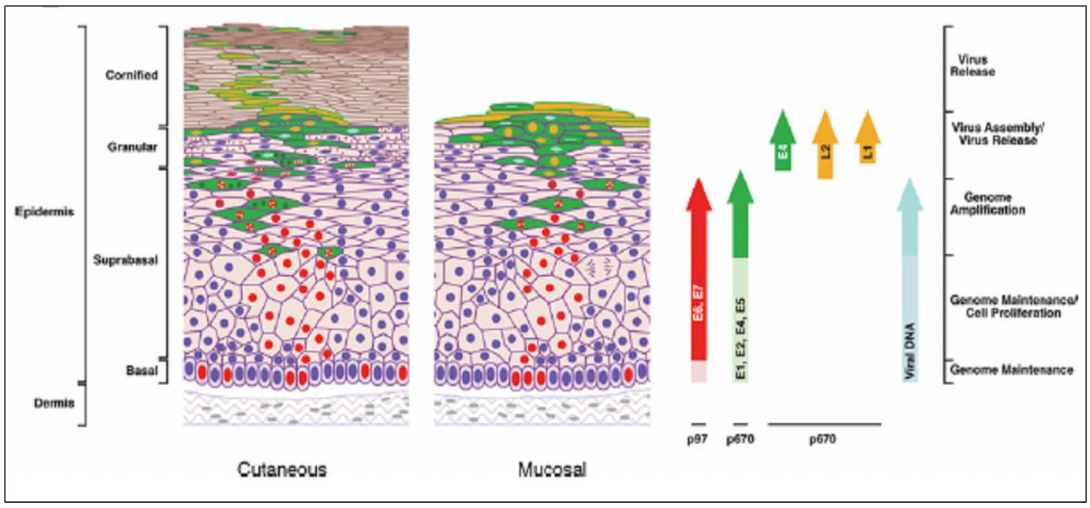

Figure 1-5 Summary of the viral lifecycle.

The different cell layers along with key viral lifecycle events are indicated at either side. Epidermal cycling cells are shown with red nuclei, whose presence in the suprabasal layer is due to viral proteins, namely E6 and E7. Cells expressing proteins necessary for viral replication are green, and yellow indicates expression of L1 and L2. Cells containing infectious particles (green with yellow nuclei) are shed from the surface. Taken from (Doorbar, 2006).

Initial viral expression in basal keratinocytes is mediated by binding of cellular transcription factors, in particular keratinocyte specific factors which may contribute to the tissue tropism (Sen et al., 2004). This leads to low expression of the E1 and E2 early genes (described, along with the other viral proteins, in more detail presently) and maintenance of HPV genomes as episomes (20-100 copies per cell). As the basal cells divide viral episomes are distributed among daughter cells to allow more cells to amplify the virus. As the cells leave the basal layer they exit the cell cycle and begin terminal differentiation. This activates the viral late promoter leading to increased expression of the E6 and E7 viral genes (Spink and Laimins, 2005), which override the typical cell cycle arrest allowing cellular DNA polymerase activity and therefore viral genome amplification (Hebner and Laimins, 2006). Recently a new model keratinocyte culture system allowing productive viral infections has been described, and showed that there was an abrupt increase in viral DNA in the mid- upper-spinous layer, and viral amplification was found to

happen after host DNA synthesis, when the cells had progressed from S to G2 phase (Wang et al., 2009a). The other viral early genes E4 (and E5 in genus-α) are also expressed and are involved in regulating viral replication. In the upper layers of the infected epithelium the structural capsid proteins L1 and L2 are expressed, which can self-assemble and are packaged with the viral genome. Viral progeny are shed from the surface with the cornified squames.

The non-lytic lifecycle of the virus means that there is no inflammatory response upon progeny virus release, and high level expression of viral proteins only occurs in the upper epidermal layers, meaning viral proteins are largely separated from immune surveillance. Additional viral mechanisms exist to evade the immune response, meaning that HPV infections can evade the immune system for some time. Despite this, the immune system usually mounts an effective adaptive response, shown by the eventual regression of cutaneous and genital warts, and seroconversion of the majority of infected individuals, with antibodies against the L1 protein expressed (Stanley, 2006). Infections of the cervix with high-risk HPVs are typically cleared within a year, and persistence of the infection for longer than this is linked to cancer progression, possibly through the accumulation of genetic instability (Rodriguez et al., 2008). Cutaneous HPV types also persist, with the same types shown to be present in skin swabs of healthy individuals after several years (Hazard et al., 2007). Hair follicles are thought to be a reservoir of persistent HPVs, with HPV presence in plucked eyebrow hairs of immunocompetent individuals suggesting persistence of at least 6 months (de Koning et al., 2007).

1.3.3 Virus structure

Despite some differences between HPV species, the genomic structure follows the same template, consisting of three main regions, illustrated in Figure 1-6. The upstream regulatory region (URR, also long control region (LCR)) contains

approximately 10% of the genome and encodes no proteins, but contains the origin of replication and several transcription factor binding sites which are important in regulation of viral expression (Zheng and Baker, 2006). The late region encodes the two structural capsid proteins, L1 and L2, and the early region includes over 50% of the genome and codes for the E1, E2, E4, E5, E6 and E7 proteins. The E5 ORF is not present in genus-β viruses. The functions of these proteins are described below.

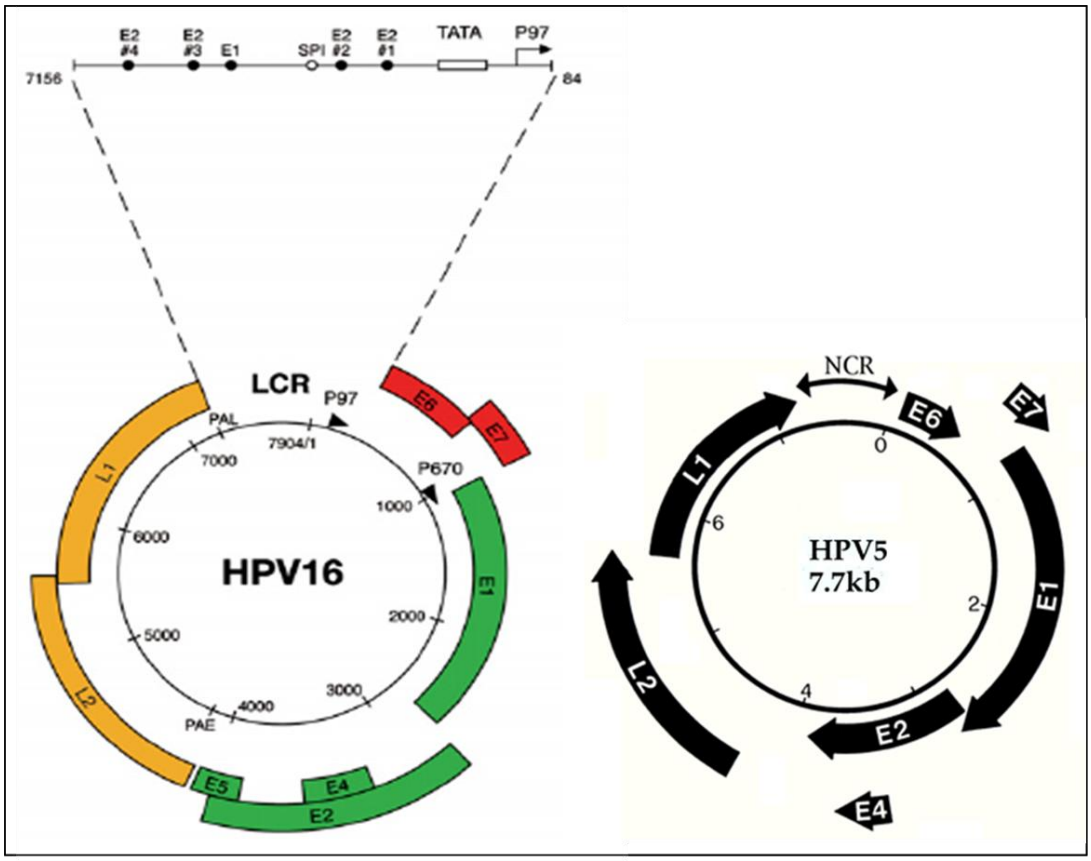

Figure 1-6 HPV genomic structure

The genus-α HPV16 genome is shown on the left as a black circle with the early (p97) and late (p670) promoters marked with arrows, and the LCR enlarged. The genus-β HPV5 genome is also shown for comparison on the right. All the viral genes are expressed from polycistronic mRNAs encoded on one strand of the double-stranded circular DNA genome. Taken from (Doorbar, 2006).

1.3.4 Viral proteins

1.3.4.1 E1 and E2

The replication proteins E1 and E2 are highly conserved throughout HPVs and are among the first viral proteins to be expressed (Sverdrup and Khan, 1994). E1 is a 70 kDa protein expressed throughout the viral lifecycle which possesses ATPase and helicase activities (Hughes and Romanos, 1993). E1 site-specific binding to the viral origin is initially weak, but complex formation with E2 leads to formation of hexameric E1/DNA complexes, initiating viral DNA replication (Wilson et al., 2002). E1 then recruits several factors to enable replication, including cellular chaperones to aid the unwinding of supercoiled DNA, DNA polymerase α, and chromatin remodelling complexes (Amin et al., 2000). Interactions with cyclins A and E lead to phosphorylation of E1 which is thought to contribute to its nuclear localisation (Deng et al., 2004).

The 50 kDa E2 protein functions as a dimer and has roles in viral replication and regulation of transcription, assembly of viral particles, and viral segregation during mitosis via interactions with the chromosomal Brd4 protein (You et al., 2004). E2 binds to specific sequences in the viral URR, facilitating E1 loading onto DNA as described. This binding also regulates transcription from the early promoter in a dose-dependent manner, with low E2 levels activating early gene expression and high levels repressing it, controlling the copy number in undifferentiated cells and regulating levels of E6 and E7 (Steger and Corbach, 1997). Upon cellular differentiation, viral transcription is activated by the late promoter which is not repressed by E2, allowing viral amplification (Klumpp and Laimins, 1999). E2 can also influence the host cell through synergistic activation of keratinocyte differentiation transcription through interaction with factors such as C/EBP (Hadaschik et al., 2003). Genus-α E2 proteins can induce apoptosis in cervical cancer cells, dependent and independent of p53, reviewed in (Hamid et al., 2009).

Genus-β E2 also displays functions other than viral replication, shown by spontaneous tumourigenesis in mice expressing HPV8-E2 in basal keratinocytes (Pfefferle et al., 2008), in contrast to the apoptosis induction of α type E2s. This may be linked to the downregulation of β-integrins and subsequent detachment of keratinocytes from the basal membrane caused by HPV8 E2 expression, which in a natural infection may contribute to commitment of the host keratinocyte to differentiation, allowing viral amplification (Oldak et al., 2004).

1.3.4.2 E4 and E5

E4 and E5 are primarily expressed in the later phases of the viral lifecycle, with E4 being the most highly expressed of all HPV proteins, accumulating in the suprabasal layers of the skin (Doorbar et al., 1997). E4 is expressed as a fusion with the first five amino acids of E1 so is also described as E1^E4, and is also modified by proteolytic cleavage which contributes to its regulation of keratinocyte proliferation (Knight et al., 2004). Its expression just prior to the capsid protein L1 suggests a role in viral amplification which has not yet been fully described, but appears to be mediated by several interactions (Nakahara et al., 2005). E4 facilitates a cellular environment suitable for viral amplification by inhibiting host DNA synthesis (Roberts et al., 2008). Additionally, binding by HPV16 E4 of cdk1/cyclinB1 tethers the active complex to the cytokeratin network, preventing its accumulation in the nucleus and leading to G2 cell cycle arrest (Davy et al., 2005). The E4 interaction with cytokeratins is conserved between HPV types 1 and 16, and in HPV16 this association leads to collapse of the cytokeratin network (Roberts et al., 1994) which may facilitate release of the progeny virus. HPV1 E4 has been found to induce relocation of promyelocytic leukemia protein (PML) from ND10 nuclear organelles to the nuclear inclusion bodies that form in HPV infected keratinocytes and are associated with E4 (Roberts et al., 2003). This disruption of

ND10 may be relevant to their possible function in viral replication and packaging (Tavalai and Stamminger, 2008). In addition, HPV16 E4 may play a role in post-transcriptional regulation as it also binds to the RNA helicase E4-DBP (Doorbar et al., 2000). Also, HPV1, 16 and 18 E4 binds and sequesters the serine-arginine specific protein kinase (SRPK1), possibly influencing SRPK1's regulation of splicing (Bell et al., 2007).

E5 is a hydrophobic membrane protein expressed at low levels primarily in differentiated cells and usually localised to the Golgi or endoplasmic reticulum, and its association with the proton-ATPase is thought to reduce endosomal acidification (Conrad et al., 1993). This leads to reduced epidermal growth factor receptor (EGFR) recycling, which in combination with upregulation of MAP kinase signalling, leads to a replication-competent environment (Crusius et al., 1997). E5 has also been proposed to mediate HPV immune evasion by decreasing antigen presentation by major histocompatability complex (MHC) I translocation to the cell surface (Ashrafi et al., 2006). Additionally, HPV16 E5 has been shown to protect cells from death receptor induced apoptosis (Kabsch et al., 2004). However the role of E5 is still debated, with high-risk genus-α E5 thought to modulate viral processes late in the lifecycle (Fehrmann et al., 2003), while genus-β HPVs do not express E5 at all, indicating that its functions are dispensable for these infections, or that they are taken over by other viral proteins in these HPV types.

1.3.4.3 E6

The E6 protein is a small multifunctional protein, with no direct cellular homologue, consisting of approximately 150 amino acids, expressed early in the viral lifecycle and localised to the nucleus and cytoplasm. In the normal viral lifecycle it is involved in episomal maintenance (Oh et al., 2004) and regulation of viral expression through co-operation with E2 (Muller-Schiffmann et al., 2006). However

one of its main roles in the normal lifecycle is thought to be the inhibition of the apoptosis that would usually be induced by viral infection and E7-mediated unscheduled DNA replication in differentiated keratinocytes. The various activities that mediate this also contribute to carcinogenesis when the normal viral lifecycle is disrupted, and lead to E6, together with E7, being characterized as one of the main oncoproteins of high-risk HPVs (Howie et al., 2009).

E6 consists of two stable folded domains each containing conserved zinc-binding domains (Cys-X-X-Cys) connected by an interdomain linker. The structure of the C-terminal domain has been solved allowing the pseudodimer model to be proposed, in which the domains associate symmetrically to mask their exposed hydrophobic patches (Nomine et al., 2006). The genus-α high-risk HPV E6s also contain a C-terminal S/TXV domain, not conserved in genus-β types 5 and 8, which mediates binding to PDZ proteins, described shortly. High-risk E6 can also be expressed as a short splice variant, termed E6*, which can inhibit the activity of full-length E6 (Pim and Banks, 1999). E6 does not appear to have enzymatic activity, and although it can bind to specific DNA structures (Ristriani et al., 2001), it mainly affects the cell through binding to multiple protein families. This varies with the genus and species of HPV, with genus-α and especially high-risk HPVs studied most intensively due to the association with tumourigenesis. Various specialised regions of exposed residues are conserved within but not between HPV species, illustrated in Figure 1-7, which could contribute to the differences in E6 binding specificity (Nomine et al., 2006). Due to these genus-dependent differences in E6 activity, genus-α effects are described prior to comparisons with genus-β.

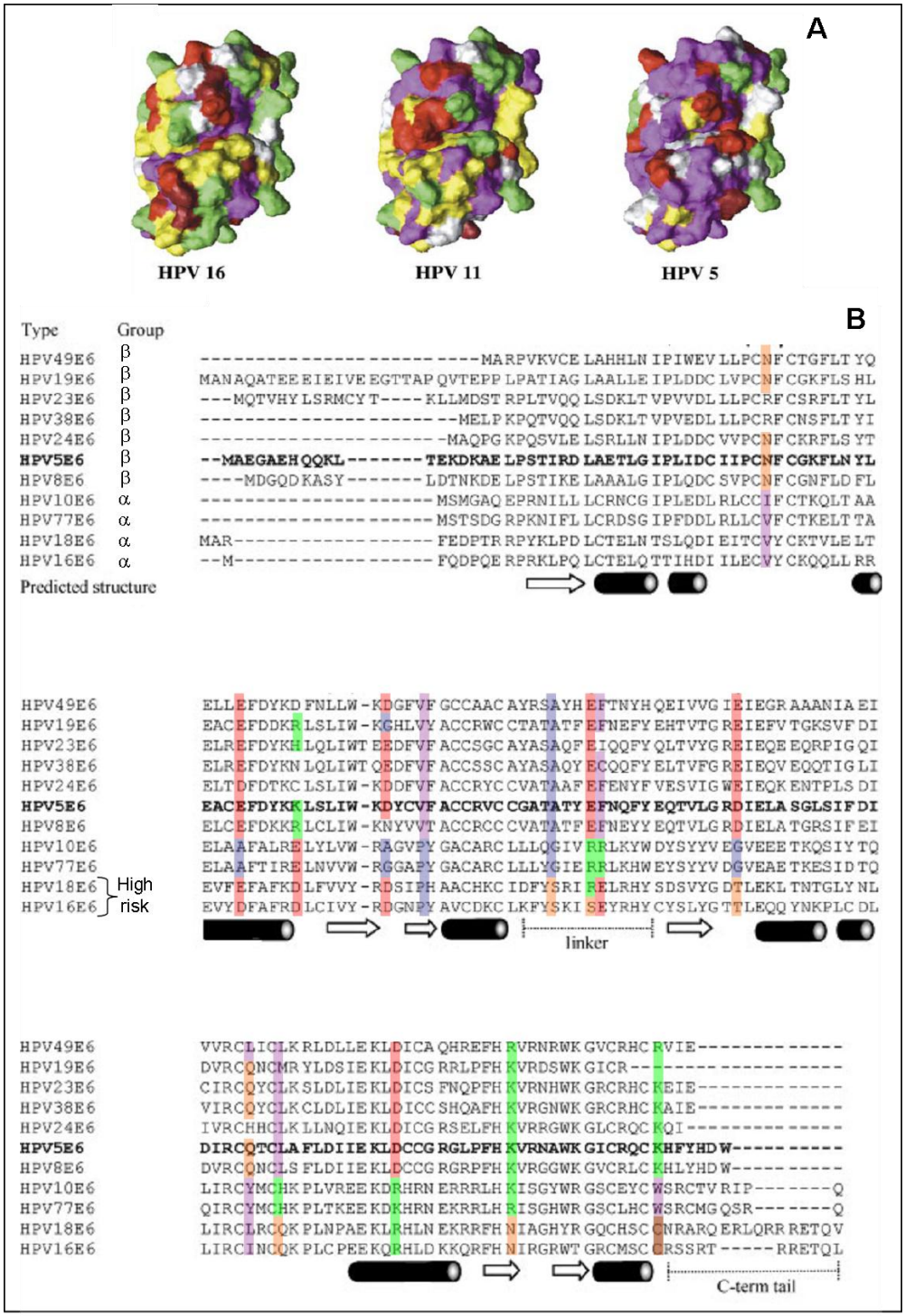

Figure 1-7 Differences in the structures of E6 of different HPV types.

A The different surface properties of E6 from HPV types 16, 11 and 5, illustrated by colouring of the residues according to their physico-chemical properties. Note for example more exposed hydrophobic areas on 5E6. Taken from (Nomine et al., 2006).

B Alignment of E6 sequences of representative HPV types illustrating conservation of certain residues, coloured according to their physico-chemical properties, with purple = hydrophobic, green = basic, red = acidic, orange = polar, brown = cysteine, blue = small; cylinder = α helix, arrow = β sheet. Adapted from (Simmonds and Storey, 2008).

One of the key functions of genus-α high-risk E6 is to bind and degrade the tumour suppressor p53 protein (Scheffner et al., 1990). As this protein is important in both cell cycle regulation and the induction of apoptosis, inhibition of p53 allows viral replication in suprabasal keratinocytes. As described in section 1.2.2.1, p53 is activated by post-translational modifications upon stress signals such as DNA damage allowing its accumulation and initiation of DNA repair, cell cycle arrest or apoptosis. The effect of high-risk E6 is to reduce p53 half life in keratinocytes from several hours to 20 minutes (Hubbert et al., 1992). This is mediated by the binding of E6 to both p53 and E6AP (E6 associated protein), an E3 ubiquitin ligase, which targets p53 for proteosomal degradation (Huibregtse et al., 1993). Although both high- and low-risk E6 can bind to the C-terminus of p53, degradation is only induced by the high-risk types which also bind to the core domain. It is also noteworthy that although E6AP is important for E6-induced degradation of several cellular substrates, degradation (of PDZ domain proteins, and p53) can still occur in E6AP-null cells (Massimi et al., 2008a). E6 also affects p53 function by means other than degradation. For example, site-specific DNA binding by p53 is reduced by HPV16, 18 and 11E6, in that order, which corresponds to the oncogenic potential of those viral types (Lechner and Laimins, 1994). E6 may also induce the mis-localisation of p53, possibly due to E6 binding masking the nuclear-localisation signal (Mantovani and Banks, 2001). E6 can also associate with CBP/p300, an interaction which inhibits p300 acetylation of p53, further reducing p53-mediated transcription (Zimmermann et al., 2000). p53 inhibition has several additional effects, including the increased expression of the anti-apoptotic survivin IAP in HPV16E6 expressing cells (Borbely et al., 2006).

However, as apoptosis can also be induced through p53-independent pathways, high-risk anogenital HPV E6 proteins have also been shown to inhibit apoptosis in cells lacking p53 (Steller et al., 1996). HPV16E6 has been shown to inhibit apoptosis induced by death receptor activation by FasL, TRAIL and TNFα ligation,

via binding and degradation of the adaptor protein FADD, and caspase 8 (Filippova et al., 2004; Garnett et al., 2006). This binding is via a novel interaction motif rather than PDZ domain binding, and so may not be restricted to high-risk E6 types (Tungteakkhun et al., 2008).

Another conserved binding region of genus-α high-risk HPV E6 is to the PDZ domain (so named due to associations with PSD-95, Dlg and ZO-1 proteins) of proteins including MAGUKs (membrane associated guanylate kinases), which includes human homologues of Drosophila discs large (hDlg and Scribble), MUPP1 and MAGI1-3 (Thomas et al., 2002). These proteins are important in cell adhesion, polarity, and are often tumour suppressors, and their degradation by E6 can deregulate epithelial proliferation (Nguyen et al., 2003) and lead to morphological changes reflecting an epithelial-mesenchymal transition (Watson et al., 2003).

PDZ domain binding can also lead to other effects, for example HPV16E6 can activate NF-κB signalling, leading to upregulation of the anti-apoptotic cIAP2 and protection from TNF-induced apoptosis, via PDZ binding (James et al., 2006).

A third major activity of genus-α high-risk HPV E6 is to activate the catalytic subunit of telomerase, hTERT. This enzyme complex prevents the eventual cellular senescence which occurs when telomeres are shortened after several rounds of replication, and is usually inactive in somatic cells. E6 forms a complex with the transcription factor Myc leading to binding and activation of the hTERT promoter (Veldman et al., 2003); with E6AP binding essential (Liu et al., 2005), as is the E6/E6AP interaction with the hTERT regulator NFX1-123 (Katzenellenbogen et al., 2007). In addition, HPV16E6 directly binds to the hTERT protein and the active telomerase complex, further increasing its activity and contributing to immortalization of the cell (Liu et al., 2009).

These activities together contribute to the transforming properties of high-risk E6, with p53 degradation important for transformation, and hTERT activation and PDZ binding important for immortalization, which can be achieved in primary human

keratinocytes by expression of high-risk E6 and E7 (Munger et al., 1989). However several cutaneous HPV types (12, 14, 15, 24, 36 and 49) have also been found to have transforming potential in oncogene cooperation assays, principally mediated by E6 (Massimi et al., 2008b). Expression of E6 may also contribute to tumourigenesis through immune evasion. HPV16E6/E7 have been found to downregulate genes involved in innate immunity, such as interferon-responsive genes, along with activation of NF-κB inducible genes (Nees et al., 2001); with downregulation of the antiviral interferon κ due to HPV16E6 (Rincon-Orozco et al., 2009). Inhibition by HPV16E6/E7 of the expression of molecules important in innate immunity such as toll-like receptor 9, and monocyte chemoattractant protein has also been observed (Hasan et al., 2007; Riethdorf et al., 1998).

In general, genus-β HPV E6s do not display the same activities as the genus-α high-risk proteins as they do not target p53 or PDZ domain proteins for degradation. However there is some overlap; in addition similar affects may be achieved through different mechanisms. For example, E6 of both genus-α and –β can inhibit intrinsic apoptosis via binding and degradation of the pro-apoptotic protein Bak. This is mediated by E6AP in some HPV types (Underbrink et al., 2008) but by a different ubiquitin ligase with other HPV types (Simmonds and Storey, 2008). Differences have also been observed in whether the degradation of Bak is constitutive (Du et al., 2004; Struijk et al., 2008) or occurs only upon apoptotic signals such as DNA damage (Jackson et al., 2000). However the end result is inhibition of release of apoptotic factors from the mitochondria (Leverrier et al., 2007) and inhibition of apoptosis in both p53 wt and null cells (Jackson and Storey, 2000; Storey, 2002). Additionally, the genus-α cutaneous HPV77E6, which does not degrade p53, has also been shown to selectively inhibit UV-induced transcription of the p53-regulated pro-apoptotic genes Fas, PUMAβ, Apaf-1, and PIG3 (Giampieri et al., 2004).

E6 of genus-α and –β have also been shown to compromise the DNA damage response. Cells expressing HPV5 or 18E6 show reduced repair of UV-induced DNA thymine dimers, and can also progress through the cell cycle despite harbouring this DNA damage (Giampieri and Storey, 2004). This may be linked to the binding and inhibition of the DNA repair protein XRCC1 by HPV1, 8 and 16E6 (Iftner et al., 2002).

It has recently been reported that E6 from genus-β cutaneous HPVs 8 and 38 can induce telomerase activity, albeit weakly compared to HPV16E6, with HPV5 and 20 E6 having no effect; and that this is mediated by E6AP interaction and could be involved in the prolonged life-span observed in cultured keratinocytes infected with these E6s (Bedard et al., 2008). In addition, the E6 and E7 of genus-β cutaneous HPV38, but not HPV10 or 20, have been shown to alter the cell cycle and senescence programmes of primary cells, and display transforming activities including extending the lifespan of keratinocytes (Caldeira et al., 2003). HPV38E6 does not degrade p53; in fact mice expressing HPV38E6/E7 in the skin accumulate p53, and the ΔNp73 isoform of the related p73 protein, however these keratinocytes do not undergo cell cycle arrest after UV irradiation (Dong et al., 2008). HPV38E6/E7 expressing cells also show reduced MHC I expression, along with inhibition of STAT-1 expression, which could contribute to immune evasion by HPV infected cells (Cordano et al., 2008).

Together these functions illustrate how the multifunctional E6 protein of both high-risk genus-α and –β HPVs could contribute to tumourigenesis in certain scenarios.

1.3.4.4 E7

The E7 protein consists of ~100 amino acids and is located in the cytoplasm and the nucleus. In the normal viral lifecycle it is involved in maintaining episomal HPV genomes by uncoupling cell cycle control and differentiation in the host cell. These

activities lend it a role in the progression and maintenance of cervical cancer which leads to its description, with E6, as one of the main oncoproteins of the genus-α high-risk HPVs (McLaughlin-Drubin and Munger, 2009). It consists of three conserved regions (CR1-3) with two zinc-finger like Cys-X-X-Cys regions that mediate E7 protein stability. E7 has no enzymatic activity but affects the cell through binding to several protein families, differences in which mediate the differences in activity between genus-α and –β, high- and low-risk HPVs.

The CR2 domain contains an LXCXE motif that enables binding to the tumour suppressor protein retinoblastoma (pRb) along with other pocket proteins p107 and p130. Pocket proteins are involved in regulating the cell cycle; pRb is continually expressed, with p107 and p130 levels changing throughout the cell cycle. In uninfected cells, unphosphorylated pRb binds to the E2F family of transcription factors, inhibiting their transcription of genes involved in progression into S-phase. Cyclin-dependent kinase phosphorylation of pRb leads to release of E2Fs and transcription of genes involved in DNA synthesis. E7 sequestration of pRb therefore leads to constitutive transcription of E2F induced genes (Patrick et al., 1994). A different region of the genus-α high-risk E7 also targets pRb to the ubiquitin degradation pathway (Wang et al., 2001). Genus-β low-risk HPV E7s bind to pRb, but frequently with reduced affinity, and do not target it for degradation, meaning they are not able to activate E2F dependent genes or cause cellular transformation (Schmitt et al., 1994). For example, the E7 of HPV77 (a genus-α cutaneous type associated with non-melanoma skin cancer) binds to pRb but does not efficiently disrupt the cell cycle (Mansour et al., 2006).

E7 also binds to the histone deacetylases (HDACs), which are also involved in the repression of E2F inducible genes. HDAC binding by E7, which is independent from pRb binding and mediated by Mi2β, is important in episomal maintenance (Longworth and Laimins, 2004a). Along with its role in cell cycle deregulation, HDAC binding by E7 can lead to gene silencing, as is the case with interferon

regulatory factor (IRF) 1, whose activity is important in the immune surveillance of HPV lesions (Park et al., 2000). Thirdly, high-risk HPV E7 deregulates cell cycle control through associations with cyclins A and E, along with the cyclin dependent kinase inhibitors p21 and p27, which have a role in phosphorylating pRb (Funk et al., 1997). A summary of the interactions leading to cell cycle disruption by E7 is shown in Figure 1-8.

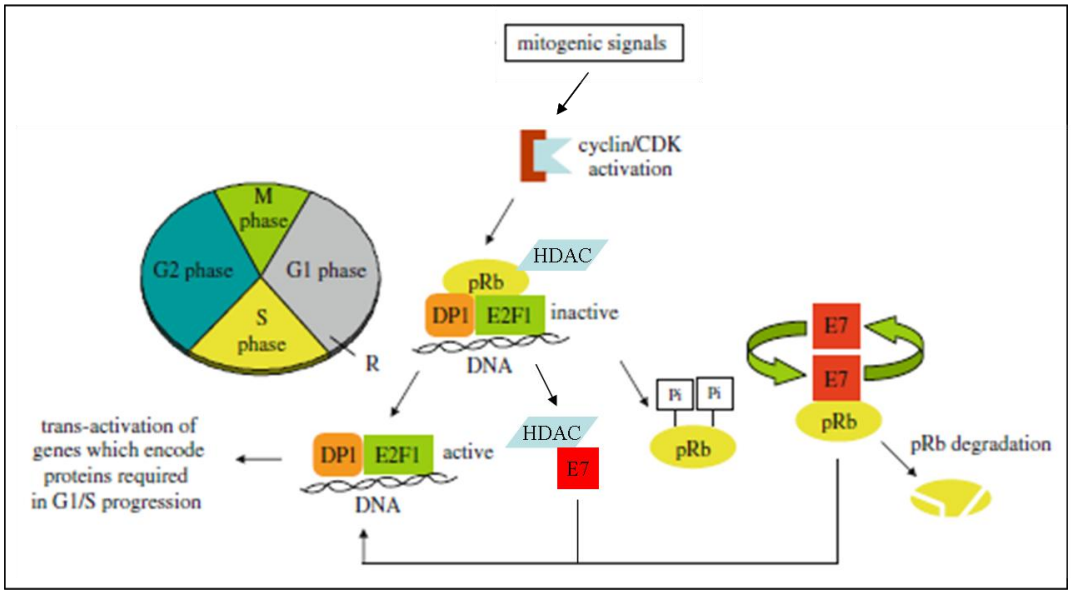

Figure 1-8 Summary of genus-α high-risk E7 disruption of the cell cycle.

E7 disrupts the cell cycle restriction point (R). pRb/HDAC complexes repress E2F transcription factors, which are released as cells move into S phase. E7 independently binds to pRb and HDACs, leading to constitutive activation of E2F inducible genes, and entry into S phase. Adapted from (Ghittoni et al., 2010).

Additionally, high-risk E7 can induce genomic instability, as seen by abnormal centrosome duplication in HPV16 E7 keratinocytes (Duensing et al., 2000). E7 proteins from different HPVs have also been shown to induce cell proliferation independently of the pRb binding capacity (Caldeira et al., 2000). These factors, in combination with the effects described above, could contribute to the ability of high-risk E7 (together with E6) to immortalize human cells (Munger et al., 1989).

Several differences have been observed between genus-α and –β E7s. The high-risk genus-β HPV5 and 8 E7 displayed low pRb binding and showed no transforming potential in rodent cell lines, however they displayed limited immortalization in combination with activated ras oncogene (Yamashita et al., 1993). In addition, although HPV8 E7 binds to pRb with lower affinity than HPV16E7, primary keratinocytes expressing HPV8E7 displayed decreased pRb expression and a disruption in the cell cycle that led to polyploidy (Akgul et al., 2007a). In contrast HPV38 E7 binds pRb with a similar efficiency to HPV16 E7 and displays transforming properties *in vivo* (Caldeira et al., 2003; Dong et al., 2005) Organotypic model systems, in which keratinocytes are grown on a scaffold allowing terminal differentiation, also demonstrated a different function of HPV8 E7. Here E7 caused increased cellular proliferation, and also increased invasion into the dermis, mediated by overexpression of extracellular matrix metalloproteinases (Akgul et al., 2005a), and further work in this model system has indicated that HPV5 and 8 E7 are able to overcome p16 induced cell cycle arrest (Westphal et al., 2009).

1.3.4.5 L1 and L2

The conserved L1 and L2 capsid proteins are expressed in differentiated suprabasal keratinocytes late in the viral lifecycle. 72 pentameric L1 capsomeres can self-assemble to form the virion, along with 12 L2 proteins (Modis et al., 2002). L1 capsomeres are assembled in the cytoplasm and transported to the nucleus. L2 is also transported to the nucleus via nuclear-localisation signals, where it localises to ND10 bodies, facilitating packaging of viral DNA into the capsid (Florin et al., 2002). The importance of L2 for efficient virion production was shown using infections of organotypic model systems with HPV31 lacking L2, leading to a 10-fold reduction in viral DNA encapsidation and 100-fold reduction in infection

efficiency (Holmgren et al., 2005). The ability of the L1 protein to self-assemble into immunogenic virus-like particles (VLPs) has led to its use in vaccines against HPV. The quadrivalent vaccine contains L1 VLPs, expressed in *Sacchromyces cerevisiae,* from HPV types 16, 18, 6 and 11; the types which cause 70% of cervical cancers and 90% of genital warts. Although not therapeutic, it has been shown to be effective in preventing infection with these HPV types, and the subsequent widespread uptake will reduce future cervical cancer, cervical intraepithelial neoplasia (CIN – precancerous dysplastic lesions), and genital wart burdens (Barr and Tamms, 2007).

1.3.5 Epidemiology

Genus-α HPVs are common sexually transmitted pathogens with an estimated 1% of the sexually active population having genital warts and 15% having subclinical infections (Koutsky, 1997). Early hypotheses that HPV types 16 and 18 were associated with cervical cancer (Gissmann et al., 1984) have been confirmed by worldwide studies (Smith et al., 2007). The HPV types 16, 18, 31, 33, 35, 39, 45, 51, 52, 56, 58, 59, 68, 73 and 82 have been classified as high-risk due to association with squamous cell cervical cancer, types 26, 53, 66 as probably high-risk, and types 6, 11, 40, 42, 43, 44, 54, 61, 70, 72 and 81 as low-risk, as they mainly cause genital warts only (Munoz et al., 2003). High-risk types are also associated with several other cancers including those from other anogenital sites and head and neck squamous cell carcinoma (Furniss et al., 2007). Cervical cancer is the 5th leading cause of cancer deaths in women, although diagnosis has declined by up to 80% in Western countries in the past 50 years due to use of Pap smear screening (Pisani et al., 2002; Singer, 1995). However given the high incidence of infection, progression to cancer is rare. This is because typical low-grade HPV lesions naturally regress in approximately one year, due to immune clearance (Hopfl et al., 2000). Cervical intraepithelial lesions (CIN) are

pathologically graded 1-3 according to severity, with the chance of regression decreasing with increasing dysplasia (Ostor, 1993). It is thought that progression to cancer is due to perturbation of the normal viral lifecycle, for example, through viral persistence with prolonged immune evasion, or infection in the transformation zone of the cervix, where neoplasia often arises (reviewed in Doorbar, 2006). Integration of high-risk HPV DNA is also seen upon progression, which typically leads to loss of the E2 gene, thus leading to constitutive expression of the oncoproteins E6 and E7 (Fujii et al., 2005). The specific activities of the high-risk oncoproteins are also thought to contribute to their association with cancer. Continued expression of E6 and E7 is required for tumour maintenance, and for continued growth of the cell lines derived from cervical cancers (Goodwin and DiMaio, 2000). The association between non-melanoma skin cancer and genus-β HPV types is somewhat different, and discussed in section 1.4.3.

1.4 Non-melanoma skin cancer

Non-melanoma skin cancer (NMSC) arises from keratinocytes and is the most commonly diagnosed cancer in fair-skinned people, with increasing worldwide incidence due to factors including increased sun-exposure and a larger immunosuppressed population (Rigel, 2008). It includes basal and squamous cell carcinomas (BCC and SCC) which in the general population are found in a 4:1 ratio. Associated conditions include: actinic keratoses (AK, precancerous UV-induced lesions, 10% of which progress to SCC), Bowen's disease (also called carcinoma *in situ* (CIS), a pre-invasive form of SCC), and keratoacanthomas (KA, a low-grade, non-invasive form of SCC) (Boukamp, 2005). In contrast to SCC, BCC development is associated with severe UV exposure incidents, often as a child, and it is relatively well-defined genetically, with abrogation of the *PTCH*/sonic hedgehog signalling pathway seen in >70% of BCC (Gailani et al., 1996; Tsao, 2001). In contrast the genetics of SCC are poorly understood, with a variety of mutations

detected at low frequencies, including the *ras* oncogene, and the cell cycle regulator $p16^{INK4}$, and high frequency of chromosomal aberrations (Boukamp, 2005). There has been no evidence to suggest a link between BCC and HPV infection; therefore further discussion will focus on SCC. SCCs are more invasive, and metastasize more than BCC, and represent a significant healthcare burden. SCCs typically arise on sun-exposed sites in patients over the age of 50, with increased risk in people prone to sunburn, indicating the role of cumulative UV exposure as the main carcinogen. The roles of both UV and HPV in the formation of SCC are outlined below.

1.4.1 UV mediated damage

The damage to keratinocytes induced by UV irradiation is a key factor in SCC development (de Gruijl and Rebel, 2008). DNA is the main cellular chromophore of UVB, with exposure resulting in formation of cyclobutane-pyrimidine dimers (CPDs) and <6-4> pyrimidine-pyrimidone photoproducts (6-4PPs), illustrated in Figure 1-9.

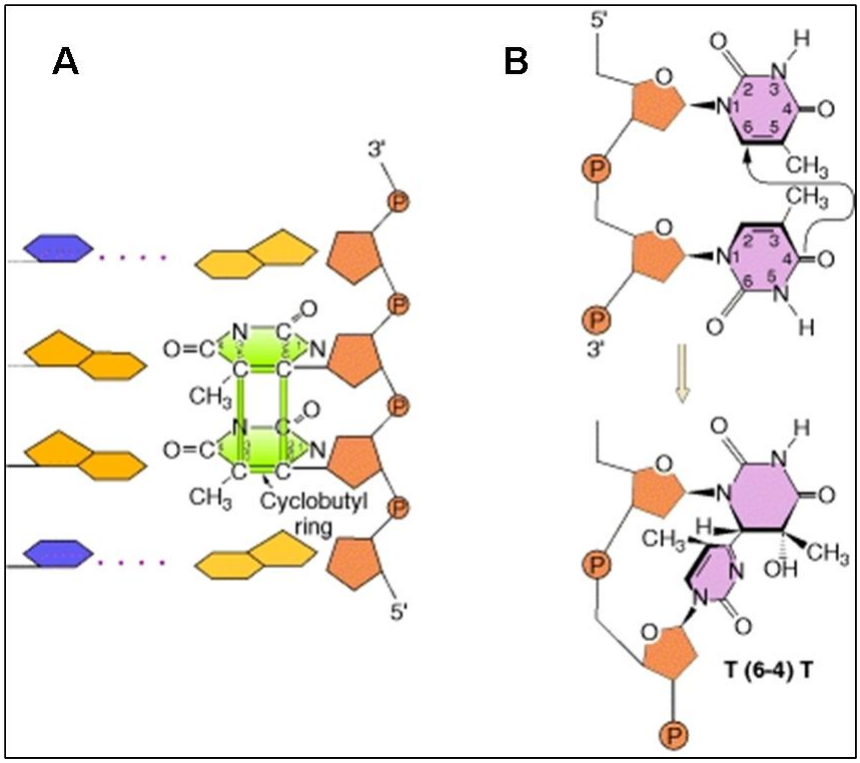

Figure 1-9 Structure of CPDs and 6-4PPs

A Structure of a cyclobutane pyrimidine dimer, the cyclobutane ring shown in green.
B Structure of a 6-4 photoproduct, which disrupts the local structure of the double helix. Taken from (Griffiths et al., 2000)

These adducts lead to mis-matching in DNA replication, giving rise to C to T mutations which are a signature of UV damage (Brash and Haseltine, 1982). Mouse models have been used to show that CPDs in basal keratinocytes are the most genotoxic and tumourigenic (Jans et al., 2006). Removal of CPDs from basal cells is essential for NMSC prevention. CPDs and 6-4PPs are repaired primarily by the Nucleotide Excision Repair (NER) system, aided by cell cycle arrest mediated by the p53 protein (Latonen and Laiho, 2005). Patients with *Xeroderma Pigmentosum*, a recessive disorder with NER defects, are susceptible to skin cancer, of which 90% have p53 mutations. In the general population 50% of skin cancers have mutations in p53, and in SCC p53 mutations often follow the UV-induced signature (Giglia-Mari and Sarasin, 2003). However p53 mutations have also been frequently observed in normal skin, indicating that p53 inactivation is an

early step in SCC development (Jonason et al., 1996). More detailed analysis of p53 mutations in both normal skin and neoplasia found that although normal skin often had p53 mutations, these were not of the same type as the mutations found in cancer (Ren et al., 1996). In addition, patients with Li-Fraumeni syndrome, who have germ line p53 mutations and an increased susceptibility to several types of cancers at an early age, are not predisposed to NMSC (Malkin et al., 1990). Changes in the apoptotic pathways important in the keratinocyte response to UV, as described in section 1.2.1, can also contribute to SCC formation (Erb et al., 2008). For example, upregulation of the anti-apoptotic Bcl-x_L has been observed in SCC compared to KA (Vasiljevic et al., 2009). The death receptor Fas is also important in regulating keratinocyte apoptosis, facilitating removal of DNA-damaged cells, as shown by an increase in epidermal UV-induced p53 mutations in FasL deficient mice compared to wild-type (wt) (Hill et al., 1999). The role of Fas has also been explored in humans; in normal skin, Fas is expressed by basal keratinocytes, and is upregulated upon UV exposure to trigger apoptosis. However prolonged UV exposure downregulates Fas, meaning damaged cells escape apoptosis, facilitating tumourigenesis, and shown by the lack of Fas in AK (Bachmann et al., 2001; Filipowicz et al., 2002). In addition, FasL expression is increased upon progression from AK to SCC, allowing tumour cells to evade the immune response by triggering Fas-induced apoptosis in infiltrating immune cells (Satchell et al., 2004). The role of the immune system in SCC development is discussed below.

1.4.2 UV mediated immune suppression

UV (both UVB and UVA) irradiation affects both local and systemic immune responses through a complex series of interactions, resulting in immune suppression and inappropriate responses to tumour and viral antigens (Murphy, 2009). The role of the immune system in keeping pre-cancerous skin lesions under

control is illustrated by the fact that immunosuppressed patients are 65-250 times more likely to develop SCC than the general population (compared to a 10-fold increase in BCC formation) (Moloney et al., 2006). Immune suppression is often measured by contact hypersensitivity (CHS) tests in the skin, and is thought to be mediated by several factors. These include the UV-induced photoisomerization of urocanic acid which accumulates in the *s.corneum* and becomes a systemic immunosuppressive agent (McLoone et al., 2005). Suppression of adaptive immune responses also occurs, one mechanism being the depletion of epidermal Langerhans cells (Murphy et al., 1993). UV can also modulate signalling pathways, for example the Epidermal growth factor receptor (EGFR) and cytokine production, as described in 1.1.3. In particular, Interleukin 10 is immunosuppressive, for example contact hypersensitivity was reduced after UV and the tolerance was mediated by regulatory T-cells and IL10 (Ghoreishi and Dutz, 2006). CPD formation also contributes to the UV mediated suppression of the memory response (Kuchel et al., 2005). UV irradiation and its associated immune suppression can interact with viral infection, an example, besides HPV, being the reactivation of herpes simplex after sunlight exposure (Norval, 2006).

1.4.3 HPV and SCC

In addition to the role of UV-induced damage and immunosuppression in SCC formation, a link with HPV infection is supported by several lines of evidence, as outlined below (and reviewed in Akgul et al., 2006a; Hengge, 2008).

1.4.3.1 Epidermodysplasia verruciformis

Epidermodysplasia verruciformis (EV) is a rare inherited disorder characterized by increased susceptibility to certain genus-β HPVs (termed EV-HPVs), which results in a large number of warts and macules from childhood. By the age of 50, 30-60% of patients also progress to SCC at sun-exposed sites, 90% of which contain DNA

from HPV5 and 8, which are termed 'high-risk' (Orth, 2006). Therefore EV has long been studied as a model for the relationship between genetic, environmental and infectious causes of cancer (Orth et al., 1979). Mutations in two adjacent novel genes, *EVER 1* and *2*, were found by linkage analysis to be associated with EV (Ramoz et al., 2002), and further mutations in these genes indicated its genetic heterogeneity, also illustrated by identification of EV patients without *EVER* mutations (Akgul et al., 2007b). *EVER1* and *2* code for transmembrane channel (TMC) 6 and 8 proteins, which were found to interact with zinc transporter 1 and regulate intracellular zinc distribution (Lazarczyk et al., 2008). Correct regulation of zinc homeostasis is important for the host cell, both in immune regulation and regulation of the viral lifecycle. Therefore it has been hypothesised that correct functioning of TMC6 and 8 is required to keep cutaneous virus amplification in check, and disruption of this allows the increased EV-HPV infections of EV patients (Lazarczyk et al., 2009).

1.4.3.2 Non-EV associations

Immunosuppressed organ transplant patients are also at increased risk of both viral warts and SCC development, possibly linked to UV-induced immune suppression as described in section 1.4.2, but also due to involvement of infectious agents such as HPV. Several studies on organ transplant recipients have found that 70-90% of SCCs contain genus-β HPV DNA, in contrast to around 30% of immunocompetent SCC; however there are often multiple types and no specific 'high-risk' types have emerged (Berkhout et al., 2000; de Villiers et al., 1997; Harwood et al., 2000; Stockfleth et al., 2004). Differences in detection methods could account for the observed differences in prevalence. HPV carriage rather than active infection could also influence results, where HPVs could simply be passengers in hyperproliferative keratinocytes, however β-HPV gene expression has been shown

by *in situ hybridisation* in SCC samples (Purdie et al., 2005). It is also interesting to note a group of patients with severe combined immune deficiency who, <10 years after haematopoietic stem cell transplant, nevertheless had an immune deficiency resulting in EV-like disease with chronic cutaneous HPV infections (Laffort et al., 2004).

Several studies have also investigated an association between HPV and SCC in the immunocompetent population, with some studies showing an increase in genus-β species 2/EV-HPV-DNA in SCC or AK (Asgari et al., 2008; Forslund et al., 2007; Harwood et al., 2004), or an increase in the number of HPV types associated with SCC (Alotaibi et al., 2006). Serologic studies have also been conducted, and several have shown an association between SCC or AK and seropositivity towards genus-β HPV and HPV8 (Karagas et al., 2006; Masini et al., 2003; Struijk et al., 2006).

However the exact role of EV-HPV in SCC formation has been difficult to delineate due to many additional studies showing that a large number of virus types are present in the majority of the worldwide general population, with infection occurring throughout life and often resulting in persistent asymptomatic infections (Antonsson et al., 2003; Boxman et al., 1997; de Koning et al., 2007). However this viral persistence could also contribute to tumourigenesis, as is the case in cervical cancers, by allowing accumulation of genetic abnormalities. Interestingly, a study which showed higher viral loads in AK than SCC or perilesional skin suggests a role for HPV early in tumourigenesis (Weissenborn et al., 2005).

1.4.3.3 Models of HPV-associated SCC formation

In addition to the activities of the viral proteins, namely inhibition of apoptosis, cell cycle and genome integrity disruption, and immune evasion, as previously described in section 1.3.4, several model systems have demonstrated potential

tumourigenicity of some genus-β HPVs. Some of these have been described previously, for example, the increased proliferation and invasion of keratinocytes expressing HPV8E7 in organotypic cultures (Akgul et al., 2005a) and the tumourigenesis in mice expressing HPV8E2 (Pfefferle et al., 2008). Organotypic cultures generated with keratinocytes expressing E6/E7 from several EV-HPV (5, 12, 15, 17, 20 and 38) have also been studied, and it was found that differentiation and stratification was disrupted or delayed to certain extents in all these HPV types (Boxman et al., 2001).

In addition, findings that expression of HPV38E6/E7 immortalized human keratinocytes were further investigated with mice expressing these proteins under the keratin 10 promoter. These mice displayed increased cellular proliferation, hyperplasia and dysplasia, and did not undergo cell cycle arrest or p21WAF1 accumulation after UV. Spontaneous tumours did not arise but carcinogen treatment led to a higher number of SCC in transgenic compared with control mice (Dong et al., 2005). Mice expressing HPV8 E2, E6 and E7 in basal keratinocytes under the control of the keratin-14 promoter have also been generated. 91% of these mice spontaneously developed benign tumours, and 6% developed SCC (Schaper et al., 2005), possibly linked to increased expression of matrix metalloproteinases (Akgul et al., 2006b). The effect of chronic UV exposure has also been studied on mice expressing E6/E7 under the keratin 10 promoter from either EV-HPV20 or genus-α HPV27 (associated with cutaneous warts). Both types showed increased proliferation, papilloma formation and disturbed differentiation, however after cessation of UV, only HPV20 transgenic mice showed continued enhanced proliferation (Michel et al., 2006).

Several studies have also investigated the effects of UV on viral promoters. For example, the URR of HPV77 contains a positive response element which is stimulated by UV-mediated p53 binding (Purdie et al., 1999), and the URR promoters of high-risk genus-β HPVs 5 and 8 are also activated by UV in primary

keratinocytes (Akgul et al., 2005b). It has also been found that a variety of UV-induced cytokines stimulate the promoter of the genus-β HPV20 but inhibit it in the genus-α cutaneous HPV27 (Ruhland and de Villiers, 2001). These findings provide further support for a role of EV-HPVs in SCC formation in combination with UV. A model describing the possible roles of EV-HPV in SCC formation is shown in Figure 1-10 and is described below.

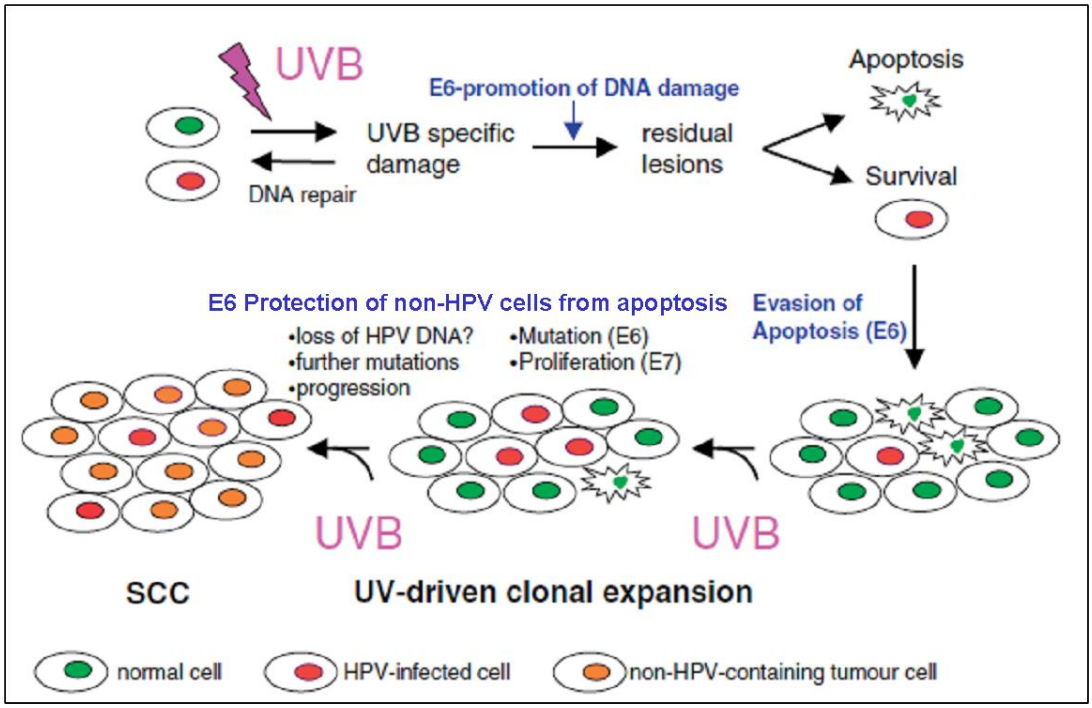

Figure 1-10 Model of the role of UV and HPV in SCC formation.

Exposure to UV leads to DNA damage, repair of which is inhibited in HPV-infected keratinocytes. E6 also protects cells from apoptosis, so normal cells are preferentially deleted following UV, allowing clonal expansion of HPV-infected cells. Accumulation of mutations allows cells to progress to SCC, independently of the proliferative and mutagenic effects of HPV, possibly assisted by HPV-mediated protection from apoptosis. Taken from (Akgul et al., 2006a).

The activity of the viral proteins, which allows accumulation of DNA damage, along with *in vitro* and epidemiological evidence, illustrates their tumourigenic potential. However their role in SCC formation has still proved difficult to clarify. In contrast to cervical cancer, where high-risk genus-α HPV proteins are continually expressed

in every cell, in SCC of immunocompetent patients viral load determinations estimate the copy number as one HPV genome per 20-5000 cells, with HPV DNA being undetectable by *in situ* hybridization in the majority of tumor cells (Dang et al., 2006), thus the model of tumourigenesis of EV-HPVs will be different to that of high-risk genus-α HPVs. One such model is that HPVs infect keratinocyte stem cells, or confer stem-like properties on basal keratinocytes, and so maintain a persistent infection but also allow accumulation of DNA damage, and become cancer stem cells (Egawa, 2003). A similar scenario of persistent viral infection is indicated by the presence of viral 'reservoirs' in hair follicles. Viral persistence may also be facilitated by UV irradiation, in which keratinocytes which are fully competent for apoptosis die preferentially, allowing expansion of surviving HPV-infected keratinocytes; similar to the expansion of mutant p53 clones in mouse skin after UV irradiation. In addition, the observation that HPV-positive SCC display greatly reduced overall apoptotic rates when compared to HPV-negative SCC, despite similar proliferation rates suggests that a low number of HPV positive cells can influence the tumour overall (Jackson et al., 2002). This fits with a model in which HPV infection can contribute to UV induced carcinogenesis at several stages, as illustrated in Figure 1-10.

1.5 Summary and Aims

The skin consists chiefly of keratinocytes which move up through the layers of the epidermis, undergoing terminal differentiation which results in the formation of a continuously replaced protective waterproof barrier made of cornified keratinocytes and extracellular lipids and proteins. Apoptosis is a crucial, tightly controlled, evolutionarily conserved, complex cellular process essential for removal of damaged cells, particularly in the skin, which is frequently exposed to damaging UV irradiation. As most keratinocytes are destined to be lost quickly, those that persist

must be protected or eliminated if damaged. Keratinocytes are the host cells of Human Papillomaviruses (HPVs) which disrupt normal differentiation to allow their own replication and release. There are over 100 HPV types, showing variation in the details of the lifecycle, infection site and activities of the viral proteins, leading to a range of pathologies from non-apparent infections, benign warts and lesions, to cancer. The link between cervical cancer and genus-α HPVs is well studied; however the link between squamous cell carcinoma (SCC) of the skin and a subset of cutaneous β-HPVs is less well delineated. The model that these EV-HPVs could act as a co-factor with UV in SCC formation is supported by the cases of EV and immunosuppressed patients, along with descriptions of molecular mechanisms by which HPVs could act. One such mechanism is the inhibition of apoptosis by HPVs, which in combination with UV damage could contribute to tumourigenesis. It has been shown that the E6 protein of several cutaneous HPVs can inhibit apoptosis, in part mediated by the inhibition of the pro-apoptotic Bak protein. However other anti-apoptotic mechanisms are thought to exist; and the aim of this work was to delineate other anti-apoptotic mechanisms that may be important in SCC formation. The E6 from a range of HPV types (5, 8, 10, 18 and 77) was used to assess protection from apoptosis in both cell lines and in primary human cutaneous keratinocytes, the natural host cell. The effect of E6 expression on the apoptosis of neighbouring but non-E6 expressing cells was also investigated, and additionally, global changes in expression levels in keratinocytes expressing E6 will also be presented.

2 Materials and Methods

2.1 Tissue culture

All chemicals were from Sigma unless stated otherwise.

2.1.1 Media composition

- Complete E4: E4 (Cancer Research UK equivalent to DMEM) + 10% foetal calf serum (FCS) + 10% L-glutamine.
- Starvation media: Dulbecco's modified Eagle medium (DMEM) without L-glutamine (Sigma # D5546) + 10% Dialysed foetal calf serum (DFCS) (Gibco # 26400-044).
- Jurkat media: RPMI 1640 + 10% L-glutamine + 10% FCS.
- Defined keratinocyte media: Gibco defined keratinocyte serum free media (Gibco # 10744) or EpiLife media plus keratinocyte supplement (Cascade Biologics # M-EPI-500-CA plus S-001-5).
- RM+ media: DMEM:Ham's F12 3:1 (Cancer Research UK) supplemented with L-glutamine, 10% FCS or DFCS, and RM+ supplement to give final concentrations of: transferrin 5 µg/ml, hydrocortisone 0.4 µg/ml, cholera toxin 10^{-10} M, epidermal growth factor 10 ng/ml (from Serotec), insulin 5 µg/ml, liothyronine $2x10^{-11}$ M, adenine 1.8×10^{-4} M.
- Starvation media II: DMEM:F12 1:1, L-glutamine free (Sigma # D6434) plus a supplement to mimic the defined media as closely as possible with the exception of glutamine (Sigma keratinocyte supplement BPE free K3136).
- Starvation media III: E4:F12 1:1 (Cancer Research UK) no supplement.
- Starvation media IV: DMEM:F12 1:1 L-glutamine free (Sigma D6434) no supplement.

2.1.2 Growth conditions

Cells were grown at 37 °C in humidified 90% air, 10% CO_2, apart from cells grown in defined keratinocyte media which were grown in 5% CO_2.

Cells were split for passage after rinsing with PBS in 1:1 trypsin:versene to cover the surface, deactivated with equal volumes of complete media or PBS + 10% FCS. Cells were pelleted at 1100 rpm (approx. 200x g) for 5 minutes and resuspended in the relevant growth media and re-seeded at the appropriate densities, for example at 1 in 10 dilution for routine passage. Where cell number was required cells were counted in a haemocytometer.

Table 2-1 Growth conditions of different cell types used.

Cell type	Cell Details	Media/s used	Use of media
HT1080	Human fibroblast sarcoma wt-p53 line (Rasheed et al., 1974)	Complete E4 Starvation media	Routine passage and growth Fas antibody induction and for conditioned media production
Jurkat	Human T lymphocyte line	Jurkat media	Routine growth and passage
NTert	Human adult cutaneous keratinocyte line (Dickson et al., 2000)	Defined KC media + 100 μL gentamycin Starvation media II Starvation media III Starvation media IV	Routine growth and passage (low calcium, proliferative basal phenotype) Fas antibody induction

Cell type	Cell Details	Media/s used	Use of media
Keratinocytes	Primary human keratinocytes isolated from middle-aged patients PA8 and PA10 Primary Adult Human Epidermal Keratinocytes, single donor (Cascade Biologics #s C-020-5C)	Defined KC media or: EpiLife media RM+	Routine growth and passage Routine growth and passage (better for extended life span of cells) More differentiated monolayer cultures and raft cultures
Human Fibroblasts	Dermal fibroblasts from Cancer Research UK cell services	Complete E4 RM+	Passage Raft culture
HaCaTs	Human keratinocyte line (Boukamp et al., 1988)	Complete E4	Routine passage

2.1.3 Storage of cells

Cells were trypsinised and resuspended in ice cold FCS + 20% filter sterilised dimethylsulphoxide (DMSO). Keratinocytes were resuspended in defined media + 10% FCS + 10% DMSO. They were aliquoted to ice-cooled cryovials, transferred to a Mr Frosty or wrapped in five layers of tissue and transferred immediately to -80 ^{o}C. From there they were transferred to liquid nitrogen. For rescue of frozen cells, aliquots were thawed quickly at 37 ^{o}C, transferred immediately to 10 ml of growth media, pelleted at 1100rpm (approx. 200x g) for 5 minutes, resuspended in growth media and seeded out.

2.1.4 Transfection of cells

HT1080 cells were plated in 6 cm dishes. Cells were transfected when 40-50% confluent. Fugene transfection reagent was used (Roche # 11815091001). A ratio of 3:1 Fugene:DNA was used, with 2 μg total DNA. For each dish to be transfected, 6 μL of fugene was added to 94 μL of serum free media. 100 μL of this mixture was added to the DNA and incubated at room temperature for twenty minutes. Media was removed from cells, and replaced with a thin layer of serum free media (900 μL in a 6 cm dish). To this was added the DNA/Fugene mix. After 5 hrs at 37 °C 2 ml of complete media was added. After a further 24 hrs the media was changed. 24 hrs later G418 selection was added at 350 μg/ml final concentration. Selection was considered to be effective when control non-transfected cells died, however G418 was still added to maintain selection pressure. Surviving cells were pooled to form polyclonal cell lines, to avoid the specific effects of integration at certain sites of the genome. Plasmids, detailed in Table 2-2, containing the E6 genes were previously generated in the lab as described in (Jackson and Storey, 2000).

Table 2-2 Cell lines generated from HT1080 cells

Name	Plasmid	Gene expressed along with resistance marker
pcDNA	pcDNA3 (Invitrogen)	Resistance marker only
pc5E6HA	pcDNA3 5E6 HA	HPV 5E6 HA tag
pc5E6	pcDNA3 5E6	HPV 5E6
pc8E6	pcDNA3 8E6	HPV 8E6
pc10E6	pcDNA3 10E6	HPV 10E6
pc18E6	pcDNA3 18E6	HPV 18E6
pc77E6	pcDNA3 77E6	HPV 77E6
EGFP	pcDNA EGFP	EGFP (enhanced green fluorescent protein)
pIRES	pIRES (Clontech)	Resistance marker only
pIRES 5E6	pIRES 5E6	HPV 5E6

2.1.5 Generation of retrovirus

Keratinocytes do not respond well to transfection, so to generate keratinocytes expressing the HPV E6 genes of interest, the retroviral vector pLXSN (Clontech) was used. This vector originates from the Moloney murine leukemia retrovirus and contains a neomycin resistance marker under the SV40 promoter. The pLXSN plasmids used here, containing E6 sequences from HPV types 5 and 8, had previously been generated in the lab (Akgul et al., 2005a). Infectious but replication incompetent virus particles were generated with the PT67 packaging cell line; briefly, PT67 cells were grown in complete E4 in 100 mm dishes until 50-60% confluent, and for each 100 mm dish, 18 µl of Fugene reagent was added dropwise directly to 567 µl of serum free DMEM, and incubated for 5 minutes at room temperature. Six µg of 1 µg/µl pLXSN plasmid DNA was added to the complex to give a ratio of Fugene:DNA of 3:1, samples were mixed by pipetting then left to incubate at room temperature for 15 minutes. This DNA/Fugene solution was then added to cells, incubated for 4-5 hrs following which the media was replaced with serum containing media and left for 24-48 hrs. Transfected cells were selected with G418 500 µg/ml, and once selected split into T175 flasks without G418. When cells reach 90-95% confluency, 16 ml of fresh media were added and the flasks incubated overnight at 32 °C, 10% CO_2. The following day media containing viral particles was collected and placed into 4x4 cm tubes, and the viral supernatant stored at -80 °C until required.

2.1.6 Retroviral infection of keratinocytes

In glass, polybrene (5 mg/ml stock) was added and mixed 1 in 1000 to serum free E4 media, 4 ml/6 cm dish or 2 ml/6 well-plate to be infected. Cells at 30-40% confluency were rinsed in PBS and incubated for 10 minutes at 37 °C in this mixture. 4 ml of viral supernatant were used to infect one or two 6 cm dishes (diluted to 8 ml with serum free media if the latter) or 2x 6 well plate wells. In glass

polybrene was added 1 in 1000. Media was removed and cells rinsed in PBS, and the virus mixture added. Cells were spun for 1hour, 350 rpm (approx. 20x g), 32 °C. Then supernatant was removed, cells rinsed, and fresh serum free keratinocyte media added. After 1-2 days media was changed, cells were split if necessary and G418 selection added at 150 µg/ml.

2.1.7 Organotypic raft culture generation

In order to mimic the natural differentiated environment of human skin, primary keratinocytes of interest can be seeded and grown along with dermal fibroblasts on a scaffold of preserved skin using the following protocol, as in (Akgul et al., 2005a). Glycerol preserved skin from the Euro Skin Bank (Beverwijk, The Netherlands) was washed 5 times in PBS to remove the glycerol, then covered in PBS with antibiotics (600 U/ml penicillin G, 600 µg/ml streptomycin sulphate, 250 µg/ml gentamycin sulphate, 2.5 µg/ml fungizone; or Gibco antibiotic/antimycotic mix used at 2x the recommended concentration) and incubated at 37 °C for 7-10 days, with daily agitation. After removal of PBS the skin was scraped to remove the dark coloured epidermis, noting which side is which. The skin (de-epidermalised dermis, DED) was cut into 1.5 x 1.5 cm squares and the remainder stored at -20 °C. The DED pieces were placed dermal side 'up' in a 6 well plate and sterilised steel rings firmly pressed down. Into these rings were seed $0.5x10^6$ dermal fibroblasts in 1 ml complete E4, plus a little media around the DED to avoid desiccation. One well of a 24 well plate was seeded in the same way to allow observation of growth. When the dermal fibroblasts reached confluence 24-48 hrs later the media was removed and the DED inverted. Sterilised steel rings were firmly pressed onto the DED and $5x10^5$ keratinocytes seeded inside in 1 ml defined keratinocyte media, again including a 24 well plate as a control.

When the keratinocytes were very confluent the media and rings were removed. Sterilised grids were placed into 6 well plates and the DEDs transferred,

keratinocyte side ‘up’, and spread out on the grids. RM+ media is added so it flows under the grids, excluding any air bubbles, until it is just level with but NOT covering the upper side of the DED. Cultures were left to differentiate for 14 days, refreshing the media every 3 days. If necessary, UV irradiation was performed at this point. Rafts were harvested after removal from the grids by cutting cleanly in half with a scalpel, immersing half in fresh 4% paraformaldehyde overnight, and snap freezing the other half in iso-propanol cooled over liquid nitrogen using CryoEmbed (store at -70 °C).

2.1.8 Induction of apoptosis and cytokine assays

Media was removed and cells are rinsed in PBS. Fas-activating antibody (Oncogene # AM01L); hereafter referred to as ’Fas-Ab’, was added to fresh media and used at different concentrations. For UVB irradiation at different doses, PBS and plasticware lids were removed and a crosslinker ‘oven’ (Ultra Violet Products, #CL-1000) with a peak emission at 312 nm or a calibrated lamp (UV source MRL 58 lamp) were used before fresh media was added.

For testing the activity of cytokines on cultures of HT1080s and primary keratinocytes, purified recombinant human OPG (R&D Systems, #805-OS) and IL6 (Sigma #I1395) were diluted in a carrier solution consisting of 0.1% bovine serum albumin (BSA) in water, stored at -20 °C, and further diluted to working concentrations prior to addition to growth media at the doses described. Negative controls employed 0.1% BSA only. After apoptosis was induced, the replacement media contained the same concentrations of cytokines.

2.1.9 CaspaseGlo assay

As an alternative measure of apoptosis, the level of activation of the executioner caspases 3 and 7 was measured with a luminescent substrate provided in Promega’s CasGlo 3/7 kit. Cells were seeded 5000 per well in white walled 96 well

plates in the appropriate media and treated with cytokines and/or UV. For measuring, the reagent and plates were equilibrated to room temperature and an equal volume of reagent to media was added. Plates were shaken at 500 rpm for 30 seconds and rocked for 45 minutes to 2 hours. Luminescence was measured with a BMG Labtech Luminometer with Fluostar software. Values from wells containing only media were used as blanks. It was observed, especially for keratinocytes, that cell disruption was not always complete so in later assays DMSO was added (10% volume of reagent) and the plate freeze-thawed to aid lysis.

2.1.10 MTT assay

Cells were seeded in 96 well plates, after the appropriate time points 50 μl of MTT (Sigma M2128-5C) at 2 mg/ml were added to each well. After incubation at 37 °C for 3 hours, the supernatant was aspirated; 100 μl of DMSO was added to each well and pipetted to dissolve the crystals. Absorbance was read at 540 nm.

2.2 Nucleic acid techniques

2.2.1 Isolation of RNA from cells

RNA was harvested from trypsinised cells with Qiagen RNEasy Mini Kit (# 74104) following the manufacturer's instructions. Cells were disrupted by addition of 350 μL Buffer RLT (which denatures RNAses), and then the lysate was homogenized on a Qiagen QIAShredder column centrifuged at 13000 rpm (approx 15000x g) for 2 minutes. 350 μL 70% Ethanol was added and mixed with the lysate, 700 μl of which was added to the RNeasy column membrane, which binds RNA longer than 200 bases during a spin step. If the RNA is to be used for sensitive applications such as Exon Microarrays the Qiagen on-column DNA digestion kit (# 79254) was

included at this stage. After a spin wash, DNase solution was pipetted onto the column membrane and incubated at room temperature for 15 minutes.
After further wash steps with buffers RW1 and RPE the column was transferred to a 1.5 ml collection tube and 40 µL of RNase-free water pipetted onto the membrane to elute the RNA. RNA was stored at -20 °C or -70 °C (longer term) and the concentration was calculated by 'Genespec' programme or Nanodrop.

2.2.2 Production of cDNA from isolated RNA

Promega's Reverse Transcription kit (# A3500) was used to make cDNA according to the manufacturer's instructions. 1 µg aliquots of the 1.2 kb positive control RNA (2 µL), poly(A)+mRNA or sample RNA were added to eppendorfs and incubated at 72 °C for 10 minutes. After a brief spin, samples are put on ice and the following reagents added:

- $MgCl_2$ 25 mM 4 µL
- Reverse transcriptase buffer 10x 2 µL
- dNTPs 10 mM 2 µL
- RNAsin 0.5 µL
- AMV reverse transcriptase 0.625 µL (15 units)
- Random (or oligo) primers 1 µL (0.5 µg)
- RNA – control or sample
- Nuclease-free water to a volume of 20 µL

The reaction can be scaled up or down according to the RNA sample concentration.
A 10 minute incubation at room temperature allows extension of the random primers, followed by incubation at 42 °C for 30 minutes for cDNA extension. The reverse transcriptase was inactivated by incubation at 92 °C for 5 minutes, then 4 °C for 10 minutes. cDNA was stored at -20 °C and quantified with a Nanodrop.

2.2.3 PCR amplifications

For each reaction use:

- 2.5 µl buffer
- 1.5 µl of 50 mM $MgCl_2$
- 0.5 µl dNTPs
- 2 µl template DNA (1 µL if plasmid)
- 0.5 µl each primer
- 0.25 µl Bioline Taq polymerase
- To 25 µl with nuclease-free water

PCRs were run as follows:

95 °C 3 minutes

95 °C 45 seconds
60 °C 45 seconds
72 °C 1 minute
} 30 cycles

72 °C 3 minutes

2.2.4 Gel Electrophoresis of DNA

1x TBE buffer consisting of 0.4 nM EDTA, 18 mM Boric acid, 18 mM Tris Base pH 8.2 was used to make and run the gels. 1.5% agarose in TBE was used to make gels along with 5 µL ethidium bromide/60 ml agarose. DNA was mixed with 6x loading buffer and run at 90 V for 1-2 hrs. Bands were illuminated with UV light. Markers used were from Fermentas (OGene Ruler 100 bp ladder).

2.2.5 Quantitative RTPCR

Quantitative real-time PCR was performed on an Opticon 2 (MJ Research) with the DyNAmo SYBRGreen kit (Finnzyme, #430-L) using cDNA template made as described in 2.2.2. The reaction was performed according to the manufacturer's

instructions. For each sample to be analysed a master mix was made, for a 20 µl final reaction each:

- 10 µl Master mix
- 0.5 µg template cDNA (not more than 10% of final reaction volume)
- Water to 18 µl.

18 µl of the master mix was then pipetted to 1 µl each of forward and reverse primers for each gene of interest, mixed and centrifuged to remove bubbles, and the vessel sealed. The reaction steps were initial denaturation at 95 °C 15 minutes, followed by 45 cycles consisting of denaturation at 94 °C 10 seconds, annealing at 57 °C 30 seconds, extension at 72 °C 30 seconds, and data acquisition. After a final extension step at 72 °C 5 minutes, a melting curve was performed from 72-95 °C, followed by reannealing at 72 °C 5 minutes. The specificity of the reaction was checked with the results of the melting curve included in each run; Figure 2-1 A and B shows an example of the narrow, superimposed curves indicative of specific amplification. The housekeeping gene GUS (Glucuronidase) was used to normalise for slight differences in starting cDNA levels, for example as illustrated in Figure 2-1 C, the orange sample crosses the threshold at a later cycle number, indicating there was a lower concentration of starting cDNA. After normalisation of the test gene according to GUS levels, the change in CT between different samples was calculated, with a lower CT indicating earlier amplification and therefore higher expression levels. The relevance of CT changes were inferred by calculating the linear fold change ratio using the $2^{\Delta\Delta CT}$ method.

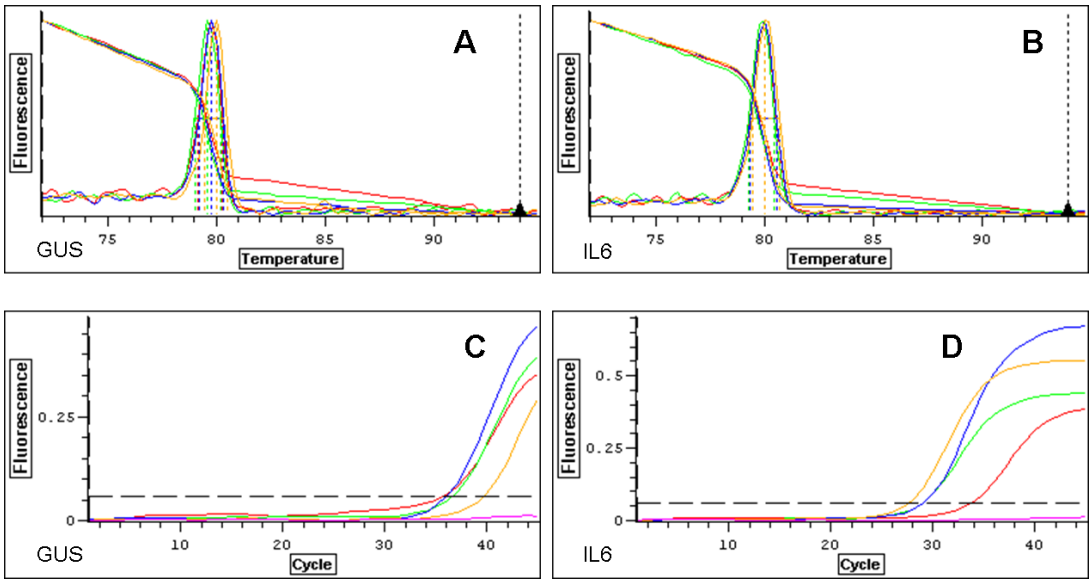

Figure 2-1 Example of QRTPCR results and analysis.

A and **B** The melting curves for GUS and the test gene (Interleukin [IL] 6) respectively. **C** and **D** The CT is the point at which the amplified products (coloured lines) cross the threshold (dashed line), GUS on the left and IL6 on the right.

2.2.6 Microarrays

RNA was extracted as described in section 2.2.1 in triplicate from early passage primary human keratinocytes which express either pLXSN empty vector or pLXSN 5E6, each of which was treated with 16 hrs of 0 or 30 mJ/cm^2 UV irradiation as described in 2.1.8. Cells which had floated up from the surface due to apoptosis were also harvested. Keratinocytes from the same patient were used in each repeat, but different viral infection repeats were used. 5.5 μg of RNA of each sample was sent to the Cancer Research UK Affymetrix Genechip Microarray Service at the Paterson Institute for Cancer Research (PICR), where it was processed for analysis with Affymetrix GeneChip Human Exon 1.0 ST arrays. Hybridised chips were scanned and quality checked at the PICR and the data uploaded onto the MIAME VICE database[1]. Data was then analysed with the

[1] http://bioinformatics.picr.man.ac.uk/vice/Welcome.vice

affylmGUI and oneChannelGUI programmes (Sanges et al., 2007; Smyth, 2004), through the Bioconductor packages on R, with help from the Computational Biology Research Group (CBRG) at the Weatherall Institute for Molecular Medicine (WIMM).

2.3 Protein Techniques

2.3.1 Generation of lysates

Media from cells to be harvested was removed. In the case of apoptotic samples, any floating cells were pelleted by centrifuging the media at 1100 rpm for 5 minutes. Ice cold RIPA buffer was used to resuspend the pellet and incubated on ice for 5 minutes. The attached cells were rinsed with PBS and ice cold RIPA was added to cover the surface (for example, 300 µL for a T75 flask) and incubated on ice for 5 minutes. A cell scraper was used to collect the sample. Lysed samples were sonicated 2 x 5 seconds and stored at -20 °C.

RIPA buffer:

- 150 mM NaCl
- 50 mM Tris HCl pH 7.5
- 1% NP40
- 0.5% NaDOC (deoxycholic acid sodium salt)
- 1% SDS
- 1 x Protease Inhibitor cocktail tablet

2.3.2 Quantification of protein

A standard curve was prepared using varying concentrations of BSA in PBS measured with the Bradford assay (BioRad Protein Assay Reagent # 500-0006). Absorbance at 595 nm was measured with a plate reader. Sample protein concentrations were determined with respect to the standard curve generated.

2.3.3 SDS-PAGE and western blotting

Protein samples were separated by SDS-PAGE (sodium dodecyl sulphate polyacrylamide gel electrophoresis). 1.5 mm thick mini gels were prepared and run with standard equipment. Gels consisted of 3% acrylamide stacking and 10 or 12% resolving gels.

Table 2-3 SDS PAGE gel components:

Percentage:	3%	10%	12%
Total ml (per gel):	3	10	10
Component (ml):			
Distilled water	2.1	4	3.3
30% Acrylamide	0.5	3.3	4
Buffer:			
1M Tris pH 6.8	0.38		
1.5M Tris pH8.8		2.5	2.5
10% SDS	0.03	0.1	0.1
10% APS	0.03	0.1	0.1
TEMED	0.003	0.004	0.004

APS and TEMED were added immediately prior to pouring. A layer of iso-propanol covers the resolving gel to ensure even setting before the stacking gel is poured. Protein samples were incubated with loading buffer at 95 °C for 5 minutes prior to loading. Gels were run at 90 -110 V for 1-2 hours.

Loading buffer:

- 4% SDS
- 0.2% Bromophenol Blue
- 20% Glycerol
- 100 nm Tris HCl pH 6.8

Running buffer:

- 3 g Tris
- 14.4 g Glycine

- 1 g SDS
- 1 L distilled water

When marker proteins were separated the gel was removed and the proteins transferred to membrane. The gel was layered with Whatman paper and nitrocellulose or PVDF membrane (activated with methanol for 1 minute) and dampened with transfer buffer, bubbles are removed. Transfers were either run at 300 mA for 1.5 hours or at 20 mA overnight.

Transfer buffer:

- 3 g Tris
- 14.4 g Glycine
- 800 ml distilled water
- 200 ml methanol

TBST:

- 2.42 g Tris
- 8 g NaCl
- 1 L distilled water
- pH to 7.6
- 1 ml Tween 20

Membranes were blocked in 10% milk TBST for at least an hour at room temperature with shaking. Primary antibodies were incubated as indicated in Table 2-4. Membranes were washed 3 x 5 minutes in TBST between antibodies and before development. Secondary antibodies were incubated in 10% milk in TBST at 1 in 1000 for 1.5 hours at room temperature with shaking. Bands were detected with the Amersham ECL Plus kit. Membranes were then exposed to film for 10 seconds to 30 minutes dependent on signal strength.

Table 2-4 Details of antibodies used (where rt = room temperature, o/n = overnight).

Antibody	Catalogue number & Supplier	Incubation details
Mouse anti-HA	Roche High Affinity anti-HA clone 3F10 #1867423	1/1000 1 hr rt 10% milk-TBST
Mouse anti-tubulin	Calbiochem CP06	1/4000 1 hr rt 10% milk-TBST
Rabbit anti Caspase 3	Cell Signalling Technology CST #9662	1/1000 o/n 4 °C 5% milk-TBST Or 1/1000 rt 3 hrs 10% milk-TBST
Rabbit anti PARP	CST #9542	1/1000 o/n 4 °C 5% milk-TBST
Rabbit anti FasR	Santa Cruz sc714, N-18	1/1000 o/n 4 °C 5% milk-TBST
Rabbit anti Bcl2	CST #2872	1/1000 o/n 4 °C 1% milk-TBST
Rabbit anti Bcl-xL	CST # 2762	1/2000 o/n 4 °C 1% milk-TBST
Mouse anti XIAP	Abcam ab28151	1/1000 o/n 4 °C 1% milk TBST
Mouse anti GAPDH	Millipore MAB374	1/4000 1 hr rt 1% milk-TBST
Rabbit anti Mcl1	Abcam ab32087	1/2000 o/n 4 °C 1% milk-TBST
Rabbit anti cIAP2	Santa Cruz sc7944	1/500 o/n 4 °C 1% milk-TBST
Mouse anti OPG	Imgenex IMG 103A	1/500 1 hr 30 rt 1% milk-TBST
Rabbit anti mouse HRP conjugated secondary	DakoCytomation P0260	1/1000 1 hr 30 rt 10% milk-TBST
Goat anti rabbit HRP conjugated secondary	DakoCytomation P0448	1/1000 1 hr 30 rt 10% milk-TBST

2.3.4 Apoptotic protein array assay

The Proteome Profiler Human Apoptosis Array kit from R+D Systems was used to investigate changes in apoptotic proteins in 5E6 expressing cells. The kit consists of membranes with antibodies specific to 35 apoptosis related proteins spotted on. The manufacturer's instructions were followed. Membranes were blocked in the buffer provided for 1hr at room temperature. Cell lysates made in the lysis buffer provided and stored at -70 °C were quantified; 500 μg of protein was normalised with blocking buffer to 250 μl and incubated with each membrane overnight at 4 °C. Membranes were washed 3 x 10 minutes in the buffer provided before addition of the diluted biotinylated detection antibody cocktail for 1 hour at room temperature, and after further washes the diluted Streptavidin-HRP was incubated for 30 minutes at room temperature. Membranes were incubated with Amersham ECL Plus reagent for 1 minute after further washes and then exposed to film. A range of exposures from 10 seconds to 5 minutes were used to get a good representation of the data points without saturation of the spots. The resulting images were analysed with software written by Dr PD Allen, Gray Institute for Radiation Oncology and Biology, University of Oxford. The software uses a template to measure pixel density of each spot, which is correlated to protein levels in the lysate. For each protein the amount is calculated by:

Amount of protein = (P-B)/(C-B)
Where P = (P1+P2)/2, P1 being the value for spot 1 of the protein pair, P2 is spot 2,
B = Background estimated by planting a set of points just outside of the array,
C = mean value of the 6 control spots.

2.4 Flow Cytometry

2.4.1 Apoptosis assays

Apoptosis was assessed by AnnexinV and vital dye staining. In the initial stages of apoptosis, phosphatidylserine (PS) flips from the inner to outer cell membrane. AnnexinV binds with high specificity to PS in the presence of calcium. AnnexinV conjugated to fluorescent proteins is therefore used to identify early apoptotic cells. Vital dyes are stains which are only expelled from living cells and therefore identify late apoptotic and necrotic cells. Different combinations of vital dye and AnnexinV conjugates can be used dependent on the cell type. Table 2-5 illustrates the combinations used. This variation was found to be necessary due to high expression levels of EGFP (488/509 nm excitation/emission) which caused bleed-through of signal into the PI detection channel. Compensation was unable to solve this problem. 7AAD, detected in the PECy5 (675/20 nm) channel was found to be compatible with EGFP expression.

Table 2-5 FACS apoptosis assay details.

Cells in assay	AnnexinV conjugate	Excitation/ Emission (nm)	Vital dye	Excitation/ Emission (nm)
HT1080 NTerts Primary Keratinocytes	Alexfluor 647	650/665	Propidium iodide	535/617
EGFP expressing cells	Alexafluor 647	650/665	7AAD	546/647

Harvesting cells for apoptosis assays:

Cells may be harvested at various time-points after induction, however 16 hrs post UV irradiation was used unless stated. Floating cells were included by centrifuging media at 1200 rpm (approx 230x g) for 5 minutes at 4 °C. Adherent cells were then rinsed with PBS and removed from the plate with 1:1 Trypsin:versene solution

(enough to cover the surface, e.g. 1 ml/well of a 6 well plate). When all cells were detached (time dependent on cell type) the trypsin was deactivated with an equal volume of E4 or PBS containing 10% serum and cells were then pelleted with those collected from the media by centrifugation for 1200 rpm 5 minutes. Cells were washed in PBS, and resuspended in AnnexinV binding buffer (Becton Dickinson #556454 10x stock AnnexinV binding buffer) with vital dye (4 µL PI [Sigma #P4864 1 mg/ml] or 2.5 µL 7AAD [0.1 mg/ml Sigma #A9400]) and AnnexinV-AlexaFluor647 (volume dependent on cell number: 1.5 µL/10 cm culture dish; 1 µL/6 cm dish; 0.75 µL/6 well plate). Cells were kept on ice in the dark and analysed within 1 hr on an LSRII (Becton Dickinson) with FACSDiva and WinMDI software, or a FACSCalibur (Becton Dickinson) or CYAN with Summit software (Dako). Fluorescence was detected in the appropriate channel and AnnexinV positivity depicted on the x-axis and vital dye positivity on the y-axis of the dotplots. In each experiment unstained samples were used to confirm adequate staining, and untreated cells used to set quadrants for the detection of dead cells. Cells in the lower left quadrant (labelled as R4) are AnnexinV and vital dye negative viable cells. As the cells progress through apoptosis they become AnnexinV positive and move to the right (quadrant R5) and subsequently become vital dye positive as well (quadrant R3). Cells in quadrant R2 are vital dye positive necrotic cells. As shown in Figure 2-2, the percentage of cells in each quadrant can be used to monitor apoptosis. As the majority of cells used in this project are epithelial there is usually not as large a move to the lower right in the early stages of apoptosis as reported for other cell types.

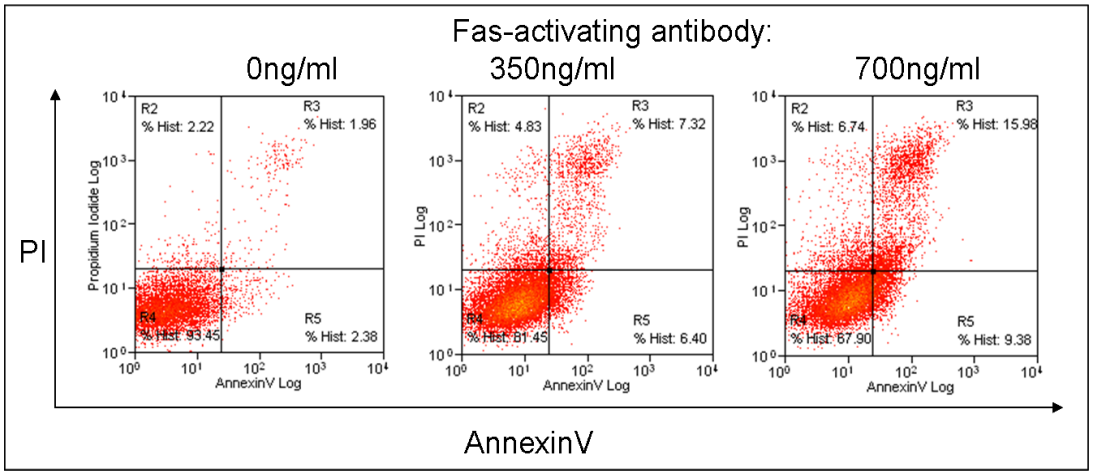

Figure 2-2 Increasing doses of Fas-activating antibody increase the amount of apoptotic HT1080 cells as shown by increased AnnexinV and PI staining.

2.4.2 Apoptosis assay including basal cell identification

To identify any changes in the level of apoptosis of primary keratinocytes of different stages of differentiation a marker of basal cells was included in some of the assays. The α6 integrin (also called CD49f) is one such marker which has been reported to be more highly expressed on the 'most basal' of a heterogeneous population of primary keratinocytes, for example (Lorenz et al., 2009; Webb et al., 2004). Therefore, a FITC-conjugated anti-CD49f antibody was included in the AnnexinV/PI protocol. After harvesting, when cells are in PBS, 5 μl of antibody/sample was added and incubated on ice, in the dark, for 30 minutes. The cells were then pelleted and resuspended in AnnexinV/PI as usual. To prevent bleedthrough of the FITC into the PI signal, PI was measured off the Violet 2 laser. Alternatively, for FACS machines without this facility, the vital dye DAPI can be used. For analysis, either the topmost 5 or 20% CD49f expressing cells were gated.

2.4.3 FACS analysis of Bak-N-terminal conformational change

The technique is based on the specificity of the Ab1 antibody (Calbiochem AM03) for Bak only in its active conformation and is adapted from a previously published

method (Griffiths et al., 1999). Cells were seeded in 6 well plates (c.150000 per well) and 24 hours later, when 70% confluent, were treated with Camptothecin (2 µl of 6 mM stock per well) or vehicle (DMSO) for 4 or 6 hours. Camptothecin binds to topoisomerase I and DNA, leading to double-strand breaks and therefore activation of apoptotic pathways. After removal of media and PBS wash, cells were fixed with 300 µl cold PBS/0.25% PFA on ice for 10 minutes (if cells are to be stored for longer before staining use 1% PFA). Cells were harvested by scraping, transferred to an eppendorf and pelleted at 9000 rpm (approx 7500x g) for 1 minute at 4 °C. The supernatant was carefully removed and cells were resuspended in 200 µl PBS (cells can then be kept at 4 °C overnight). Cells were pelleted at 9000 rpm for 1 minute at 4°C, resuspended in 100 µl PBS/0.01% saponin and incubated for 5 minutes at room temperature to permeabilise. Cells were pelleted and resuspended in either 100 µl Bak Ab-1 primary antibody diluted 1/50 with PBS/0.01% saponin or 100 µl mouse IgG1 (Pharmingen) diluted 1/30 with PBS/0.01% saponin. Cells were incubated for 30 minutes at 4 °C on a mixing wheel. Cells were pelleted and washed in 100 µl PBS/0.01% saponin for 3 minutes. Cells were pelleted and resuspended in 100 µl rabbit anti-mouse phycoerythrin (Dako, 500 mg/L) secondary antibody diluted 1/30 with PBS/0.01% saponin and incubated for 30 minutes at 4 °C on a mixing wheel. Cells were pelleted and resuspended in PBS and analysed, detecting PE fluorescence in the FL2 channel.

A no stain control sample was used to gate the cell population and an IgG control to determine the negatively stained population. Figure 2-3 shows how increased PE fluorescence indicates increased active Bak. Specific Bak fluorescence was calculated by taking the IgG median value from the sample medians, then multiplying the adjusted medians by the percentage Bak positive cells for each sample.

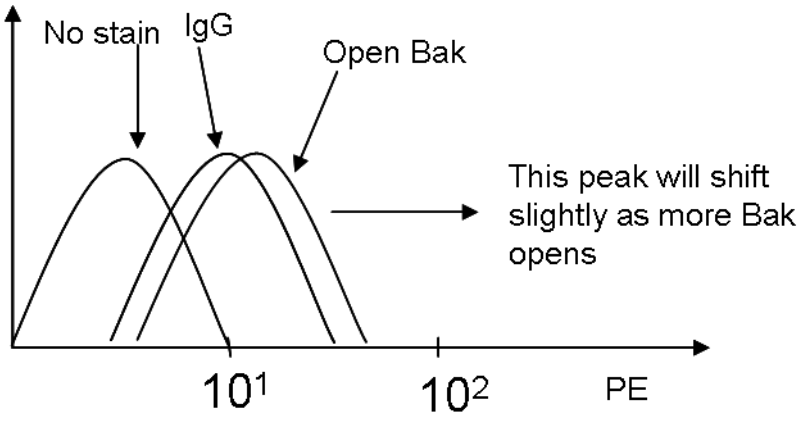

Figure 2-3 Diagrammatic representation of the FACS machine PE histogram setup for detection of increased active Bak.

2.5 Conditioned media

2.5.1 Conditioned media generation

Cells were plated at the same densities in T150 flasks. After being allowed to settle (8-24 hrs) they were rinsed with PBS and 40 ml of the appropriate growth media added. For media which will be used in protection from Fas-induced apoptosis assays on HT1080s, glutamine free media must be used. G418 was routinely added to cell cultures to maintain selection pressure and expression; however it was omitted for conditioned media generation. Upon harvesting, media was centrifuged at 1100 rpm for 10 minutes to remove cell debris ('clarified media') then stored at -20 °C. Where possible depending on the further use of the cells, cells were trypsinised and counted to give final cell numbers.

2.5.2 Cytokine arrays

Arrays spotted with specific antibodies to 174 different cytokines/growth factors/signalling molecules were purchased from Raybiotech (www.raybiotech.com). Taken from the product insert, Figure 2-4 outlines the principle of the assay.

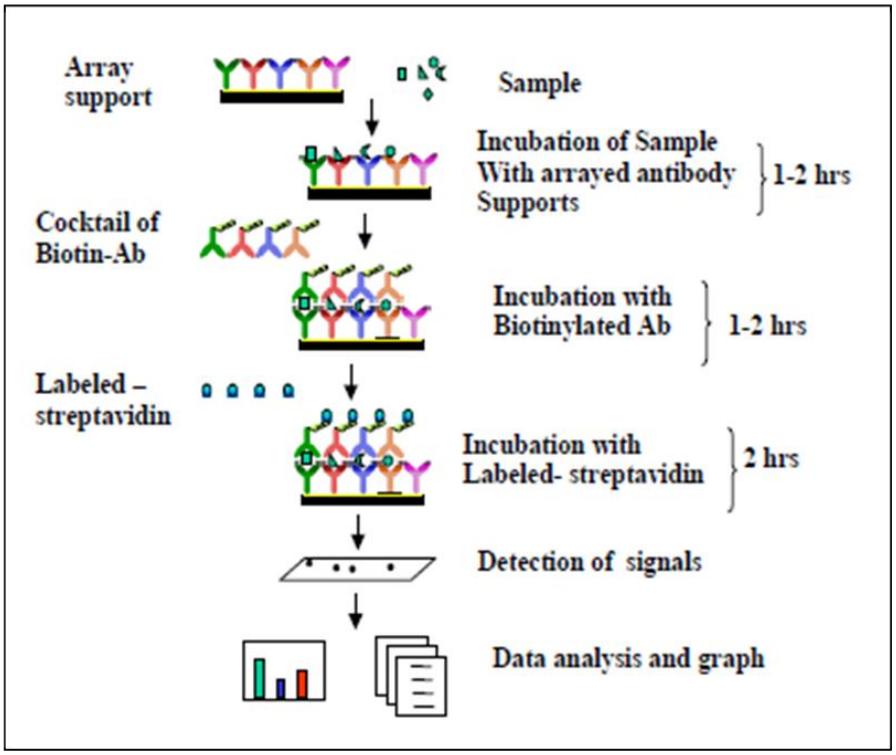

Figure 2-4 The principal of the cytokine array assay.

Arrays were placed in 8 well plates provided and blocked with the buffer provided for 30 minutes at room temperature. Media was added and incubated at 4 °C overnight with shaking. The volume of media used was normalised to account for differences in the final cell count and where necessary diluted with blocking buffer to at least 1.2 ml. Membranes were then washed, 3 x 2 ml Wash Buffer A, 2 x 2 ml Wash Buffer 2 (provided) for 5 minutes each. Primary antibody cocktails were diluted in blocking buffer and 1 ml added to each of the appropriate wells and incubated overnight, at 4 °C with shaking. After washing as before, 1 ml of the HRP-conjugated streptavidin, diluted 1 in 1000 in Blocking buffer, was added to each membrane and incubated overnight at 4 °C with shaking. After a further wash as before, 1 ml of detection reagent (1:1 detection buffers A and B) was added to each membrane and incubated at room temperature for 3 minutes. The membranes were then exposed to film for 5-120 seconds. Low exposure images were analysed with Image J software (W. Rasband, NIH) to quantify pixel density,

which was normalised according to positive and negative control spots from different parts of the array. Values were compared to results from wt cell conditioned media to allow differences in E6 expressing media to be seen.

2.6 Immunohistochemistry

2.6.1 Immunofluorescence

The immunofluorescent Bak activation assay was performed as described (Griffiths et al., 1999). Cells were seeded in EpiLife in 8 well chamber slides (Nunc) and then swapped into RM+ with 100 ng/ml IL6 or 0.1% BSA for 24 or 48 hrs, plus 4 or 6 hrs treatment time with camptothecin (CPT) (0.5 µl of 6 mM stock per well) or vehicle (DMSO). Cells were then fixed for 10 minutes in 4% PFA in PBS. Anti-Bak Ab1 (Calbiochem AM03) was incubated 1/50 in PBS with 0.05% digitonin (Calbiochem # 300411) to permeabilise the cells at 4 °C overnight. After washing the Alexafluor488 conjugated anti-mouse secondary (Molecular Probes Invitrogen #11059) was incubated 1/1000 in PBS for 30 minutes at room temperature. Slides were mounted in Fluoromount G (Southern Biotech # 0100-01) with DAPI.

2.6.2 Immunohistochemistry

Immunohistochemistry (IHC) was used to quantify and localise osteoprotegerin (OPG) and Interleukin 6 (IL6) in paraformaldehyde fixed paraffin embedded (PFPE) sections of both organotypic raft cultures and human tissue sections. 4 µm sections were cut and mounted on Superfrost Plus slides. Morphology was observed with Heamatoxylin and Eosin (H+E) staining and IHC performed with Vectastain ABC Mouse and Rabbit kits (Vector Labs, anti-rabbit # PK 4001 and anti-mouse Elite # PK 6102) according to the manufacturer's instructions.
The panel of 18 different SCC sections were characterized by the dermatology and pathology departments of the Royal London Hospital (London, UK). They were

HPV typed by degenerate nested PCR followed by sequencing (Harwood et al., 1999), except for section number 5, which was typed by the newer PM-PCR-RHA (reverse hybridization assay) method (de Koning et al., 2006). As this method is more sensitive than degenerate nested PCR, yet still returned an HPV-negative result, the difference in method is not relevant in this case.

H+E staining was carried out according to a standard protocol, in which sections are firstly dewaxed and hydrated through a series of xylene and alcohols: xylene 5 minutes, xylene 3 minutes, 100% IMS (Industrial methylated spirits) 3 minutes, 100% IMS 3 minutes, 90% IMS 3 minutes, 70% IMS 3 minutes. After a 5 minute rinse in water, sections are stained in Gil's No 3 Heamatoxylin for 5 minutes. The excess is removed with a 5 minute tap water rinse and differentiation is achieved by 2-6 short dips in acid alcohol (99 ml 70% IMS 1 ml conc. HCl). Sections are incubated 5-8 minutes in the mildly alkali Scott's tap water (3.5 g Sodium bicarbonate, 20 g Magnesium sulphate, 1 L water) until the nuclei are blue, then stained in Eosin Y (acidified with 0.5 ml glacial Acetic acid per 100 ml stain) for 1 minute. After a 5 minute water wash, sections are dehydrated through the alcohol/xylene series: 70% IMS 2 minutes, 90% IMS 2 minutes, 100% IMS 2 minutes, 100% IMS 2 minutes, xylene 2 minutes, xylene 2 minutes. Slides are mounted straight from xylene in a thin layer of Depex or Vectamount on a coverslip, pressing out any bubbles, and left to set overnight.

For IL6 and OPG staining, no antigen retrieval was used. The sections are dewaxed and hydrated through xylene and graded alcohols as before. After a water rinse the tissue is surrounded with an ImmEdge pen to contain the solutions – sections of tissue are partitioned as negative controls. Sections are blocked by incubation with the horse serum solution provided for 30 minutes at room temperature, after which the primary antibody is incubated 1/400 in blocking serum, at 4 °C overnight in a sealed humidified chamber. Negative sections are incubated with serum alone. The antibodies used were: mouse monoclonal to human OPG,

Imgenex IMG-103A; rabbit polyclonal to IL6, Abcam ab6672. All further incubations are at room temperature. After a 5 minute PBS wash, endogenous peroxidise activity is quenched with a 30 minute incubation with 0.3% hydrogen peroxide in water. After a further 5 minute PBS wash, the biotinylated secondary is incubated for 30 minutes. After 3 x 5 minute PBS washes, the ABC reagent is incubated for 30 minutes, followed by a 5 minute PBS wash. Each section is then incubated separately for 30 seconds in DAB reagent (Vector Laboratories # SK4100) to achieve brown staining. Sections are counterstained with haematoxylin for 5 minutes, differentiated, cleared and mounted as described previously for H+E staining.

An Axioskop 2 Plus microscope (Zeiss) with Axiovision software was used to save images. Staining was quantified according to positivity, intensity and localisation. The keratinocyte portions of the tumours were assigned scores for nuclear staining and cytoplasmic staining, however it was observed that for both OPG and IL6 there was very little nuclear staining, so the cytoplasmic staining only was used in the final scores. The percentage of cells in at least 3 fields of view for each SCC were recorded as negative, weak, moderate, and strong, for which the scores 0-4 were assigned. The overall score = percentage x intensity.

2.7 Statistics

Significance was calculated with two-tailed T Tests in most cases, except for the results of the IHC SCC panel, where a one-way ANOVA was used. In all cases significance was taken to be 5%, P= 0.05.

3 Expression of intracellular anti-apoptotic factors in cells expressing cutaneous Human Papillomaviruses E6 protein

3.1 Introduction

Squamous cell carcinoma (SCC) is a common cancer occurring at sun-exposed body sites of fair-skinned people. Ultraviolet (UV) radiation is the main aetiological agent of SCC for several reasons (Hussein, 2005). Primarily it induces damage to cellular DNA and cytotoxic reactive oxygen species (ROS), both of which can lead to apoptosis if the damage is irreparable. Apoptosis in keratinocytes is an essential process as persistence of mutant cells may lead to tumourigenesis.

Evidence for a link between infection with a subset of high-risk cutaneous HPVs (termed β-HPVs) and SCC development includes the examples of EV patients and immunosuppressed transplant recipients, along with several epidemiological studies (Akgul et al., 2006a). The high-risk members of the α-HPVs have a clear role in the formation of cervical cancer, by mechanisms including the degradation of p53 by the HPV E6 protein, which leads to the inhibition of apoptosis. Although β-HPVs do not target p53 for degradation, it has previously been shown that expression of E6 from several cutaneous HPVs (β type 5 along with the α-types 10 and 77) reduces apoptosis in both p53-null and wt p53 cell lines in response to UV (Jackson and Storey, 2000). The expression of these E6 types in the HT1080 cell line prevented the post-UV accumulation of the apoptotic regulator protein Bak by targeting it for degradation (Jackson et al., 2000). Bak is a key protein in the mitochondrial pathway, forming pores in the outer mitochondrial membrane upon activation leading to release of apoptotic factors such as cytochrome c (CytC), apoptosis inducing factor (AIF) and HtrA2/Omi. Further work also showed that

expression of HPV5 and 18E6 decreased UV-induced mitochondrial morphological changes and release of AIF, CytC and HtrA2/Omi in HT1080 cells (Leverrier et al., 2007). The anti-apoptotic activity of various E6 proteins has also been tested in human keratinocytes, the natural host cell of HPVs. This work also showed that expression of HPV8E6 in keratinocytes used to generate organotypic raft cultures also prevented the relocation of AIF post UV. Other studies have also shown the reduction of apoptosis, and a decrease in CytC release, in HT1080 cells expressing HPV types 5, 8, 38 and 16E6. Expression of E6 from HPV types 16, 8 and 38 also reduced CytC release in primary keratinocytes (Underbrink et al., 2008). Post UV Bak accumulation was also tested in keratinocytes, and found to be reduced or prevented in cells expressing HPV types 5, 8, 16, 20, 22, 38, 76, 92 and 96E6. Similarly further work showed that expression of E6 (along with E7) from HPV types 5, 8, 15 and 20 reduced apoptosis to different extents (Struijk et al., 2008). HPV types 5 and 38 E6/E7 also reduced baseline Bak expression, but there was no reduction in post-UV Bak accumulation observed. Therefore, although the targeting of Bak for degradation by E6 is important in protection of cells from UV-induced apoptosis, it is not the only factor involved in the protection of cells by cutaneous HPV E6. This is indicated not only by slight inconsistencies in the above mentioned works, which could also be due to differences in cell (particularly keratinocyte) culture methods, but also by several reports of other anti-apoptotic activities. For example it was shown that HPV77E6 inhibits the post-UV p53-dependant transcription of pro-apoptotic genes such as *PIG3, Fas, PUMAβ* and *Apaf1* (Giampieri et al., 2004). In has also been noted that mutants of HPV5E6 that have lost the ability to target Bak for degradation still protect cells from UV-apoptosis to different extents (Simmonds and Storey, 2008). It is known that the E6 protein has many cellular binding partners, which vary between HPV types, and could therefore affect many cellular processes. As has been noted, the inhibition of UV induced apoptosis in the skin could lead to accumulation of mutant cells and

therefore tumourigenesis, and it is therefore of interest to delineate the anti-apoptotic effects of cutaneous HPV E6 expression.

3.1.1 Aims

It has previously been shown that expression of the E6 protein from several cutaneous HPV types reduces apoptosis in cell lines in response to UV irradiation and triggering of the death receptor pathway by activation of Fas. As outlined above, this is partially mediated by inhibition of the apoptotic activity of Bak. The aims of these experiments was to investigate changes in other cellular apoptotic pathways; different from Bak activation, or that may co-operate with Bak inhibition, for example by up-regulation of anti-apoptotic proteins. Dissection of the apoptotic pathways involved and therefore the mechanisms employed by cutaneous HPVE6 to inhibit host cell apoptosis would be relevant to studies on SCC formation.

3.2 Results

3.2.1 Expression of HPV E6 proteins

The human fibrosarcoma cell line, HT1080 (Rasheed et al., 1974) were chosen as they are a well-characterised system that have previously been used in work on HPVE6 inhibition of apoptosis (Jackson et al., 2000) and they express wt p53 protein. Primary human keratinocytes were obtained from several sources. Skin samples donated by cosmetic surgery patients were processed by previous lab members and the isolated keratinocytes, called PA8 and PA10, used in initial studies. However the majority of the work was performed with keratinocytes purchased from Cascade Biologics, from two donors.

HT1080 cells stably expressing the E6 protein from different HPV types were created with plasmids previously generated in the lab – pcDNA (empty vector), pcDNA 5E6 HA tag, pcDNA 5E6, pcDNA 8E6, pcDNA 10E6, pcDNA 18E6, pcDNA 77E6, pcDNA EGFP (enhanced green fluorescent protein), pIRES (empty vector),

and pIRES 5E6. HT1080 cells were grown until 40-50% confluent and then transfected with 2 μg plasmid DNA with a 3:1 ratio of Fugene. G418 selection at 350 μg/ml was subsequently added until negative control non-transfected cells were all dead to achieve stable expression of E6. These HPV types were chosen to be representative of cutaneous HPVs, as it has been shown that the β-types 5 and 8 are associated with SCC in EV patients, type 77 is a cutaneous α-type associated with SCC in transplant recipients; whereas type 10 is a cutaneous α-type usually associated with benign lesions but also found in SCC from transplant recipients, and type 18 is a high-risk anogenital α-type included for comparison. Primary keratinocytes do not respond well to transfection so were made to stably express HPV types 5 and 8E6 using a retroviral infection protocol, in which they were infected with replication-incompetent pLXSN retroviruses containing HPV5 and 8E6 and a drug selection marker. Cells were cultured with 150 μg/ml G418 until negative control cells were all dead, and then used within 6 passages. Figure 3-1 shows the confirmation of E6 expression in the cells used throughout this work. There are no antibodies available against HPV5E6 so expression was initially confirmed by PCR. RNA was extracted from HT1080 cells transfected with different plasmids and used in reverse transcription to make cDNA as described in Materials & Methods, sections 2.2.1 and 2.2.2. Reverse transcription can be performed with random or oligo primers, cDNA made with both methods were then used as templates in PCR alongside a positive control pcDNA5E6 plasmid and negative control untransfected cell cDNA, and the products resolved on an agarose gel. Figure 3-1 A shows bands corresponding to HPV5E6 in the cDNA made with both reverse transcription primers in the transfected cell types. The pIRES HPV5E6 vector was used alongside the pcDNA vector series as it had been shown to give a higher level of expression, and a difference in E6 protein expression level could affect the results. Figure 3-1 B shows PCR products corresponding to the expression of the other HPV E6 types used along with the relevant positive control

plasmids. The two bands seen in HPV18E6 most likely correspond to the splice variants of HPV18E6 (Czegledy et al., 1994; Schneider-Gadicke and Schwarz, 1986). Figure 3-1 C shows an agarose gel of representative products of real-time PCR in which primers for HPV5E6 were included to test for HPV5E6 expression in the retrovirally infected keratinocytes used along with the HT1080s. Figure 3-1 D shows the expression of HA-tagged HPV5E6 in HT1080s which were made and tested at the beginning of this work. A faint band of the appropriate size corresponding to HPV5E6 expression can be seen in the HPV5E6 lysate lane, agreeing with the expected low level of HPV5E6 expression. However, it is suspected from previous unpublished observations in the lab that the presence of an HA tag interferes with the binding of HPV5E6 to cellular proteins, so it was decided to continue with the untagged version, with expression confirmed by PCR.

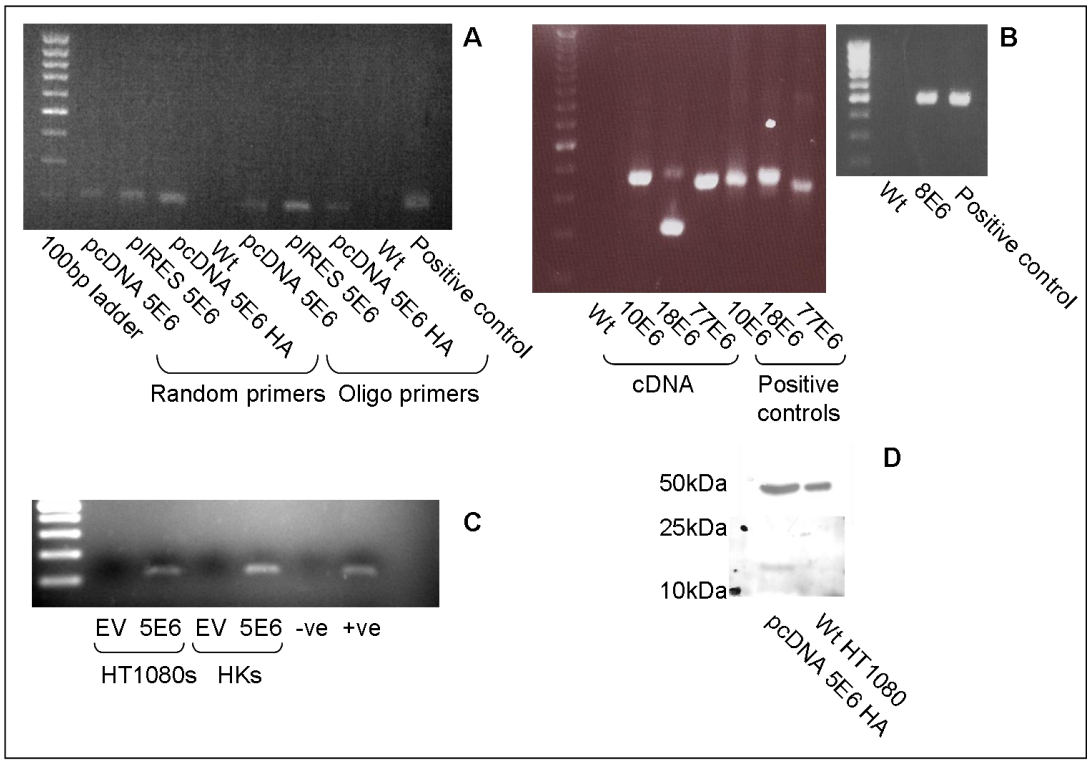

Figure 3-1 Confirmation of E6 expression.

A cDNA made from the indicated cell types with either random or oligo primers were used as templates along with a positive control expression plasmid to detect HPV5E6 expression, seen as a band at 200 bp.

B cDNA from the indicated cell types was used in PCRs along with the corresponding expression plasmids as positive controls to detect E6 expression, seen as bands of around 350bp.

C The products of real-time PCR were run on an agarose gel to show expression of HPV5E6 in the indicated cell types; HK – human keratinocytes, EV – empty vector cells (pcDNA in HT1080s, pLXSN in keratinocytes), positive control is the pcDNAHPV5E6 expression plasmid, negative control contained the negative cDNA control as a template.

D Western blot showing a band at approximately 18 kDa corresponding to HA tagged HPV5E6 expressed at low levels in transfected HT1080s, with α tubulin at 50 kDa as a loading control.

3.2.2 Changes in apoptosis-related proteins in HT1080s caused by HPV5E6 expression and UV irradiation

To identify the factors that may be involved in the protection of cells expressing HPV5E6 from apoptosis, Proteome Profiler apoptotic protein arrays were used as instructed by the manufacturer and described in Materials and Methods, section 2.3.4. HT1080s expressing HPV5E6 or empty vector pcDNA were induced with 0 or 5 mJ/cm^2 UV, and harvested 16 hrs later with the lysis buffer supplied. Lysates were quantified and 500 μg of total protein of each sample loaded onto blocked arrays. After incubation at 4 °C overnight, membranes were washed, incubated with detection antibody cocktail, washed, incubated with streptavidin conjugates, washed, developed and exposed to film. Figure 3-2 A shows the 1 minute exposure which was used with the software as described in Materials and Methods to calculate the relative protein levels. As an example of the changes in protein levels, the highlighted boxes indicate phospho-p53(S392) which is upregulated in pcDNA empty vector cells post 5 mJ/cm^2 UV. The software allows detailed comparison of the relative protein levels.

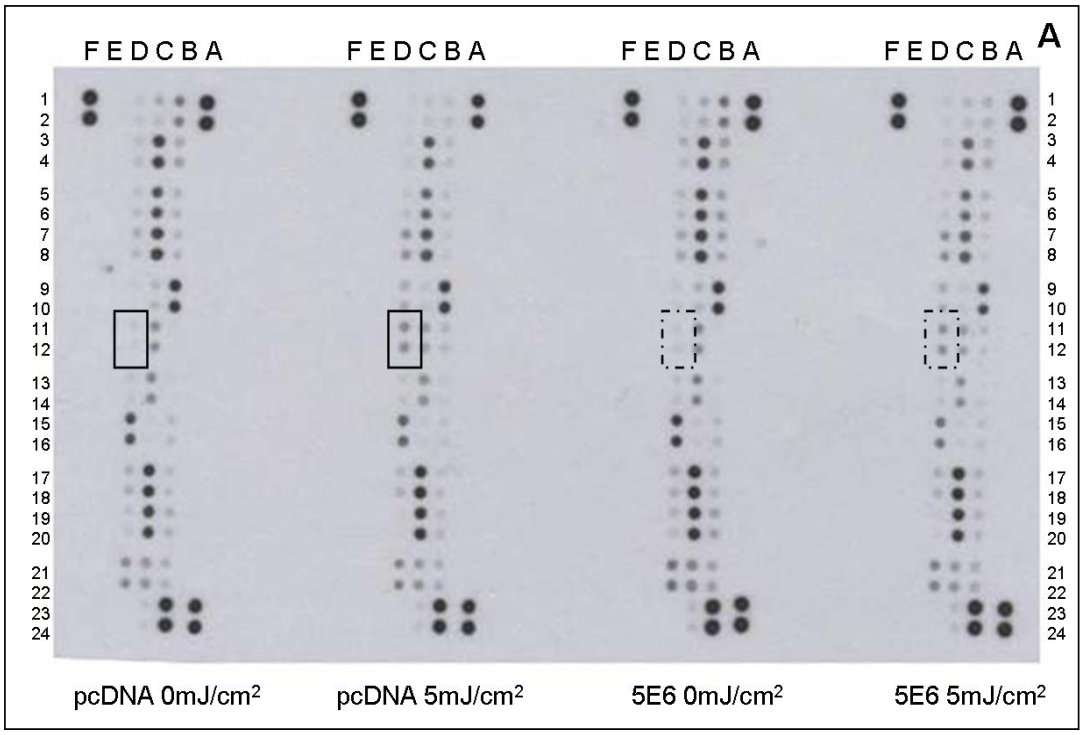

Figure 3-2 Changes in apoptotic proteins in HPV5E6 expressing HT1080s measured by Proteome Profiler arrays.

A The 1 minute exposure to film was used with the software to calculate the relative protein levels. For a complete map of the array see Appendix 1. As an example the boxes indicate the upregulation of phospho-p53(S392) in pcDNA 5 mJ/cm^2 cells compared to untreated cells, with the same change in 5E6 cells shown by dashed boxes.

B Relative levels of apoptotic proteins in pcDNA empty vector cells and HPV5E6 expressing cells 16 hrs post 0 or 5 mJ/cm^2 UV.

C Changes in the levels of apoptotic proteins in HT1080s 16 hrs after exposure to 5 mJ/cm^2 UV.

D Changes in the levels of apoptotic proteins compared to pcDNA 0 mJ/cm^2 UV.

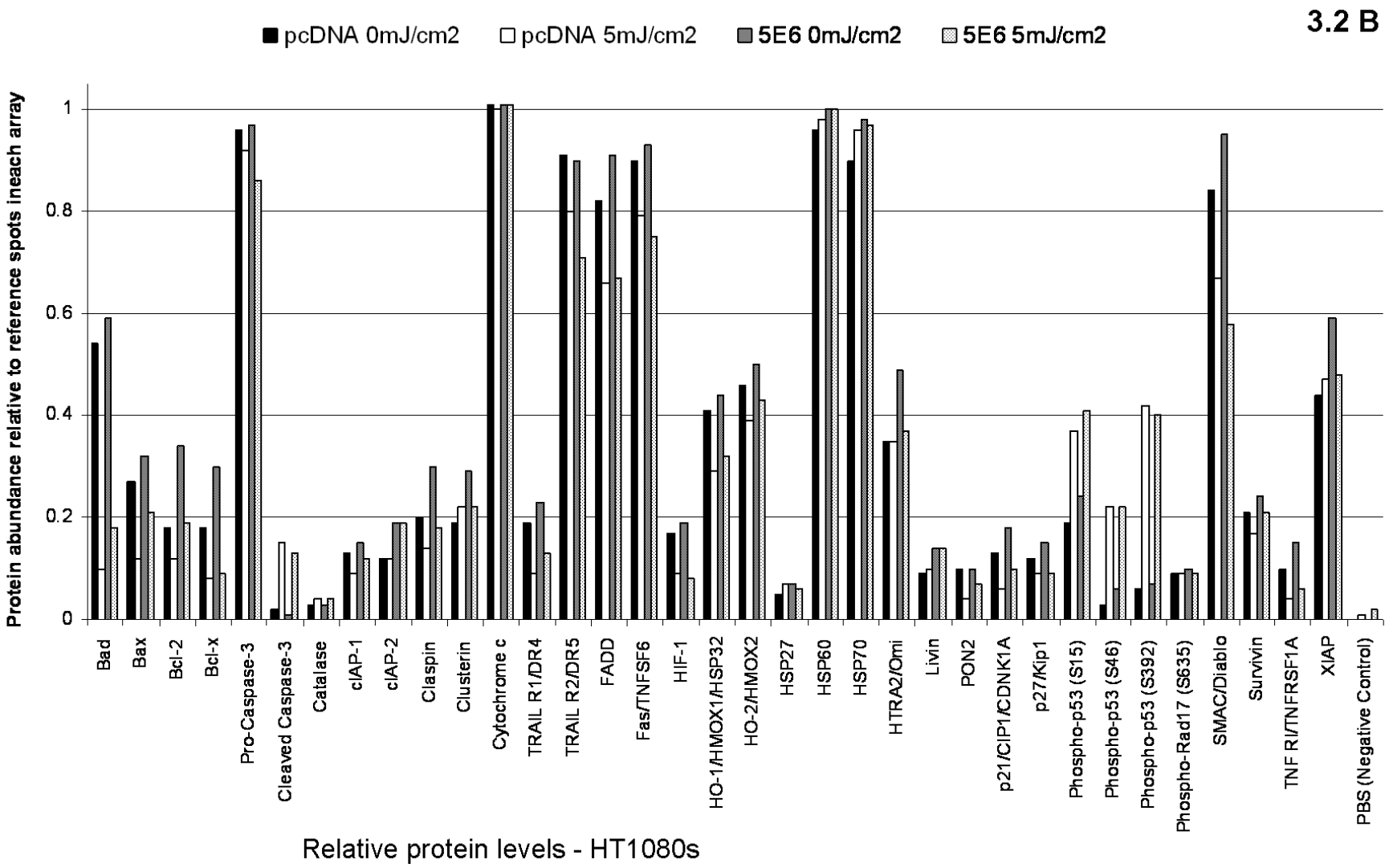
3.2 B
pcDNA 0mJ/cm2
pcDNA 5mJ/cm2
5E6 0mJ/cm2
5E6 5mJ/cm2
Protein abundance relative to reference spots ineach array
0
0.2
0.4
0.6
0.8
1
Bad
Bax
Bcl-2
Bcl-x
Pro-Caspase-3
Cleaved Caspase-3
Catalase
cIAP-1
cIAP-2
Claspin
Clusterin
Cytochrome c
TRAIL R1/DR4
TRAIL R2/DR5
FADD
Fas/TNFSF6
HIF-1
HO-1/HMOX1/HSP32
HO-2/HMOX2
HSP27
HSP60
HSP70
HTRA2/Omi
Livin
PON2
p21/CIP1/CDNK1A
p27/Kip1
Phospho-p53 (S15)
Phospho-p53 (S46)
Phospho-p53 (S392)
Phospho-Rad17 (S635)
SMAC/Diablo
Survivin
TNF RI/TNFRSF1A
XIAP
PBS (Negative Control)
Relative protein levels - HT1080s

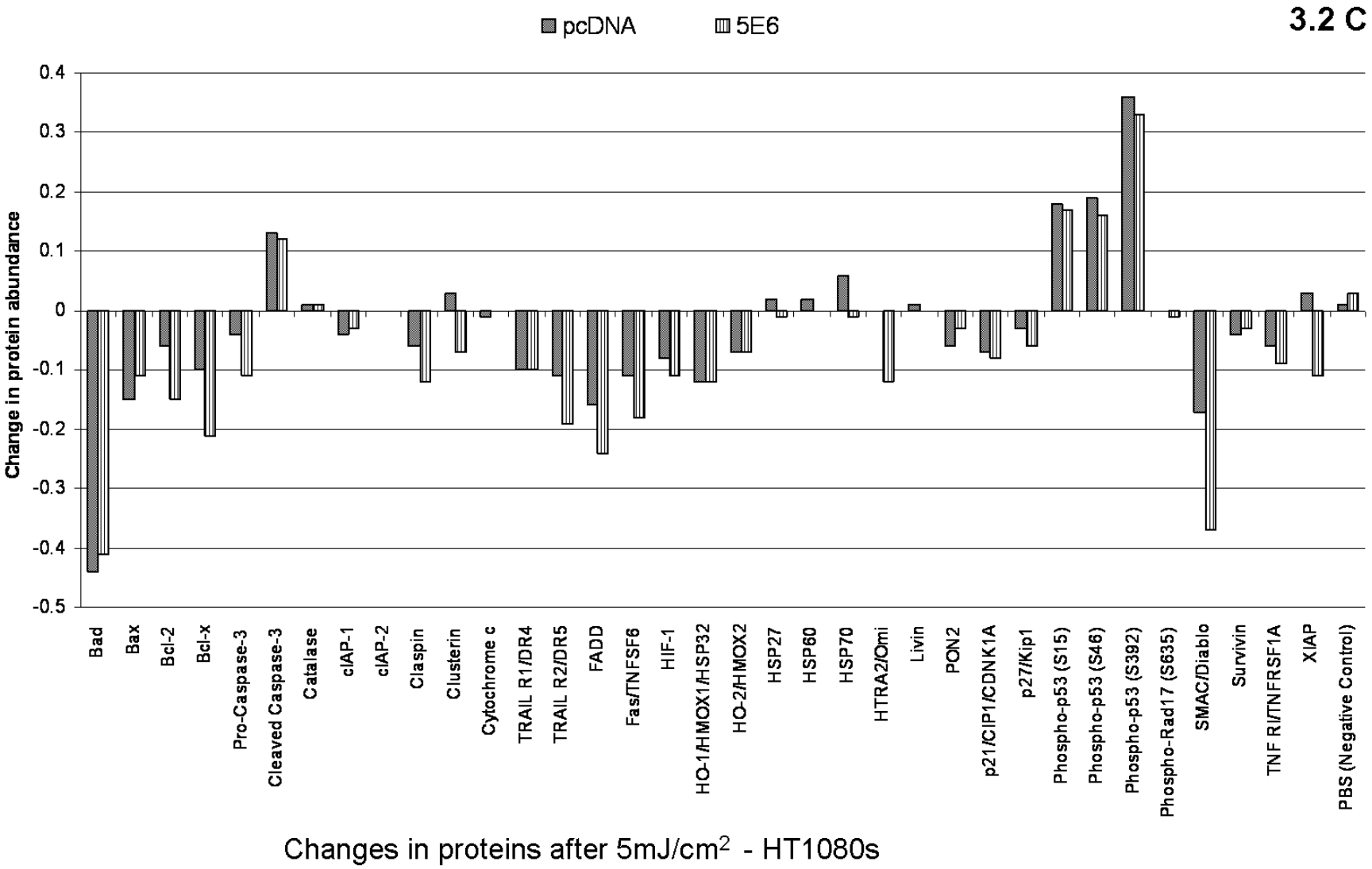

Changes in proteins after 5mJ/cm^2 - HT1080s

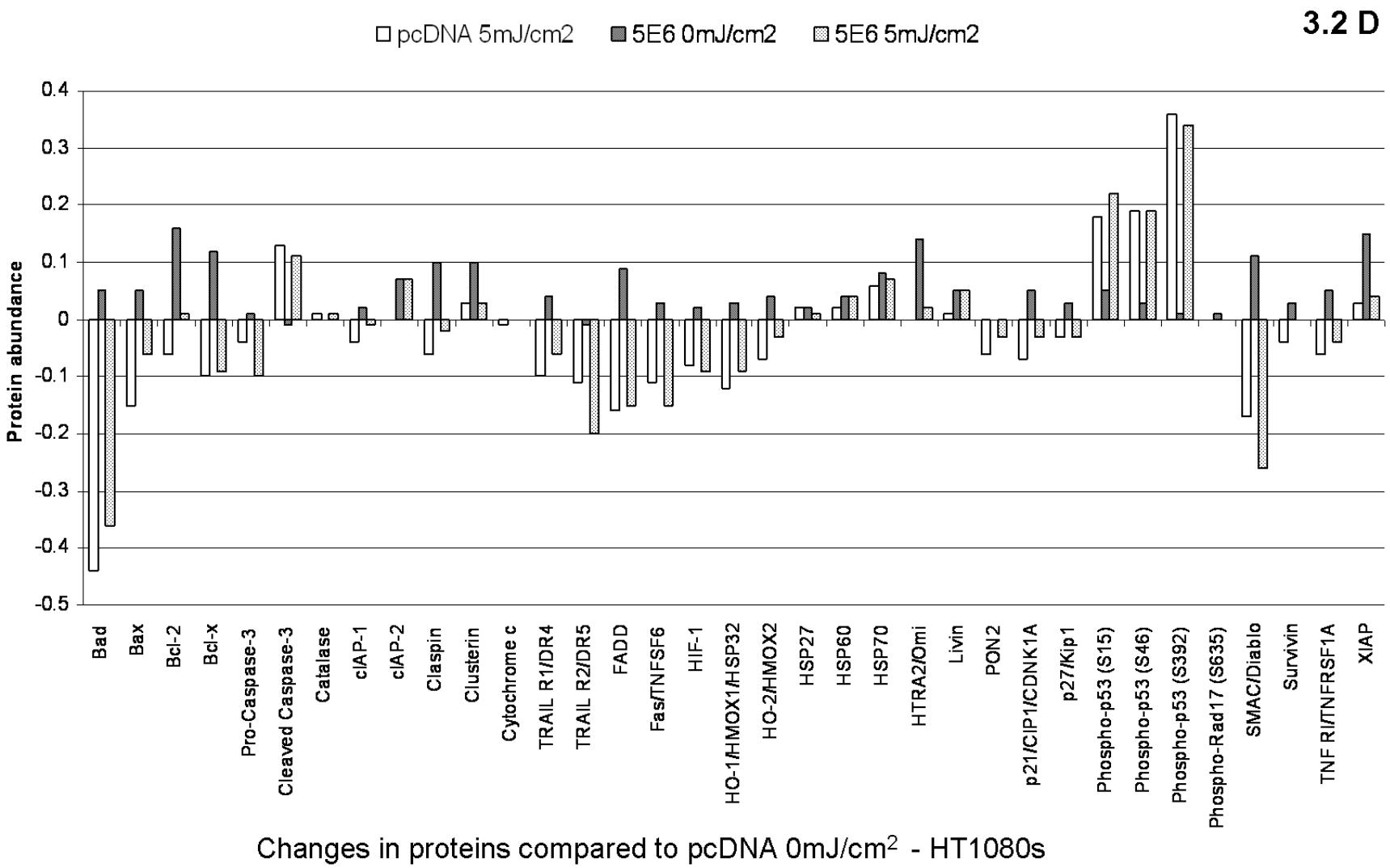
3.2 D
pcDNA 5mJ/cm2
5E6 0mJ/cm2
5E6 5mJ/cm2
Protein abundance
0.4
0.3
0.2
0.1
0
-0.1
-0.2
-0.3
-0.4
-0.5
Bad
Bax
Bcl-2
Bcl-x
Pro-Caspase-3
Cleaved Caspase-3
Catalase
cIAP-1
cIAP-2
Claspin
Clusterin
Cytochrome c
TRAIL R1/DR4
TRAIL R2/DR5
FADD
Fas/TNFSF6
HIF-1
HO-1/HMOX1/HSP32
HO-2/HMOX2
HSP27
HSP60
HSP70
HTRA2/Omi
Livin
PON2
p21/CIP1/CDNK1A
p27/Kip1
Phospho-p53 (S15)
Phospho-p53 (S46)
Phospho-p53 (S392)
Phospho-Rad17 (S635)
SMAC/Diablo
Survivin
TNF RI/TNFRSF1A
XIAP
Changes in proteins compared to pcDNA 0mJ/cm2 - HT1080s

Firstly a comparison of all the arrays is shown in Figure 3-2 B. This allows differences in baseline expression of apoptotic protein levels between empty vector pcDNA and HPV5E6 expressing cells to be seen. The following proteins are upregulated (by at least 1.5 fold) in HPV5E6 cells: Bcl2, Bcl-x, cIAP2, claspin, clusterin, livin, phospho-p53 (S46), and TNFR1. Only cleaved caspase 3 is downregulated (by 0.5 fold) in untreated HPV5E6 cells. The total protein levels shown in Figure 3-2 B should be considered along with the fold changes, for example in the case of phospho-p53 (S46), an apoptotic modification of p53, which is on the above list of HPV5E6 upregulated 'baseline' proteins. However it can be seen that the relative protein level is very low in untreated cells compared to apoptotic cells, as would be expected, indicating that the HPV5E6 'upregulation' at baseline is not significant. Apart from TNFR1, the main receptor of tumour necrosis factor α (TNF) which can initiate both survival and apoptotic messages, the rest of the proteins upregulated by HPV5E6 prior to UV treatment have anti-apoptotic activity.

Figure 3-2 B also allows general patterns of regulation upon UV to be seen. In both cell types, the following proteins are downregulated to different degrees after 5 mJ/cm^2 UV: Bad, Bax, Bcl2, Bcl-x, procaspase 3, DR4, DR5, FADD, Fas, HO, and SMAC/DIABLO. Conversely cleaved caspase 3 and Phospho-p53 (S15, S46 and S392) are upregulated in both cell types after UV, which is as expected, as cleaved caspase 3 is a well-known marker of apoptosis, and the phosphorylation of p53 is important for the stabilization and subsequent activity of p53 upon damage to the cell. However a significant reduction of cleaved caspase 3 in the lysates of HT1080 cells expressing HPV5E6 is not observed, which could be expected if HPV5E6 protected cells from apoptosis.

To clarify the results, the changes in apoptotic proteins upon UV irradiation in each cell type were calculated by subtracting the 0 mJ/cm^2 value from the 5 mJ/cm^2 value, and the results shown in Figure 3-2 C. In summary, this appears to show

greater downregulation in HPV5E6 cells after UV of: Bcl2, Bcl-x, procaspase 3, claspin, clusterin, DR5, FADD, Fas, HSP70, HTRA2/Omi, SMAC/DIABLO and XIAP. However when considering the actual protein levels, none are significantly different between pcDNA and HPV5E6 cells. This agrees with the result showing no difference between the amounts of cleaved caspase 3 in pcDNA or HPV5E6 cells. There is a decrease after UV in both cell types of Bad, Bax, Bcl2, Bcl-x, DR4, DR5, FADD, Fas, HO1 and SMAC/DIABLO. None of the proteins measured are more upregulated after UV in HPV5E6 than pcDNA cells.

For further clarification of the changes in apoptotic proteins, the levels were compared to the levels in non-irradiated pcDNA cells, to normalise for the differences in baseline expression. This is shown in Figure 3-2 D, and provides further elucidation of the results. For example the upregulation of Bcl-2 in HPV5E6 0 mJ/cm^2 cells is more apparent; and although it appears in Figure 3-2 C that Bcl-x is more downregulated post-UV in HPV5E6 cells than pcDNA cells, Figure 3-2 D shows approximately the same amount is present in pcDNA and HPV5E6 expressing cells post UV; the difference in Figure 3-2 C is due to the baseline upregulation in non-UV treated HPV5E6 expressing cells.

Figure 3-3 E shows a list of the proteins upregulated in HPV5E6 expressing HT1080s along with HPV5E6 expressing primary keratinocytes and is discussed presently. A full list of the fold changes of all the proteins on the arrays can also be found in Appendix 2.

3.2.3 Changes in apoptosis-related proteins in primary keratinocytes caused by HPV5E6 expression and UV irradiation

As outlined previously, primary keratinocytes are the natural host cell of HPV and their apoptotic response to UV irradiation is an important factor in SCC formation. Therefore Proteome Profiler apoptotic protein arrays were also used to identify changes in HPV5E6 or empty vector pLXSN primary keratinocytes at baseline and after UV irradiation. Keratinocytes were seeded in EpiLife, and transferred into RM+ medium for 48hrs to allow cell differentiation to begin, treated with 0 or 30mJ/cm^2 UV and harvested 16hrs later in the lysis buffer provided. Membranes were probed according to the manufacturer's instructions, as described previously. Figure 3-3 A shows the 1 minute exposure which was used with the software described to calculate relative protein levels. As an illustration the boxes highlight the upregulation of Bcl-x in HPV5E6 expressing cells compared to pLXSN empty vector cells. As stated before the software allows detailed analysis of the changes in apoptotic proteins. Figure 3-3 B shows a comparison of all the arrays. The 0mJ/cm^2 cells allow comparison of the 'baseline' levels of apoptotic proteins, with HPV5E6 expressing cells showing upregulation (by at least 1.5 fold) of the following: Bax, Bcl2, Bcl-x, cleaved caspase 3, cIAP1, cIAP2, claspin, clusterin, DR4, DR5, FADD, Fas, HIF, HO1, HO2, HSP 70, HTRA2/Omi, PON2, p27, phospho-p53 (S46 and S392), phospho-rad17 (S635), SMAC/DIABLO, survivin, TNFR1 and XIAP. There are no proteins downregulated by HPV5E6 expression on the array. A complete map of the array is shown in Appendix 1.

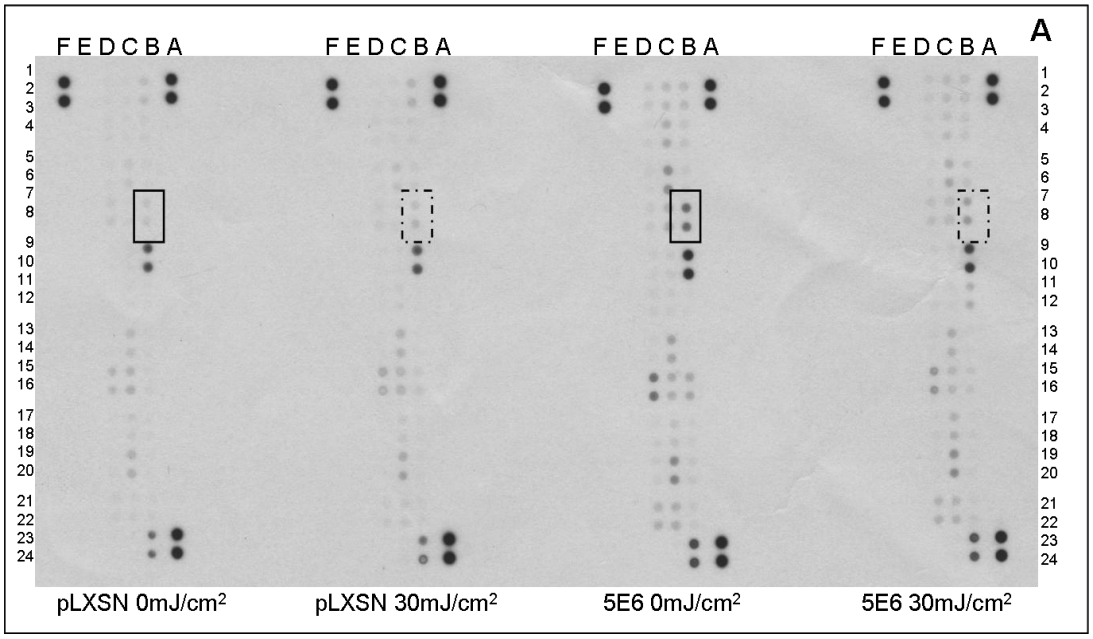

Figure 3-3 Changes in apoptotic proteins in HPV5E6 expressing primary keratinocytes measured by Proteome Profiler arrays.

A The 1 minute exposure to film was used with the software to calculate the relative protein levels. As an example the boxes indicate the upregulation of Bcl-x in HPV5E6 expressing cells compared to empty vector pLXSN cells, with dashed boxes indicating Bcl-x in UV treated samples.

B Relative levels of apoptotic proteins in pLXSN cells and HPV5E6 expressing cells 16 hrs post 0 or 30 mJ/cm^2 UV.

C Changes in the levels of apoptotic proteins in primary keratinocytes 16 hrs after exposure to 30 mJ/cm^2 UV.

D Changes in the levels of apoptotic proteins compared to pLXSN cells at 0 mJ/cm^2 UV.

E Table summarising the fold changes of apoptosis related proteins in non-UV irradiated HPV5E6 expressing cells compared to the relative empty vector cells, pcDNA or pLXSN in HT1080s or primary keratinocytes.

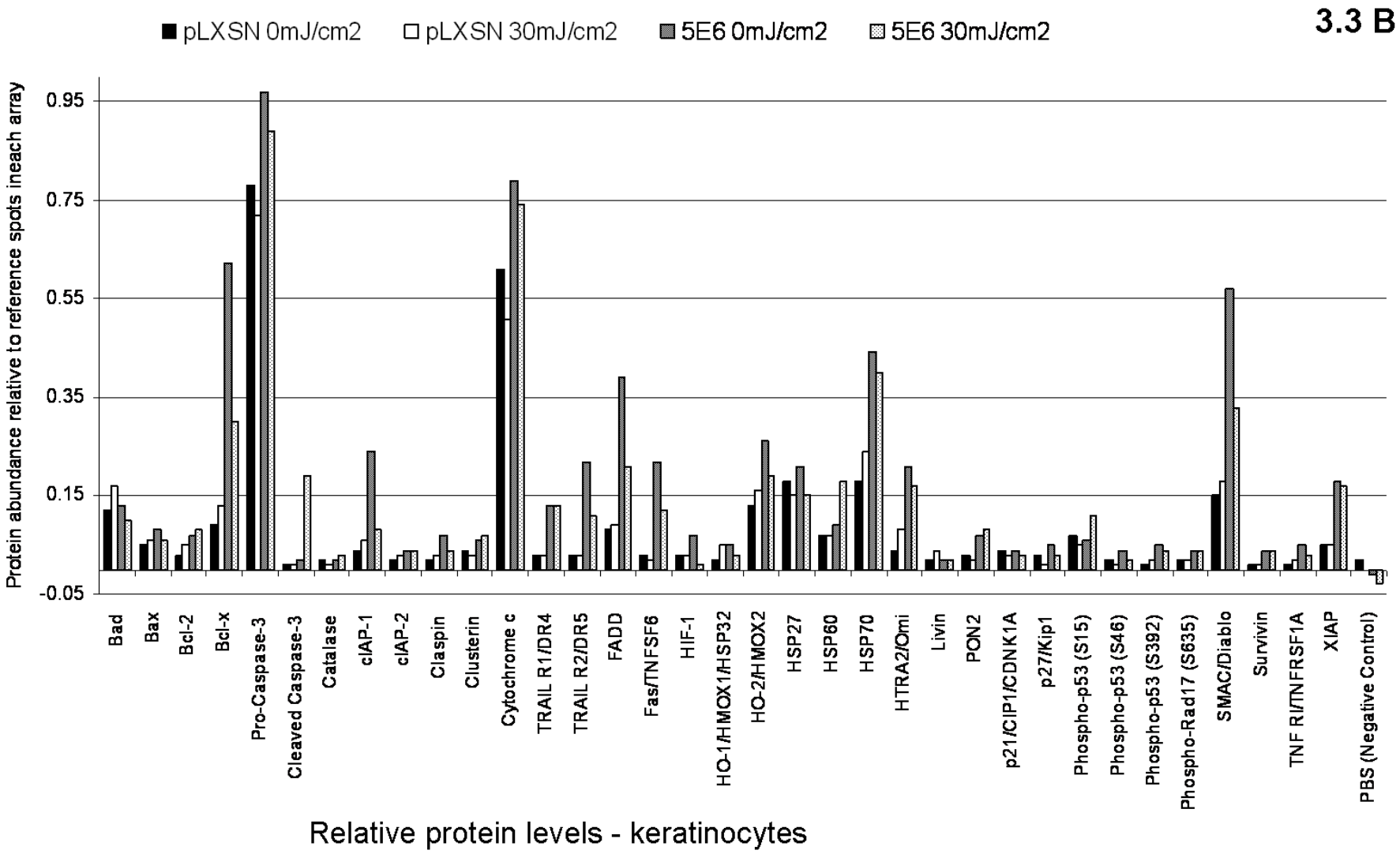
3.3 B
pLXSN 0mJ/cm2
pLXSN 30mJ/cm2
5E6 0mJ/cm2
5E6 30mJ/cm2
Protein abundance relative to reference spots ineach array
0.95
0.75
0.55
0.35
0.15
-0.05
Bad
Bax
Bcl-2
Bcl-x
Pro-Caspase-3
Cleaved Caspase-3
Catalase
cIAP-1
cIAP-2
Claspin
Clusterin
Cytochrome c
TRAIL R1/DR4
TRAIL R2/DR5
FADD
Fas/TNFSF6
HIF-1
HO-1/HMOX1/HSP32
HO-2/HMOX2
HSP27
HSP60
HSP70
HTRA2/Omi
Livin
PON2
p21/CIP1/CDNK1A
p27/Kip1
Phospho-p53 (S15)
Phospho-p53 (S46)
Phospho-p53 (S392)
Phospho-Rad17 (S635)
SMAC/Diablo
Survivin
TNF RI/TNFRSF1A
XIAP
PBS (Negative Control)
Relative protein levels - keratinocytes

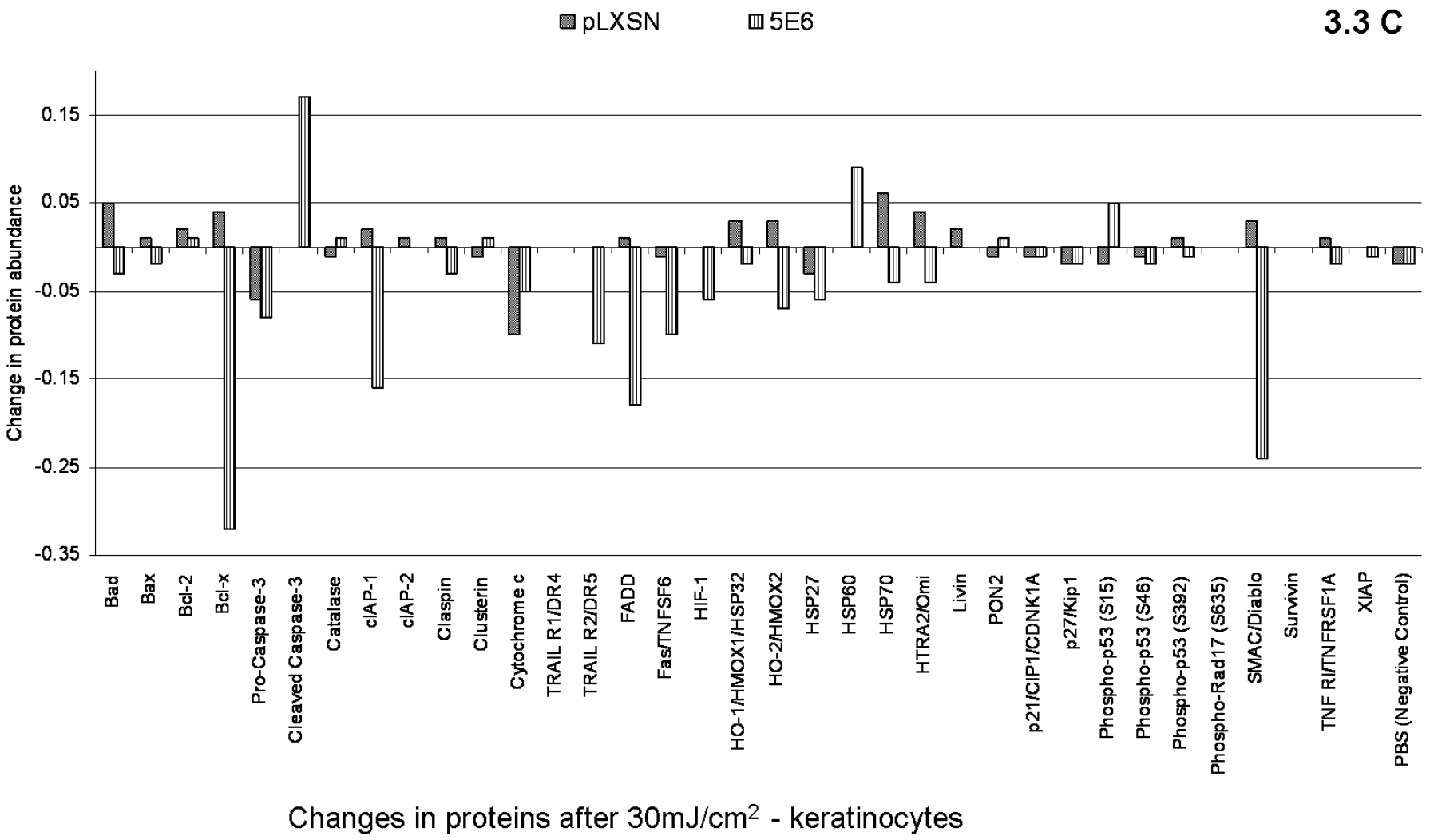

Changes in proteins after 30mJ/cm^2 - keratinocytes

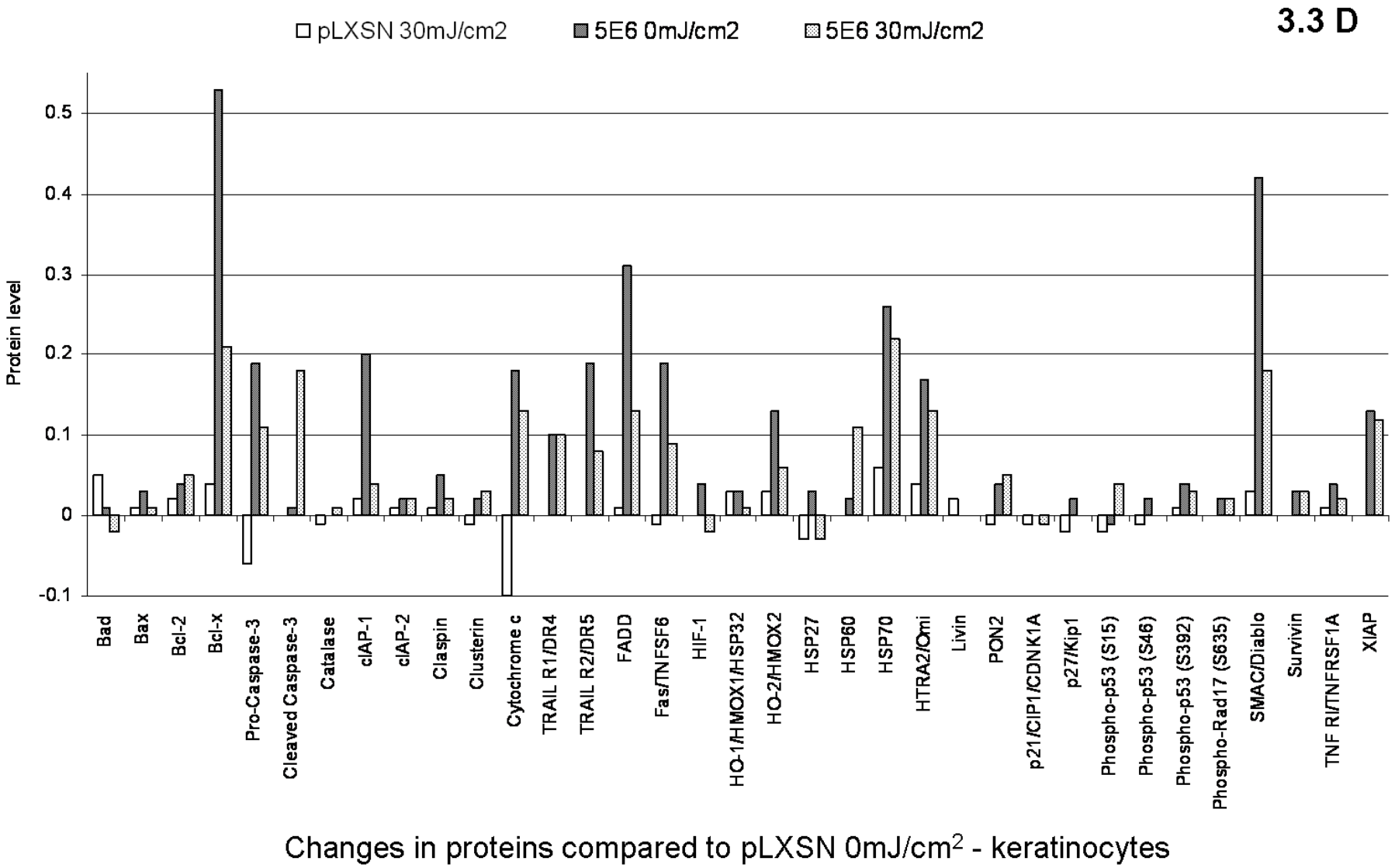

Changes in proteins compared to pLXSN 0mJ/cm^2 - keratinocytes

E

HT1080s		Keratinocytes	
Protein	Upregulation	Protein	Upregulation
		Bax	1.60
Bcl-2	1.89	Bcl-2	2.33
Bcl-x	1.67	Bcl-x	6.89
		Cleaved Caspase-3	2.00
		cIAP-1	6.00
cIAP-2	1.58	cIAP-2	2.00
Claspin	1.50	Claspin	3.50
Clusterin	1.53	Clusterin	1.50
		TRAIL R1/DR4	4.33
		TRAIL R2/DR5	7.33
		FADD	4.88
		Fas/TNFSF6	7.33
		HIF-1	2.33
		HO-1/HMOX1/HSP32	2.50
		HO-2/HMOX2	2.00
		HSP70	2.44
		HTRA2/Omi	5.25
Livin	1.56		
		PON2	2.33
		p27/Kip1	1.67
Phospho-p53 (S46)	2.00	Phospho-p53 (S46)	2.00
		Phospho-p53 (S392)	5.00
		Phospho-Rad17 (S635)	2.00
		SMAC/Diablo	3.80
		Survivin	4.00
TNF R1/TNFRSF1A	1.50	TNF RI/TNFRSF1A	5.00
		XIAP	3.60

Summary table of the fold changes of apoptosis related proteins in non-UV irradiated HPV5E6 expressing cells compared to the relative empty vector cells, pcDNA or pLXSN in HT1080s or primary keratinocytes. Apoptotic proteins are indicated in red, anti-apoptotic in blue, and those receptors which can mediate apoptotic or survival signalling in purple. For additional information on the role of some of these proteins please refer to the Overview of apoptotic pathways, Figure 1-3.

Figure 3-3 B also allows the effect of UV to be seen. In contrast to HT1080s, the proteins downregulated upon UV in both cell types include only procaspase 3, cytochrome c (CytC) and HSP27. Figure 3-3 C illustrates the changes in apoptotic proteins upon UV irradiation in each cell type which were calculated as before, and shows greater downregulation post UV in HPV5E6 cells compared to pLXSN cells of: Bcl-x, cIAP1, DR5, FADD, Fas, HSP70 and SMAC/DIABLO. However when looking at the actual levels of these proteins in Figure 3-3 B, they are actually at the same or slightly higher levels post UV in HPV5E6 than pLXSN cells. There is an increase of cleaved caspase 3 in HPV5E6 keratinocytes that is not seen in pLXSN cells after UV, which would suggest that HPV5E6 expression increases apoptosis

following UV rather than inhibiting it. The information from Figure 3-3 C should be considered along with the results as given in Figure 3-3 D, which shows the levels of apoptotic proteins compared to pLXSN 0 mJ/cm^2 as a baseline. For example, in Figure 3-3 C Bcl-x is more downregulated after UV in HPV5E6 expressing cells then pLXSN cells, however Figure 3-3 D shows that the actual protein abundance is still higher in HPV5E6 expressing cells than pLXSN cells after UV.

It can be seen in the table summarising changes in apoptosis related proteins, Figure 3-3 E, that there are a few overlaps between HT1080 cells and primary keratinocytes. For example, the anti-apoptotic proteins Bcl2, Bcl-x, cIAP2, clusterin and claspin are upregulated in HPV5E6 expressing cells of both types, albeit to different extents. However, although the overall expression of proteins involved in apoptosis appears to be higher in HT1080 cells, there are more differences observable between empty vector control and HPV5E6 expressing cells in primary keratinocytes. This could be due to the transformed nature of the cell line, derived from cancer and therefore with deregulation of apoptotic pathways, as opposed to the primary cells. In general the HPV5E6 expressing keratinocytes display greater upregulation of more proteins, of which some are pro- and some anti-apoptotic, and which are discussed in section 3.3.

3.2.4 Fas-induced apoptosis of HT1080 cells

Apoptosis assays were carried out to investigate if the upregulation of the anti-apoptotic proteins observed in both HT1080s and primary keratinocytes resulted in reduction of apoptosis. Initial work was carried out using Fas-activating antibody (Fas-Ab) to induce apoptosis. Fas (CD95) is a death receptor which triggers the extrinsic apoptotic cascade upon binding by its ligand FasL, or a Fas-Ab. Fas induction was initially used as it is a more delineated pathway then UV-induced apoptosis which, as described, triggers many cellular events. Unpublished

observations in the lab had indicated that HT1080s are sensitive to Fas-induced apoptosis, and suggested that apoptosis was inhibited by expression of the E6 proteins of HPV types 5, 10, 18 and 77. To investigate these observations, HT1080s were swapped into starvation media several hours prior to treatment with different doses of Fas-Ab, and then assayed for apoptosis by AnnexinV/PI as described in Materials & Methods, section 2.4.1. Figure 3-4 A shows a representative result with a decrease in the percent of viable cells, from c.95% to 70%, as the dose of Fas-Ab increases.

Initial work indicated that the type of media used affected the response of HT1080s to Fas activation, and cells have to be incubated in starvation media (without glutamine) for at least 8 hrs prior to addition of Fas-Ab. In addition, variability in the results obtained at the outset led to investigation of growth conditions used. Therefore HT1080s were grown in different media prior to addition of Fas-Ab and apoptosis measured 16 hrs later. Figure 3-4 B shows the increase in apoptotic cells 16 hrs post Fas-Ab treatment of HT1080s grown in different types of media. It was found that this Cancer Research UK E4 formulation contains glutamine and it can be seen that there was no increase in Fas-induced apoptosis in any media which contained glutamine. Thereafter all Fas-Ab assays were completed on cells grown in starvation media without glutamine. There have been reports of glutamine modulating the apoptotic response (Fuchs and Bode, 2006) and it could be concluded that glutamine starvation sensitises HT1080s to Fas-induced apoptosis. 100 ng/ml Fas-Ab was thereafter used as a dose which would induce apoptosis in approximately 30% of cells. Confirmation of Fas-induced apoptosis of HT1080s was seen with a western blot as shown in Figure 3-4 C, where increasing Fas-Ab causes an increase in cleaved caspase 3. Caspase 3 is an executioner caspase which is cleaved from the inactive procaspase form to produce active cleaved caspase 3 which then cleaves cellular targets and is therefore a marker of apoptosis, as described in the Introduction section 1.2.3.

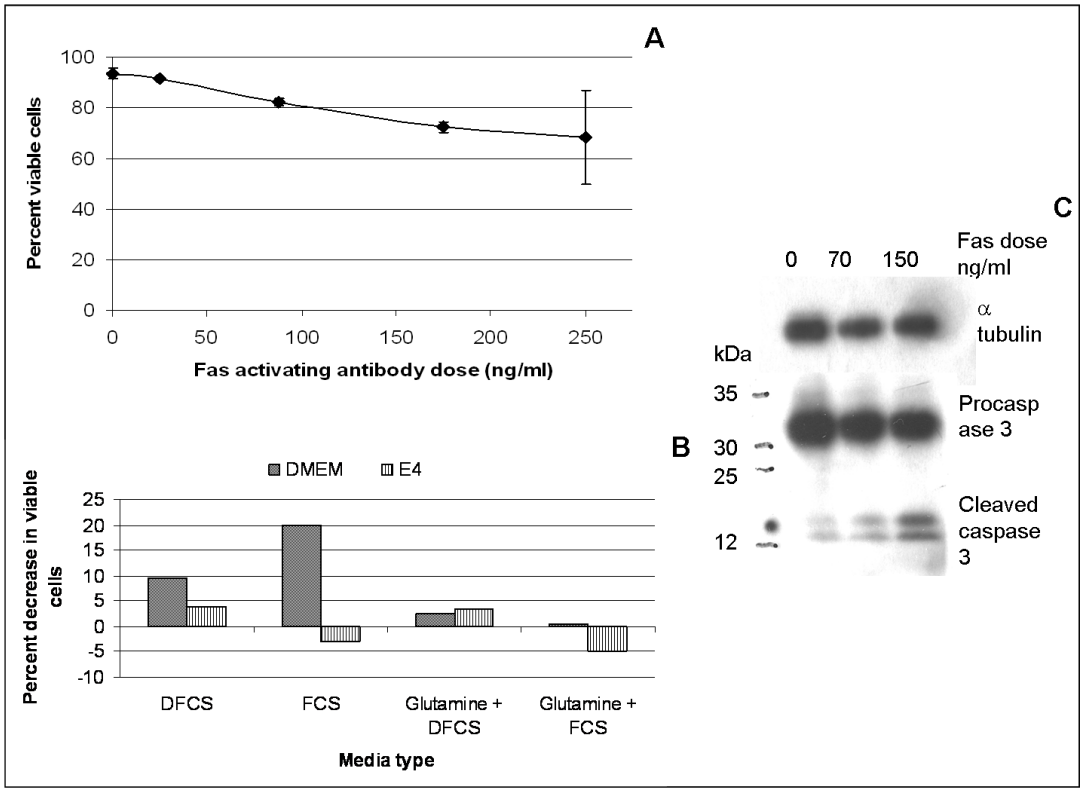

Figure 3-4 Apoptosis of HT1080s induced by Fas-activating antibody.

A HT1080s were harvested 16 hrs post Fas-Ab treatment and the amount of apoptosis measured by AnnexinV/PI staining. Error bars indicate standard deviation of 2 replicates.
B HT1080s were grown in different types of media for 8 hrs prior to addition of 100 ng/ml Fas-Ab and apoptosis was measured 16 hrs later with AnnexinV/PI staining. DFCS = Dialysed foetal calf serum, FCS = foetal calf serum, Glutamine = supplemented with fresh L-glutamine.
C HT1080s were grown in starvation media, Fas-Ab was added and the cells harvested with RIPA 16 hrs later. Lysates were resolved on SDS-PAGE and probed for cleaved caspase 3, a marker of apoptosis. αtubulin shows equivalent loading, and as the Fas-Ab dose increases from 0 to 150 ng/ml the amount of cleaved caspase 3 increases.

3.2.5 Reduction of Fas-induced apoptosis in HT1080 cells expressing HPV5, 18 or 77E6

To investigate the effect of HPV E6 expression on Fas-Ab apoptosis, HT1080 cells which express E6 from HPV types 5, 8, 10, 18 or 77 were treated with 100 ng/ml Fas-Ab and assayed for apoptosis with AnnexinV/PI staining. Figure 3-5 shows the decrease in viable cells in Fas-Ab treated samples compared to untreated samples of each cell type. As expected, Fas-Ab causes a 40% decrease in viable empty vector pcDNA control cells. Figure 3-5 also shows that expression of HPV types 5, 18 and 77E6 significantly reduce the amount of Fas-induced apoptosis from 40% in control cells to c.15, 20 and 17% respectively. Interestingly, HPV8E6 did not decrease Fas-Ab apoptosis of HT1080 cells, despite being closely related to HPV5 and having an association with SCC formation in EV patients. In contrast HPV8E6, along with HPV5, 10, 18 and 77E6, has been shown to reduce UV-induced apoptosis in HT1080s (Jackson and Storey, 2000). Differences in the induction of apoptosis by Fas-Ab or UV could contribute to this variation. Fas activation is an important component in UV apoptosis of keratinocytes, induced either by FasL binding or UV-induced receptor clustering and auto-activation (Aragane et al., 1998; Leverkus et al., 1997).

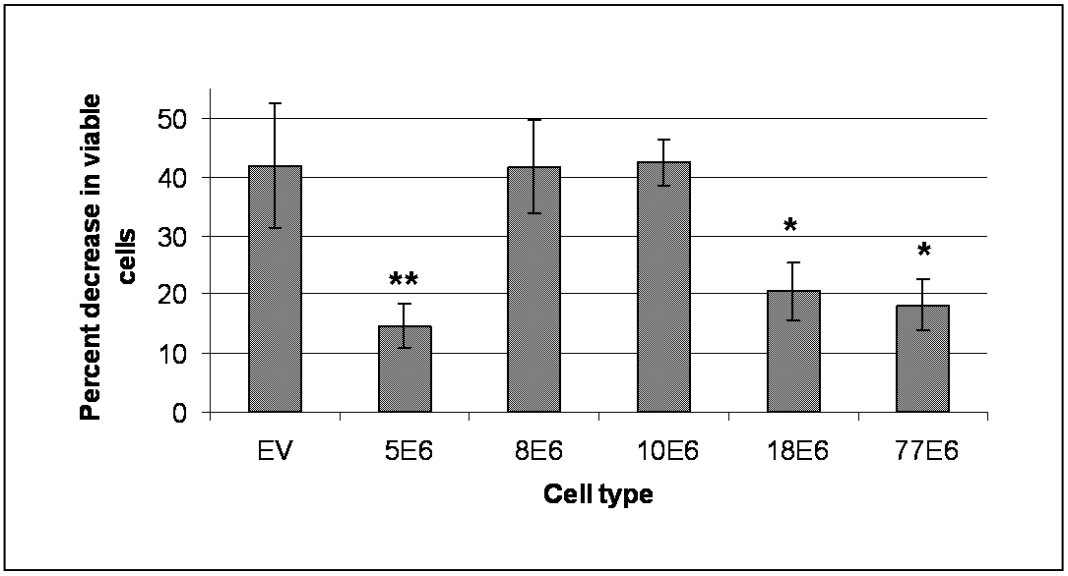

Figure 3-5 Reduction of Fas-induced apoptosis of HT1080s by E6 expression.

HT1080 cells expressing HPV5, 8, 10, 18 or 77E6 were grown in starvation media prior to treatment with 100 ng/ml Fas-Ab, apoptosis was measured by AnnexinV/PI staining 16 hrs later and the decrease in viable cells plotted. A reduction in the amount of apoptosis is significant compared to empty vector (EV) cells in cells expressing HPV5E6 (P= 0.003), HPV18E6 (P= 0.025) and HPV77E6 (P= 0.015), error bars represent the standard deviation, 3 replicates.

3.2.6 Reduction of UV-induced apoptosis of HT1080 cells expressing HPV5, 8, 10 or 18E6

To expand on the finding that HT1080s expressing E6 from HPV types 5, 18 and 77 are protected from Fas-induced apoptosis (Figure 3-5), and to investigate the effect of HPVE6 expression on UV-induced apoptosis, UV irradiation was used with HT1080 cells. UV irradiation is a potent inducer of apoptosis triggering both the extrinsic and intrinsic caspases cascades, along with production of Reactive Oxygen Species (ROS) and DNA damage. HT1080 cell lines expressing HPV5, 8, 10, 18 and 77E6 were generated as described, and treated with UV irradiation at various doses, harvested 16 hrs later and apoptosis assayed with AnnexinV/PI. Figure 3-6 shows that, as expected, as the UV dose increases from 2 to 10 mJ/cm^2 apoptosis (expressed as percent decrease in viable cells) increases in empty vector pcDNA cells from 22% to 40%. It can also be seen that in the cell lines expressing HPV5, 8, 10 and 18E6, in at least 2 of the UV doses tested, there is a significant decrease in apoptosis compared to the level of apoptosis in pcDNA cells at the same UV dose. The cell line expressing HPV77E6 alone displays no difference in apoptosis from pcDNA cells, except after 4 mJ/cm^2, where the level of apoptosis is significantly increased (P= 0.0001). There is also no difference between any of the cells expressing E6 and pcDNA cells in the levels of apoptosis after 10 mJ/cm^2. This is in all probability due to the high UV dose being very cytotoxic, and causing irreversible commitment to apoptosis which E6 expression is not able to reduce. The greatest protection from apoptosis appears to be conferred by HPV8 and 10E6 expression as these reduce UV induced apoptosis the most, especially at 2 and 4 mJ/cm^2.

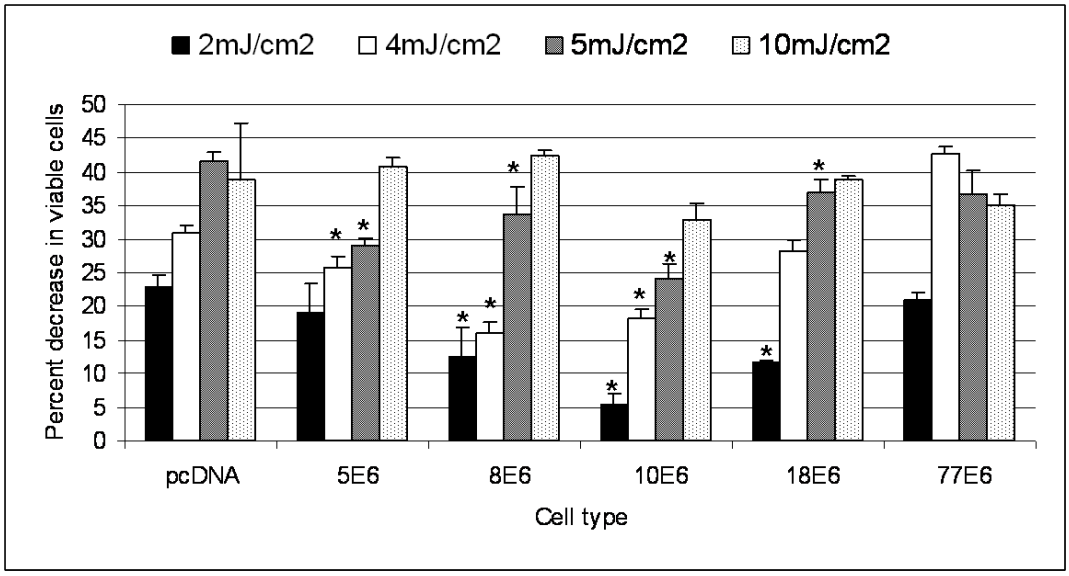

Figure 3-6 UV induced apoptosis of HT1080s expressing either HPV type 5, 8, 10, 18 or 77 E6.

HT1080 cells expressing the indicated E6 types were irradiated with UV and apoptosis assayed 16 hrs later with AnnexinV/PI. The decrease in viable cells was calculated from the percentage of viable cells in untreated samples of each cell type, which was approximately 80% for each. * = significant reduction in apoptosis compared to empty vector pcDNA cells, 3 replicates (for HPV5E6 at 4 mJ/cm^2 P= 0.009, 5 mJ/cm^2 P= 0.0002; for HPV8E6 at 2 mJ/cm^2 P= 0.023, 4 mJ/cm^2 P=0.0002, 5 mJ/cm^2 P=0.033; for HPV10E6 at 2 mJ/cm^2 P= 0.0004, 4 mJ/cm^2 P= 0.0002, 5 mJ/cm^2 P= 0.0003; for HPV18E6 at 2 mJ/cm^2 P=0.0008, 5 mJ/cm^2 P= 0.026).

Apoptotic inducer:	5E6	8E6	10E6	18E6	77E6
100ng/ml Fas-Ab	✓			✓	✓
2 mJ/cm^2 UV		✓	✓	✓	
4 mJ/cm^2 UV	✓	✓	✓	✓	
5 mJ/cm^2 UV	✓	✓	✓	✓	
10 mJ/cm^2 UV					

Figure 3-7 Summary of anti-apoptotic activity of the indicated E6 types in HT1080s

As a summary of the effect of E6 on apoptosis of HT1080 cells, Figure 3-7 indicates under which of the conditions tested expression of E6 of the HPV type indicated significantly reduces apoptosis. It can be noted that HPV5 and 18E6 protect from apoptosis induced by both Fas-Ab and certain doses of UV, and that HPV8 and 10E6 reduce apoptosis induced by several UV doses.

3.2.7 Fas-activating antibody does not induce apoptosis in primary keratinocytes or NTerts in the conditions tested

In order to test if E6 expression can protect keratinocytes from Fas-induced apoptosis, both primary human cutaneous keratinocytes and the keratinocyte cell line NTert (Dickson et al., 2000) were treated with Fas-Ab. PA8 and PA10 primary keratinocytes were grown in defined serum-free media, used at passage 2 or 3, treated with various doses of Fas-Ab, and apoptosis measured with AnnexinV/PI staining at 18, 43, 46 and 70 hr time-points. Firstly it can be seen that cells untreated by Fas-Ab still display approximately 80% viability only. The finding that untreated cells do not display 100% viability was repeatedly seen in apoptosis assays in the different cell types and culture media, indicating that low levels of apoptosis occur normally in the culture of cells, with the baseline viability typically ranging from 80 to 95% depending on cell type. Therefore in all experiments the baseline apoptotic rate was taken into account and changes in viability calculated according to viability levels of corresponding untreated cells, rather than arbitrarily using 100%. Figure 3-8 A and B show there is no significant increase in apoptosis at any Fas-Ab dose or time point tested, with the cells displaying c80% viability after 18, 43 and 46 hrs with doses of Fas-Ab ranging from 0-1500 ng/ml. The notable exception is PA8 cells which had been incubated with 1500 ng/ml Fas-Ab media for 70 hrs, which display a viability of c.30%. However the corresponding cells not treated with Fas-Ab but also grown in the same media for 70 hrs display a

low level of viable cells (c.50%), indicating the cells are starving, and that the lower viability is not wholly due to Fas-induced apoptosis. As in the HT1080s, starvation of cells may sensitise them to Fas-induced apoptosis. Incubating the cells for 70 hrs with Fas-Ab would not be useful in the intended assays as the starvation signalling events could mask the apoptotic pathways of interest.

To test the effect of starvation on Fas-induced apoptosis of keratinocytes, the NTert cell line was used. This cell line is derived from keratinocytes but avoids the problem of senescence seen when culturing primary cells, as NTert cells express the telomerase catalytic subunit and are deficient in p16(INK4a). As the media type has been shown to affect both the response of HT1080 cells to Fas-Ab and the growth patterns of keratinocytes, several different media were used to grow NTert cells; starvation media II, III and IV as described in Materials and Methods, section 2.1.1. Fas-Ab was then added at different doses and apoptosis measured 16 and 24 hrs later with AnnexinV/PI staining. Figure 3-8 C is a representative result of two of the media tested, showing that the amount of viable cells does not significantly decrease after addition of up to 1000 ng/ml Fas-Ab in any conditions tested. The cells in starvation media IV (DMEM:F12, no glutamine or keratinocyte supplement) display lower overall viability than those grown in complete media (c.60% viable compared to c.90%) in agreement with the more minimal media, however the amount of viable cells does not decrease from c.60% even with the addition of the highest Fas-Ab doses.

Western blots for the apoptotic marker cleaved caspase 3 were carried out on lysates from PA8 and PA10 primary keratinocyte samples to confirm the FACS results. There was no cleavage of procaspase 3 in cell lysates which had been incubated with Fas-Ab for 46 hrs, however Figure 3-8 D shows the lysates of cells which had been incubated with Fas-Ab for 70 hrs, and in PA8 cells there is a slight increase in cleaved caspase 3 at the highest dose, corresponding to the slightly increased apoptosis seen in the AnnexinV/PI assay (Figure 3-8 A). The N-18

antibody (Santa Cruz sc714) was also used to confirm the expression of Fas in the keratinocytes, which has previously been reported, for example (Sayama et al., 1994). Fas is reported to migrate at 44 kDa, however Figure 3-8 D shows a band at c.50 kDa which does not alter with increasing Fas-Ab dose. This could correspond to Fas, the slightly increased apparent size possibly due to post-translational modifications, for example phosphorylations which have been reported on Fas (Lautrette et al., 2006).

Keratinocytes have previously been shown to have different sensitivities to Fas-induced apoptosis, as the studies use different cell types, doses, and time points. Several studies also include the inflammatory cytokine Interferon-γ as it sensitises cells to Fas-induced apoptosis (Konur et al., 2005). However as Fas-Ab does not induce apoptosis in the conditions used here, it was decided not to continue and include Interferon-γ as it would add further complexity to the signalling pathways we are attempting to delineate.

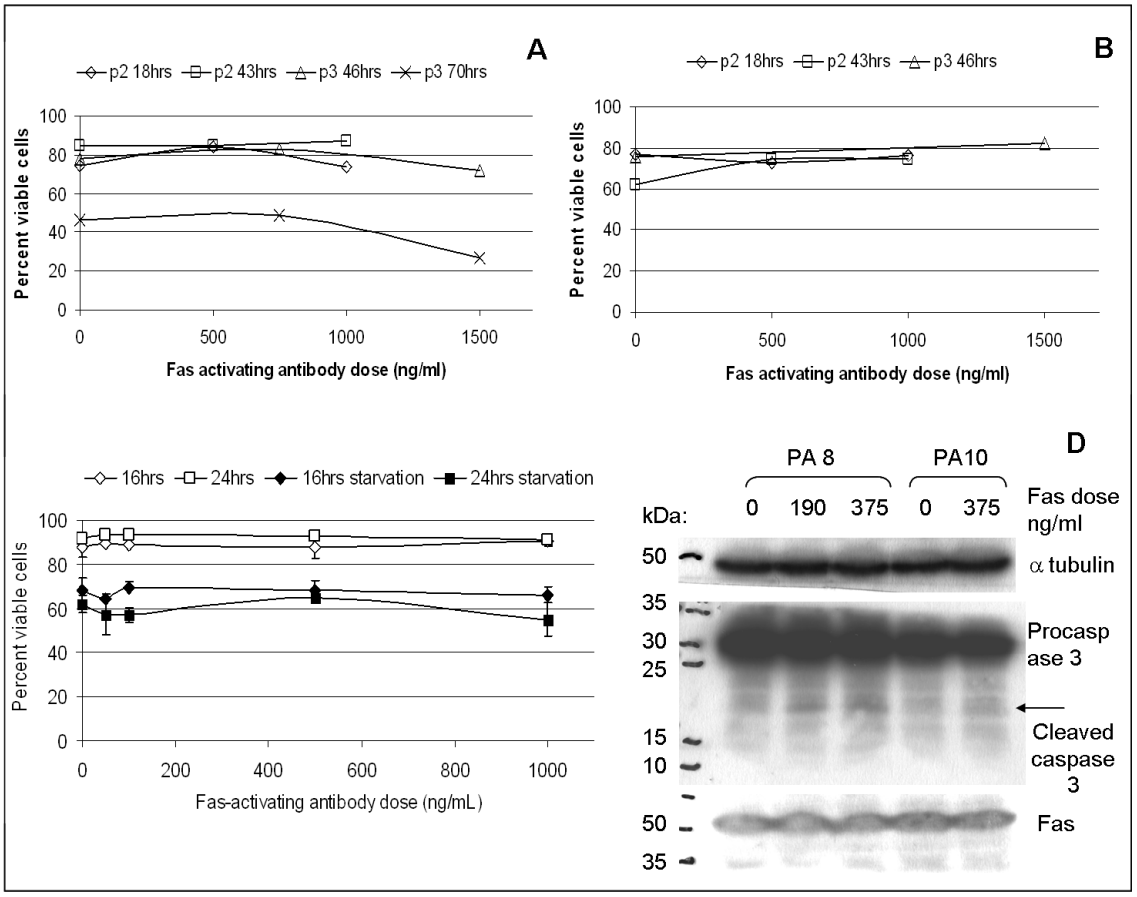

Figure 3-8 Fas-activating antibody does not induce apoptosis in primary keratinocytes or NTert cells.

Keratinocytes of the indicated passage number were cultured in defined serum-free keratinocyte media prior to addition of different doses of Fas-Ab and apoptosis was measured with AnnexinV/PI staining at the indicated time points. **A** shows the viability of PA8 keratinocytes and **B** the viability of PA10 cells.

C NTert cells were cultured in defined serum free media or starvation media IV prior to addition of Fas-Ab and apoptosis measured 16 and 24 hrs later. Error bars indicate the standard deviation, 2 replicates.

D PA8 and PA10 keratinocytes were grown for 70 hrs with Fas-Ab, lysed in RIPA, separated by SDS-PAGE, and probed for α tubulin, which shows equal loading, and cleaved caspase 3, which increases slightly as the dose of Fas-Ab increases from 0 to 375 ng/ml in PA8 cells. The lysates were also probed for Fas. Here a band can be seen at c.50 kDA that does not alter with increasing Fas-Ab dose, which shows the expression of Fas on primary keratinocytes.

3.2.8 UV induced apoptosis of primary keratinocytes, HaCaT and NTert cells

As Fas-Ab did not induce apoptosis of keratinocytes in the conditions tested, UV irradiation was used. As described apoptosis is induced by UV through several cellular pathways, and is an important process in keratinocytes as it removes damaged, potentially tumourigenic cells. Primary keratinocytes, along with cell lines derived from keratinocytes, HaCaT (Boukamp et al., 1988) and NTert (as described) were used in initial experiments testing the apoptotic response to UV. HaCaT are a spontaneously immortalized adult keratinocyte cell line with normal differentiation, while NTert cells can also still undergo normal differentiation. Cells were UV irradiated as described in Materials and Methods, section 2.1.8. As expected, UV irradiation induced apoptosis of the cell lines at a range of doses from 5 to 20 mJ/cm^2, as measured by AnnexinV/PI staining and illustrated in Figure 3-9 A. NTert cells are more susceptible to UV induced apoptosis in these conditions, with fewer than 5% viable cells remaining 16 and 24 hrs post 10 and 15 mJ/cm^2 UV. The difference in the amount of apoptosis in NTert cells at 5 mJ/cm^2, with 70% of the cells viable 24 hrs post UV compared to 20% viability 16 hrs post UV, could be due to the processing of the damage received, as at a low dose of UV the extra time has allowed repair of DNA damage and so fewer NTert cells are undergoing apoptosis. HaCaT cells are more resistant to UV induced apoptosis although the percentage of viable cells does decrease to 50% 16 hrs post 20 mJ/cm^2 UV. Apoptosis induction was also tested on primary keratinocytes (from Cascade Biologics) grown in different types of media. The different media types give rise to differences in the morphology and differentiation of the cells. Initial experiments were performed in the defined serum-free media EpiLife, and it was also observed that the density of the cells had an effect upon UV induced apoptosis. Figure 3-9 B shows that the number of viable cells decreased from a

baseline of 70-85% to 0-20% after increasing doses of UV from 5 to 40 mJ/cm^2. Cells that were plated at higher densities and allowed to proliferate for 24 hrs longer displayed slightly increased levels of viable cells at the corresponding UV doses, with 50, 40 and 20% viable cells remaining after 10, 15 and 20 mJ/cm^2 UV respectively, compared to 60, 20 or 40, and 10% viable cells remaining after 5, 10 and 15 mJ/cm^2 UV in less confluent cells, presumably due to the protective effect of cell clustering. As seen in the NTert cells in Figure 3-9 A, there is a difference in the less confluent cells with 20% viable cells remaining 16 hrs post 10 mJ/cm^2 UV compared to 40% viable 24 hrs post UV, which again is probably due to the extra time post-irradiation allowing repair of the damage and so more viable cells are seen. Primary keratinocytes grown in RM+ media, which allows early differentiation of the cells and therefore more colony formation, was also tested. Figure 3-9 C shows that cells grown in this media are more resistant to apoptosis, with a significant decrease in viable cells only seen at 15 mJ/cm^2 and above, from 80% viable to 55% 16 hrs after and 20% viable 24 hrs after 40 mJ/cm^2. This slightly increased resistance to apoptosis is presumably due to the clustering of the cells which occurs in this media type as the cells grow in colonies. The difference in cell morphology in this media can also explain the large error bars. As the cells become more differentiated they adhere more to the plate and each other, and this makes the trypsinisation part of the harvesting protocol more variable as it takes longer to detach the majority of the cells. Also some of the cells may stay attached to the plate and this may affect the distribution of apoptotic cells seen in the analysis. As a significant increase in apoptosis was always observed 16 hrs after a sufficient dose of UV irradiation this time point was used subsequently.

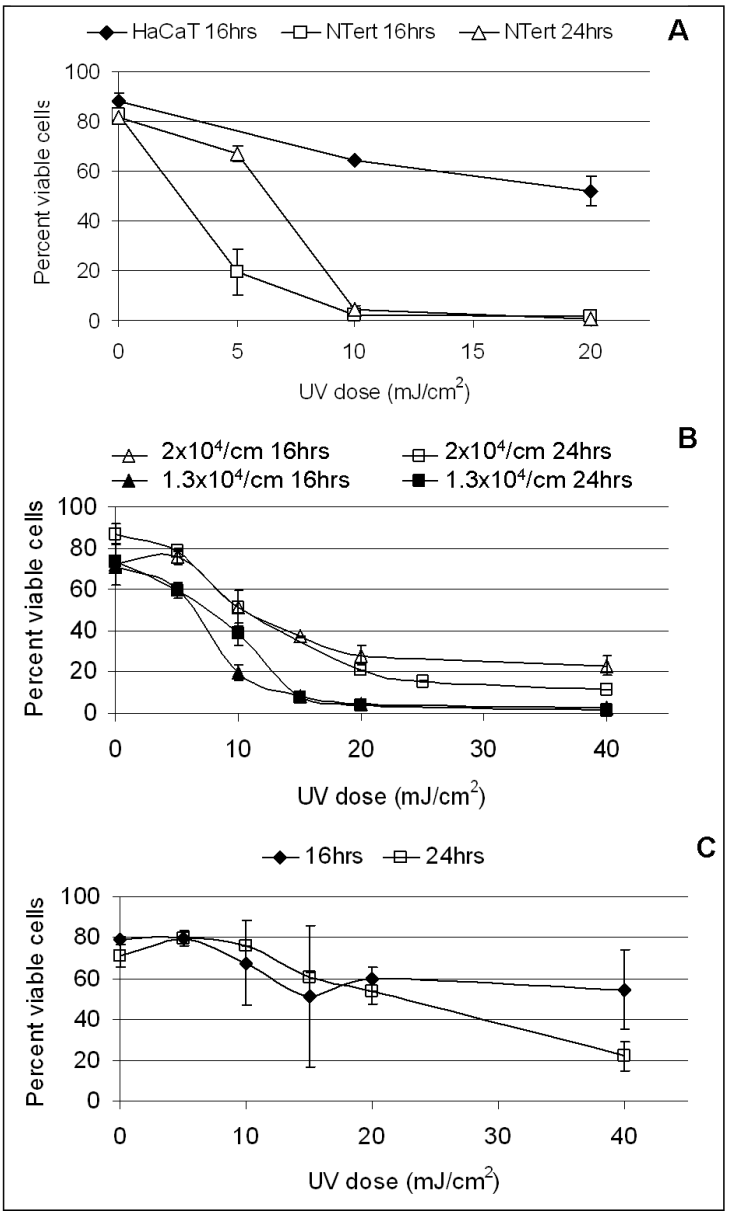

Figure 3-9 UV irradiation induces apoptosis of keratinocytes.

A HaCaT and NTert cells were treated with different doses of UV irradiation and apoptosis measured 16 and 24 hrs later. A decrease in viable NTert cells can be seen at both time points at 5 mJ/cm^2 with an almost complete induction of apoptosis at the higher UV doses (>10 mJ/cm^2). HaCaT cells demonstrate a smaller but still significant reduction in viable cells at higher UV doses. Error bars represent standard deviation, 2 replicates for NTert and 3 for HaCaT cells.

B Primary keratinocytes were seeded at the indicated densities, UV irradiated and apoptosis measured 16 and 24 hrs later. 2x10^4/cm cells were cultured for 72 hrs before induction, 1.3x10^4/cm cells for 48 hrs.

C Primary keratinocytes grown in the early differentiation media RM+ prior to UV irradiation show slightly increased resistance apoptosis. For B and C error bars indicate standard deviation, 2 replicates.

3.2.9 UV induced apoptosis of HPV5 and 8E6 expressing keratinocytes

To test if the expression of the E6 protein from β-HPV types 5 and 8 reduced apoptosis in primary keratinocytes, cells stably expressing these proteins following retroviral infection were treated with UV irradiation and apoptosis was measured with AnnexinV/PI staining as described in Materials and Methods, section 2.4.1. Keratinocytes were grown in both EpiLife and RM+ to test if the differentiation state of the cells affected the response to UV. Initial results showed that expression of HPV5 and 8E6 increased apoptosis in response to UV, as illustrated in Figure 3-10 A and B, in contrast to the apoptotic response of HT1080 cells expressing E6 and to previously published data. Figure 3-10 A shows that pLXSN empty vector control primary keratinocytes grown in EpiLife decrease from 80% viable to 60% viable 16 hrs post 15 mJ/cm^2 UV whereas cells expressing HPV5 and 8E6 are only 40% viable; and keratinocytes grown in RM+ decrease to 30% viable pLXSN cells and 20% viable HPV5 and 8E6 cells post 20 mJ/cm^2 UV, as shown in Figure 3-10 B. This is unexpected given the reduction of Fas-induced apoptosis seen in HT1080 cells expressing HPV5E6 (Figure 3-5) and of UV-induced apoptosis in HT1080s expressing HPV5 and 8E6 (Figure 3-6), and also differs from results from other groups, who have observed protection from apoptosis in keratinocytes expressing HPV5E6 (Struijk et al., 2008; Underbrink et al., 2008). However the balance of pro- and anti- apoptotic factors which control cellular commitment to apoptosis could be affected by changes in culture and assay conditions meaning that here we do not consistently see a reduction in apoptosis in E6 expressing cells. It was also observed that although the actual percentage of viable HPV5E6 cells is lower than the empty vector pLXSN cells post UV, seen in Figure 3-10 C, the decrease in viable cells is less in HPV5E6 expressing cells than pLXSN cells, seen in Figure 3-10 D. This figure shows a significant difference in the decrease in viable cells for keratinocytes grown in RM+, for example, viable pLXSN cells

decrease by 20% after 30 mJ/cm^2, whereas there is no decrease in viable HPV5E6 cells. This pattern of apoptosis could be consistent with the retroviral infection and expression of E6 genes causing a decrease in baseline viability in the 'normal' cellular state, however when apoptosis is triggered, HPV5E6 expression induces some protection from cell death. It is also possible that the effect of E6 is not being seen in the tissue culture systems or assays being used, or that only specific populations of the cells are being affected.

To test if the anti-apoptotic effects of E6 in these assays were limited to immortalised cell lines the keratinocyte HaCaT cell line was used as an intermediate between HT1080s and primary keratinocytes. HaCaT cells expressing HPV5 and 8E6 proteins were made by retroviral infection with pLXSN vectors and selection, they were irradiated and apoptosis measured 16 hrs later by AnnexinV/PI staining, as described in Materials and Methods, section 2.4.1. Figure 3-10 E shows that although there is a small but significant increase, of c.10%, in viable HPV8E6 cells at 10 mJ/cm^2, there is no protection from apoptosis by HPV5 or 8E6 expression at 20 mJ/cm^2. It was also observed that the growth of HaCaT cells was different to that of NTert and primary keratinocyte, for example the G418 dose required to select E6 expressing cells was very high, so it was decided to continue to work principally with primary keratinocytes.

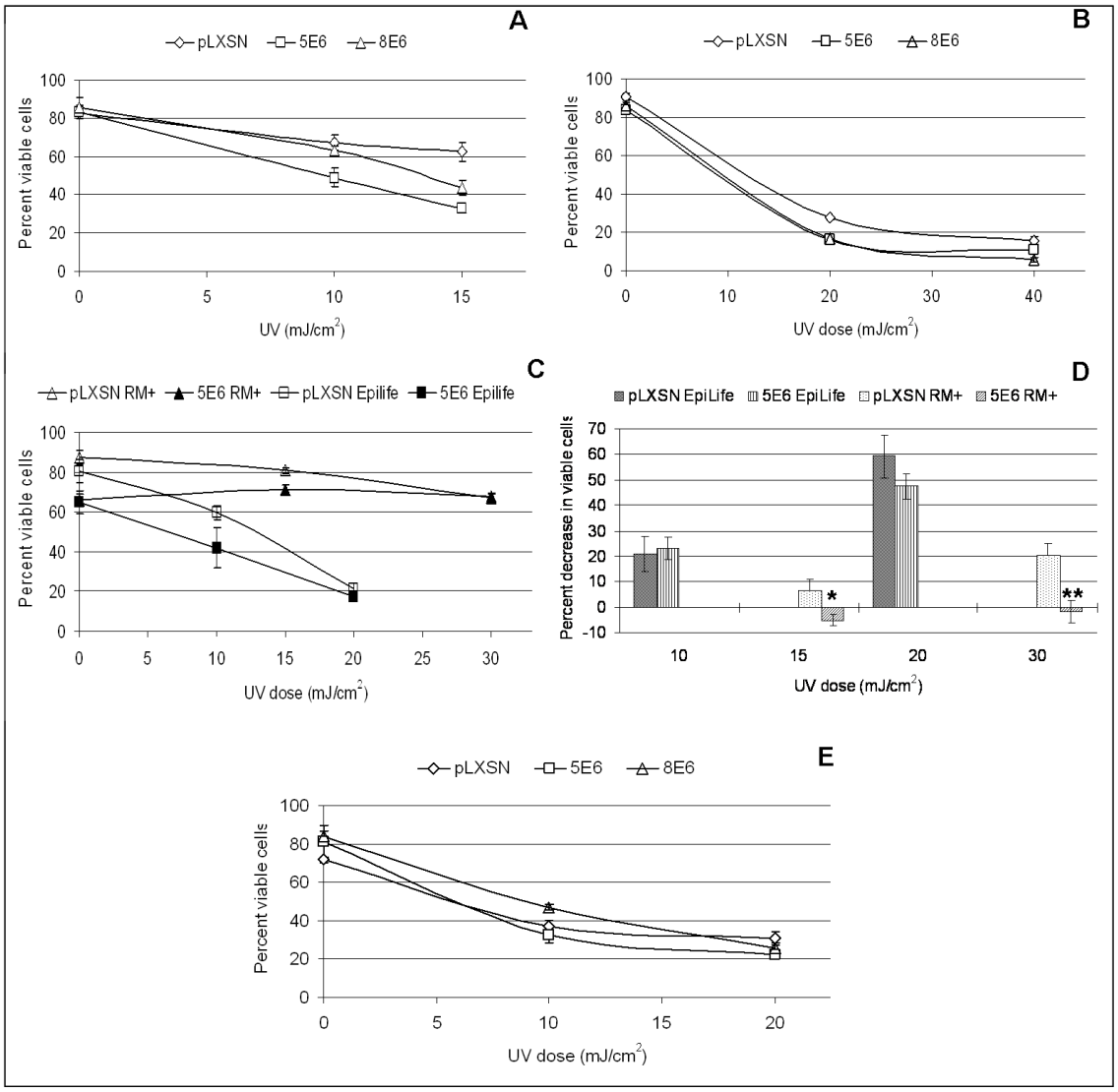

Figure 3-10 UV induced apoptosis in E6 expressing keratinocytes, measured by AnnexinV/PI staining.

A Keratinocytes were grown in EpiLife media, apoptosis induced and measured 24 hrs later. Cells expressing HPV5 and 8E6 are less viable than empty vector pLXSN cells (for HPV5E6 at 10 mJ/cm^2 P=0.0075 and 20 mJ/cm^2 P= 0.0006, for HPV8E6 at 20 mJ/cm^2 P= 0.006). Error bars indicate standard deviation, 3 replicates.

B Keratinocytes were grown in EpiLife then swapped into RM+ to begin differentiation for 48 hrs before apoptosis was induced with UV irradiation. Cells expressing E6 are significantly less viable than empty vector pLXSN cells (for HPV5E6 at 20 mJ/cm^2 P= 0.0002, at 40 mJ/cm^2 P= 0.03; for HPV8E6 at 20 mJ/cm^2 P= 0.00005, at 40 mJ/cm^2 P= 0.002). Error bars indicate standard deviation, 3 replicates.

C Viable keratinocytes, grown in either EpiLife or RM+, remaining 16 hrs post UV irradiation. Empty vector pLXSN cells are more viable than HPV5E6 cells at lower UV doses (in EpiLife P= 0.045, in RM+ P= 0.005). Error bars indicate standard deviation, 3 replicates.

D The decrease in viable keratinocytes grown in different media 16 hrs post UV is shown. For EpiLife the differences did not reach significance, for RM+, HPV5E6 expressing cells display significantly less decrease in viability, * = P= 0.011, ** = P= 0.004.
E HaCaT cells expressing HPV5 and 8E6 were UV irradiated and apoptosis measured 16 hrs later. HPV8E6 cells are significantly more viable than pLXSN empty vector cells at 10 mJ/cm^2 (P= 0.005) but there is no protection from apoptosis seen at 20 mJ/cm^2. Error bars indicate standard deviation, n of 3.

3.2.10 Apoptosis of basal primary keratinocytes

To investigate the hypothesis that the expression of E6 may cause a reduction in apoptosis only of a certain population of keratinocytes, a marker for basal cells was included in the AnnexinV/PI apoptosis assay to measure apoptosis of the less differentiated cells. As primary cells, keratinocytes form a heterogeneous population in tissue culture, with cells of different sizes and morphology evident, along with the differences in differentiation and morphology seen with RM+ media that have been mentioned. This is due to the growth pattern of keratinocytes in the skin, where they progress up through the epidermis whilst undergoing terminal differentiation to form the cornified squames which are shed from the surface, as has been described in the Introduction. It has been hypothesised that cutaneous HPVs infect the most basal of the keratinocytes, or the epidermal stem cells which remain in the basal layer, and therefore allow the HPV to replicate and persist (Egawa, 2003). Therefore E6 may only protect basal keratinocytes from apoptosis, and this was tested by inclusion of a basal cell marker in the FACS assay for apoptosis. The marker chosen to identify basal keratinocytes was an antibody specific for α6 integrin, also called CD49f, which has previously been shown to be expressed on keratinocytes which contact the basement membrane (Sonnenberg et al., 1991) and is used in combination with other markers to identify pools of keratinocytes that may contain stem cells. The inclusion of this antibody allows the keratinocytes most strongly expressing α6 integrin to be identified from within the population by FACS and the level of apoptosis determined.

Keratinocytes grown in both EpiLife and RM+ were tested due to the known variations in differentiation caused by these media. The 20% of cells with the strongest staining for α6 integrin were taken as basal cells in this analysis. Figure 3-11 shows the apoptosis of basal keratinocytes, with Figure 3-9 A showing an example of the patterns of UV induced apoptosis seen in the total and basal populations of keratinocytes grown in both RM+ and EpiLife. In EpiLife-grown cells, with no UV treatment the basal cells are c.10% less viable than the total population (P= 0.0009), as the UV dose increases the viability of the basal population is approximate to the total population, and at the higher dose there is a small but significant increase (9%) in viability of the basal population (P= 0.039). However in the RM+ cells, with no UV treatment the basal cells have the same 90% viability as the total population, and as the UV dose increases the basal cells are significantly more viable than the total population (at 20 mJ/cm^2 there is a 14% increase in viable cells, P= 0.0007; at 40 mJ/cm^2 an 11% increase, P= 0.014). To test if a more stringent system identifying basal cells made a difference, the apoptosis of the total population, the basal population (top 20% α6 integrin), and the top 5% of cells staining for α6 integrin were compared, and shown in Figure 3-11 B. Here keratinocytes were grown in RM+ and as expected the basal cells are 15-20% more viable than the total population at all UV doses; however there is no difference between the topmost 5% and 20% α6 integrin expressing cells.

To test the hypothesis that E6 protects basal cells from apoptosis, keratinocytes expressing HPV5E6 were UV treated, and apoptosis measured, with the marker for α6 integrin included in the assay. Figure 3-11 C shows that, as seen previously in EpiLife cells, at 0 mJ/cm^2, the basal cells are less viable than the total population. pLXSN and HPV5E6 total populations have the same baseline viability at 88% and 86% respectively, however the pLXSN basal baseline is more viable than the HPV5E6 basal baseline, at 78% compared to 64% viable. Also as seen previously, the total population of HPV5E6 expressing cells are less viable than total pLXSN

empty vector cells after UV, with 10% fewer viable HPV5E6 cells after 7.5 mJ/cm^2 and 25% fewer after 15 mJ/cm^2. However, basal pLXSN cells display 67% viability, the same as the total pLXSN population after 15 mJ/cm^2, whereas basal HPV5E6 cells are 15% more viable than the total HPV5E6 population at this dose, although this difference does not reach significance (P= 0.07). Cells expressing HPV8E6 were also included in this assay however there was no significant difference observed between either the total or basal populations of HPV8E6 and pLXSN cells. Cells expressing HPV5E6 were also tested in RM+ media, and Figure 3-11 D shows the viability of the total and basal populations after UV treatment. As seen before with RM+ media, there is no significant difference between any of the cell populations at 0 mJ/cm^2. However the total population of HPV5E6 expressing cells are 5 and 10% more viable than pLXSN cells at 20 and 40 mJ/cm^2 respectively (P= 0.049, P= 0.003). At the lower UV dose, both basal cell populations are c.20% more viable than the total population, a significant difference (for HPV5E6 cells P= 0.003, for pLXSN P= 0.001), however at 40 mJ/cm^2, pLXSN basal cells are not significantly more viable than the total population (P= 0.07) whereas HPV5E6 basal cells are still c.20% more viable (P= 0.0001). This could indicate that HPV5E6 is protecting basal cells from apoptosis. However as it was previously observed (Figure 3-11 A), in parental keratinocytes grown in RM+, that basal cells are more viable than the total population at this dose, the increase in viability of HPV5E6 basal cells may not be meaningful.

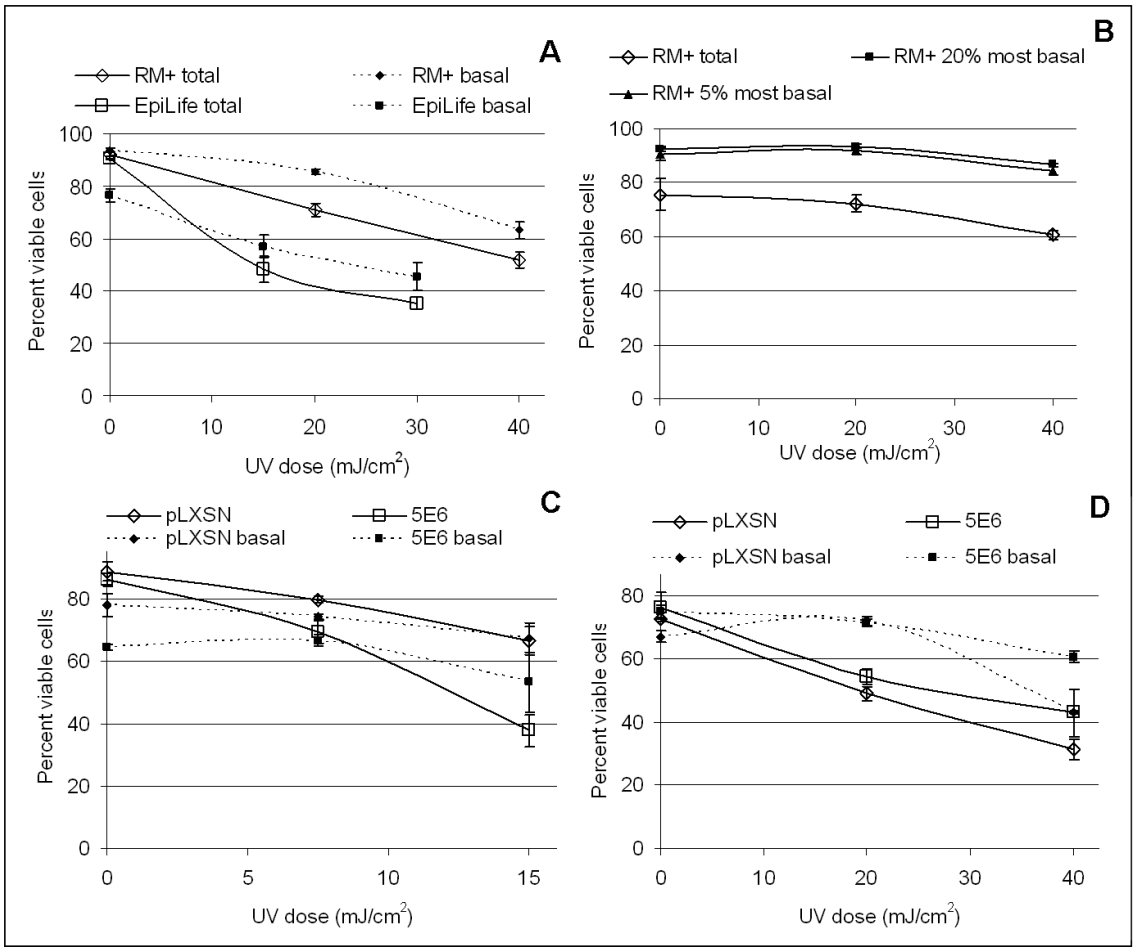

Figure 3-11 Apoptosis of basal keratinocytes, induced by UV and measured after 16hrs by AnnexinV/PI staining including a marker for basal cells.

A Primary keratinocytes were grown in either EpiLife or RM+, which give different results for the levels of basal cell viability.

B Primary keratinocytes were grown in RM+. The amount of viable cells in the top 20% and top 5% expressing α6 integrin populations are not significantly different.

C Primary keratinocytes expressing HPV5E6 were grown in EpiLife. The total population of HPV5E6 cells are less viable than empty vector pLXSN cells after UV. The viability of the basal populations does not decrease as much as the total population after UV.

D Primary keratinocytes expressing HPV5E6 were grown in RM+. HPV5E6 expressing cells are more viable post UV than pLXSN cells and for both cell types the basal cells are more viable after UV than the total populations.

For all results error bars indicate standard deviation, 3 replicates.

3.2.11 Changes of apoptosis-related proteins in HT1080 cells and primary keratinocytes expressing HPV E6 proteins assessed by western blotting

Western blots were performed to detect a number of apoptosis-related proteins to further investigate several of the changes seen on the Proteome Profiler arrays (Figure 3-2 B and Figure 3-3 B); as well as to investigate any changes which occur in cells expressing the E6 from other HPV types, and to test apoptosis-related proteins which were not included on the arrays.

HT1080s containing the pcDNA empty vector or expressing HPV5, 8, 10, 18, and 77E6 were grown to 85% confluence and harvested with RIPA buffer plus protease inhibitor which was incubated with the cells on ice for 5 minutes then scraped, and the lysates were stored at -20 °C until they were quantified and separated by SDS-PAGE, after which proteins were transferred to membranes and blocked. Primary keratinocytes expressing the pLXSN empty vector, HPV5 or 8E6 were grown in either EpiLife or RM+ media and processed as described above. Both media types were included as the culture system of primary keratinocytes can affect the expression profile and apoptotic response as has previously been demonstrated. Keratinocytes generated from several different retroviral infections were used to minimise the effects of random incorporation of E6 into the genome on the results. The lysates of both cell types harvested as described for the Proteome Profiler arrays were also included (in which the keratinocytes were grown in RM+).

Probing for various apoptotic proteins was carried out under various conditions as described in Materials & Methods, section 2.3.3. Image J was used to quantify the pixel density, which was normalised according to the background and loading control, and the fold change in the protein of interest calculated according to levels of the relevant empty-vector lysate.

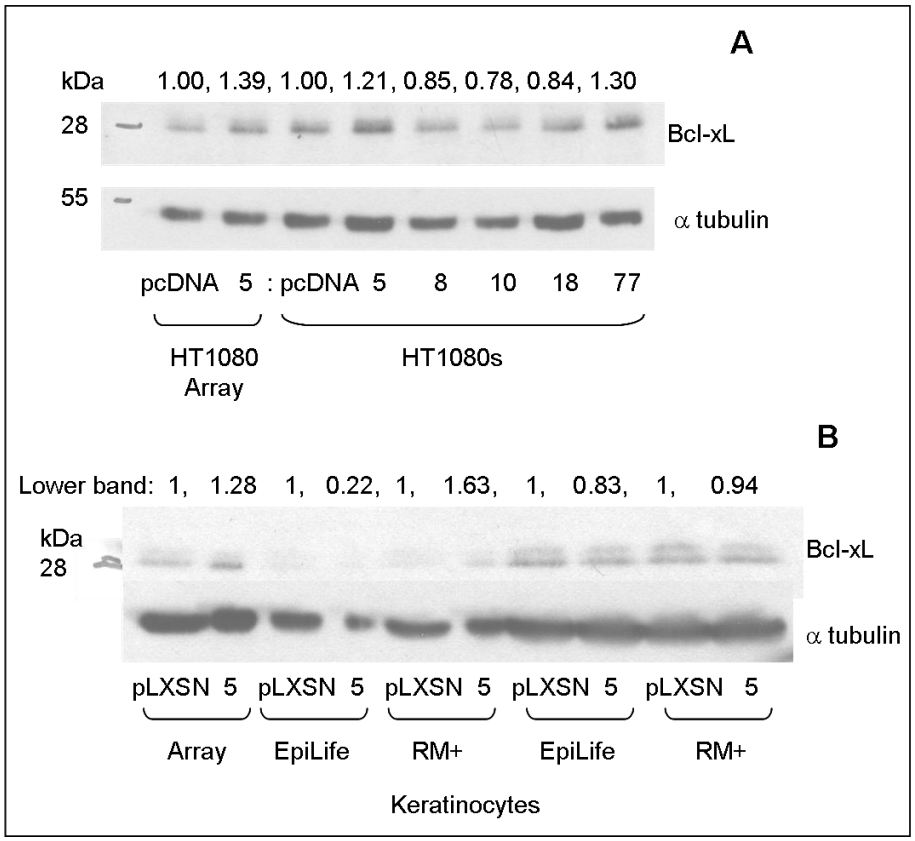

Figure 3-12 Levels of Bcl-x_L

HT1080s (**A**) and primary keratinocytes (**B**) (including replicate retroviral infections; array samples grown in RM+) expressing either empty vector or the HPVE6 type indicated are shown. α tubulin was used as a loading control and the fold changes compared to the relevant empty vector control are indicated.

Figure 3-12 shows the levels of the anti-apoptotic Bcl2 family member Bcl-x_L. It can be seen that in HT1080s there is a small increase in HPV5 and 77E6 lysates, which is similar to the small upregulation seen on the arrays. The keratinocyte HPV5E6 lysates show a small but not consistent increase in Bcl-x_L, not as great as that seen on the arrays. The blots also show a double band. Bcl-x is expressed as two splice variants, Bcl-x_L (30 kDa) which is anti-apoptotic and the shorter Bcl-x_S (19 kDa) which is pro-apoptotic (Minn et al., 1996). This size difference, and the specificity of the antibody used here for Bcl-x_L, suggests that the double bands do not correspond to both Bcl-x_L and Bcl-x_S. However phosphorylation of Bcl-x_L could result in double bands, which has been observed (Poruchynsky et al., 1998). Phosphorylation has been reported to reduce the anti-apoptotic activity and has

also been found to be involved in the link between mitotic arrest and apoptosis (Terrano et al., 2010).

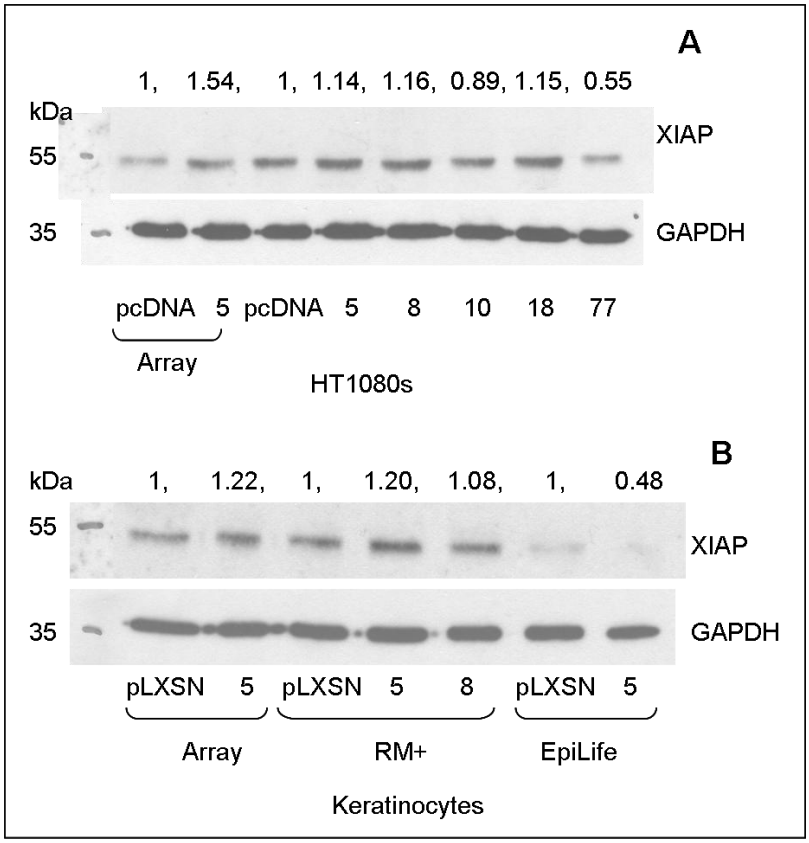

Figure 3-13 Levels of XIAP

HT1080s (**A**) and primary keratinocytes (**B**) (including replicate retroviral infections; array samples grown in RM+) expressing either empty vector or the HPVE6 type indicated are shown. GAPDH was used to ensure equal loading and the fold changes compared to the relevant empty vector control are indicated.

Figure 3-13 shows the levels of the anti-apoptotic XIAP are slightly increased in HT1080s expressing HPV5, 8 and 18E6, which agrees with the small increase in XIAP in HPV5E6 HT1080s on the array, and slightly decreased in 10 and 77E6. Primary keratinocytes grown in RM+, but not in EpiLife, expressing HPV5E6 also show slightly increased XIAP levels, which are smaller than the increase seen on the array.

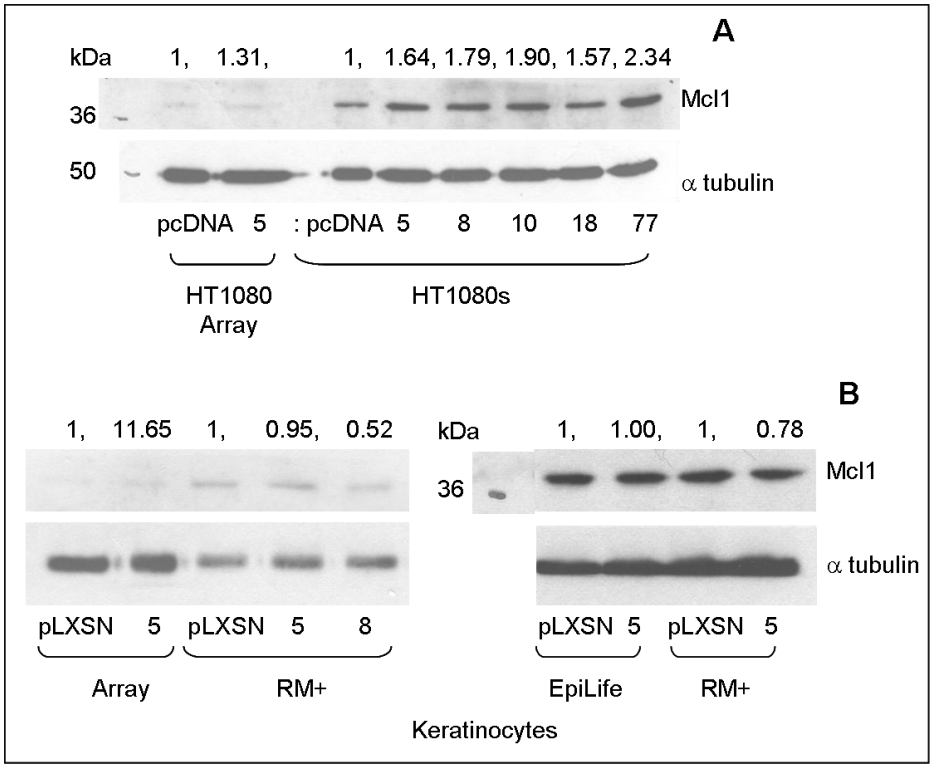

Figure 3-14 Levels of Mcl1

HT1080s (**A**) and primary keratinocytes (**B**) (including replicate retroviral infections; array samples grown in RM+) expressing either empty vector or the HPVE6 type indicated are shown. α tubulin was used to ensure equal loading and the fold changes compared to the relevant empty vector control are indicated.

Mcl1 was not included on the Proteome Profiler arrays, but it is an important anti-apoptotic member of the Bcl2 family which inhibits the activity of Bak, therefore the levels of Mcl1 in HT1080s and keratinocytes expressing HPVE6 proteins were investigated. Figure 3-14 A shows an increase in Mcl1 in HT1080s expressing HPV5, 8, 10, 18 and 77E6. However Figure 3-14 B shows no difference in the majority of the keratinocyte lysates. The upregulation of 11-fold shown in the array lysates is probably skewed due to the low intensity of the bands combined with slight differences in background.

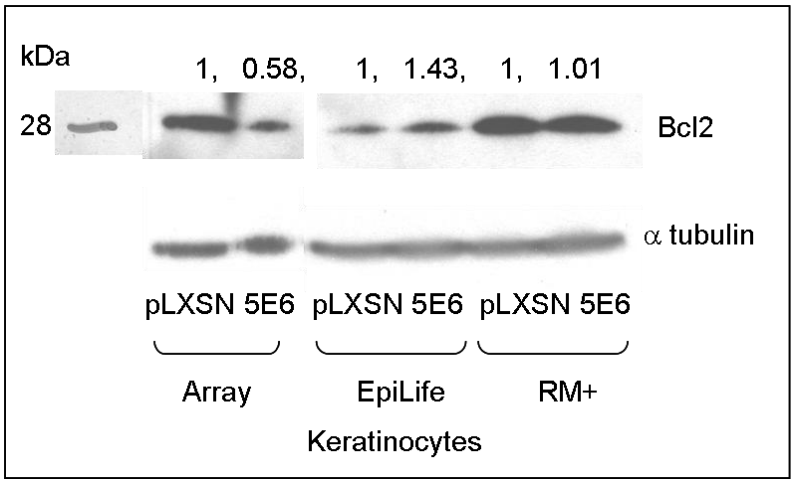

Figure 3-15 Levels of Bcl2

Primary keratinocytes expressing either empty vector or the HPVE6 type indicated are shown. α tubulin was used to ensure equal loading and the fold changes compared to the relevant empty vector control are indicated.

Figure 3-15 shows the levels of the anti-apoptotic Bcl2 are increased in HPV5E6 keratinocytes grown in EpiLife but not in RM+. The decrease in the array samples is contrary to the increase seen on the arrays and could be due to the slightly uneven loading on the western.

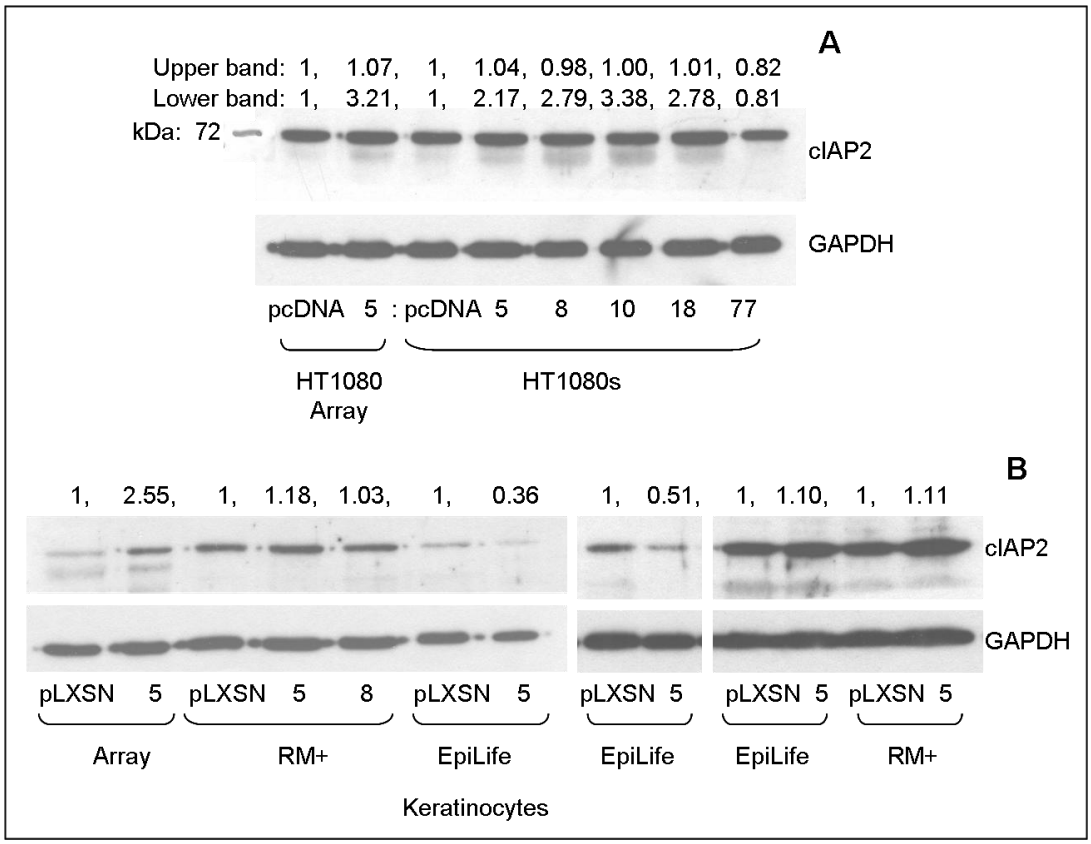

Figure 3-16 Levels of cIAP2

HT1080s (**A**) and primary keratinocytes (**B**) (including replicate retroviral infections; array samples grown in RM+) expressing either empty vector or the HPVE6 type indicated are shown. GAPDH was used to ensure equal loading and the fold changes compared to the relevant empty vector control are indicated.

The larger of the bands seen in Figure 3-16 A corresponds to cIAP2; however no difference is observed in any of the lysates. However this could be due to the high level of protein loaded obscuring any differences. If the smaller bands represent degradation products and therefore reflect cIAP2 levels, an increase in HPV5, 8, 10 and 18E6 lysates can be seen. This is also observed in Figure 3-16 B, where the heavily loaded samples (far right hand side) do not show any differences, whereas in the lighter loaded lanes, an increase in cIAP2 in HPV5E6 lysates from RM+, and a decrease in HPV5E6 lysates from EpiLife, becomes apparent.

3.3 Discussion

3.3.1 General conclusions

A detailed discussion of the results presented in this chapter follows, however a general summary can be drawn. The proteome profiler arrays, Figure 3-2 and Figure 3-3, show that several anti-apoptotic proteins are upregulated by at least 1.5 fold in both HT1080s and keratinocytes expressing HPV5E6, including Bcl2, Bcl-x, cIAP2, claspin and clusterin. In addition more anti-apoptotic proteins are upregulated in HPV5E6 keratinocytes, as shown in Figure 3-3 E.

To test if these changes in the levels of apoptotic regulators resulted in a reduction of apoptosis in E6 expressing cells, HT1080s expressing HPV5, 8, 10, 18 and 77E6 were assessed with apoptosis induced by Fas-Ab and UV. In addition keratinocytes expressing HPV5 and 8E6 were tested with UV. As summarised in Figure 3-7, HPV5, 18 and 77E6 protect HT1080s from Fas induced apoptosis, and HPV5, 8, 10 and 18E6 protect from UV induced apoptosis. In contrast, HPV5 and 8E6 expression in keratinocytes did not result in more viable cells remaining after UV irradiation. However, expression of HPV5E6 in keratinocytes grown in RM+ resulted in a slightly lesser degree of apoptosis, shown in Figure 3-10 D. Nonetheless, even a small reduction in keratinocyte apoptosis in the skin could be relevant to the process of SCC formation, as discussed below.

3.3.2 Sensitivity to death receptor activation

The sensitivity of HT1080 cells to Fas-induced apoptosis was found to be dependent on the composition of the media, as cells grown with glutamine did not undergo apoptosis following incubation with a level of Fas-activating antibody that causes a 30% increase in apoptosis of HT1080s in starvation media. Fas-activating antibody was therefore used to show that expression of HPV5, 18 and 77E6 reduced Fas-induced apoptosis of HT1080s.

High-risk HPV types have been shown to inhibit death receptor apoptosis, in cell lines and keratinocytes (for example Kabsch et al., 2004). There have been several studies which attempt to delineate the mechanism of mucosal high-risk HPVE6 inhibition of apoptosis induced via the death receptor pathway. For example it was observed that the differing sensitivities to Fas-Ab in the cervical cancer cell lines HeLa (HPV18+ve), SiHa and CaSki (both HPV16+ve) and C33A (HPV-ve) depended on differences in levels of apoptotic proteins Fas, caspase 8 and Bid (Hougardy et al., 2005). Several studies have shown that HPV16E6 (but not low risk mucosal HPV6b and 11E6) binds and promotes the degradation of FADD (Fas-associated death domain), therefore inhibiting apoptosis induced by Fas in the U2OS osteosarcoma cell line (Filippova et al., 2004) and TRAIL in the HCT116 epithelial cell line (Garnett et al., 2006). HPV16E6 also inhibits TNF (tumour necrosis factor)-apoptosis by binding to and inhibiting the activity of TNFR1 (TNF receptor 1) in the U937 monocyte and U2OS cell lines (Filippova et al., 2002). It has been shown that the different splice variants of HPV16E6 have different effects, with the ratio of full-length E6 to the short E6* also being important in the reduction of Fas-apoptosis and the reduction or sensitisation to TNF-apoptosis (Filippova et al., 2007) depending on different binding to procaspase 8. As β-HPV types do not express the short E6 splice variant and show many differences in cellular binding partners, along with the differences observed between cell types in response to Fas activation, it could be that the mechanisms of the inhibition of apoptosis seen in this work are different. Indeed, although keratinocyte apoptosis assays could not be used to test the effect of cutaneous HPVE6 expression upon Fas-induced apoptosis specifically (as discussed below), the results of the Proteome Profiler arrays can be used to compare with previous findings on the effect of HPVE6 on the death receptor pathway. The death receptor-associated proteins included on the arrays are TRAILR1, TRAILR2, FADD, Fas and TNFR1. In HT1080s stably expressing HPV5E6, there is a slight increase in FADD, and this

increase is greater in primary keratinocytes expressing HPV5E6 compared to the empty vector control cells. This implies that HPV5E6 does not inhibit Fas-apoptosis by mediating the degradation of FADD as do the high-risk types described above. In keratinocytes expressing HPV5E6, TRAILR1, TRAILR2 and Fas are also slightly upregulated compared to empty vector cells, which suggests these cells would be more susceptible to death receptor activated apoptosis. However changes in apoptotic regulatory proteins further down the cascade could still result in an inhibition of apoptosis, as discussed presently. The activity of the death receptors also depends on their position on the cell surface, which is unknown from the total cellular protein incubated on the arrays. There are no other significant changes in the death receptors tested in either cell type. It is also interesting to consider the non-apoptotic functions of the death receptors, which have been investigated more in recent years (Guicciardi and Gores, 2009). For example, the receptor of TNF (tumour necrosis factor), TNFR1 is constitutively expressed at low levels, and is involved in signalling inflammation along with cell death. The Receptor Interacting Protein (RIP) 1, which can bind to all the death receptors, has several functions mediated by various post-translational modifications. Poly-ubiquitination leads to TNFR1 activation of NF-κB (and therefore survival signals) whereas de-ubiquitination leads to caspase 8 activation (Ea et al., 2006; O'Donnell et al., 2007). Fas activation has also been reported to promote proliferation, migration and cytokine production, through the activation of MAPK pathways and NF-κB (Kreuz et al., 2004), especially in apoptosis-resistant cells. It has been reported that Fas activation of keratinocytes induces a caspase-independent inflammatory response (Farley et al., 2006). Therefore it could be hypothesised that cutaneous HPVE6 upregulates 'death' receptors, along with downstream factors which inhibit apoptosis, and so benefit from the increased survival signalling.

The same Fas-activating antibody was used with primary keratinocytes with the aim of investigating if the reduction of Fas-induced apoptosis by the cutaneous HPVE6 proteins also occurs in the relevant cell type, however no significant Fas-induced apoptosis was observed in the conditions tested. The Fas system of apoptosis induction is thought to be important in the skin's response to UV, for example FasL deficient mice have increased accumulation of mutant p53 following chronic UV exposure (Hill et al., 1999). Several studies have shown an increase in apoptosis in cultured keratinocytes following Fas-activating treatment alone, for example (Leverkus et al., 1997; Sung et al., 1997; Wang et al., 2004a). However frequently other treatment combinations are used; including Interferon-γ which is required for, or increases, Fas-induced apoptosis, for example (Konur et al., 2005; Matsue et al., 1995; Sayama et al., 1994). Interferon-γ is an inflammatory cytokine involved in anti-viral responses, and it sensitises cells to Fas-induced apoptosis by upregulation of pro-apoptotic genes (Ossina et al., 1997). The differences in Fas-induced apoptosis observed may also be due to differences in the differentiation state of the keratinocytes, as basal cells have been suggested to be more resistant to apoptosis, both UV and Fas-induced (Norris et al., 1997). In this work only primary keratinocytes grown in defined serum-free media were tested for Fas-induced apoptosis, whereas growth of the cells in RM+, allowing early differentiation to begin, may result in primary cells becoming sensitive to Fas-Ab. However the NTert keratinocyte cell line were tested in different types of media and still no Fas-induced apoptosis was observed. The Fas death receptor system is important in cutaneous immune responses (Daehn et al., 2009), and it has been hypothesised that reduction of keratinocyte Fas-apoptosis by HPV contributes to immune evasion and viral persistence. Fas has also been implicated in cutaneous autoimmune disorders such as eczematous dermatitis (Trautmann et al., 2000),

which may mean that Fas-induced apoptosis of keratinocytes is augmented by immune co-factors not found in tissue culture systems used here.

3.3.3 Sensitivity to UV-induced apoptosis

The use of Fas-induced apoptosis was supplemented by use of UV irradiation to induce apoptosis in HT1080s, as this is the most relevant stimulus in the formation of skin cancer. The results shown here, that HPV5, 8, 10, and 18E6 expression reduces apoptosis of HT1080s after exposure to a variety of low UV doses, also agrees with previous work (Jackson and Storey, 2000), with the exception that HPV77E6, the HPV type which displayed the weakest anti-apoptotic effect, here did not display significant reduction of apoptosis. In addition it has been shown here that the cutaneous HPV8E6, a 'high-risk' β-type associated with SCC in EV patients, also reduces UV induced apoptosis. These results are important in formulating the hypothesis that cutaneous HPV infection plays a complementary role with UV in the formation of SCC. The reduction of apoptosis following UV irradiation in HPVE6 expressing cells, although not total, could be important in giving a small number of E6-expressing cells a survival advantage, and tipping the balance of apoptosis regulation in favour of allowing UV-damaged cells to proliferate, leading to the accumulation of mutations and increasing the chance of tumourigenesis. However the use of primary keratinocytes in the assays described here is also important in investigating the activity of the E6 proteins in the natural host cell.

As no significant Fas-induced apoptosis of keratinocytes was observed in the assays described here UV irradiation was used to test the effect of cutaneous HPVE6 upon apoptosis in primary keratinocytes. Despite the inhibitory effects of HPV5, 8, 10 and 18E6 on UV-induced HT1080 apoptosis, an increase in viable primary keratinocytes remaining after UV irradiation was not consistently observed

with cells expressing HPV5 and 8E6. However an indication that HPV5 and 8E6 provide some protection from apoptosis is given by the finding that the decrease in viable cells after UV is significantly less in HPV5E6 keratinocytes grown in RM+ (early differentiating) media. This could be due to the retroviral transfection and E6 expression causing cells to have lower 'normal' viability, with the slight protection from apoptosis only apparent after UV irradiation. These results differ from previously published work which has shown inhibition of UV-induced apoptosis of keratinocytes expressing E6 from several HPV types (including 5, 8, 15, 16, 20 and 38, Struijk et al., 2008; Underbrink et al., 2008) possibly due to several reasons. As mentioned, the tissue culture systems used to grow primary keratinocytes vary significantly and affect the growth, morphology and differentiation of the cells, which therefore also affects the apoptotic response. Both EpiLife (serum-free defined) and RM+ (serum replete) were used in this work to enable any differences in apoptosis in HPV5E6 cells to be identified irrespective of the culture system, and indeed the lessening of the decrease in viable cells was only observed in RM+ HPV5E6 keratinocytes. Lethally irradiated fibroblast feeder cells were not included in the keratinocyte culture system here as contamination of the apoptosis assays by these cells gave a high apoptotic reading which masked any changes in the keratinocytes themselves. Previous work has demonstrated an inhibition of UV-induced apoptosis, as shown by decreased CytC release from the mitochondria, in keratinocytes expressing HPV16, 8 and 38E6 (Underbrink et al., 2008). However the cells used were derived from foreskin keratinocytes and as neonatal cells they may have slightly different growth patterns and apoptotic responses to the adult cutaneous keratinocytes used in this work. Further studies have also showed inhibition of UV-induced apoptosis in keratinocytes measured by TUNEL and active caspase 3; however in this case the cells were expressing both E6 and E7 from HPVs 5, 8, 15 and 20 (Struijk et al., 2008). HPV8E6 alone was used to demonstrate that E6 is responsible for the inhibition of apoptosis, however the

inclusion of E7 could have stabilised the effect of E6 making it more robust in this study. The variability in apoptotic responses in primary keratinocytes is also highlighted by the different effects of HPV16E6, included in both the above studies as a comparative high-risk α type, and which decreased UV-induced apoptosis in the former but increased it in the latter.

3.3.4 Apoptosis in basal keratinocytes

It has been proposed that keratinocyte resistance to UV-induced apoptosis is greater in the basal compartment allowing protection of the amplifying stem cells by 'integrin-mediated survival signals' (Norris et al., 1997). The importance of the basal keratinocyte compartment is also highlighted by the fact that UV-induced DNA damage in these cells is an important factor in tumour formation (Jans et al., 2006). Therefore UV-induced apoptosis of basal keratinocytes was investigated with respect to the activity of HPV5E6 by the inclusion of the basal marker α6 integrin in the flow cytometry assays. It was seen here that, especially in RM+ media, the 20% of keratinocytes expressing the most α6 integrin (taken to be basal cells) are more viable post UV-irradiation that the total population. This agrees with previous work on keratinocyte anoikis (cell death induced by detachment from the extracellular matrix) where 'stem cell' keratinocytes highly expressing α6β4 integrin are protected from apoptosis (Tiberio et al., 2002). When retrovirally infected keratinocytes were tested, at higher UV doses, the basal fraction of the pLXSN population were not significantly more viable then the total population, whereas the HPV5E6 expressing basal cells were more viable that the total HPV5E6 population. However although the effect of HPV5E6 was different from the pLXSN cells, it was not sufficiently different from the non-transduced cells used to investigate further.

3.3.5 Changes on the apoptotic protein arrays

Although the assays described here measuring apoptosis showed no reproducible increase in viable keratinocytes expressing HPV5E6 post UV, as discussed above, it is possible that even though the end point of apoptosis as measured by downstream markers of AnnexinV/PI is unchanged, apoptotic proteins further upstream may be modified by HPV5E6 expression, which although not enough to inhibit apoptosis in the system used here, may nevertheless affect the balance of pro- and anti-apoptotic factors enough to inhibit apoptosis in the skin, and therefore be important in HPV-associated UV-induced SCC formation. As a result the Proteome Profiler arrays are useful in investigating possible mechanisms of cutaneous HPVE6 modification of apoptosis. Changes in death receptor related proteins have been discussed above. Of the other changes highlighted by the arrays, we first considered those which were seen in HPV5E6 HT1080s and primary keratinocytes. As shown in Figure 3-3 E, these include baseline upregulation (of >1.5 fold) by HPV5E6 of Bcl2, Bcl-x, cIAP2, claspin, clusterin, p53(S46) and TNFR1. The inclusion of an apoptotic form of p53 on this list is unexpected as it is derived from viable cell populations, however it can be seen that the actual protein levels are very low and so this apparent upregulation is unlikely to be biologically significant. The same is true of TNFR1 where the upregulation seen is due to the initial very low levels. cIAP2 also has a low expression level in HPV5E6 HT1080s and keratinocytes, and Bcl2, claspin and clusterin display low levels in keratinocytes, which makes it more difficult to assign significance to the upregulation. However small changes in some of these proteins may still have significant effects on apoptosis due to their regulatory function. For example Bcl2 and Bcl-x are pro-survival members of the Bcl2 family which antagonize the activity of the apoptotic Bak and Bax proteins through a system of interactions which also involves the BH3-only Bcl2 family members (Lessene et al.,

2008) and the balance of which affects release of apoptotic factors from the mitochondria. The western blot of Bcl2 in keratinocyte lysates is inconclusive, showing an increase in EpiLife, but a decrease in the HPV5E6 lysates which previously showed an increase on the array. Bcl2 seems to be expressed at low levels in normal keratinocytes, mostly in basal cells, but over-expression has been shown to inhibit UV-induced apoptosis *in vitro* and *in vivo* (Assefa et al., 2003; Takahashi et al., 2001). It appears that other anti-apoptotic Bcl2 family members also have an important role in keratinocyte apoptosis. The upregulation of Bcl-x by HPV5E6 seen on the array and repeated in 2 out of 3 of the western blots of RM+ keratinocytes could be relevant to SCC formation. Over-expression in mouse skin (driven by the Keratin14 promoter) increased resistance to UV irradiation (Pena et al., 1997), and Bcl-x_L knockdown in the basal keratinocytes of mice increased UV-induced apoptosis (Kim et al., 2009). Bcl-x is expressed in basal keratinocytes which are protected from anoikis (Tiberio et al., 2002), and an increase in expression has been observed in SCCs compared to keratoacanthomas (a benign skin lesion) (Vasiljevic et al., 2009). It has also been found in a study on epithelial mesenchymal transition using gingival keratinocytes expressing HPV16E6/E7 that Bcl-x is upregulated (Chamulitrat et al., 2009).

The Inhibitor of Apoptosis (IAP) protein family is also important in the regulation of apoptosis as they inhibit caspases (Roy et al., 1997), with more recent work describing the variation in their structure and function (Mace et al., 2010). cIAP1, Survivin and XIAP are upregulated (by >1.5 fold) in keratinocytes expressing HPV5E6, Livin is upregulated in HT1080s expressing HPV5E6, and cIAP2 in both. Several of the IAP family members are expressed in keratinocytes and therefore could be involved in the UV response. Primary foreskin keratinocytes have been shown to express Livin, and low levels of XIAP, cIAP1 and 2 (Bowen et al., 2003). XIAP expression has also been noted in primary keratinocytes (Leverkus et al., 2003), and the western blots performed here showed XIAP expression along with

slight upregulation by HPV5E6 keratinocytes grown in RM+. It has also been observed that oral keratinocytes expressing HPV16E6/E7 show increased cIAP2 expression which has a role in resistance to apoptosis (Yuan et al., 2005), and the western blots for cIAP2 performed here also show an increase in cIAP2 in RM+ HPV5E6 keratinocytes.

Claspin is a checkpoint protein which is phosphorylated upon DNA damage, and during apoptosis is cleaved by caspase 3/7 and degraded by the proteosome, and the increase in apoptotic human fibrosarcoma cells in which Claspin has been downregulated by siRNA points to a role in apoptosis regulation (Semple et al., 2007). Clusterin is expressed as a secreted glycoprotein and a nuclear form and is thought to inhibit the effects of Reactive Oxygen Species (ROS), for example protein aggregation and precipitation, and it is this which gives it cytoprotective prosurvival properties (Trougakos and Gonos, 2009). Although both claspin and clusterin are upregulated in HPV5E6 expressing keratinocytes, the protein levels as indicated by the array are low, so it is more difficult to identify if they are have a significant role.

Of the other proteins that are described as upregulated in HPV5E6 expressing keratinocytes, several display low absolute protein levels which again makes it more difficult to ascribe biological significance. These include the pro-apoptotic protein Bax, HIF1 (hypoxia inducible factor 1), HO1 (heme oxygenase 1, or Hsp32), PON2 (paraoxonase 2), p27, p53(S392), and pRad17(S635). However several of the upregulated proteins could be important in HPVE6 mediated inhibition of keratinocyte apoptosis. For example, HO2 (heme oxygenase 2) is an enzyme which cleaves heme to release products with anti-oxidant, and also anti-apoptotic, properties, and has been shown to inhibit apoptosis, for example in endothelial cells (Basuroy et al., 2006).

The heat shock protein, Hsp 70, which is upregulated in HPV5E6 expressing keratinocytes at both 0 and 30 mJ/cm^2, is well known to inhibit apoptosis induced

by stressors including TNF, ROS, and radiation (Jaattela et al., 1998), through its function as a chaperone protein which refolds or targets for degradation proteins damaged by these stressors. It is also known that Hsp70 is expressed in the skin and upregulated upon UV irradiation (Jonak et al., 2006) which agrees with the results from this array seen with pLXSN keratinocytes. Expression of HPV16E6 in human foreskin keratinocytes also causes upregulation of Hsp70 (Merkley et al., 2009). Hsp70 has been found to reduce UV induced apoptosis and inflammation *in vitro* and *in vivo* (Matsuda et al., 2009); therefore its upregulation by HPV5E6 could play an important part in reduction of keratinocyte apoptosis. The upregulation of the apoptotic mediator proteins HtrA2/Omi and Smac/DIABLO seen in HPV5E6 expressing keratinocytes seems contrary to the proposed inhibition of apoptosis by E6. HtrA2/Omi (high temperature requirement protein A2) is a serine protease which is transported to the mitochondrial intermembrane space where it is processed to its active form and has a role in maintaining mitochondrial integrity (Vande Walle et al., 2008). Smac/DIABLO (second mitochondria-derived activator of caspases/Direct IAP binding protein with low PI) is also located in the mitochondria. However the apoptotic function of both of these proteins only occurs when they are released from the mitochondria and can inhibit the activity of the IAPs (Wang and Youle, 2009), therefore the level of these proteins seen in the total cellular lysates applied to the arrays is not necessarily related to their activity levels. This is also true of CytC, which is released from the mitochondria during apoptosis, but there is no difference in the levels seen on the arrays after UV treatment, even when an increase in cleaved caspase 3 indicates apoptosis is progressing. A possible upregulation of pro-apoptotic proteins by the cell in response to expression of a viral protein would be ineffective if their release from the mitochondria or subsequent activity is inhibited.

The anti-apoptotic Bcl2 family member Mcl1 was not included on the Proteome profiler arrays but its expression in HT1080s and keratinocytes expressing HPVE6s

was tested by western blot, as it has been shown to be expressed in keratinocytes, and its degradation is essential for UV-induced apoptosis to proceed (Nijhawan et al., 2003; Sitailo et al., 2009). However although it was upregulated in HT1080s expressing HPV5, 8, 10 and 18E6, there was no reproducible increase in the keratinocyte lysates tested. Also, in a study investigating apoptosis in HPVE6 expressing keratinocytes, HPV16, 8 and 38E6 had no significant effect on Mcl1 levels (Underbrink et al., 2008).

3.3.6 Further work

More work utilising different keratinocyte culture systems could be used to further investigate apoptosis of primary cells, for example Fas-Ab induced apoptosis in RM+ media, and the affect on apoptosis when HPVE6 keratinocytes are used for organotypic raft generation. Different assays may also shed more light on the apoptotic responses of HPVE6 keratinocytes, for example immunofluorescence detecting apoptotic markers in keratinocytes grown in different media with a range of apoptosis-inducers. Additionally assays looking at other aspects of mitochondrial integrity such as membrane potential and release of apoptotic factors could be used to further investigate the roles of Bcl2 family members, and the effect of HPVE6. Further work on the response of basal keratinocytes to apoptosis may also be beneficial in delineating the role of HPVE6 in this cell population. Lysates generated from both HT1080s and primary keratinocytes treated with both Fas-Ab and UV irradiation could be used for western blots to look at any changes in apoptosis regulators and markers to identify any changes caused by HPVE6 expression. It would also be useful to follow up the most interesting changes seen on the Proteome Profiler arrays, namely Bcl-x_L, cIAP1 and Hsp70 especially in primary keratinocytes, to investigate the mechanism of apoptosis inhibition. The observation that Bcl-x_L appears to be phosphorylated is also interesting and further

work to confirm this and investigate the effect on apoptosis would be beneficial. Additionally it would be interesting to investigate the upregulation of death receptors in HPV5E6 expressing primary keratinocytes as seen on the arrays, with respect to recent elucidation of the non-apoptotic survival signalling mediated by these receptors, particularly in apoptosis-resistant cells.

4 Investigation of the changes in factors secreted by cells expressing cutaneous Human Papillomaviruses E6 protein

4.1 Introduction

Preliminary unpublished observations from this lab during experiments on Fas-induced apoptosis of HT1080s which had been transfected with plasmids expressing E6 from HPV types 5, 10, 18 and 77, along with GFP (green fluorescent protein) as an expression marker, found that apoptosis was reduced in the E6/GFP expressing cells, but also in the non-GFP and therefore non-E6 expressing cells. The explanations put forward for this were that the level of transfection was too low to allow visible GFP expression but E6 expression was still protecting the cells; or that E6 expression was reducing apoptosis in neighbouring, non-E6 expressing cells. It has also been observed that in HPV-positive SCC sections the level of apoptosis (as judged by TUNEL staining) was significantly lower than in HPV-negative SCCs (Jackson et al., 2002), despite similar levels of proliferation and lack of HPV-positivity in all cells. In cervical cancer caused by high-risk mucosal HPVs, expression of the viral E6 and E7 oncoproteins, and the inhibition of apoptosis this results in, is detected in every cell and is required for maintenance of the transformed cellular state (Doorbar, 2006). Viral load analysis has also revealed high HPV DNA levels in hair follicles and skin lesions of EV patients (Dell'Oste et al., 2009). However the viral load of HPV in SCCs of immunosuppressed transplant patients is low, with an estimated copy number of one HPV genome per 20-5000 cells, and HPV DNA is undetectable by *in situ* hybridization in the majority of tumour cells (Dang et al., 2006). This has meant that the mechanism of tumour formation in HPV-associated SCC has been difficult to delineate. However when

this is considered together with the observed reduction in overall apoptotic rates in HPV-positive SCCs, it can be hypothesised that high-risk cutaneous HPV expression reduces apoptosis in neighbouring non-infected cells. Such a 'bystander effect' could play an important role in tumourigenesis, with persistent low levels of HPV providing neighbouring cells with protection from apoptosis, permitting cell survival and allowing accumulation of UV-induced DNA damage. This hypothesis could also help explain the proposed role of cutaneous HPV early in tumourigenesis (Weissenborn et al., 2005) and the low levels of HPV in SCC.

4.1.1 Aims

As has been described above, various lines of evidence suggest that expression of E6 from several HPV types could inhibit apoptosis of expressing cells but also of non-E6 expressing, neighbouring cells. The aim of these experiments was to investigate this bystander effect and to delineate the mechanism, in both HT1080 cells and primary human keratinocytes. The relevance of the protection of non-E6 expressing cells by cutaneous HPVs in SCC formation was also investigated.

4.2 Results

4.2.1 Co-culture of EGFP and E6 expressing HT1080s

Preliminary observations in the lab made during investigations of the inhibition of Fas-induced apoptosis of HT1080s suggested that cutaneous HPV E6 expression also reduced apoptosis in non-E6 expressing cells. In that work (unpublished data) HT1080s were transfected with HPV 5, 10, 18 and 77E6 plasmids along with a plasmid expressing Green Fluorescent Protein (GFP) used as a marker of E6 expression. Fas-induced apoptosis was then assayed with AnnexinV/PI flow cytometry, along with cell sorting based on GFP fluorescence. It was observed that GFP-negative cells from the same cultures as E6/GFP expressing cells also

displayed reduced Fas-induced apoptosis. It was suggested that this could be due to cells being transfected with low levels of the plasmids, meaning E6 expressing cells did not appear GFP positive, or that E6 expressing cells affected apoptosis in non-E6 expressing cells. To investigate this observation more thoroughly, the HT1080 cells stably expressing HPV5, 8, 10, 18 and 77E6, as described previously and shown in Figure 3.1, were used along with HT1080s stably expressing Enhanced Green Fluorescent Protein (EGFP). EGFP was expressed from a pcDNA vector which was transfected into HT1080s and selected for as described. EGFP expression was confirmed by fluorescent microscopy observation of the cells showing more than 90% of the cells glowing green. Use of the cells in FACS assays also allowed continuous observation of green fluorescence. In the AnnexinV/PI FACS assay with EGFP expressing cells, it was observed that the high levels of EGFP expression caused bleed-through of the EGFP signal into the PI detection channel, which compensation was not able to resolve. This caused unstained, viable EGFP cells to appear PI positive, which corresponds to the upper left quadrant of the viability dotplot in which necrotic cells are usually seen in AnnexinV/vital dye apoptosis assays, as illustrated in Figure 4-1 A, and also masks any shift in PI positivity caused by cells undergoing apoptosis. As a result the vital dye 7AAD was used in place of PI, with detection in the PECy5 channel, which allowed quantification of apoptosis.

Mixing experiments were first performed in which HT1080s stably expressing EGFP were cultured alone, or with HT1080s expressing HPV5, 8, 10, 18 and 77E6, in a 1:1 ratio for 24 hrs. Apoptosis was then induced with 100ng Fas-activating antibody (Fas-Ab) and cells harvested 16 hrs later. Flow cytometry was used to measure apoptosis as described, with the additional measurement of EGFP fluorescence. The amount of apoptosis of the EGFP positive portion of either the co-cultures or the respective EGFP-only cultures was calculated and Figure 4-1 B

shows the fold change in apoptosis in EGFP cells co-cultured with HPV5, 8, 10, 18 or 77E6 expressing cells compared to EGFP cells cultured alone.

It can be observed that there is no significant difference in apoptosis when EGFP cells are cultured with empty vector pcDNA cells, however the amount of Fas-induced apoptosis in EGFP cells is significantly reduced when they are co-cultured with HPV5 and 18E6 expressing cells. The amount of apoptosis in co-cultures with HPV8 and 10E6 appeared lower, but this did not reach significance as there was a large variation in the apoptotic response of EGFP cells. It was also observed that EGFP cells have a higher baseline rate of death in culture and are more sensitive to Fas-induced apoptosis, as shown in Figure 4-1 C, where there are 20% fewer viable EGFP cells than parental HT1080 cells 16 hrs after the same dose of Fas-Ab. This may be due to the stress on the cells of continually over-expressing EGFP. It also became apparent that cells lose EGFP fluorescence as they undergo apoptosis, making it very difficult to distinguish in the co-cultures between E6 expressing cells and EGFP cells undergoing apoptosis.

The finding that HT1080s stably expressing HPV5 and 18E6 significantly reduce Fas-induced apoptosis in co-cultured EGFP expressing cells may be significant in the formation of SCC. Cutaneous HPV E6 expression may mediate this protection from apoptosis by influencing factors secreted from E6 expressing cells, or cell-cell contact may be necessary.

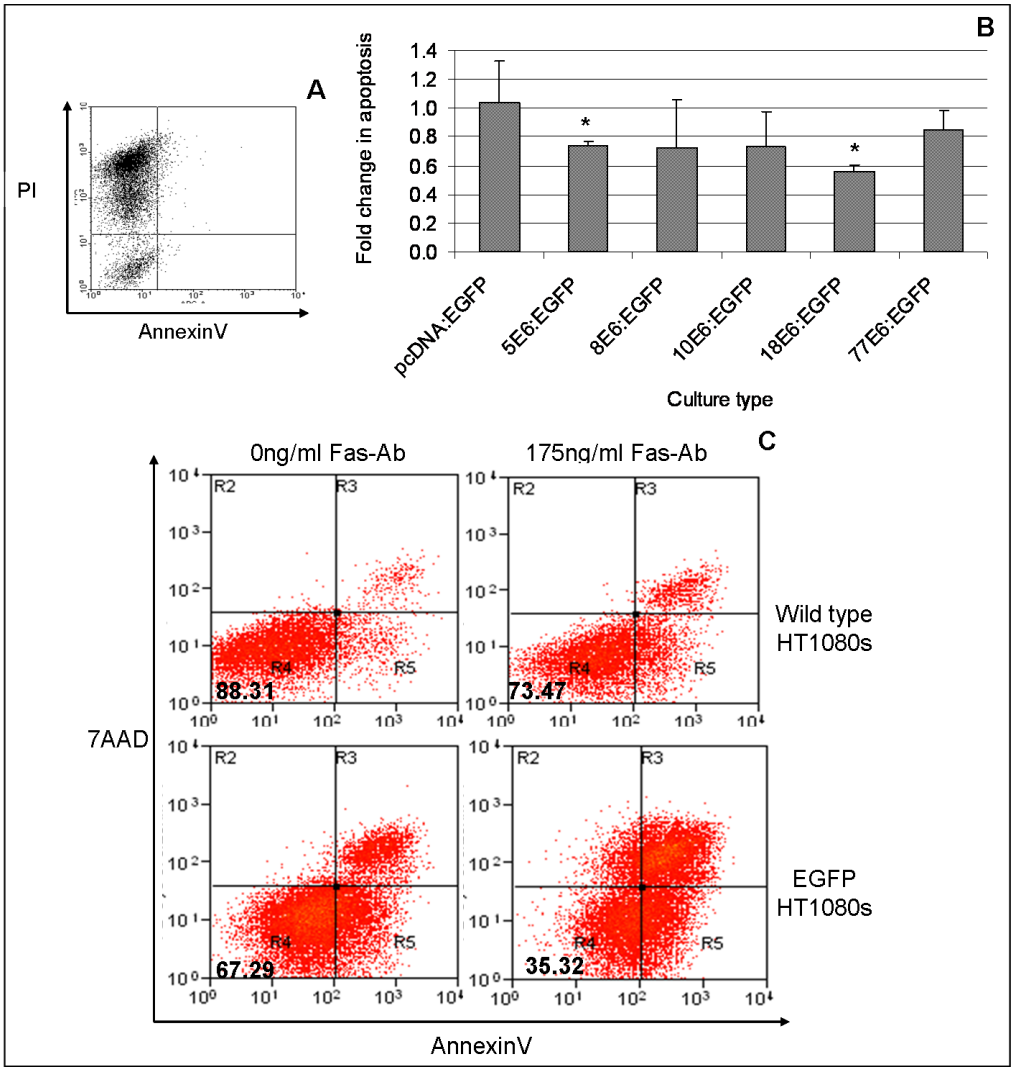

Figure 4-1 HT1080s expressing EGFP cultured with HPV E6 expressing HT1080s are protected from Fas-induced apoptosis

A Viability dotplot of EGFP-expressing HT1080s which were harvested and analysed for apoptosis by AnnexinV/PI flow cytometry.

B EGFP-expressing HT1080s were cultured alone, or with equal numbers of HPV E6-expressing cells as indicated, treated with 100 ng/ml Fas-Ab and apoptosis measured 16 hrs later. The amount of apoptosis in the EGFP positive portion of each co-culture was compared to the amount of apoptosis in the EGFP positive portion of concurrent EGFP-only cultures, and the fold change in apoptosis displayed. * Apoptosis of EGFP positive cells is significantly reduced in HPV5E6 (P= 0.0001) and HPV18E6 (P= 0.0007) co-cultures, 3 replicates.

C EGFP-expressing and parental HT1080s were treated with 0 or 175 ng/ml Fas-Ab, harvested after 16 hrs and apoptosis measured with AnnexinV/7AAD. Viability dotplots displaying the percentage of cells remaining in the viable quadrant are shown, indicating the increased susceptibility to Fas-induced apoptosis of EGFP cells.

4.2.2 Conditioned media from HPV E6 expressing HT1080s reduces apoptosis in untransfected HT1080s

To define how cutaneous HPV E6 expression protects neighbouring non-expressing cells from apoptosis and to avoid the problems inherent with the use of EGFP cells in the co-culture assays (with respect to their differing apoptotic response as outlined above), conditioned media swap experiments were performed. HT1080s stably expressing HPV5 and 8E6 were cultured in media not containing glutamine, to allow subsequent testing of Fas-induced apoptosis, and supplemented with dialysed serum to reduce possible affects of other growth factors. The media was harvested after 48 hrs and stored at -20 °C until it was used to culture parental HT1080 cells for 24 hrs. Apoptosis was then induced with 100 ng/ml Fas-Ab in fresh aliquots of the conditioned media and measured 16 hrs later with AnnexinV/PI. It can be seen in Figure 4-2 A that untransfected HT1080s cultured in media conditioned by growth with HT1080s expressing HPV5 and 8E6 undergo significantly less Fas-induced apoptosis than cells cultured in media conditioned with untransfected HT1080s (reduced from 40% apoptosis to 30% for HPV5E6 [P= 0.0037] and 25% for HPV8E6 [P= 0.0034]). The results of further experiments carried out using media conditioned by growth of HT1080s containing empty vector pcDNA or HPV5, 8, 10, 18 and 77E6 are presented in Figure 4-2 B. Here the levels of apoptosis of parental HT1080s cultured in the indicated media type have been compared to the level of apoptosis in the concurrent cells cultured in parental HT1080 conditioned media, and the fold change presented. Fas-induced apoptosis is significantly reduced in untransfected cells cultured in media conditioned by HPV5, 8, and 18E6 (by 0.6 fold with HPV5E6 [P= 0.024]; 0.7 fold with HPV8E6 [P= 0.0002]; and 0.16 fold with HPV18E6 [P= 0.03]). There is no significant difference in the level of apoptosis in cells cultured in pcDNA and 77E6

HT1080 conditioned media, and growth in 10E6 conditioned media significantly increases apoptosis (by 2 fold, P= 0.019).

To further investigate the inhibition of apoptosis by HPV E6 conditioned media, apoptosis in response to UV was tested. HT1080s stably expressing pcDNA, HPV5, 8, 10, 18 and 77E6 were cultured in media supplemented with dialysed serum for 72 hrs, the media was harvested and used to culture parental HT1080s for 24 hrs. Cells were UV irradiated, fresh aliquots of conditioned media added back and apoptosis measured 16 hrs later by AnnexinV/PI. Due to the length of time the media was conditioned for, it was supplemented with 1/3 (final volume) fresh non-conditioned media to ensure nutrient supply for the parental cells. Figure 4-2 C shows that culture of parental cells in media conditioned with growth of pcDNA cells significantly decreases apoptosis following UV irradiation, from 17% to 5.5% at 2.5 mJ/cm^2, and from 34% to 12% at 5 mJ/cm^2. This is presumably due to the fact that the standard production of growth or survival factors by these cells provides some protection from apoptosis. However growth of parental cells in media conditioned with HPV5 and 18E6 further reduces apoptosis (to 3% with HPV5E6 at 5 mJ/cm^2 [P= 0.001], and to 0.5% with HPV18E6 at 2.5 mJ/cm^2 [P= 0.031]), indicating that HPV5 and 18E6 expression influences the secretory profile of cells which confers additional, nearly complete, resistance to apoptosis at these low UV doses. This could be due to HPV5 and 18E6 increasing levels of the survival factors already secreted by empty vector control cells, or due to the induction of different factors. Interestingly growth of parental cells in HPV77E6 conditioned media significantly increased apoptosis after 5 mJ/cm^2, to 16% (P= 0.005).

Although HPV types 5 and 8 are both from HPV species 1 of the β-genus and are both closely associated with SCC in EV patients (Pfister, 2003), it is interesting to note while conditioned media from both confers protection from Fas-induced apoptosis, the protection from UV-induced apoptosis by HPV8E6 conditioned

media did not reach significance, due to the large variability observed here. When considered with the results from Chapter 3, which showed reduction in UV-induced apoptosis but no reduction of Fas-induced apoptosis of HPV8E6 expressing cells, it appears that HPV8E6 may have a subtle effect which was not significantly detected in all of the assays described here. Further repetition of this assay may allow subtle differences to reach significance. However conditioned media from HPV8E6 expressing HT1080s was included in subsequent assays to investigate any changes.

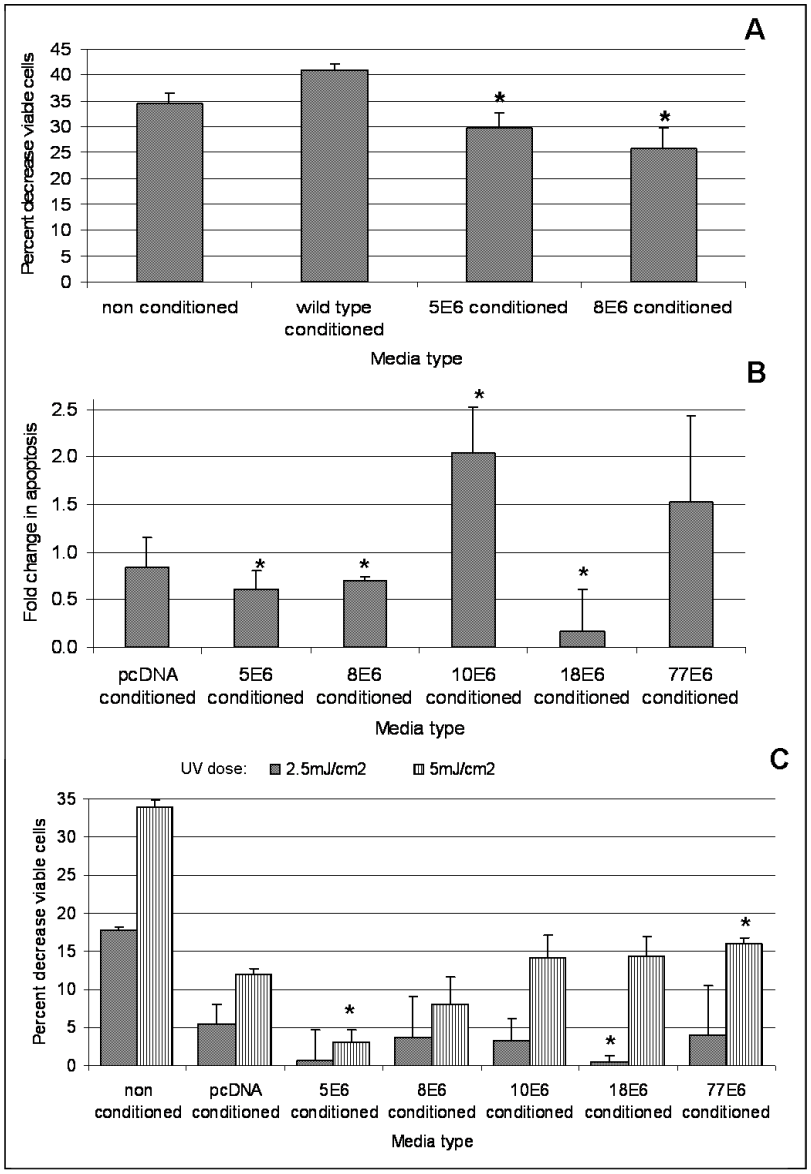

Figure 4-2 Conditioned media from HT1080s expressing HPV5, 8, and 18E6 reduces apoptosis in parental HT1080s.

A HT1080s were cultured for 24 hrs in media conditioned for 48 hrs with HT1080s expressing the indicated E6 types, and apoptosis measured 16 hrs after addition of 100 ng/ml Fas-Ab. The decrease in viable cells compared to 0 ng/ml Fas-Ab is presented, for **A**, **B** and **C**, error bars indicate standard deviation, 3 replicates.

B Media conditioned by 24 hrs growth with pcDNA, HPV10, 18 and 77E6 or 48 hrs growth with HPV5 and 8E6 cells was used to culture parental HT1080s for 24 hrs, and apoptosis induced with 100 ng/ml Fas-Ab and measured 16 hrs later with AnnexinV/PI. The amount of apoptosis was compared to apoptosis in the respective parental cells cultured in parental conditioned media, and the fold change is presented.

C HT1080s were cultured for 24 hrs in media conditioned with the indicated cell type for 72 hrs; apoptosis induced with UV irradiation and measured 16 hrs later with AnnexinV/PI. The decrease in viable cells compared to 0 mJ/cm^2 UV samples is presented.

4.2.3 Conditioned media from HPV5E6 expressing keratinocytes reduces apoptosis in parental keratinocytes

To test if HPV5E6 has a comparable effect on UV induced apoptosis of non-E6 expressing primary keratinocytes, the natural host cell of HPV, conditioned media experiments were also performed on these cells. Primary keratinocytes stably expressing pLXSN empty vector or HPV5E6, generated as described previously, were cultured in both EpiLife and RM+ medias for 48 hrs. The harvested media was then used to culture primary keratinocytes for 24 hrs; apoptosis was induced with UV irradiation and measured after 16hrs with AnnexinV/PI. Figure 4-3 shows the decrease in viable parental cells post UV when cultured in the indicated media types, EpiLife in A and RM+ in B. Parental cells cultured in HPV5E6 conditioned RM+ media undergo significantly less apoptosis than parental cells cultured in pLXSN media post 40 mJ/cm^2 UV (19% compared to 28%, P= 0.008). There is a small decrease in apoptosis in parental cells cultured in HPV5E6 conditioned EpiLife post 30 mJ/cm^2 (53% compared to 59%) however it does not reach significance. In the baseline non-conditioned media, cells cultured in RM+ are more resistant to UV induced apoptosis, as seen in Chapter 3 and as shown here by a 33% increase in apoptotic cells after 40 mJ/cm^2 UV, while in EpiLife media there is a 33% increase after 15 mJ/cm^2. Similarly to the response to UV irradiation of HT1080s cultured in conditioned media, RM+ media conditioned by pLXSN cells provides some protection from apoptosis induced by 40 mJ/cm^2 UV (28% compared to 34% apoptosis), presumably due to the secretion of normal growth factors, which is modified by HPV5E6 expression to further increase the resistance to UV-induced apoptosis of keratinocytes, resulting in 10% fewer apoptotic cells. A small but significant reduction in apoptosis would nevertheless have an impact on keratinocyte survival in the skin and be relevant to SCC formation. That the protective effect of HPV5E6 conditioned media is only observed in RM+ could

indicate that the survival signalling is activated to a significant level only in keratinocytes grown in media with certain supplements, which may potentiate the signalling pathways. Media conditioned by growth of primary keratinocytes expressing HPV8E6 was also used to culture parental keratinocytes, however no significant difference in the apoptotic response was observed in the conditions tested.

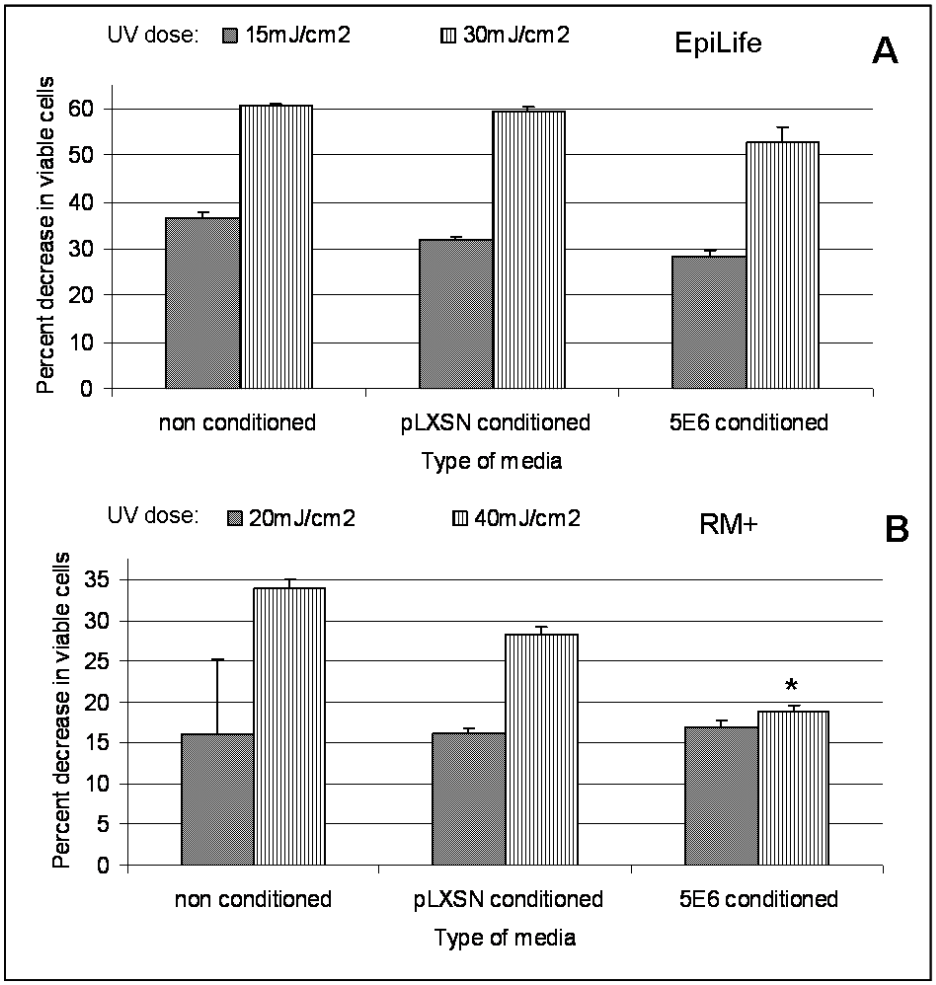

Figure 4-3 UV induced apoptosis of primary keratinocytes cultured in conditioned media.

Keratinocytes were cultured for 24 hrs in media conditioned with the indicated cell type for 48 hrs, and the decrease in the percentage of viable cells remaining after UV irradiation indicated, for EpiLife media in A and RM+ in B, * P = 0.008, 2 replicates.

4.2.4 Identification of changes in secreted factors from HT1080s

To identify E6-specific changes in the secretion of factors that could mediate the reduction in apoptosis in neighbouring HT1080 cells, media conditioned by growth for 72 hrs with HT1080s or HT1080s expressing HPV5 and 8E6 was incubated overnight with cytokine arrays, which were then washed, probed with detection antibodies and developed as described in Materials & Methods, section 2.3.4. To allow comparison, 174 cytokines and growth factors are included along with control spots on each array. Image J was used to quantify the pixel density for each spot which was normalised according to the background, and positive control spots, and the relevant protein abundance calculated relevant to levels in parental conditioned media. Figure 4-4 shows the results of the arrays, with Figure 4-4 A showing an example of changes in the secretion of two cytokines, Interleukin (IL) 6 and Osteoprotegerin (OPG), and the quantified results presented in Figure 4-4 B. Additionally, the results are presented graphically along with the results of the same arrays performed with keratinocyte conditioned media in Figure 4-5 C to allow visualisation of significant changes, which are discussed presently.

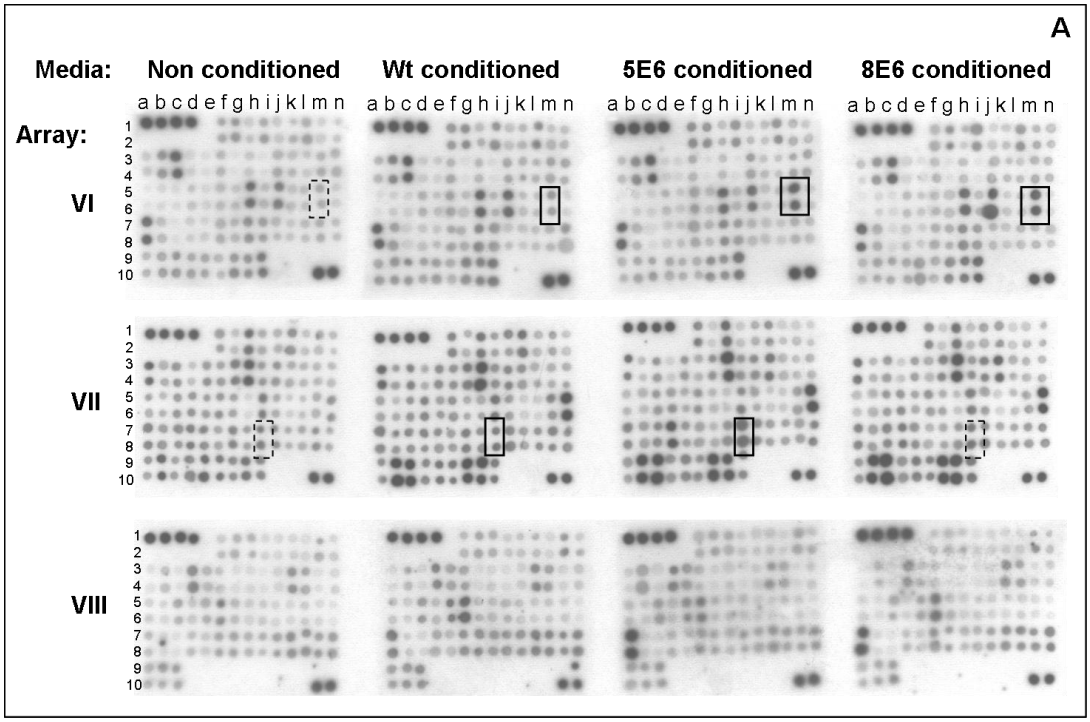

Figure 4-4 Results of the cytokine arrays showing changes in cytokine secretion relative to normal HT1080 conditioned media.

A Arrays are incubated with the indicated media type and the spots, arranged in vertical pairs for each cytokine, are then quantified to allow calculation of relative protein abundance. The boxes show the upregulation of IL6 on Array VI (M 5,6) in HPV5 and 8E6 conditioned media, and of OPG on Array VII(I 7,8) in HPV5E6 conditioned media, with the dashed boxes showing the baseline and unchanged levels.

B Table showing the fold changes (test value/control value), and significance, of the relative abundance of each protein in the indicated conditioned media compared to parental conditioned media (split over two pages), with IL6 and OPG highlighted in yellow.

Array VI		Conditioned media type				Array VII		Conditioned media type			
		5E6		8E6				5E6		8E6	
Position	Cytokine	Fold	P	Fold	P	Position	Cytokine	Fold	P	Fold	P
A 3,4	Eotaxin2	0.51	0.016	0.67	0.389	A 3,4	CTACK	0.69	0.038	0.84	0.013
A 5,6	IGF4	-1.92	0.0002	1.25	0.351	A 5,6	ICAM-1	0.68	0.001	0.73	0.049
A 7,8	Leptin	0.88	0.146	1.02	0.836	A 7,8	I-TAC	0.89	0.514	0.88	0.396
A 9,10	PDGF-BB	0.42	0.036	0.82	0.237	A 9,10	TECK	1.10	0.554	1.15	0.075
B 3,4	Eotaxin 3	0.92	0.244	0.94	0.396	B 3,4	Dtk	0.58	0.061	0.79	0.224
B 5,6	IL 10	0.44	0.033	0.97	0.808	B 5,6	ICAM - 3	1.25	0.339	1.48	0.104
B 7,8	LIGHT	0.51	0.044	0.92	0.432	B 7,8	Lymphotactin	1.17	0.086	1.23	0.048
B 9,10	RANTES	0.58	0.059	0.92	0.645	B 9,10	TIMP-1	1.00	0.957	1.00	0.973
C 3,4	FGF-6	0.93	0.347	1.02	0.297	C 3,4	EGF-R	0.85	0.181	0.93	0.417
C 5,6	IL 13	0.68	0.107	0.90	0.508	C 5,6	IGFBP-3	1.13	0.327	1.08	0.384
C 7,8	MCP-1	0.16	0.021	0.94	0.560	C 7,8	MIF	1.22	0.073	1.32	0.078
C 9,10	SCF	0.68	0.189	0.93	0.457	C 9,10	TIMP-2	1.14	0.098	1.18	0.036
D 3,4	FGF-7	0.65	0.170	1.03	0.739	D 3,4	ENA-78	0.70	0.064	0.80	0.126
D 5,6	IL15	0.68	0.011	0.89	0.093	D 5,6	IGFBP-6	0.92	0.379	0.92	0.287
D 7,8	MCP-2	0.56	0.073	1.30	0.152	D 7,8	MIP-1alpha	2.10	0.029	1.39	0.180
D 9,10	SDF-1	0.81	0.046	1.27	0.007	D 9,10	Thrombopoietin	1.31	0.029	1.25	0.022
E 3,4	Flt-3 ligand	0.41	0.015	0.77	0.393	E 3,4	Fas	0.86	0.246	0.80	0.039
E 5,6	IL 16	0.62	0.135	0.89	0.582	E 5,6	IGF1-sr	0.88	0.057	0.93	0.076
E 7,8	MCP-3	0.82	0.148	1.05	0.633	E 7,8	MIP-1beta	1.02	0.787	1.19	0.051
E 9,10	TARC	0.51	0.005	1.53	0.020	E 9,10	TRAIL R3	1.22	0.007	1.21	0.002
F 1,2	Angiogenin	1.07	0.505	0.98	0.906	F 1,2	Acrp30	1.03	0.701	0.99	0.915
F 3,4	Fractaline	0.75	0.288	0.97	0.880	F 3,4	FGF-4	0.72	0.005	0.83	0.094
F 5,6	IL1 alpha	1.01	0.688	0.80	0.041	F 5,6	IL1 R4	0.99	0.826	1.01	0.881
F 7,8	MCP-4	1.19	0.489	1.15	0.336	F 7,8	MIP3 beta	1.21	0.032	0.89	0.415
F 9,10	TGF-beta 1	0.75	0.086	1.21	0.242	F 9,10	TRAIL R4	1.12	0.598	1.12	0.531
G 1,2	BDNF	0.84	0.159	0.94	0.209	G 1,2	AgRP	0.75	0.187	0.95	0.755
G 3,4	GCP-2	-0.03	0.010	1.13	0.311	G 3,4	FGF-9	0.66	0.009	0.85	0.197
G 5,6	IL1 beta	0.91	0.610	1.24	0.150	G 5,6	IL1-R1	1.10	0.504	1.22	0.250
G 7,8	M-CSF	0.64	0.065	0.99	0.876	G 7,8	MSP-alpha	0.61	0.039	0.63	0.000
G 9,10	TGF-beta 3	0.73	0.070	1.07	0.516	G 9,10	uPAR	1.09	0.100	1.08	0.103
H 1,2	BLC	0.53	0.050	0.91	0.715	H 1,2	Angiopoietin 2	1.24	0.025	1.14	0.020
H 3,4	GDNF	0.57	0.072	1.07	0.617	H 3,4	GCSF	0.99	0.823	0.96	0.420
H 5,6	IL-1ra	0.91	0.153	1.10	0.227	H 5,6	IL 11	0.76	0.249	0.69	0.176
H 7,8	MDC	0.80	0.091	1.08	0.448	H 7,8	NT-4	1.23	0.246	1.05	0.794
H 9,10	TNF-alpha	0.69	0.011	1.16	0.053	H 9,10	VEGF	1.00	0.995	1.13	0.295
I 1,2	BMP-4	0.86	0.546	1.31	0.346	I 1,2	Amphiregulin	0.76	0.125	1.00	0.951
I 3,4	GM-CSF	-0.20	0.043	0.68	0.215	I 3,4	GITR-ligand	1.05	0.619	0.95	0.246
I 5,6	IL2	0.96	0.698	1.29	0.429	I 5,6	IL 12 p40	0.82	0.193	0.95	0.406
I 7,8	MIG	0.74	0.027	0.96	0.639	I 7,8	Osteoprotegerin	1.83	0.008	1.23	0.205
I 9,10	TNF beta	0.99	0.960	1.22	0.029	I 9,10	VEGF-D	0.99	0.910	1.29	0.065
J 1,2	BMP-6	0.41	0.037	0.76	0.456	J 1,2	Axl	0.69	0.243	0.89	0.619
J 3,4	I-309	0.96	0.690	1.16	0.122	J 3,4	GITR-ligand	1.03	0.626	1.06	0.481
J 5,6	IL 3	0.82	0.118	1.33	0.273	J 5,6	IL12 p70	0.94	0.759	1.05	0.606
J 7,8	MIP 1 delta	1.17	0.405	1.54	0.112	J 7,8	Oncostatin M	0.95	0.659	0.90	0.645
K 1,2	CK beta 8-1	0.41	0.107	0.83	0.474	K 1,2	bFGF	0.61	0.023	0.60	0.023
K 3,4	IFN-gamma	0.50	0.074	0.76	0.136	K 3,4	GRO	1.40	0.006	1.50	0.033
K 5,6	IL 4	0.87	0.411	0.89	0.723	K 5,6	IL 17	1.19	0.032	0.95	0.645
K 7,8	MIP 3 alpha	1.09	0.676	1.37	0.202	K 7,8	PIGF	0.97	0.715	0.81	0.007
L 1,2	CNTF	0.80	0.285	1.11	0.530	L 1,2	b-NGF	0.66	0.042	0.72	0.109
L 3,4	IGFBP-1	0.31	0.018	0.92	0.352	L 3,4	GRO alpha	1.04	0.516	0.93	0.671
L 5,6	IL 5	1.25	0.157	1.32	0.146	L 5,6	IL2 R alpha	1.18	0.415	1.31	0.226
L 7,8	NAP-2	0.67	0.018	1.42	0.012	L 7,8	sgp 130	0.89	0.026	0.81	0.097
M 1,2	EGF	0.72	0.574	1.02	0.969	M 1,2	BTC	0.70	0.131	0.76	0.101
M 3,4	IGFBP-2	0.59	0.112	0.87	0.089	M 3,4	HCC 4	0.75	0.147	0.93	0.374
M 5,6	IL6	2.19	0.009	2.43	0.004	M 5,6	IL6 R	0.93	0.515	0.71	0.094
M 7,8	NT-3	0.98	0.868	1.01	0.925	M 7,8	sTNF rII	0.88	0.613	0.78	0.393
N 1,2	Eotaxin	0.40	0.205	0.95	0.855	N 1,2	CCL-28	0.78	0.391	1.05	0.812
N 3,4	IGFBP-4	0.98	0.923	0.73	0.282	N 3,4	HGF	1.01	0.465	0.89	0.393
N 5,6	IL7	1.76	0.009	1.21	0.158	N 5,6	IL8	1.03	0.188	0.88	0.112
N 7,8	PARC	0.40	0.001	0.46	0.063	N 7,8	sTNF rII	1.04	0.396	0.82	0.047

4.4B

Array VIII		Conditioned media type			
		5E6		8E6	
Position	Cytokine	Fold	P	Fold	P
A 3,4	Endoglin	-2.57	0.014	0.46	0.416
A 5,6	IL-21R	2.22	0.001	1.31	0.651
A 7,8	PDGF AA	1.28	0.073	1.31	0.098
A 9,10	VE-cadherin	1.54	0.055	1.20	0.524
B 3,4	ErbB3	3.23	0.022	1.57	0.070
B 5,6	IL-5 R alpha	3.35	0.003	1.99	0.090
B 7,8	PDGF-AB	3.15	0.013	2.29	0.061
B 9,10	VEGF R2	0.96	0.632	0.90	0.355
C 3,4	E-selectin	6.88	0.020	4.39	0.058
C 5,6	IL 9	1.48	0.029	1.24	0.300
C 7,8	PDGF R alpha	1.93	0.022	1.59	0.039
C 9,10	VEGF R3	0.98	0.764	0.95	0.609
D 3,4	FasL	1.14	0.419	1.11	0.001
D 5,6	IP-10	1.76	0.058	1.37	0.415
D 7,8	PDGF R beta	0.90	0.226	0.78	0.127
E 3,4	ICAM 2	1.36	0.028	0.91	0.561
E 5,6	LAP	1.13	0.282	0.94	0.483
E 7,8	PECAM-1	1.05	0.839	0.95	0.548
F 1,2	Activin A	2.20	0.095	1.12	0.750
F 3,4	IGF-II	1.02	0.795	0.76	0.064
F 5,6	Leptin R	0.78	0.139	0.92	0.532
F 7,8	Prolactin	1.03	0.778	1.22	0.131
G 1,2	ALCAM	1.44	0.067	1.17	0.285
G 3,4	IL1 R II	3.84	0.031	2.10	0.156
G 5,6	LIF	1.35	0.041	1.42	0.146
G 7,8	SCF R	0.85	0.374	0.77	0.217
H 1,2	B7-1	1.79	0.005	0.96	0.893
H 3,4	IL10 R beta	3.08	0.040	1.33	0.538
H 5,6	L selectin	1.61	0.098	1.05	0.718
H 7,8	SDF -1 beta	0.97	0.875	0.79	0.207
I 1,2	BMP-5	3.50	0.068	1.53	0.557
I 3,4	IL13 R alpha 2	14.91	0.014	4.49	0.193
I 5,6	M-CSF-R	1.30	0.038	0.76	0.301
I 7,8	Siglec-5	0.90	0.452	0.76	0.083
J 1,2	BMP-7	3.13	0.146	1.31	0.751
J 3,4	IL18 BP alpha	2.69	0.088	1.40	0.218
J 5,6	MMP-1	1.74	0.034	0.96	0.796
J 7,8	TGF-alpha	1.04	0.632	0.81	0.107
K 1,2	Cardiotrophin 1	3.41	0.055	0.66	0.754
K 3,4	IL18 R beta	0.96	0.807	0.96	0.708
K 5,6	MMP 13	1.96	0.001	1.18	0.032
K 7,8	TGF beta 2	0.96	0.517	0.76	0.009
L 1,2	CD14	10.11	0.049	-0.15	0.844
L 3,4	MMP 3	1.08	0.647	0.82	0.413
L 5,6	MMP 9	1.59	0.450	1.36	0.306
L 7,8	Tie-1	0.95	0.467	0.80	0.166
M 1,2	CXCL-16	1.46	0.228	0.60	0.549
M 3,4	IL 2 R beta	1.60	0.290	0.44	0.410
M 5,6	MPIF 1	2.96	0.012	0.75	0.358
M 7,8	Tie-2	1.20	0.220	0.94	0.671
N 1,2	RF6	2.83	0.102	0.16	0.521
N 3,4	IL2 R gamma	1.50	0.108	0.05	0.017
N 5,6	NGF R	-3.98	0.022	1.97	0.030
N 7,8	TIMP 4	0.89	0.371	0.78	0.175

4.4 B cont

4.2.5 Identification of changes in secreted factors from primary keratinocytes

To investigate the changes in secreted factors induced by HPV5 and 8E6 expression in primary keratinocytes, cytokine arrays were incubated as described previously in EpiLife media conditioned by 48 hrs growth of either keratinocytes or keratinocytes stably expressing HPV5 and 8E6. The results are shown in Figure 4-5, with the example of the upregulation of IL6 and OPG shown in Figure 4-5 A, and the quantification of all the results shown in Figure 4-5 B. Furthermore, Figure 4-5 C represents all the significant results of both the HT1080 and keratinocyte arrays to allow comparison.

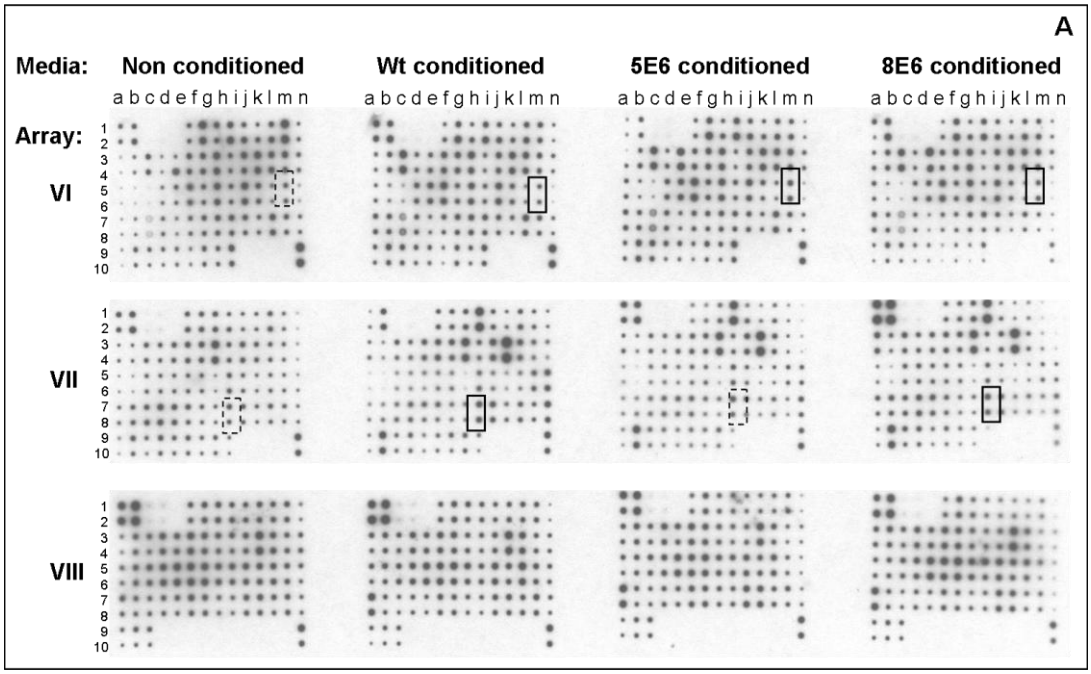

Figure 4-5 Results of the cytokine arrays showing changes in cytokine secretion relative to normal primary keratinocyte conditioned media.

A Arrays are incubated with the indicated media type and the spots, arranged in vertical pairs for each cytokine, are then quantified to allow calculation of relative protein abundance. The boxes show the upregulation of IL6 on Array VI (M 5,6) in HPV5 and 8E6 conditioned media, and of OPG on Array VII(I 7,8) in HPV8E6 conditioned media, with the dashed boxes showing the baseline and unchanged levels.

B Table showing the fold changes (test value/control value), and significance, of the relative abundance of each protein in the indicated conditioned media compared to parental conditioned media (split over two pages), with IL6 and OPG highlighted in yellow.

C Diagram representing changes in media from HT1080s and keratinocytes expressing HPV5 or 8E6. Non-significant changes are white (where P>0.05), significant upregulation is shown in red (>2fold) and orange (>1fold). Significant downregulation is shown in blue (<0.5 fold) and pale blue (1 to 0.5 fold). IL6 and OPG are highlighted in yellow (split over two pages).

Array VI		Conditioned media type				Array VII		Conditioned media type			
		5E6		8E6				5E6		8E6	
Position	Cytokine	Fold	P	Fold	P	Position	Cytokine	Fold	P	Fold	P
A 3,4	Eotaxin2	1.80	0.694	2.02	0.083	A 3,4	CTACK	0.67	0.278	0.72	0.315
A 5,6	IGF4	5.23	0.001	2.09	0.074	A 5,6	ICAM-1	7.21	0.033	3.31	0.049
A 7,8	Leptin	3.49	0.000	1.34	0.042	A 7,8	I-TAC	0.66	0.075	0.53	0.079
A 9,10	PDGF-BB	3.42	0.018	0.71	0.450	A 9,10	TECK	0.66	0.404	0.33	0.134
B 3,4	Eotaxin 3	2.78	0.034	1.49	0.010	B 3,4	Dtk	0.63	0.030	0.57	0.107
B 5,6	IL 10	3.66	0.004	1.31	0.210	B 5,6	ICAM - 3	2.19	0.073	1.95	0.046
B 7,8	LIGHT	3.14	0.005	1.09	0.074	B 7,8	Lymphotactin	0.56	0.137	0.49	0.106
B 9,10	RANTES	3.84	0.012	0.94	0.884	B 9,10	TIMP-1	0.52	0.053	0.28	0.018
C 3,4	FGF-6	3.09	0.000	1.16	0.007	C 3,4	EGF-R	0.48	0.042	0.35	0.031
C 5,6	IL 13	2.87	0.000	0.86	0.014	C 5,6	IGFBP-3	0.64	0.050	0.47	0.001
C 7,8	MCP-1	3.48	0.012	1.00	0.991	C 7,8	MIF	0.52	0.018	0.34	0.010
C 9,10	SCF	3.96	0.048	0.86	0.731	C 9,10	TIMP-2	0.62	0.126	0.37	0.044
D 3,4	FGF-7	3.09	0.061	1.22	0.069	D 3,4	ENA-78	0.43	0.010	0.28	0.006
D 5,6	IL15	3.19	0.001	0.99	0.943	D 5,6	IGFBP-6	0.60	0.035	0.41	0.008
D 7,8	MCP-2	3.72	0.002	0.99	0.937	D 7,8	MIP-1alpha	0.48	0.029	0.33	0.018
D 9,10	SDF-1	1.18	0.756	2.45	0.305	D 9,10	Thrombopoietin	1.04	0.921	2.27	0.179
E 3,4	Flt-3 ligand	5.62	0.002	2.24	0.044	E 3,4	Fas	0.36	0.001	0.21	0.000
E 5,6	IL 16	3.46	0.001	1.11	0.232	E 5,6	IGF1-sr	0.45	0.149	0.33	0.105
E 7,8	MCP-3	3.71	0.015	0.80	0.366	E 7,8	MIP-1beta	0.54	0.144	0.34	0.079
E 9,10	TARC	1.18	0.726	2.31	0.276	E 9,10	TRAIL R3	1.67	0.250	2.42	0.255
F 1,2	Angiogenin	3.35	0.082	1.23	0.673	F 1,2	Acrp30	0.31	0.024	0.25	0.018
F 3,4	Fractaline	2.71	0.013	1.07	0.185	F 3,4	FGF-4	0.34	0.002	0.19	0.002
F 5,6	IL1 alpha	3.71	0.001	1.20	0.120	F 5,6	IL1 R4	0.45	0.006	0.25	0.001
F 7,8	MCP-4	3.76	0.024	0.99	0.959	F 7,8	MIP3 beta	0.54	0.154	0.25	0.065
F 9,10	TGF-beta 1	2.15	0.281	1.92	0.593	F 9,10	TRAIL R4	1.43	0.368	2.24	0.242
G 1,2	BDNF	3.55	0.071	1.37	0.307	G 1,2	AgRP	0.30	0.022	0.24	0.013
G 3,4	GCP-2	3.26	0.000	1.26	0.104	G 3,4	FGF-9	0.38	0.006	0.21	0.003
G 5,6	IL1 beta	3.82	0.003	1.34	0.010	G 5,6	IL1-R1	0.47	0.002	0.21	0.001
G 7,8	M-CSF	1.00	0.980	2.86	0.044	G 7,8	MSP-alpha	1.22	0.559	1.74	0.150
G 9,10	TGF-beta 3	1.12	0.764	1.79	0.317	G 9,10	uPAR	1.02	0.960	1.08	0.907
H 1,2	BLC	3.58	0.129	1.37	0.537	H 1,2	Angiopoietin 2	0.39	0.051	0.26	0.032
H 3,4	GDNF	3.29	0.002	1.31	0.073	H 3,4	GCSF	0.42	0.010	0.22	0.006
H 5,6	IL-1ra	3.69	0.005	1.45	0.010	H 5,6	IL 11	0.64	0.030	0.27	0.006
H 7,8	MDC	1.03	0.856	3.24	0.061	H 7,8	NT-4	1.12	0.761	1.60	0.263
H 9,10	TNF-alpha	1.30	0.563	1.46	0.749	H 9,10	VEGF	1.10	0.757	0.73	0.595
I 1,2	BMP-4	3.76	0.037	1.27	0.415	I 1,2	Amphiregulin	0.46	0.006	0.25	0.002
I 3,4	GM-CSF	3.11	0.015	1.39	0.112	I 3,4	GITR-ligand	0.39	0.010	0.18	0.006
I 5,6	IL2	3.62	0.006	1.45	0.003	I 5,6	IL 12 p40	0.45	0.001	0.18	0.000
I 7,8	MIG	1.06	0.746	3.58	0.115	I 7,8	Osteoprotegerin	0.99	0.978	1.79	0.031
I 9,10	TNF beta	1.34	0.448	1.97	0.492	I 9,10	VEGF-D	0.69	0.570	0.04	0.280
J 1,2	BMP-6	3.46	0.101	1.22	0.599	J 1,2	Axl	0.41	0.082	0.15	0.029
J 3,4	I-309	3.36	0.006	1.28	0.088	J 3,4	GITR-ligand	0.35	0.009	0.14	0.005
J 5,6	IL 3	1.04	0.727	4.09	0.000	J 5,6	IL12 p70	1.04	0.539	1.24	0.007
J 7,8	MIP 1 delta	1.16	0.377	3.73	0.064	J 7,8	Oncostatin M	0.85	0.532	1.70	0.025
K 1,2	CK beta 8-1	3.28	0.150	1.16	0.778	K 1,2	bFGF	0.97	0.932	1.18	0.547
K 3,4	IFN-gamma	3.51	0.002	1.24	0.131	K 3,4	GRO	1.00	0.962	1.59	0.034
K 5,6	IL 4	0.95	0.808	3.82	0.002	K 5,6	IL 17	0.80	0.564	0.93	0.790
K 7,8	MIP 3 alpha	1.17	0.521	3.09	0.192	K 7,8	PIGF	0.85	0.570	1.66	0.044
L 1,2	CNTF	2.94	0.053	1.20	0.588	L 1,2	b-NGF	0.74	0.385	0.70	0.247
L 3,4	IGFBP-1	3.44	0.004	1.29	0.055	L 3,4	GRO alpha	0.80	0.060	0.91	0.190
L 5,6	IL 5	1.21	0.358	4.06	0.000	L 5,6	IL2 R alpha	0.79	0.395	0.99	0.966
L 7,8	NAP-2	1.11	0.449	2.39	0.157	L 7,8	sgp 130	0.86	0.322	1.29	0.395
M 1,2	EGF	1.05	0.793	4.28	0.040	M 1,2	BTC	0.43	0.092	0.10	0.039
M 3,4	IGFBP-2	1.55	0.053	5.64	0.000	M 3,4	HCC 4	0.45	0.031	0.47	0.131
M 5,6	IL6	1.73	0.008	5.57	0.001	M 5,6	IL6 R	0.64	0.028	0.93	0.578
M 7,8	NT-3	1.00	0.987	1.91	0.352	M 7,8	sTNF rII	0.60	0.083	1.14	0.765
N 1,2	Eotaxin	1.11	0.768	5.23	0.078	N 1,2	CCL-28	0.05	0.044	-0.94	0.015
N 3,4	IGFBP-4	1.73	0.038	5.03	0.043	N 3,4	HGF	0.21	0.031	-0.20	0.033
N 5,6	IL7	7.61	0.083	6.81	0.256	N 5,6	IL8	0.54	0.007	0.61	0.077
N 7,8	PARC	1.22	0.311	1.02	0.983	N 7,8	sTNF rII	0.79	0.345	1.12	0.615

4.5 B

Array VIII		Conditioned media type			
		5E6		8E6	
Position	Cytokine	Fold	P	Fold	P
A 3,4	Endoglin	1.24	0.410	1.39	0.228
A 5,6	IL-21R	1.16	0.584	1.15	0.525
A 7,8	PDGF AA	1.46	0.058	1.34	0.072
A 9,10	VE-cadherin	1.70	0.484	2.17	0.325
B 3,4	ErbB3	1.32	0.217	1.39	0.169
B 5,6	IL-5 R alpha	1.14	0.607	1.09	0.714
B 7,8	PDGF-AB	1.50	0.202	1.45	0.137
B 9,10	VEGF R2	1.86	0.178	1.66	0.312
C 3,4	E-selectin	1.21	0.178	1.26	0.055
C 5,6	IL 9	1.20	0.098	1.22	0.174
C 7,8	PDGF R alpha	1.64	0.077	1.31	0.256
C 9,10	VEGF R3	2.00	0.161	1.48	0.371
D 3,4	FasL	1.24	0.189	1.26	0.010
D 5,6	IP-10	1.17	0.098	1.27	0.116
D 7,8	PDGF R beta	1.78	0.048	1.52	0.101
E 3,4	ICAM 2	1.24	0.128	1.40	0.029
E 5,6	LAP	1.27	0.039	1.46	0.024
E 7,8	PECAM-1	2.05	0.079	1.65	0.130
F 1,2	Activin A	1.04	0.768	1.17	0.501
F 3,4	IGF-II	1.33	0.077	1.52	0.012
F 5,6	Leptin R	1.21	0.016	1.45	0.058
F 7,8	Prolactin	1.57	0.090	1.40	0.222
G 1,2	ALCAM	1.23	0.019	1.39	0.023
G 3,4	IL1 R II	1.26	0.102	1.50	0.032
G 5,6	LIF	1.25	0.215	1.52	0.098
G 7,8	SCF R	1.27	0.107	1.27	0.171
H 1,2	B7-1	1.04	0.371	1.21	0.396
H 3,4	IL10 R beta	1.35	0.004	1.71	0.008
H 5,6	L selectin	1.18	0.346	1.59	0.131
H 7,8	SDF -1 beta	1.31	0.325	1.33	0.246

Array VIII		Conditioned media type			
		5E6		8E6	
Position	Cytokine	Fold	P	Fold	P
I 1,2	BMP-5	1.68	0.126	1.03	0.861
I 3,4	IL13 R alpha 2	1.30	0.199	1.94	0.047
I 5,6	M-CSF-R	1.44	0.014	1.99	0.172
I 7,8	Siglec-5	1.57	0.213	1.70	0.191
J 1,2	BMP-7	1.38	0.120	1.17	0.419
J 3,4	IL18 BP alpha	1.15	0.234	1.63	0.032
J 5,6	MMP-1	0.86	0.203	1.39	0.169
J 7,8	TGF-alpha	1.43	0.110	1.69	0.070
K 1,2	Cardiotrophin 1	0.82	0.227	0.94	0.843
K 3,4	IL18 R beta	0.86	0.173	1.39	0.025
K 5,6	MMP 13	0.86	0.382	1.46	0.237
K 7,8	TGF beta 2	1.26	0.253	1.45	0.160
L 1,2	CD14	0.76	0.014	0.72	0.170
L 3,4	MMP 3	0.65	0.050	1.16	0.032
L 5,6	MMP 9	0.69	0.078	0.95	0.806
L 7,8	Tie-1	0.89	0.307	0.90	0.645
M 1,2	CXCL-16	1.07	0.825	0.84	0.342
M 3,4	IL 2 R beta	0.56	0.043	0.96	0.236
M 5,6	MPIF 1	0.52	0.024	0.85	0.706
M 7,8	Tie-2	0.71	0.328	0.69	0.267
N 1,2	RF6	1.33	0.616	0.04	0.448
N 3,4	IL2 R gamma	0.67	0.124	0.73	0.206
N 5,6	NGF R	0.31	0.013	0.37	0.100
N 7,8	TIMP 4	0.74	0.424	0.18	0.107

4.5 B cont

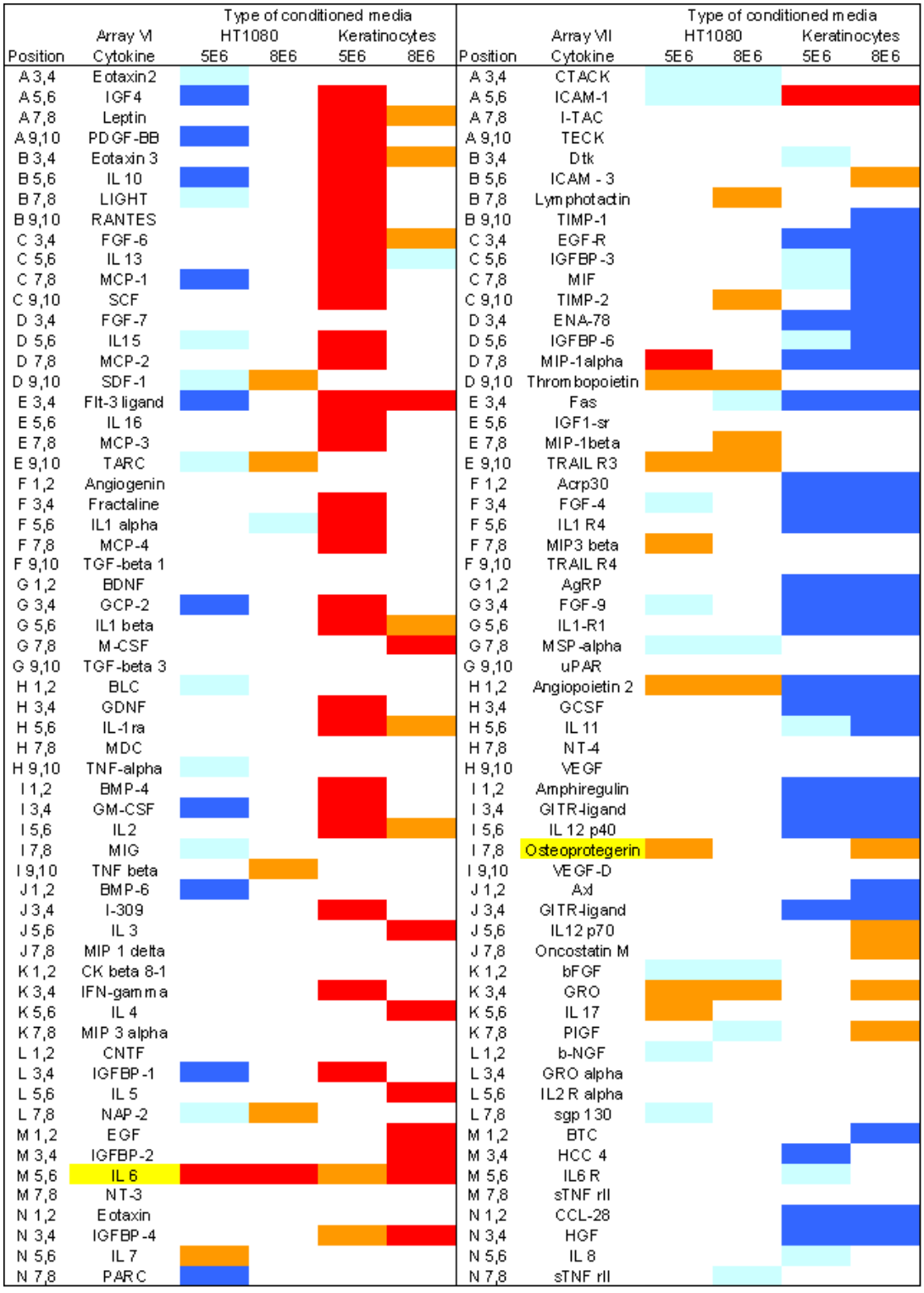
Type of conditioned media
Array VI
HT1080
Keratinocytes
Position
Cytokine
5E6
8E6
5E6
8E6
A 3,4 Eotaxin2
A 5,6 IGF4
A 7,8 Leptin
A 9,10 PDGF-BB
B 3,4 Eotaxin 3
B 5,6 IL 10
B 7,8 LIGHT
B 9,10 RANTES
C 3,4 FGF-6
C 5,6 IL 13
C 7,8 MCP-1
C 9,10 SCF
D 3,4 FGF-7
D 5,6 IL15
D 7,8 MCP-2
D 9,10 SDF-1
E 3,4 Flt-3 ligand
E 5,6 IL 16
E 7,8 MCP-3
E 9,10 TARC
F 1,2 Angiogenin
F 3,4 Fractaline
F 5,6 IL1 alpha
F 7,8 MCP-4
F 9,10 TGF-beta 1
G 1,2 BDNF
G 3,4 GCP-2
G 5,6 IL1 beta
G 7,8 M-CSF
G 9,10 TGF-beta 3
H 1,2 BLC
H 3,4 GDNF
H 5,6 IL-1ra
H 7,8 MDC
H 9,10 TNF-alpha
I 1,2 BMP-4
I 3,4 GM-CSF
I 5,6 IL2
I 7,8 MIG
I 9,10 TNF beta
J 1,2 BMP-6
J 3,4 I-309
J 5,6 IL 3
J 7,8 MIP 1 delta
K 1,2 CK beta 8-1
K 3,4 IFN-gamma
K 5,6 IL 4
K 7,8 MIP 3 alpha
L 1,2 CNTF
L 3,4 IGFBP-1
L 5,6 IL 5
L 7,8 NAP-2
M 1,2 EGF
M 3,4 IGFBP-2
M 5,6 IL 6
M 7,8 NT-3
N 1,2 Eotaxin
N 3,4 IGFBP-4
N 5,6 IL 7
N 7,8 PARC
Type of conditioned media
Array VII
HT1080
Keratinocytes
Position
Cytokine
5E6
8E6
5E6
8E6
A 3,4 CTACK
A 5,6 ICAM-1
A 7,8 I-TAC
A 9,10 TECK
B 3,4 Dtk
B 5,6 ICAM - 3
B 7,8 Lymphotactin
B 9,10 TIMP-1
C 3,4 EGF-R
C 5,6 IGFBP-3
C 7,8 MIF
C 9,10 TIMP-2
D 3,4 ENA-78
D 5,6 IGFBP-6
D 7,8 MIP-1alpha
D 9,10 Thrombopoietin
E 3,4 Fas
E 5,6 IGF1-sr
E 7,8 MIP-1beta
E 9,10 TRAIL R3
F 1,2 Acrp30
F 3,4 FGF-4
F 5,6 IL1 R4
F 7,8 MIP3 beta
F 9,10 TRAIL R4
G 1,2 AgRP
G 3,4 FGF-9
G 5,6 IL1-R1
G 7,8 MSP-alpha
G 9,10 uPAR
H 1,2 Angiopoietin 2
H 3,4 GCSF
H 5,6 IL 11
H 7,8 NT-4
H 9,10 VEGF
I 1,2 Amphiregulin
I 3,4 GITR-ligand
I 5,6 IL 12 p40
I 7,8 Osteoprotegerin
I 9,10 VEGF-D
J 1,2 Axl
J 3,4 GITR-ligand
J 5,6 IL12 p70
J 7,8 Oncostatin M
K 1,2 bFGF
K 3,4 GRO
K 5,6 IL 17
K 7,8 PIGF
L 1,2 b-NGF
L 3,4 GRO alpha
L 5,6 IL2 R alpha
L 7,8 sgp 130
M 1,2 BTC
M 3,4 HCC 4
M 5,6 IL6 R
M 7,8 sTNF rII
N 1,2 CCL-28
N 3,4 HGF
N 5,6 IL 8
N 7,8 sTNF rII

4.5

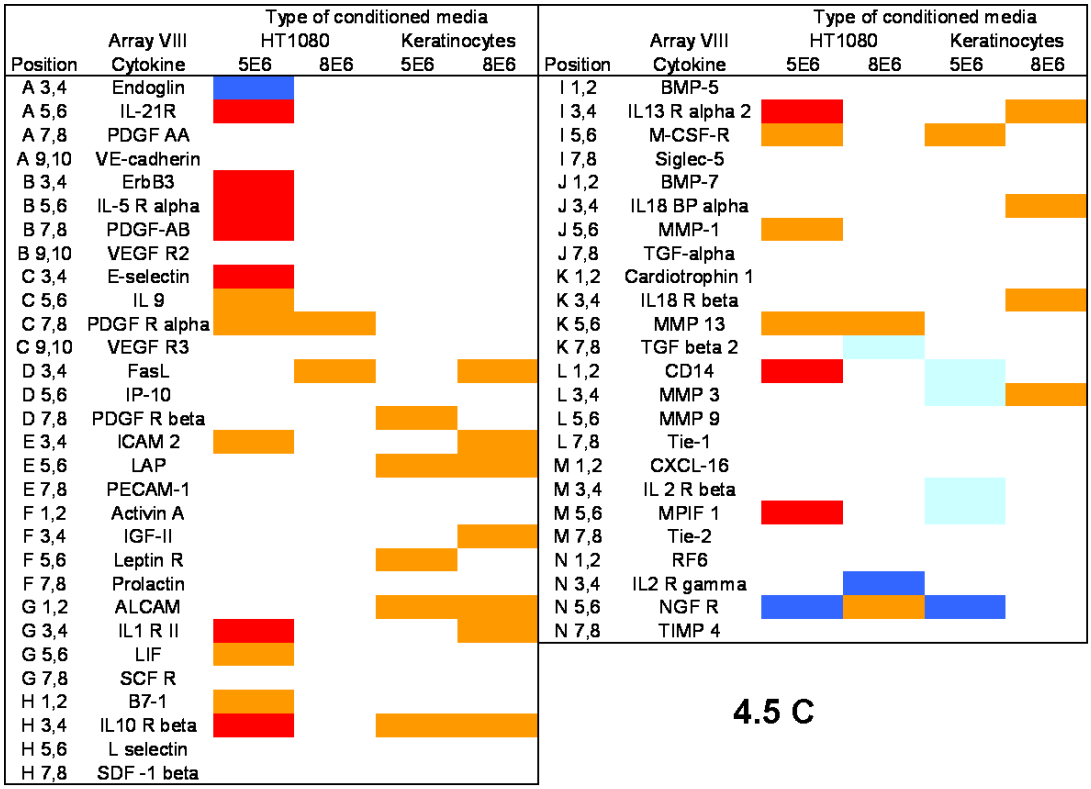

4.5 C

It is interesting to note that the patterns of changes seen in HT1080 and primary keratinocyte media vary, with only a few changes common to both cell types, and that there are many differences between HPV5 and 8E6 conditioned media of the same cell type, even though both types can inhibit UV-induced apoptosis in HT1080 cells. This implies that either each cell type requires a number of different factors to protect them from apoptosis, or that the protection is mediated by a small number of factors found in both types of conditioned media. Inspection of the induced factors that were common to both E6 types, but that were also independent of cell type, shows that Interleukin 6 is the only cytokine to show significant up-regulation in all the E6 media types, by factors of 2.19, 2.43, 1.73 and 5.57 in HT1080 HPV5E6, HT1080 HPV8E6, keratinocyte HPV5E6 and keratinocyte HPV8E6 media respectively, while Osteoprotegerin is up-regulated by factors of 1.83, (1.23, and 0.99 - not statistically significant) and 1.79 respectively. These factors have also been shown to have anti-apoptotic effects, as outlined presently; therefore further investigation into the role of Interleukin 6 (IL6) and

Osteoprotegerin (OPG) in the protection of non-E6 cells from apoptosis was undertaken.

4.2.6 Changes in Osteoprotegerin expression

Osteoprotegerin is a secreted TNFR (tumour necrosis factor receptor) family member whose primary ligand is RANKL (receptor activator of NFκB ligand), a member of the TNF family. Bone remodelling is regulated in part by OPG in the bone marrow, as osteoclastogenesis is prevented by OPG binding RANKL thereby inhibiting activation of RANK. However OPG is also found in the general circulation and it also binds to and inhibits TNF-related apoptosis inducing ligand (TRAIL) (Zauli et al., 2009), and several studies have shown that it inhibits apoptosis of different cell types (Neville-Webbe et al., 2004). Therefore its potential role in protection of non-E6 expressing cells from UV-induced apoptosis, including keratinocytes, was investigated, beginning with its expression levels.

HT1080s and keratinocytes stably expressing either empty vectors (pIRES or pLXSN respectively) or HPV5E6, generated as described previously, were cultured to 70-90% confluence (keratinocytes in RM+) and harvested for RNA extraction. mRNA was then used in reverse transcription reactions to generate cDNA templates, which were used in quantitative real-time PCR (QRTPCR) to assess levels of gene expression as described in Materials and Methods, section 2.2.5. Gene expression was normalised to the housekeeping gene GUS and the fold change calculated using the $2^{\Delta\Delta}$CT method.

Figure 4-6 A shows there is no significant increase in the expression of OPG in HPV5E6 expressing HT1080s or keratinocytes. The large error bar is a result of the transformation used to calculate fold change. HT1080s and keratinocytes expressing empty vector (pcDNA or pLXSN respectively) or HPV5, 8, 10, 18 and 77E6 were also used to analyse OPG expression by western blotting. Cells were cultured to 70-90% confluence, harvested by scraping in RIPA lysis buffer, the

lysates separated by SDS-PGE, and transferred to membranes which were then probed for OPG, and quantified with Image J then normalised according to the background and loading control, as described. Figure 4-6 B shows a band at 55 kDa corresponding to OPG which is increased in lysates expressing the indicated E6 types relative to the empty vector control.

The finding that OPG mRNA transcription is not affected by HPV5E6 expression but the protein levels are increased suggests that E6 expression instead has an effect on the processing or secretion of OPG. Additionally the upregulation of OPG in HPV8E6 HT1080s and HPV5E6 keratinocytes seen on the western blots is greater than the non-significant changes seen on the arrays.

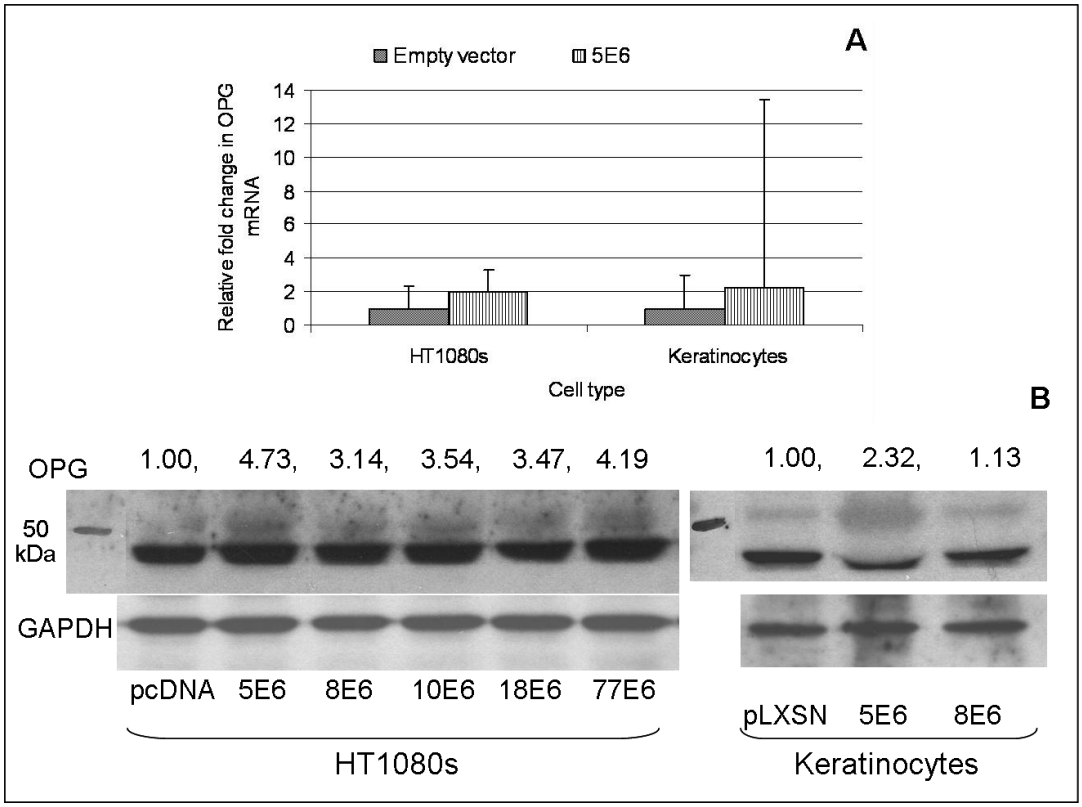

Figure 4-6 Changes in OPG expression in E6 expressing HT1080s and keratinocytes.

A QRTPCR was used to calculate the relative fold change in expression levels of OPG in the cell type indicated. Error bars indicate $2^{\text{standard deviation of } \Delta\Delta CT}$, 4 replicates.

B Western blot showing HT1080 and keratinocyte lysates expressing either empty vector or the HPVE6 type indicated, OPG is the upper band (predicted size 55kDa). GAPDH was used to ensure equal loading and the fold changes compared to the relevant empty vector control are indicated.

4.2.7 Changes in Interleukin 6 expression

IL6 is a multifunctional proinflammatory cytokine and has been shown to influence cell survival through activation of anti-apoptotic and proliferative STAT3, MAPK and PI3K pathways (Hodge et al., 2005), so its possible role in protection of non-E6 cells from apoptosis was investigated, beginning with gene expression levels. HT1080s and keratinocytes expressing either empty vector (pIRES or pLXSN respectively) were cultured to 70-90% confluence (keratinocytes in RM+) and RNA extracted as before. This was used to make cDNA templates which were then used in QRTPCR to test IL6 mRNA levels. Gene expression was normalised to the housekeeping gene GUS and the fold change calculated using the $2^{\Delta\Delta}$CT method as before. Figure 4-7 A shows no significant difference in IL6 gene expression in HT1080s expressing HPV5E6, however there is a striking 100-fold increase in keratinocytes expressing HPV5E6. To further test this, keratinocytes were cultured in both EpiLife and RM+, and treated with UV irradiation. QRTPCR was performed as described, and the results shown in Figure 4-7 B. It can be seen that both UV irradiation and HPV5E6 expression alone greatly increase IL6 expression, and this increase is synergistic in UV-irradiated cells expressing HPV5E6. In all cases the upregulation is also greater in cells cultured in RM+. It appears that HPV5E6 is altering the transcription of IL6 in keratinocytes but not in HT1080s, despite the upregulation in secretion seen in both cell types.

Lysates of HT1080s and keratinocytes expressing empty vector or E6 of the various HPV types were also used in western blots to identify changes in IL6 expression. However it was not possible to detect a specific band corresponding to IL6, possibly due to the processing which occurs during secretion from the cell. Samples of conditioned media were also tested by western blot for IL6 but again no specific band was observed, probably because the media had not been concentrated prior to loading onto the gel.

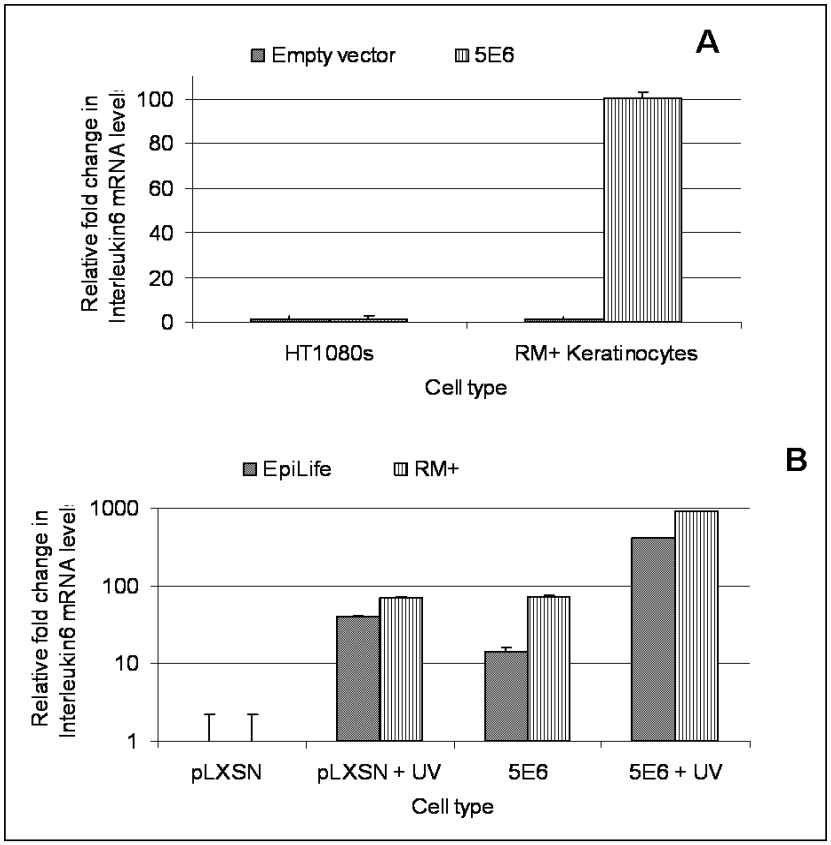

Figure 4-7 Changes in IL6 expression in HPV5E6 expressing HT1080s and keratinocytes

A QRTPCR was used to calculate the relative fold change in expression levels of IL6 in the cell type indicated. Error bars indicate $2^{\text{standard deviation of } \Delta\Delta CT}$, 4 replicates.
B QRTPCR was used to calculate the relative fold change in expression levels of IL6 in keratinocytes cultured in both EpiLife and RM+ as indicated, with or without UV irradiation (10 mJ/cm^2 in EpiLife, 15 mJ/cm^2 in RM+). Error bars indicate $2^{\text{standard deviation of } \Delta\Delta CT}$, 4 replicates. Note the log scale.

4.2.8 Changes in IL6 and OPG expression in organotypic skin cultures

In an attempt to further investigate the production of IL6 and OPG by HPV5E6 expressing keratinocytes, the organotypic culture system was used to more closely mimic the natural environment of the skin. Keratinocytes expressing pLXSN or HPV5E6 were used to generate the organotypic cultures as described in Materials and Methods, section 2.1.7. After 14 days differentiation at the air-liquid interface, the epidermal skin equivalents were harvested and sections cut.

Immunohistochemistry for OPG and IL6 was carried out as described. Briefly, after blocking, sections are incubated overnight at 4 °C with the primary antibody, and subsequent steps used ABC kits and DAB staining, with haematoxylin counterstaining.

Figure 4-8 shows examples of the staining, and it can be seen that the keratinocytes do not display a great degree of stratification or cornification in the upper layers. Previous unpublished observations from the lab have indicated that it is difficult to generate good-quality organotypic cultures from keratinocytes expressing HPV5E6 alone. Although there appears to be an increase in brown staining, indicating OPG and IL6, in rafts generated from HPV5E6 keratinocytes, there were not enough sections to properly quantify this.

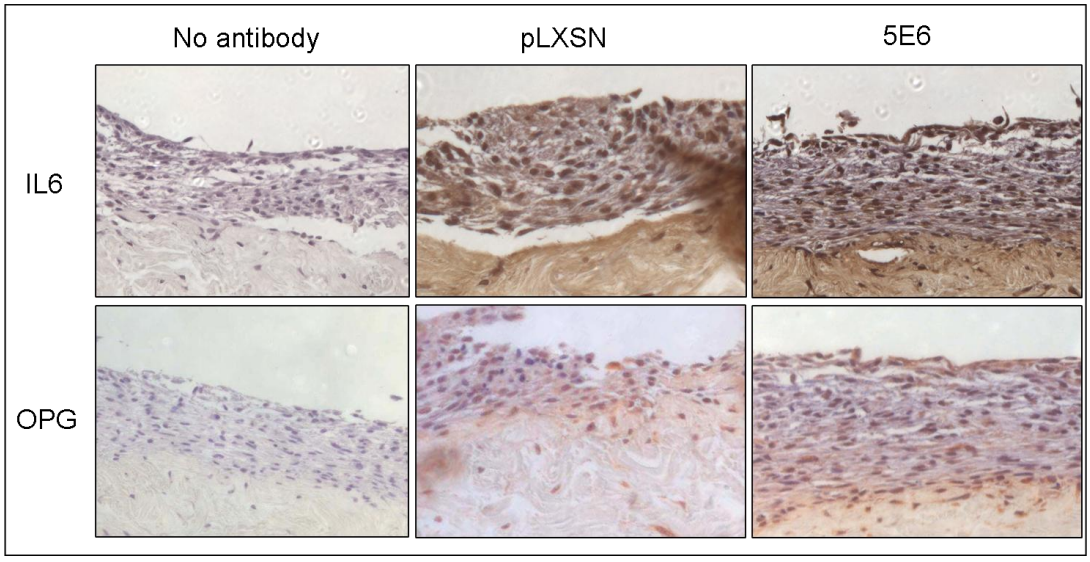

Figure 4-8 OPG and IL6 expression in organotypic raft cultures.

Keratinocytes expressing pLXSN or HPV5E6 were used to generate raft cultures, which were then stained for OPG and IL6 as indicated, shown by brown staining, with blue nuclear counterstaining. Negative control sections (of pLXSN rafts) were incubated without the primary antibody to demonstrate specificity.

4.2.9 Osteoprotegerin and Interleukin 6 alone do not protect from UV-induced apoptosis

In addition to investigating the expression levels of IL6 and OPG, their effect on apoptosis was tested to help elucidate their possible role in E6-mediated protection of non-E6 cells from UV. To test the effect of these cytokines on UV-induced apoptosis, recombinant purified human OPG and IL6 were added to HT1080s or keratinocytes prior to UV exposure, and apoptosis levels measured 16 hours later, as described. Review of the literature and pilot experiments were performed to find appropriate doses of cytokines which ranged initially from 1, 10, 50, 100 and 150 ng/ml, as these have previously shown inhibition of apoptosis, for example 100 ng/ml of IL6 inhibits Fas-induced apoptosis of multiple myeloma cells (Chauhan et al., 1997), and 100 ng/ml of OPG decreased osteoclast apoptosis caused by withdrawal of stimulatory factors (Chamoux et al., 2008). When added separately to HT1080 cells or primary keratinocytes OPG or IL6 had no effect on UV-induced apoptosis as measured by AnnexinV/PI flow cytometry. Figure 4-9 shows representative results of these experiments, and no significant difference in apoptosis is observed in any case.

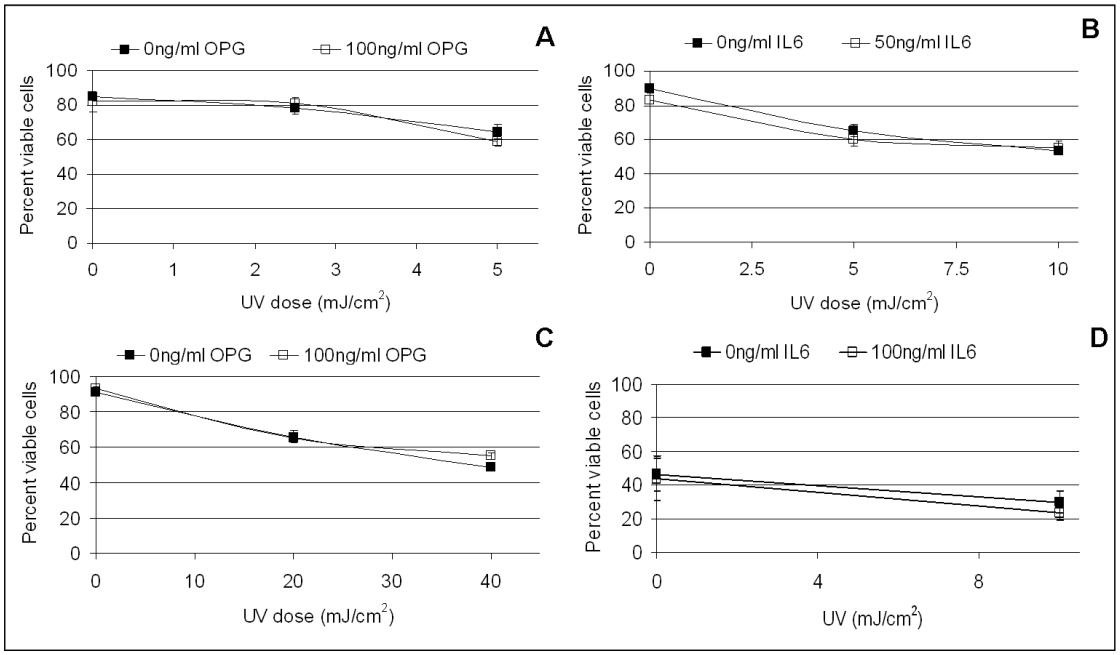

Figure 4-9 OPG and IL6 added individually do not inhibit UV-induced apoptosis in HT1080s or primary keratinocytes.

A There is no increase in the amount of viable HT1080 cells remaining 16 hrs post UV when cultured for 24 hrs with OPG (in all cases error bars indicates standard deviation, for **A**, **B** and **C** - 3 replicates).

B There is no increase in the amount of viable HT1080s remaining 16 hrs post UV when cultured for 24 hrs with IL6.

C There is no difference in the amount of viable primary keratinocytes remaining 16 hrs post UV when cultured for 48 hrs in RM+ with OPG.

D There is no difference in the amount of viable primary keratinocytes remaining 16 hrs post UV when cultured 24 hrs with IL6 in EpiLife, 2 replicates.

4.2.10 Osteoprotegerin and Interleukin 6 together protect HT1080s and primary keratinocytes from UV-induced apoptosis

As the conditioned media which provided protection from UV-induced apoptosis for non-E6 expressing cells showed changes in several factors, OPG and IL6 were added together to cultures of HT1080s and keratinocytes, and apoptosis induced and measured. HT1080s were cultured for 24 hrs with OPG and IL6, UV irradiated and incubated with the cytokines for a further 16 hrs, after which cells were harvested and apoptosis measured with AnenxinV/PI as described. Figure 4-10 A

shows that there are significantly more viable HT1080 cells after UV irradiation in the presence of 100 ng/ml OPG and 50 ng/ml IL6, with a 9% increase in viable cells at 2.5 mJ/cm^2 and a 13% increase at 5 mJ/cm^2. Primary keratinocytes were also tested, with cells cultured in EpiLife for 24 hrs with 150 ng/ml OPG and 100 ng/ml IL6, and in RM+ for 48 hrs with 100 ng/ml OPG and 50 ng/ml IL6, then UV irradiated and incubated with the cytokines for a further 16 hrs before the cells were harvested and apoptosis measured with AnnexinV/PI. Figure 4-10 B shows that in both media types, there are more significantly more viable cells remaining after UV irradiation in the presence of the cytokines. As observed before, cells cultured in the media which allows early differentiation and cell clustering, RM+, are more resistant to UV-induced apoptosis. Growth with the cytokines confers a small but significant increase of 5% in the percent viable cells remaining after 20 mJ/cm^2 UV irradiation, and a 7% increase (which does not reach significance) at 40 mJ/cm^2. Although the overall apoptotic rates were higher in cells cultured in EpiLife, the addition of the cytokines in this media gave a greater relative degree of protection from UV-induced apoptosis, with a 15% increase in viable cells at 15 mJ/cm^2, and an 11% increase at 30 mJ/cm^2. This could be due to the slightly higher cytokine doses which were being tested with the EpiLife media (150 ng/ml OPG 100 ng/ml IL6 compared to 100 ng/ml OPG 50 ng/ml IL6 in RM+). In addition, the longer incubation time with the cytokines in RM+ could have led to some inactivation. The observation that both cytokines are required for protection from apoptosis implies they have differing yet complementary roles in the inhibition of different apoptotic pathways.

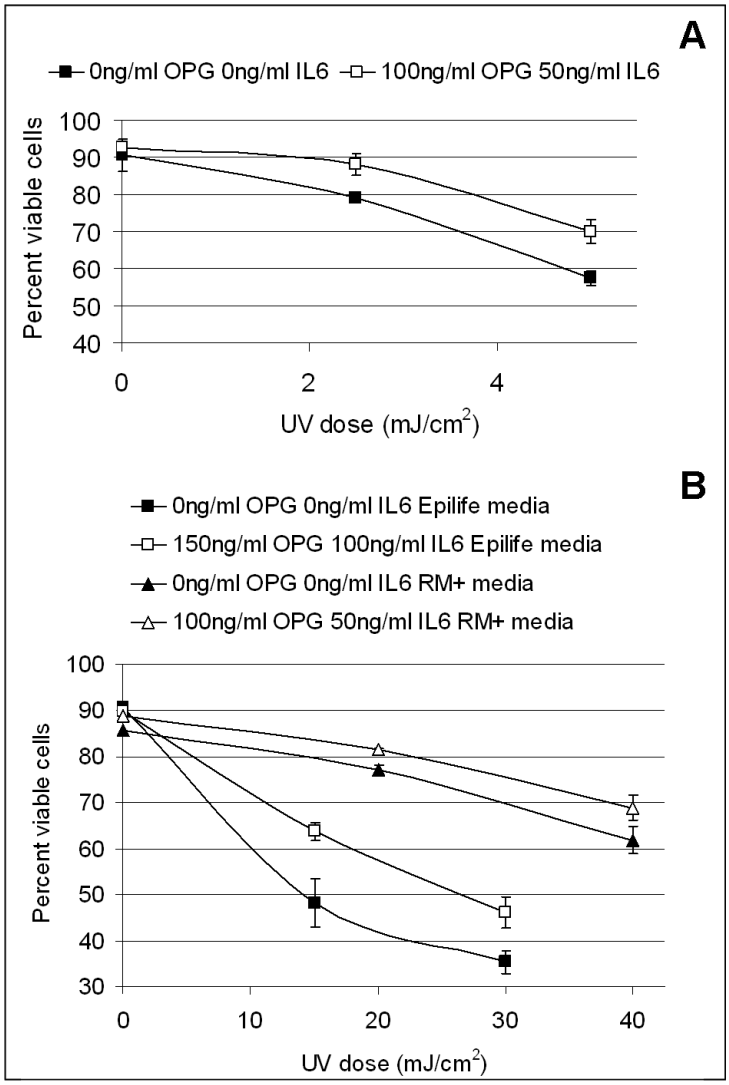

Figure 4-10 Addition of OPG and IL6 together decreases UV induced apoptosis in non-E6 cells.

A HT1080 cells cultured for 24 hrs, plus the 16 hrs post UV, with cytokines undergo significantly less apoptosis than those without cytokines; at 2.5 mJ/cm^2 P = 0.007; at 5 mJ/cm^2 P = 0.004.

B Keratinocytes cultured with cytokines also undergo less apoptosis than those without. Squares indicate cells cultured in EpiLife with cytokines for 24 hrs plus the 16 hrs post UV, at 15 mJ/cm^2 P = 0.008, at 30 mJ/cm^2 P = 0.011. Triangles indicate cells cultured in RM+ with cytokines for 48 hrs plus the 16 hrs post UV, at 20 mJ/cm^2 P = 0.019.

4.2.11 Mechanism of Osteoprotegerin inhibition of apoptosis

As mentioned, OPG is a secreted decoy receptor which prevents binding of the apoptosis-inducing ligand TRAIL to its cell surface receptor. This implies that it is involved in inhibiting the extrinsic apoptotic pathway through prevention of death receptor activation. Therefore its role as an inhibitor of TRAIL-induced apoptosis was studied, firstly in HT1080s.

HT1080s were treated with various doses ranging from 0, 10, 20, 50, 100 to 200 ng/ml of TRAIL and harvested after various time points ranging from 2 to 24 hrs. Figure 4-11 A shows representative results in which increasing doses of TRAIL cause a decrease in the remaining viable cells, with 20 ng/ml of TRAIL leaving 53% of the HT1080s viable after 4 hrs, and 41% viable after 16 and 24 hrs. At the higher TRAIL doses viability ranges from 19 to 31% after all time points. Thereafter cells were harvested after 16 hrs incubation with TRAIL, and lower concentrations of 10 and 20 ng/ml of TRAIL were used, to allow any inhibitory effects of OPG to be seen without being overwhelmed by large amounts of TRAIL.

To test the effect of OPG and IL6, HT1080s were incubated with OPG for 30minutes and with IL6 for 4 hrs prior to addition of TRAIL, harvested after 16 hrs and apoptosis measured with AnnexinV/PI as described. Figure 4-11 B shows that IL6 has no significant effect on apoptosis induced by TRAIL death receptor activation (44% [+/-4%] viable compared to 34% [+/-9%] viable cells treated with 0.1%BSA carrier solution only 20 ng/ml TRAIL, P= 0.08), whereas incubation with OPG increases the amount of viable cells remaining after treatment with 20 ng/ml of TRAIL from 34% to 79% (P=0.0003).

TRAIL induced apoptosis in HT1080s was also measured with a different apoptosis marker, activation of the executioner caspases 3/7, using a specific fluorogenic substrate, as described in Materials and Methods, section 2.1.9. HT1080s were cultured in 96-well plates, and media containing both TRAIL and OPG at the

indicated concentrations prepared just prior to addition to the cells. Apoptosis was measured by addition of the substrate after 6 hrs, and the fluorescence measured after 1hr30 in relative light units (RLU). Figure 4-11 C shows that increasing doses of OPG decreases the fluorescence of the caspase substrate, with 200 ng/ml OPG returning levels of apoptosis after 20 ng/ml TRAIL from 640 +/-117 RLU to the approximate basal level (196 +/-86 RLU) seen with no TRAIL (134 +/-20 RLU). Primary keratinocytes (cultured in RM+) were also incubated with varying doses of TRAIL ranging from 0, 10, 50 to 100 ng/ml, and apoptosis was measured by AnnexinV/PI after 16 hrs, however no increase in apoptosis was observed under these conditions. TRAIL sensitivity in keratinocytes has been reported, to a greater extent in transformed or dividing cells. It appears to be dependent on cell type, environmental factors, and structural differences in the TRAIL preparations (Qin et al., 2002) which may account for the lack of apoptosis seen in this culture system. However TRAIL-induced apoptosis appears to be important in UV irradiation of the skin (Bachmann et al., 2001) and so upregulation of OPG in keratinocytes could have a role in inhibition of apoptosis, supported by its inhibition of the extrinsic pathway in HT1080s, and so in SCC formation also.

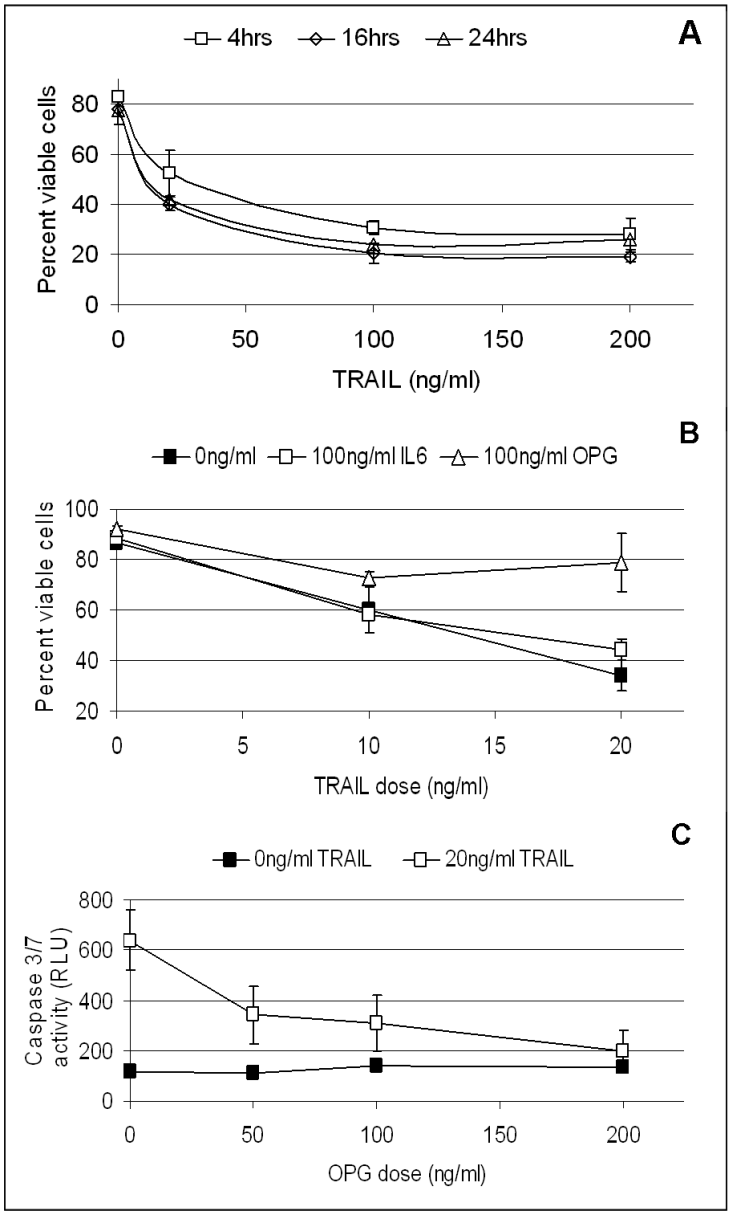

Figure 4-11 Osteoprotegerin inhibits TRAIL induced apoptosis.

A HT1080s treated with various doses of TRAIL were harvested at the time points indicated and apoptosis measured. For **A**, **B** and **C** error bars indicate standard deviation, 3 replicates.

B HT1080s were cultured with OPG for 30 minutes, IL6 for 4hrs, or 0.1% BSA carrier solution only, prior to addition of TRAIL, harvested 16 hrs later and apoptosis measured.

C HT1080s were cultured in 96-well plate, and apoptosis measured 6 hrs after addition of OPG and TRAIL at the indicated concentrations. Apoptosis is indicated by increased fluorescence of the caspase substrate (measured as RLU).

4.2.12 Mechanism of Interleukin 6 inhibition of apoptosis

As OPG inhibits the extrinsic/death receptor apoptosis pathway, it was hypothesised that IL6 may inhibit apoptosis by affecting activation of the intrinsic/mitochondrial pathway. This is also suggested by previous studies which have shown that IL6 exerts a cytoprotective effect through modification of levels of Bcl2 family members, important regulators of mitochondrial apoptosis (Cavarretta et al., 2007; Waxman and Kolliputi, 2009). Additionally, HPV E6 proteins have been shown to target the key mitochondrial apoptotic effector Bak (Jackson et al., 2000), so the effect of IL6 on Bak activation was tested. Bak is found in the outer mitochondrial membrane and upon apoptotic signals, such as DNA damage, undergoes conformational changes which allow it to multimerize, forming pores in the mitochondrial membrane and allowing release of apoptotic factors (Antignani and Youle, 2006; Griffiths et al., 1999; Mikhailov et al., 2003). One of these conformational changes yields a form of the protein labelled 'active Bak', which is able to multimerize and release apoptotic factors from the mitochondria. The levels of Bak activation were tested with a specific antibody which only detects this 'active' form of Bak, in combination with the DNA damaging drug camptothecin (CPT) to induce apoptosis. CPT binds to DNA and the enzyme Topo1, blocking its activity which leads to the generation of double-strand breaks (DSBs) in genomic DNA. This is particularly relevant as DSBs generated by the processing of cyclopyrimidine dimers are believed to be the most genotoxic lesion in skin produced after UV irradiation (Garinis et al., 2005).

HT1080s and keratinocytes were cultured for 16 hrs (plus treatment time) with IL6 (keratinocytes in EpiLife), CPT (or DMSO vehicle-only control) was added for the indicated treatment time and cells harvested, and levels of active Bak assayed by flow cytometry to give the specific Bak fluorescence as described in Materials & Methods, section 2.4.3. IL6 significantly reduces Bak activation 4 hrs post CPT in

HT1080s (from 484 +/-118 to 111 +/-30, arbitrary units, Figure 4-12 A) and 6 hrs post CPT in keratinocytes (from 691 +/47 to 380 +/30, Figure 4-12 B). Keratinocytes cultured in RM+ and IL6 were also assayed this way; however the morphology of the cells in this media makes them unsuitable for the FACS assay. The high Ca^{2+} levels in RM+ induce the formation of cell-cell junctions (desmosomes) meaning the colonies of keratinocytes are fixed together by the PFA during processing, making a single cell suspension for the flow cytometer unobtainable. As an alternative method of measuring active Bak, the same conformation-specific antibody was used in immunocytochemistry (ICC) as described in Materials & Methods, section 2.6.1. Figure 4-12 C shows examples of the staining resulting from activation of Bak, with an increase in strong, punctuate, green staining after CPT treatment corresponding to active Bak; and a total absence of green staining in the negative control, which was incubated without the primary antibody to demonstrate specificity. Keratinocytes were cultured in chamber slides with RM+, with 0.1% BSA carrier solution or 100 ng/ml IL6 for 4 or 6 hrs, and CPT as indicated. IFC was performed as described, and the percent of cells with active Bak scored as shown in Figure 4-12 D. When this was quantified it can be seen in Figure 4-12 E that growth of keratinocytes with IL6 significantly reduces the percentage of cells with active Bak 4hrs after CPT treatment from 18.5% to 5.5%. This indicates that IL6 affects the intrinsic apoptotic pathway involving an inhibition of Bak activation which in turn can affect release of apoptotic factors such as cytochrome c (CytC) from the mitochondria and commitment to apoptosis.

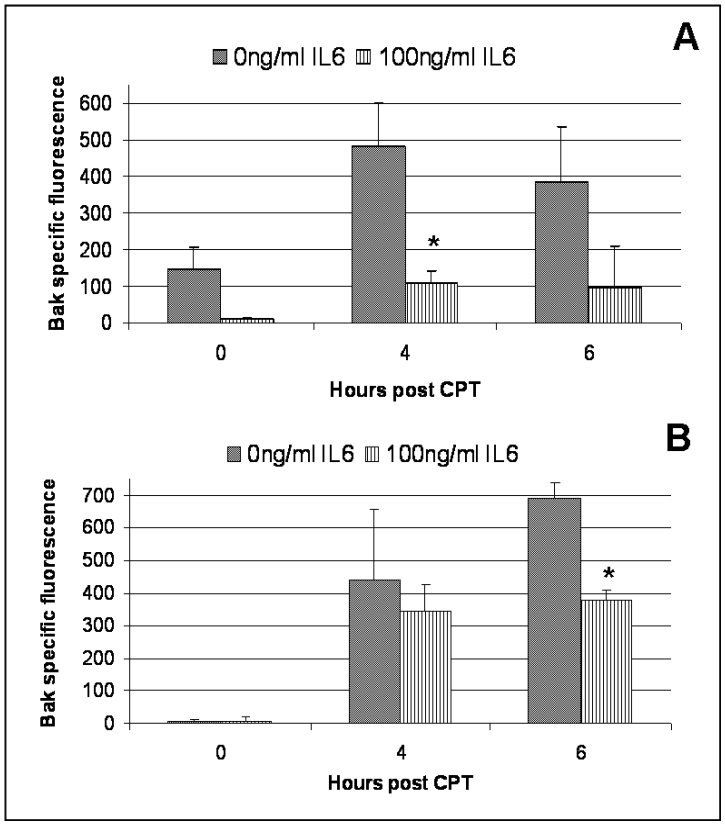

Figure 4-12 IL6 inhibits Bak activation

A Bak activation measured by FACS is reduced in HT1080s cultured overnight plus treatment time in IL6, 4 hrs post CPT * P = 0.034. For **A** and **B**, error bars indicate standard deviation, 2 replicates.

B Bak activation measured by FACS is reduced in keratinocytes cultured in EpiLife overnight plus treatment time in IL6, 6 hrs post CPT * P = 0.016.

C Examples of Bak activation in keratinocytes cultured in RM+ with IL6 measured with Ab1 IFC. Negative control was incubated with serum in place of the primary antibody; nuclei are blue (DAPI) and Ab1 is green (AlexaFluor488 secondary). Strong punctuate staining indicates active Bak.

D Example of the scoring used to quantify active Bak in keratinocytes cultured in RM+ with IL6, white arrows indicate positive cells.

E Quantification of active Bak staining by calculating the average percentage of Ab1 positive cells in three fields shows growth of keratinocytes in RM+ with IL6 reduces Bak activation significantly at 4 hrs post CPT treatment, * P = 0.021. Error bars indicate standard deviation, 3 replicates.

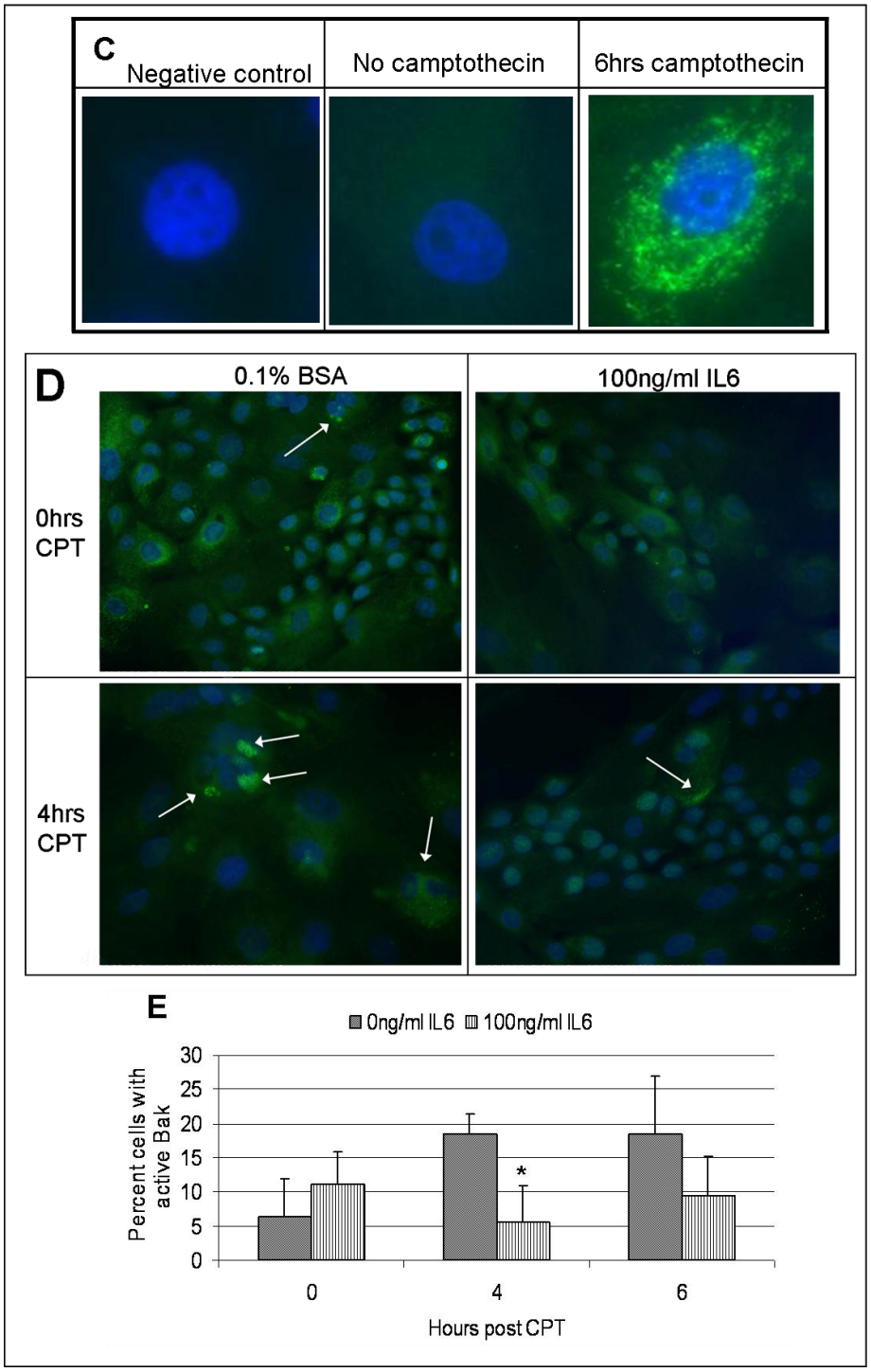

4.2.13 Osteoprotegerin and Interleukin 6 expression in SCC

To investigate whether the observed increase in OPG and IL6 in HPV5E6 expressing keratinocytes and the subsequent protection of cells from UV-induced apoptosis could be involved in HPV-associated SCC formation; sections from a

panel of HPV-typed SCCs were analyzed for OPG and IL6 expression patterns. As has been discussed, the increased expression of anti-apoptotic factors such as OPG and IL6 by a small number of HPV expressing cells in the skin could have an important role in SCC formation through inhibition of UV-induced apoptosis, allowing accumulation of mutations.

Sections from 18 different SCCs which had been characterized by the dermatology and pathology departments of the Royal London Hospital were used. HPV typing was performed and sections were stained by immunohistochemistry with antibodies to OPG and IL6 as described in Materials & Methods, section 2.6.2. A minimum of 3 fields-of-view of each section were scored blind, counting only the keratinocyte portions of the section (rather than connective tissue for example). As no nuclear staining was observed, cytoplasmic staining was scored with a protocol assigning scores (from 0 to 5) for both increased intensity of staining and higher percentage stained positively throughout the field-of-view. The overall staining score was calculated by intensity multiplied by percentage scores. Nine of the SCCs were HPV-negative and 9 contained HPV of various types, shown in Table 4-1.

Number	HPV type	Diff. status	Body site	Number	HPV type	Diff. status	Body site
1	Negative	WD	L hand	10	Z95969 β type	MD	Scalp
2	Negative	WD	Nose	11	5, 20	WD	R temple
3	Negative	WD	R forearm	12	36	MD	R forearm
4	Negative	WD	L forehead	13	21	MD	R temple
5	Negative	MD	Scalp	14	5	WD	R ear
6	Negative	WD	R forehead	15	Novel	WD	R forearm
7	Negative	WD	L knee	16	5	WD	R buttock
8	Negative	WD	L cheek	17	24	WD	L cheek
9	Negative	MD	Scalp	18	15	WD	R upper chest

Table 4-1 Details of the SCC sections used.

Diff. = differentiation, WD = well differentiated, MD = moderately differentiated.

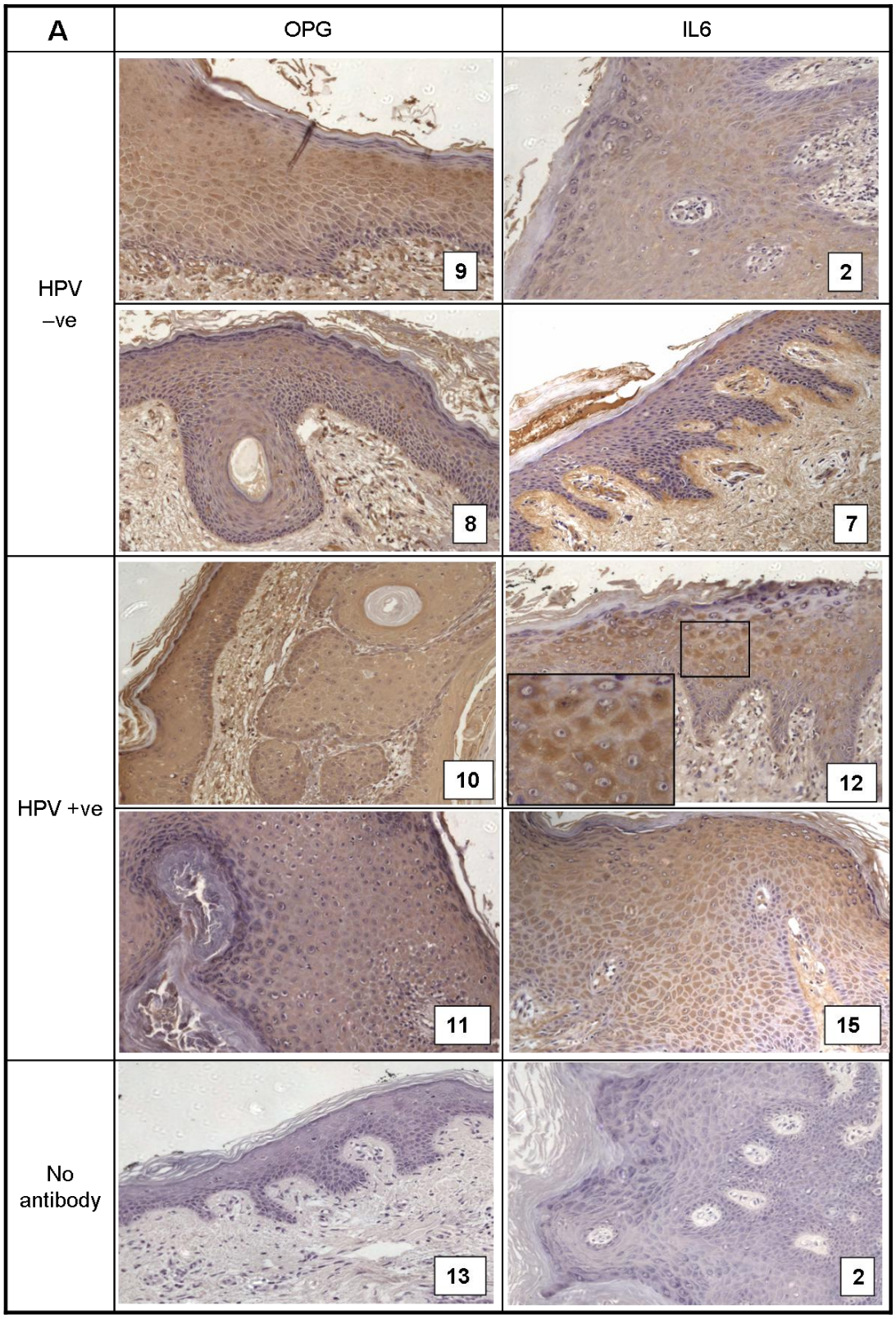

Figure 4-13 OPG and IL6 expression in HPV-positive and negative SCCs

A Examples of HPV positive and negative sections stained for OPG and IL6. Staining was scored in a minimum of 3 fields of view per section according to intensity and percentage

stained. Overall staining score = percentage x intensity. Section number is indicated in the lower right. Original magnification 200x, insert 500x.

B Average overall staining scores indicate no difference in OPG levels, but a significant increase in IL6 in HPV positive SCCs, when tested by one-way ANOVA, P = 0.0003. The SCCs along the x-axis are presented in the same order as in Table 4-1.

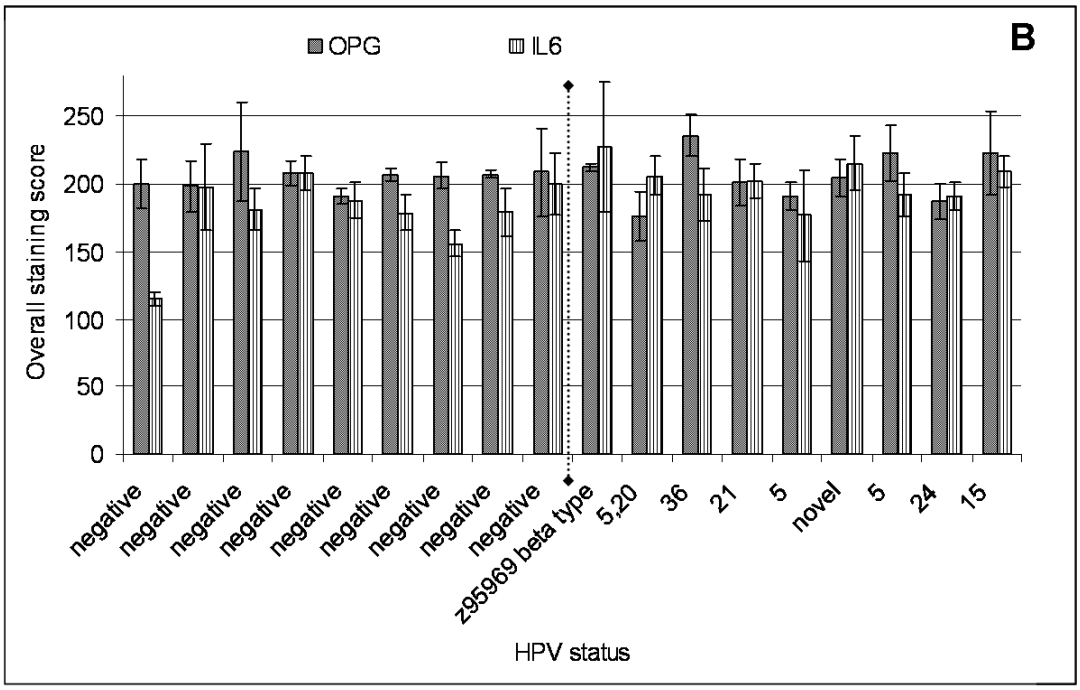

Figure 4-13 A illustrates the staining for OPG and IL6 with examples of both HPV-positive and -negative SCCs, along with the negative no primary antibody controls, which show specificity of the staining by the absence of brown staining. While a generally uniform staining pattern was seen for IL6 in HPV-negative tumors, in HPV-positive tumors strong cytoplasmic staining was observed in regions of the suprabasal cell layers, along with increased overall levels of staining.

Quantification of the data and analysis for statistical significance with a one-way ANOVA test showed that the HPV-positive tumors express significantly more IL6 than HPV-negative tumors, (Figure 4-13 B, F = 14.5, P = 0.0003). There was no significant difference in the staining scores for OPG in SCC sections that was associated with HPV status (F = 0.016, P = 0.9).

4.3 Discussion

4.3.1 Co-culture and conditioned media experiments

The use of HT1080 cells stably expressing EGFP allowed mixed cultures of E6 and non-E6 expressing cells to be grown, and the apoptotic response of each of the cell types in the co-culture to be tested. This allowed the protection of HT1080s from Fas-Ab apoptosis by other HT1080 cells expressing HPV5, 8 and 18E6 to be seen. Further studies presented here indicated this protection from apoptosis was likely to be mediated by changes in factors secreted from the cells, rather than cell-cell contact, as conditioned media, from both HT1080s expressing HPV5, 8 and 18E6, and primary keratinocytes expressing HPV5E6 also protected non-E6 expressing cells from Fas-Ab and/or UV-irradiation induced apoptosis. This result is important as it suggests a mechanism by which a low number of cutaneous HPV-expressing cells could contribute to the reduction in apoptosis seen in HPV-positive SCC. The mechanism was further investigated with cytokine arrays which allowed comparison of 174 different cytokines and growth factors between normal and E6 conditioned media of HT1080s and keratinocytes.

4.3.2 Most significant changes from the conditioned media arrays

Inspection of the arrays revealed that Interleukin (IL) 6 was the only cytokine significantly upregulated compared to parental conditioned media in media conditioned with HT1080 and keratinocyte HPV5 and 8E6; and Osteoprotegerin (OPG) was upregulated in HT1080 HPV5E6 and keratinocyte HPV8E6 conditioned media. These cytokines were selected for further study; however other changes on the array could be interesting. For example, GRO and IL10Rβ were significantly upregulated, and Fas, FGF-4 and FGF-9 are significantly downregulated, in three of the conditioned media types. GRO (Growth related oncogene, also called CXCL1 and melanoma growth stimulating activity) is a chemokine associated with

tumourigenesis, especially with activation of NFκB in melanoma (Dhawan and Richmond, 2002). Fibroblast growth factors are involved in regulating a range of activities, with FGF-4 implicated in stem cell development and FGF-9 in tissue homeostasis and the proliferative response to injury (Turner and Grose, 2010). The Fas downregulation observed here differs to the result showing upregulation of Fas in HPV5E6 expressing keratinocytes observed in Chapter 3; however these apparently contrary results could correspond to less shedding of Fas into the media and therefore retention on the cells.

4.3.3 Additional changes on the conditioned media arrays

Several factors were also upregulated in both HPV5 and 8E6 conditioned media in keratinocytes, these include Leptin, Eotaxin 3, FGF-6, Flt3 ligand, IL1β, IL1Rα, IL2, IGFBP4, ICAM1, latency associated peptide (LAP), and ALCAM. Several of these factors have some association with cancer or the skin which could be relevant to investigations of HPV-associated SCC formation. Leptin is structurally similar to IL6, has a role in immune modulation, is involved in the JAK/STAT signalling pathway and a role in some cancers has been reported (Nkhata et al., 2009). Eotaxin 3 (CCL26) is a chemokine for eosinophils and has recently been shown to be involved in the skin lesions of atopic dermatitis (Owczarek et al., 2010). Flt3 (fms-like tyrosine kinase receptor 3) ligand is involved in regulating dendritic cell development, as receptor activation leads to proliferation and survival signalling, with constitutive activation common in the leukaemia AML (Advani, 2005; Jonsson et al., 2004). IL1β and IL1Rα form part of the Interleukin 1 pro-inflammatory signalling pathway. IL1β is expressed by keratinocytes especially after UV irradiation (Kupper et al., 1987) and is also one of the components that stimulated keratinocyte proliferation in a recent study (Domaszewska-Szostek et al., 2009). Expression of HPV16 and 38E6/E7 increases IL1β expression in keratinocytes especially after UV (Dell'oste et al., 2008). Interleukin 2 is another pro-

inflammatory cytokine which is involved in the survival and differentiation of T cells, as receptor activation can trigger the Ras/MAPK, JAK/Stat and PI3-kinase signalling pathways. Its regulation of T cell homeostasis and the consequent anti-tumour immune response has led to its use for treatment of several cancers (Overwijk and Schluns, 2009). IGFBP (insulin-like growth factor binding protein) 4 is expressed by a wide range of tissues including many types of cancer but its role is unclear, with some reports of cell growth inhibition (Durai et al., 2006). LAP binds to and inhibits TGF (transforming growth factor) β, affecting immune modulation, along with other functions (Ali et al., 2008). ALCAM (activated leukocyte cell adhesion molecule) is expressed by several cell types mainly at cell-cell boundaries, as well as in several cancer types (Ofori-Acquah and King, 2008). ICAM (intercellular adhesion molecule) is essential for leukocyte trafficking out of blood vessels, and is also widely expressed and upregulated by inflammatory cytokines. Interestingly ICAM has also been shown to be upregulated by expression of HPV5 and 38E6/E7 in keratinocytes (De Andrea et al., 2007), along with MCP1 (monocyte chemotactic protein), which is also upregulated in the HPV5E6 expressing keratinocyte media tested here (Figure 4-5). A recent study (Akgul et al., 2010) has also shown that HPV5 and HPV8E6 downregulate IL8 expression in primary keratinocytes, in agreement with the result presented here that IL8 is significantly down regulated in HPV5E6 conditioned media, although this downregulation in HPV8E6 conditioned media did not reach significance in our assay. IL8 is also a pro-inflammatory cytokine with chemoattractant properties, whose production by keratinocytes is increased by UV irradiation as part of the warning to surrounding tissue of UV damage (Li et al., 2001a).

The protection from UV-induced apoptosis provided by the addition of IL6 and OPG to HT1080 and keratinocyte cultures is not complete, but as previously mentioned, a shift in the balance of pro-and anti-apoptotic factors in the skin microenvironment

could be enough to confer a survival advantage to cells after UV irradiation and therefore permit the persistence of damaged cells. Additionally, secretion of immuno-modulating cytokines by even a small number of HPV-positive cells could locally protect transformed cells or part of a tumour by affecting the local immune response. Therefore it would be interesting to investigate the changes in factors which have an immuno-modulatory role along with the apoptosis related cytokines.

4.3.4 Upregulation of OPG

The observed upregulation of OPG could have an important role in protecting keratinocytes (both E6 and non-E6 expressing) from apoptosis, as keratinocytes have been shown to be susceptible to TRAIL (Wachter et al., 2004). In contrast to the mechanism proposed here, high-risk anogenital HPV16 has been shown to inhibit TRAIL-induced apoptosis via E5 inhibition of DISC (Death-inducing signalling complex) formation (Kabsch and Alonso, 2002), and E6 mediated degradation of FADD (Fas-associated death domain) (Garnett et al., 2006). In addition, a study of the epithelial-mesenchymal transition of keratinocytes expressing either HPV16, 38 or 8E6/E7 showed upregulation of OPG by the cutaneous HPV types 8 and 38 (Azzimonti et al., 2009).

4.3.5 Upregulation of IL6

The results shown here illustrating the upregulation of IL6 by HPV5E6 are in agreement with previous studies showing IL6 upregulation in keratinocytes by HPV5 and 16E6/E7 (De Andrea et al., 2007) and by HPV38E6/E7 (Dell'oste et al., 2008). It is also interesting to note findings that persistent DNA damage leads to an increase in IL6 secretion by fibroblasts (Rodier et al., 2009); as previous work in the lab has shown that HPV5E6 expression impairs the repair of thymine dimers induced by UV (Giampieri and Storey, 2004) and this could therefore contribute to IL6 upregulation. IL6 is also one of the cytokines upregulated in media from

irradiated human dermal fibroblasts which increase the DNA damage response in non-irradiated cells (Dieriks et al., 2010). As mentioned, IL6 is a pleiotropic cytokine, which is known to be expressed, along with its receptor, by keratinocytes (Yoshizaki et al., 1990), with roles including regulation of barrier formation in the skin (Wang et al., 2004b). Activation of JAK tyrosine kinases by receptor binding can in turn activate the mitogen-activated protein kinase (MAPK), PI-3 kinase and signal transducers and activators of transcription (STAT) pathways (for example Ogata et al., 1997). These lead to cell survival and proliferation by transactivation of anti-apoptotic and growth factors, and inactivation of pro-apoptotic factors. Constitutive activation of STAT3 in particular is linked to many types of cancer (Hodge et al., 2005). IL6 has been shown to affect the balance of the Bcl2 family apoptotic regulators, for example in multiple myeloma cells deprived of IL6 there is a downregulation of anti-apoptotic Bcl2, Mcl1 and Bcl-x_L, and upregulation of apoptotic Bax (Spets et al., 2002). Prostate cancer cells have also been shown to be resistant to apoptosis through upregulation of Mcl1 via an autocrine IL6 loop (Cavarretta et al., 2007). IL6 also increases Bcl2 expression, inhibits hydrogen peroxide-induced mitochondrial membrane depolarization, and affects activation of Bak in transgenic mouse cells (Waxman and Kolliputi, 2009). This upregulation of anti-apoptotic Bcl2 family members correlates with the upregulation seen in Chapter 3, where Bcl2 and Bcl-x were upregulated in lysates of HT1080 cells and primary keratinocytes expressing HPV5E6 on the Proteome arrays (Figure 3.3 E), and Mcl1 is upregulated in HPV5E6 expressing HT1080 cells as seen by western blot (Figure 3.13). Therefore the upregulation of IL6 by HPV5E6 could contribute to this upregulation of anti-apoptotic Bcl2 family members through autocrine signalling.

4.3.6 Summary

These studies, along with the results shown here (Figure 4-10) that OPG and IL6 are both required to inhibit UV-induced apoptosis in keratinocytes, suggested that IL6 functions by inhibiting the intrinsic/mitochondrial pathway, whereas OPG inhibits the extrinsic/death receptor pathway by preventing binding of TRAIL. The results shown here support this theory, with IL6 treatment inhibiting active Bak formation in HT1080s and keratinocytes (Figure 4-12) and OPG reducing TRAIL-induced apoptosis in HT1080s (Figure 4-11).

The results presented here suggest that increased OPG and IL6 secretion by cells expressing HPV5E6 may serve to protect the infected host cell from UV-induced apoptosis via an autocrine mechanism, while a paracrine effect may protect neighbouring non-HPV infected cells through a 'bystander effect'. A small number of keratinocytes exposed to higher cytokine concentrations may preferentially survive UV-induced apoptosis, contributing to tumourigenesis. This is in contrast to tumourigenesis in cervical cancer, where there is no UV-irradiation and high-risk mucosal HPV DNA and proteins are found in every cell, and therefore a paracrine anti-apoptotic effect may not be as important. A related tumourigenesis model involving a bystander effect has been proposed for hepatocellular carcinoma arising from chronic infection with Hepatitis C virus (HCV), where HCV inhibits Fas-induced apoptosis of infected hepatocytes, but also impairs the immune response by affecting CD8(+) T cells (Castello et al., 2009).

It has been established that the E6 proteins of both high-risk and low-risk mucosal and cutaneous types have multiple binding partners and affect many cellular pathways (Howie et al., 2009). The results shown here demonstrate how different activities of HPV5E6 work in combination to reduce UV-induced apoptosis, and the finding that IL6 is increased in HPV-positive SCC imply that the protection from UV-induced apoptosis this provides may be important in tumour formation.

4.3.7 Further work

It would be of interest to test cells and conditioned media from both HT1080s and keratinocytes expressing other HPV types (8, 10, 18 and 77) for similar changes, especially of OPG and IL6, by QRTPCR but also at the protein level. It would also be valuable to analyse conditioned media by mass spectrometry (MS) to gain a complete picture of the spectrum of secreted factors, rather than only those spotted on the arrays. This would require optimisation of preliminary MS work which yielded mainly serum proteins and keratins. Further work to optimise ELISAs to quantify the levels of IL6 and OPG found in conditioned media would also be useful; with the aim of correlating with the doses used in the apoptosis assays. Further confirmation of some of the other most interesting changes seen on the arrays along with investigations of possible mechanisms of action would also be valuable. In addition, as the cytokine arrays were performed with conditioned EpiLife, it would be of particular interest to repeat the assay with RM+ conditioned media, given the known effect the culture conditions have on keratinocytes.
More detailed investigations into how IL6 regulates Bak activation would be worthwhile, especially with respect to work being done in this lab on the regulation of conformational changes leading to Bak activation by various kinases and phosphatases. Further investigation into OPG and IL6 protection from apoptosis could also be carried out, for example IL6 could be silenced in keratinocytes and these cells used in organotypic raft cultures in which UV-apoptosis could be tested. Mouse models of HPV-associated SCC formation (Schaper et al., 2005) could also be used to investigate the bystander effect.

5 Global expression changes in primary keratinocytes with HPV5E6 expression and UV irradiation

5.1 Introduction

As described in detail in Chapter 1, UV irradiation is a major inducer of apoptosis in keratinocytes, mediated by its damaging effects on DNA, generation of reactive oxygen species (ROS) and activation of the death receptor pathways (Van Laethem et al., 2009). The association between the development of squamous cell carcinoma (SCC) and infection with a subset of cutaneous HPV types has also been described previously. Aside from their role as a co-factor with UV irradiation, the mechanisms of viral tumourigenesis have not been completely elucidated. The work presented in the previous chapters addressed the possible mechanisms of inhibition of UV-induced apoptosis by cutaneous HPV E6, which could contribute to accumulation of potentially tumourigenic mutations, both in E6 expressing cells and non-E6 expressing neighbouring cells. However, as has been described in section 1.3.4.3, the E6 protein has previously been shown to have multiple effects through different interactions. Therefore to increase our understanding of the effects of HPV5E6 expression in keratinocytes, and the relationship with UV irradiation, investigation into cellular gene expression patterns was undertaken.

5.1.1 Aims

To gain insight into the overall gene expression changes induced by expression of the high-risk genus-β HPV5E6 in primary human adult keratinocytes, microarray analysis was performed. Further investigations into the apoptotic responses to UV irradiation of primary keratinocytes were also carried out using microarrays, and

consequently the effect of both HPV5E6 expression and UV irradiation could be compared.

5.2 Results

5.2.1 Clustering of replicate arrays

Primary human keratinocytes stably expressing either empty vector control pLXSN or HPV5E6 were made as described previously. Keratinocytes from the same donor were used but 3 different replicate retroviral infections were used for the microarray repeats. Once drug selection was complete, early passage keratinocytes were grown to 60% confluence in EpiLife, exchanged into RM+ for 48 hrs, and induced with 0 or 30 mJ/cm^2 UV, and harvested 16 hrs later. This dose and time point was used as it is known to induce apoptosis in a proportion (30-40%) of the keratinocytes, as it corresponds to the experimental conditions used in previous AnnexinV/PI apoptosis FACS assays. Cells which had detached from the surface were also collected. RNA was extracted as described in Materials and Methods (section 2.2.1) and submitted to the Cancer Research UK Affymetrix Genechip Microarray Service at the Paterson Institute for Cancer Research (PICR), Manchester, for processing on Affymetrix Human Exon arrays. These arrays contain over a million probes, with approximately four probes per exon and forty probes per gene, meaning that as well as information on gene expression, additional exon analysis can be performed for information on the expression of different isoforms of genes. A summary of the workflow is presented in Figure 5-1. The resulting files are quality checked by the PICR staff and uploaded onto the MIAME VICE database, from whence they were downloaded for analysis, with assistance from the Computational Biology Research Group (CBRG) at the Weatherall Institute for Molecular Medicine (WIMM). Data was then analysed with the affylmGUI and oneChannelGUI programmes (Sanges et al., 2007; Smyth, 2004).

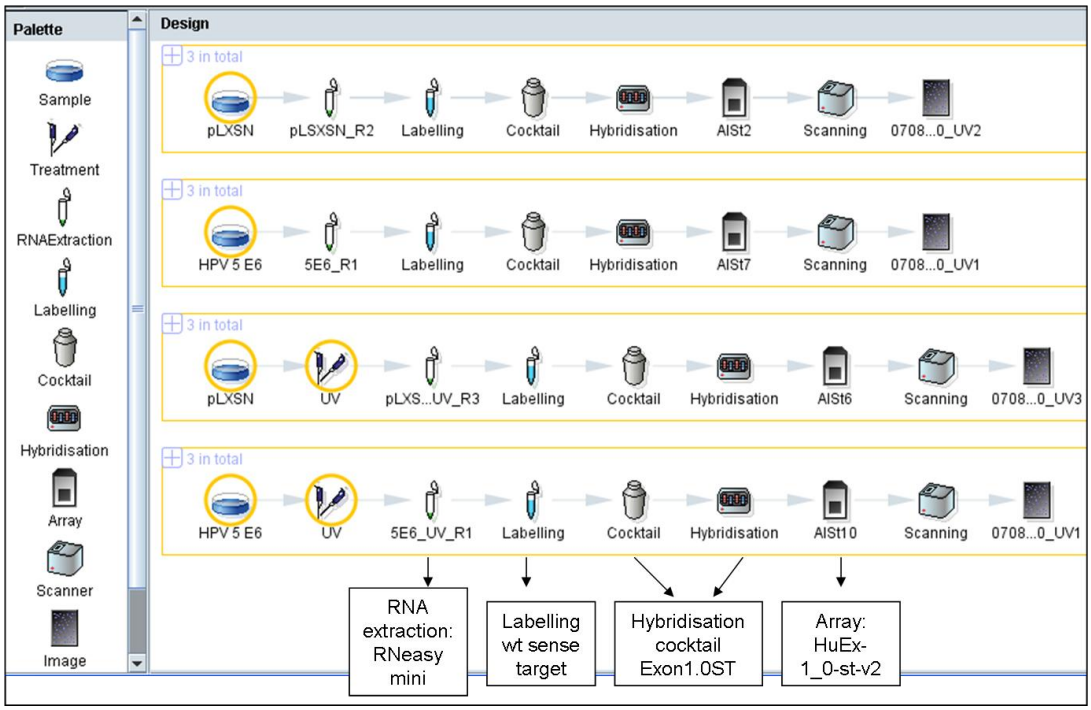

Figure 5-1 Summary of the workflow for microarray analysis.

The steps involved in microarray analysis using Affymetrix Human Exon Arrays (taken from the MIAME VICE online database).

The oneChannelGUI programme allows analysis of exon arrays, however the analysis presented here is at the gene level. Data was normalized (Robust Multiarray Average [RMA] method was used) and the linear model fit computed. This allows comparison between the groups of replicates. In addition to the quality checks performed on the arrays themselves, the biological replicates can also be quality-control checked by Principle component analysis (PCA) and by performing hierarchical clustering (HCL). The results of these tests are shown Figure 5-2.

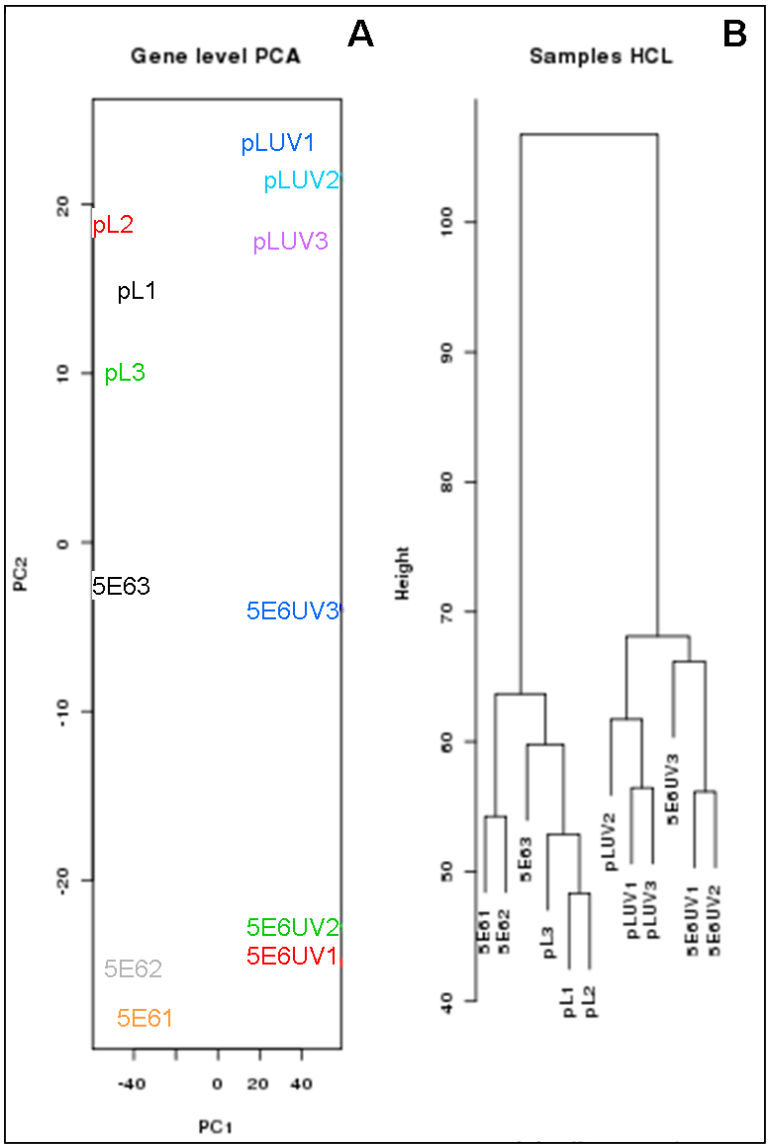

Figure 5-2 PCA and HCL analysis of microarray replicates

A The PCA space showing the grouping of the pLXSN repeats in the upper left, pLXSN +UV in the upper right, HPV5E6 lower left, and HPV5E6 +UV lower right.

B The HCL dendrogram showing the grouping of the replicates.

PCA is a statistical tool that aims to simplify visualisation of large datasets by reducing the large number of observations (Ringner, 2008). It does this by combining all the variables to identify the key variables, called principle components, along which the samples differ, which in this case allows the separation of the samples according to the experimental conditions. Therefore it can be seen in Figure 5-2 A that the replicates are quite well separated into four

corners of the plot, with the exception of the 5E63 and 5E6UV3 samples which are more central. A similar result can be seen in Figure 5-2 B, in which the replicates cluster together, firstly according to the presence or absence of UV, then the presence or absence of HPV5E6. The only exception to this is the 5E63 sample, which is an outlier in the pLXSN branch. 5E6UV3 also appears slightly apart from the other 5E6UV samples. These findings could indicate a difference in this infection repeat, which perhaps led to lower expression levels of HPV5E6 in that replicate.

5.2.2 Pathway analysis

The Ingenuity Pathway Analysis (IPA) software (Ingenuity® Systems, www.ingenuity.com) was used for further analysis of the differentially expressed genes. The 'top table' lists of differentially expressed genes, generated with oneChannelGUI as described above, consisting of AffyID identifiers, and expression values of M (fold change) and the P value, were uploaded into Ingenuity. The molecules are mapped to Ingenuity's 'Knowledge base', which is manually curated from the literature to provide information on relationships between molecules, pathways and diseases. This allows large gene lists to be analysed on a wider scale, showing information on affected pathways. Some of the gene changes from the oneChannelGUI results tables are presented in combination with IPA results below.

5.2.3 Expression changes in keratinocytes with HPV5E6 expression

The presence of expression data from replicate arrays allows the software to calculate a 'top table' of differentially expressed genes, which along with the fold change in expression levels, also allows calculation of the Bayes statistic (B, the log odds ratio of differential expression), which takes into account both the fold change and the variance between replicate arrays. Firstly, differences in expression between pLXSN and HPV5E6 expressing keratinocytes, without UV,

were calculated, with the absolute fold change cut-off set as 1, and the P value cut-off set as 0.05. A graphical overview of the results is shown in Figure 5-3, with the MA plot showing the normalization is correct by the horizontal distribution of the datapoints, and the volcano plot in Figure 5-3 B showing the significant gene changes. Here, the horizontal axis shows the fold change or the biological impact of the change, and the vertical axis the statistical reliability of the change. It can be seen that there is a relatively small number of significantly changed genes, with more down- than up-regulated with HPV5E6 expression. The full details of the changes are shown in the top table at the end of the chapter, in Table 5-10.

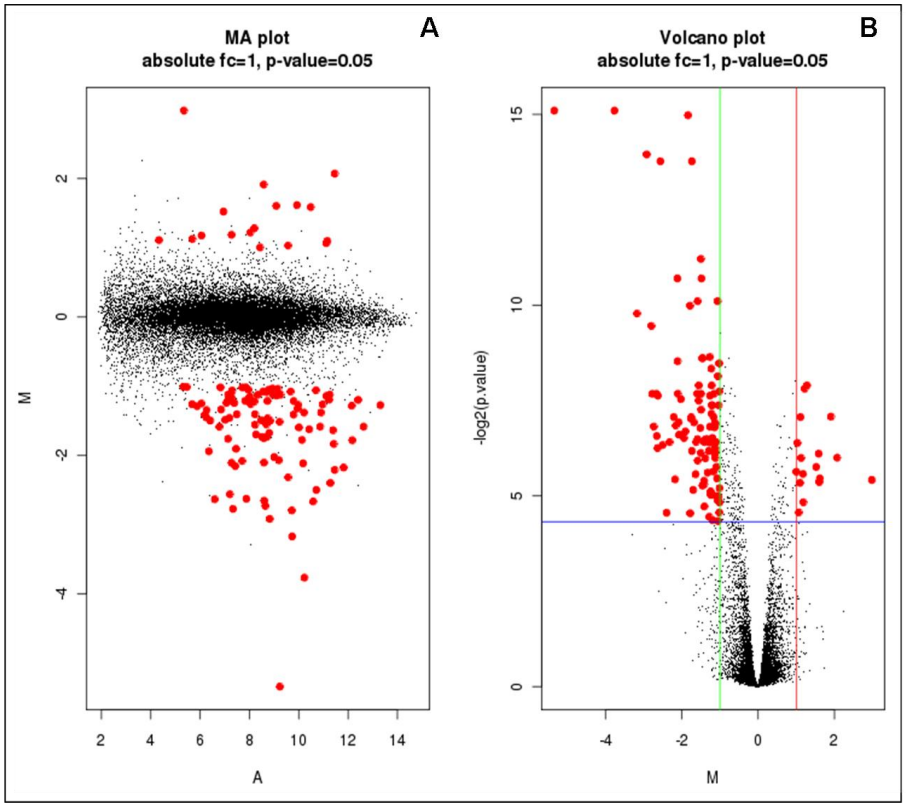

Figure 5-3 Graphical representation of expression changes in HPV5E6 expressing primary keratinocytes compared to pLXSN controls.

A The MA plot shows significantly upregulated and downregulated genes in red, comparing the log ratios (M) and log intensities (A).

B The volcano plot shows the significantly upregulated (right) and downregulated (left) genes in red.

The majority of genes are downregulated and the list includes several which are involved in regulation and formation of the cornified envelope of the skin, which have been collected and shown in Table 5-1.

Table 5-1 Genes downregulated in HPV5E6 expressing keratinocytes compared to pLXSN controls, without UV.

The gene is shown by GenBank symbol and description. The table is ordered according to descending B statistic, which incorporates P and M (= absolute fold change).

SYMBOL	DESCRIPTION	M	P Value	B
SPRR3	small proline-rich protein 3	-3.76	0.0000	10.75
ECM1	extracellular matrix protein 1	-1.83	0.0000	10.08
KRT24	keratin 24	-1.48	0.0006	7.14
SPRR2A	small proline-rich protein 2A	-1.58	0.0009	6.64
SPRR2D	small proline-rich protein 2D	-1.78	0.0010	6.49
KRT4	keratin 4	-3.17	0.0011	6.31
LCN2	lipocalin 2	-2.21	0.0075	3.15
KRT10	keratin 10	-2.07	0.0103	2.59
CLDN4	claudin 4	-1.38	0.0112	2.35
PPL	periplakin	-1.27	0.0118	2.23

For example, the small proline-rich protein (SPRR) family are structural proteins encoded, along with loricrin and involucrin, on the epidermal differentiation complex on chromosome 1q21 (Cabral et al., 2001). Lipocalin 2 (also called neutrophil gelatinase-associated lipocalin, NGAL) has anti-microbial properties, has been induced in keratinocyte tissue culture models by calcium-induced differentiation, but is not observed in normal skin, but expressed in inflammatory conditions and neoplasias, indicating it has a role in maintenance of skin homeostasis (Lee et al., 2008). ECM1 also has a role in the control of keratinocyte differentiation (Chan, 2004), whereas claudin 4 has a role in tight junction formation, which plays a role in barrier function (Yuki et al., 2007). Periplakin is a cytoskeletal protein also involved in the assembly of the cornified envelope and regulation of keratinocyte differentiation (Boczonadi et al., 2007). Keratin 4 is upregulated in mucosal epithelia, however the expression patterns and function of Keratin 24 are not well

studied (Moll et al., 2008). Keratin 10 is expressed by differentiated keratinocytes in the upper layers of the cutaneous epidermis, is important in giving mechanical integrity to the keratinizing cells, and it has also been found that loss of K10 leads to increased keratinocyte proliferation (Reichelt et al., 2004).

The downregulation of these genes involved in keratinocyte differentiation and formation of the cornified envelope suggests that expression of HPV5E6 is disrupting this process, which could be important in the viral lifecycle, and also contribute to tumourigenesis.

Previous studies on the effects of HPVE6 expression on global gene expression have also seen differential regulation of differentiation-related genes. Expression of HPV18E6/E7 in organotypic cultures showed the category with the most significant changes was 'differentiation and proliferation' (Garner-Hamrick et al., 2004). Another study giving a more detailed list of genes differentially regulated by HPV16E6/E7 also shows several overlaps with the results shown here (Duffy et al., 2003), including downregulation of Involucrin, lipocalin 2 (NGAL), ECM1, keratin 4, and several SPRRs; and upregulation of mitochondrial aldehyde dehyrogenase (ALDH) 1, whereas ALDH2 was slightly upregulated by HPV5E6, shown in Table 5-2.

As there are only a small number of genes significantly upregulated in HPV5E6 keratinocytes compared to pLXSN controls, these are shown separately in Table 5-2. It can be seen that, contrary to the results presented in Chapter 4, which showed a significant upregulation of interleukin (IL) 6 mRNA in HPV5E6 expressing keratinocytes, IL6 does not appear on this list.

Table 5-2 Significantly upregulated genes in HPV5E6 expressing keratinocytes.

The gene is shown by GenBank symbol and description. The table is ordered according to descending B statistic, which incorporates P and M (= absolute fold change).

SYMBOL	DESCRIPTION	M	P Value	B
MCAM	melanoma cell adhesion molecule	1.28	0.0042	4.45
PCDH7	protocadherin 7	1.22	0.0045	4.28
SLCO2A1	solute carrier organic anion transporter family, member 2A1	1.91	0.0074	3.22
PDPN	podoplanin	1.03	0.0120	2.19
BNIP3	BCL2/adenovirus E1B 19kDa interacting protein 3	1.59	0.0145	1.81
MT1G	metallothionein 1G	2.07	0.0156	1.71
AS3MT	arsenic (+3 oxidation state) methyltransferase	1.13	0.0157	1.68
RPS10P7	ribosomal protein S10 pseudogene 7	1.52	0.0185	1.43
ALDH2	aldehyde dehydrogenase 2 family (mitochondrial)	1.01	0.0202	1.27
SLC1A1	solute carrier family 1 (neuronal/epithelial high affinity glutamate transporter, system Xag), member 1	1.18	0.0210	1.20
IVNS1ABP	influenza virus NS1A binding protein	1.62	0.0227	1.09
IL28A	interleukin 28A (interferon, lambda 2)	2.98	0.0234	1.04
FAP	fibroblast activation protein, alpha	1.61	0.0243	0.98
TGFBI	transforming growth factor, beta-induced, 68kDa	1.10	0.0246	0.95
GPR155	G protein-coupled receptor 155	1.19	0.0351	0.32
CXCL1	chemokine (C-X-C motif) ligand 1 (melanoma growth stimulating activity, alpha)	1.07	0.0422	0.03

A brief overview of these upregulated genes does not immediately reveal a specific area of keratinocyte biology that was affected. The most upregulated gene shown here is IL28A, which is a member of the type III interferon family, expression of which can be induced by viral infection and which activates an antiviral response, similar to but weaker than type I interferons (Meager et al., 2005). This could therefore be a cellular response to expression of the HPV5E6 protein. MT1G is part of a metal-binding family which can be involved in different cellular processes, for example zinc homeostasis, and it has been shown to be a methylated tumour suppressor in hepatocellular carcinoma (Kanda et al., 2009). SLCO2A1 is a member of the organic anion transporter family, and is linked to transport of Prostaglandin, which regulates mucosal integrity but has also been linked to cancer progression (Mandery et al., 2010). MCAM, also called CD146, has been found on melanoma and smooth muscle cells, and has a role in angiogenesis. It has also

been linked to melanoma and prostate cancer progression, is thought to activate AKT signalling in melanomas, and is also upregulated on suprabasal keratinocytes in inflammatory skin conditions such as psoriasis, and in viral warts (Ouhtit et al., 2009; Weninger et al., 2000). BNIP3 is a member of the Bcl2 family of apoptotic regulators, but as a BH3-only protein it is pro-apoptotic. However it is also important in regulating autophagy via an association with Beclin-1, in particular during hypoxia and via mitophagy (a type of autophagy where mitochondria are targeted for degradation) (Zhang and Ney, 2009). An induction of autophagy rather than apoptosis could contribute to cell survival.

Additionally, the comparison between pLXSN and HPV5E6 expressing cells was analysed by IPA. The summary of the pathways and functions with the most significant differential expression is shown in Table 5-3. In addition, the 19 Function groups with the most significant differential expression (and the number of molecules involved) between pLXSN and HPV5E6 expressing keratinocytes are shown in Figure 5-4.

Table 5-3 Summary of IPA of genes differentially expressed in pLXSN and HPV5E6 keratinocytes.

Top Networks:	*Molecule Score:*
Cell-To-Cell Signalling and Interaction, Cancer, Gastrointestinal Disease	57
Lipid Metabolism, Small Molecule Biochemistry, Cell Death	35
Drug Metabolism, Endocrine System Development and Function, Lipid Metabolism	25
Cell Cycle, Small Molecule Biochemistry, Infection Mechanism	22
Cellular Development, Hair and Skin Development and Function, Drug Metabolism	18
Top Bio Functions:	
Diseases and Disorders:	
Cancer	30
Reproductive System Disease	14
Infection Mechanism	4
Infectious Disease	6
Gastrointestinal Disease	13
Molecular and Cellular Functions:	
Cell to Cell signalling and interaction	19
Drug metabolism	7
Lipid metabolism	14
Small molecule biochemistry	20
Cellular movement	15
Physiological system development and function:	
Endocrine system development and function	5
Nervous system development and function	3
Tumour morphology	4
Lymphoid tissue structure and development	2
Reproductive system development and function	9
Top Canonical Pathways:	
Glycerolipid metabolism	
C21-steroid hormone metabolism	
Metabolism of xenobiotics by cytochrome P450	
Androgen and oestrogen metabolism	
Fatty acid metabolism	

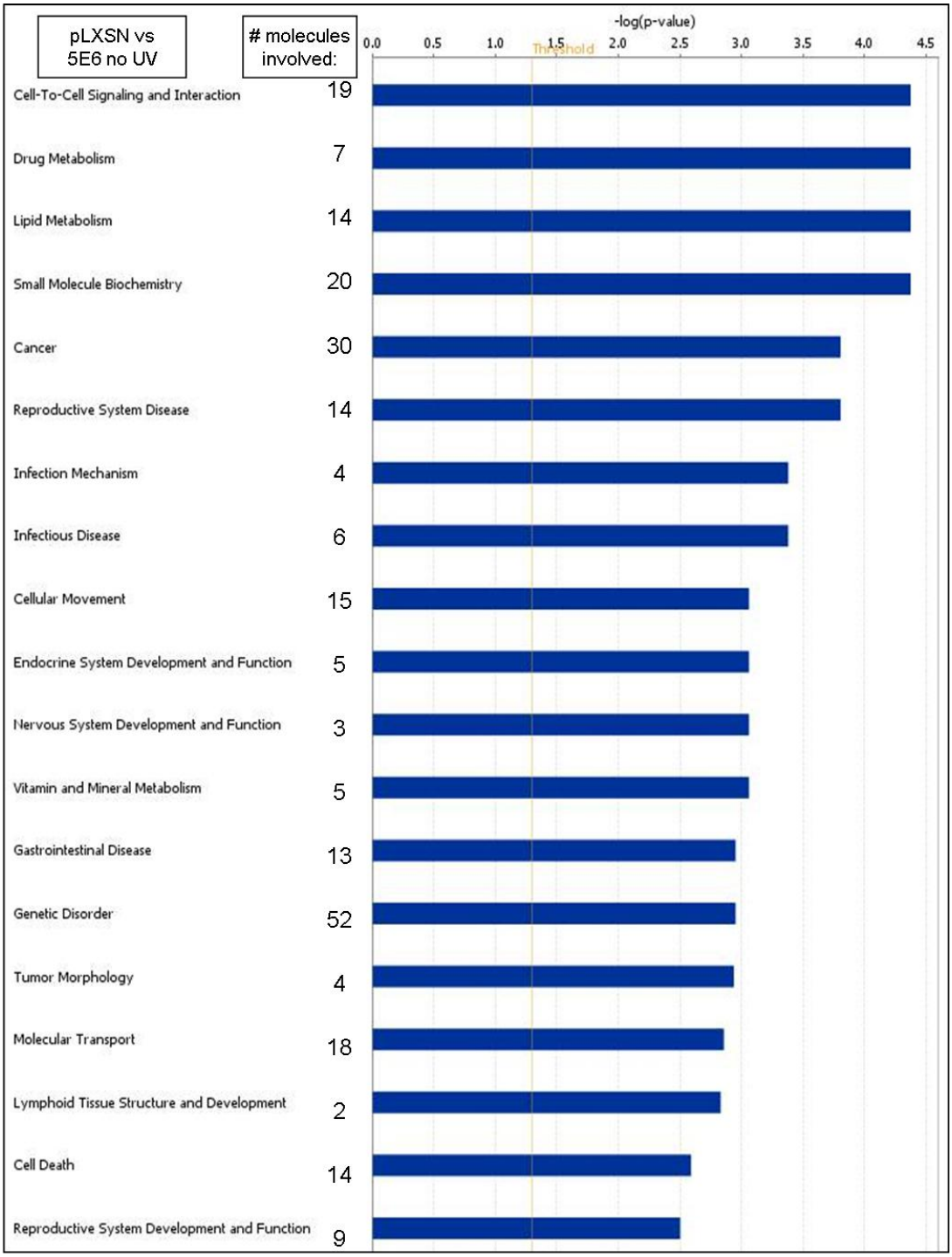

Figure 5-4 Function groups with the most significant differential expression between pLXSN and HPV5E6 keratinocytes, without UV irradiation.

Many of the pathways and functions indicated in both Table 5-3 and Figure 5-4 appear to be related to the basic functions of keratinocytes, for example lipid, drug and hormone metabolism, hair and skin development, and signalling, as described

in the Introduction. The appearance of these pathways and functions could indicate they are being perturbed by expression of the HPV5E6 protein, which concurs with the hypothesis that HPV5E6 is de-regulating keratinocyte differentiation, as discussed previously. The inclusion of the cell death and cell cycle networks in the summary Table 5-3 is also interesting as expression of HPV5E6 is known to have a role in these pathways (Giampieri and Storey, 2004; Jackson and Storey, 2000). The identification of cancer as the disease most significantly associated with the differential expression also suggests that the activity of HPV5E6 in keratinocytes may contribute to tumourigenesis. This could also be linked to the perturbation of metabolic pathways. Rapidly dividing cells need to manufacture biomolecules to incorporate into new cellular structures, for example it has been shown that highly-proliferative cells increase *de novo* fatty acid synthesis to provide for membrane biogenesis (Zambell et al., 2003). Accordingly, studies have also shown that inhibition of metabolic enzymes early in synthetic pathways can inhibit proliferation of tumour cells *in vitro* and reduce tumour growth *in vivo* (Hatzivassiliou et al., 2005). Therefore perturbation of synthetic pathways by HPV5E6 expression could contribute not only to the hyper-proliferation of keratinocytes but also to tumourigenesis.

IPA also allows the networks identified in the summary table to be visualised, and the most significant network in Table 5-3 is shown in Figure 5-5. This diagram illustrates how signalling pathways may be activated even though the signalling molecules themselves are not upregulated at the mRNA level, for example three of the upregulated genes, ALDH2, CXCL1 and BNIP3 are involved in the p38 MAP kinase pathway. NF-κB presence in this network could also be relevant as it is important in many aspects of skin biology including homeostasis and inflammatory responses (Sur et al., 2008). HPV16E6 has been shown to activate NF-κB leading

to survival signalling, although this is mediated by the PDZ binding domain not found in HPV5E6 (James et al., 2006).

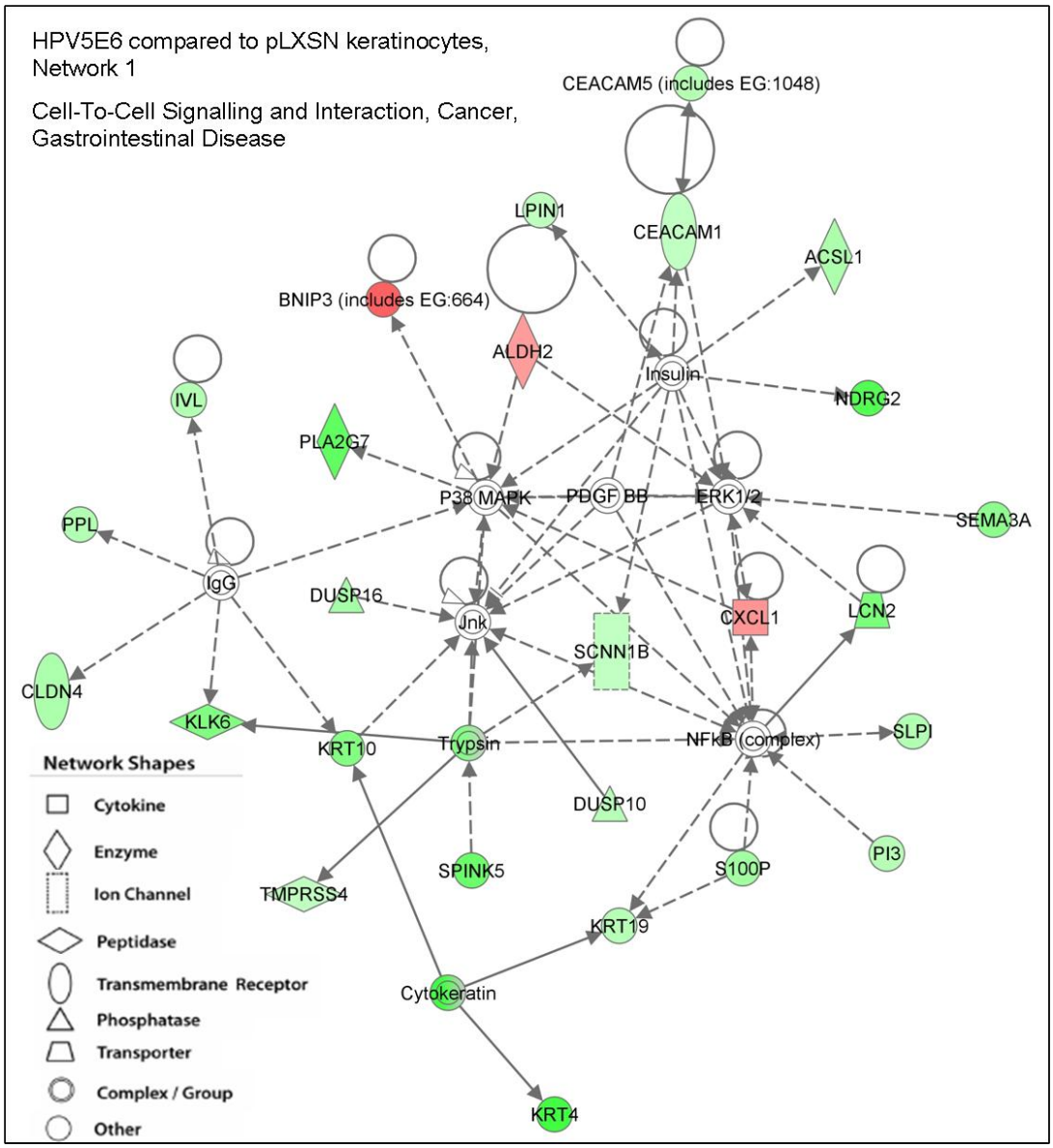

Figure 5-5 The network most significantly differentially regulated in HPV5E6 keratinocytes.

Genes upregulated in HPV5E6 keratinocytes compared to pLXSN cells are shown in red, downregulated in green. A dotted line indicates an indirect interaction.

Several of the genes involved in keratinocyte differentiation and cornified envelope formation are also present in this network, including CLDN4 (claudin 4) and the keratins (KRTs).

5.2.4 Expression changes in pLXSN keratinocytes after UV

The expression levels in pLXSN keratinocytes after 0 and 30 mJ/cm^2 UV irradiation for 16 hrs were compared next. Figure 5-6 summarises the results, and it can be seen that there are more differentially regulated genes after UV irradiation than with HPV5E6 expression, with a large number of downregulated genes. The details of the 200 most significant changes (out of 2112 where P<0.05), again ordered according to the value of B, are shown at the end of the chapter, in Table 5-11.

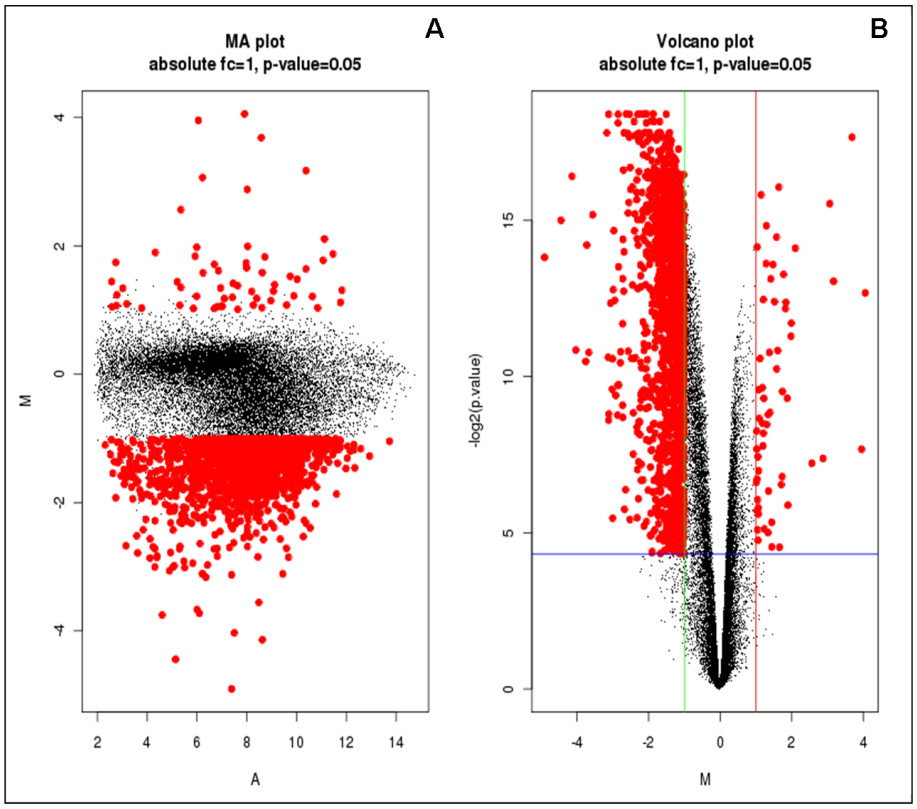

Figure 5-6 Graphical representation of expression changes in primary pLXSN keratinocytes 16 hrs after 30 mJ/cm^2 UV

A The MA plot shows significantly upregulated and downregulated genes in red, comparing the log ratios (M) and log intensities (A).

B The volcano plot shows the significantly upregulated (right) and downregulated (left) genes in red.

For ease of comparison, the most significantly upregulated genes in pLXSN cells after UV irradiation are shown in Table 5-4.

Table 5-4 Significantly upregulated genes in pLXSN keratinocytes post UV

The gene is shown by GenBank symbol and description. The table is ordered according to descending B statistic, which incorporates P and M (= absolute fold change).

SYMBOL	DESCRIPTION	M	P Value	B
CCL20	chemokine (C-C motif) ligand 20	3.69	0.0000	10.83
C12orf57	chromosome 12 open reading frame 57	1.64	0.0000	8.42
MAFB	v-maf musculoaponeurotic fibrosarcoma oncogene homolog B (avian)	1.15	0.0000	8.02
ARL14	ADP-ribosylation factor-like 14	3.06	0.0000	7.57
FOSB	FBJ murine osteosarcoma viral oncogene homolog B	1.04	0.0001	5.67
CXCL1	chemokine (C-X-C motif) ligand 1 (melanoma growth stimulating activity, alpha)	2.11	0.0001	5.62
HIST2H2BE	histone cluster 2, H2be	1.77	0.0001	4.63
HCST	hematopoietic cell signal transducer	1.42	0.0001	4.47
IL8	interleukin 8	3.17	0.0001	4.36
CXCL2	chemokine (C-X-C motif) ligand 2	4.06	0.0002	3.95
PHLDA2	pleckstrin homology-like domain, family A, member 2	1.21	0.0002	3.72
PMAIP1	phorbol-12-myristate-13-acetate-induced protein 1	1.52	0.0002	3.64
KRTAP4-9	keratin associated protein 4-9	1.84	0.0002	3.61
CXCL3	chemokine (C-X-C motif) ligand 3	1.83	0.0002	3.40
TNF	tumor necrosis factor (TNF superfamily, member 2)	1.99	0.0003	2.90
INSL4	insulin-like 4 (placenta)	1.98	0.0004	2.46
MT1X	metallothionein 1X	1.61	0.0005	1.99
TRA2A	transformer 2 alpha homolog (Drosophila)	1.38	0.0006	1.93
HCP5	HLA complex P5	1.58	0.0008	1.41
RASL11A	RAS-like, family 11, member A	1.18	0.0013	0.83
MT1G	metallothionein 1G	1.87	0.0016	0.49
IL23A	interleukin 23, alpha subunit p19	1.39	0.0022	0.07
RPS10P7	ribosomal protein S10 pseudogene 7	1.34	0.0023	0.00
ANP32C	acidic (leucine-rich) nuclear phosphoprotein 32 family, member C	1.09	0.0025	-0.12
HIST1H3H	histone cluster 1, H3h	1.18	0.0027	-0.27
IER3	immediate early response 3	1.31	0.0028	-0.31
PTX3	pentraxin-related gene, rapidly induced by IL-1 beta	1.03	0.0033	-0.50
IL6	interleukin 6 (interferon, beta 2)	1.21	0.0034	-0.56
KRTAP19-7	keratin associated protein 19-7	1.20	0.0046	-0.94
KRTAP19-1	keratin associated protein 19-1	3.95	0.0049	-1.04
IL20	interleukin 20	1.06	0.0058	-1.27
IL6	interleukin 6 (interferon, beta 2)	2.88	0.0060	-1.32
CXCL10	chemokine (C-X-C motif) ligand 10	2.56	0.0067	-1.46
ID2	inhibitor of DNA binding 2, dominant negative helix-loop-helix protein	1.08	0.0079	-1.68
S100A7A	S100 calcium binding protein A7A	1.73	0.0090	-1.85
KRTAP4-12	keratin associated protein 4-12	1.90	0.0169	-2.68
CXCL11	chemokine (C-X-C motif) ligand 11	1.07	0.0206	-2.95
CYP1A1	cytochrome P450, family 1, subfamily A, polypeptide 1	1.66	0.0431	-3.91

It is interesting to note, with regards to data presented in Chapter 4 showing the upregulation of IL6 in keratinocytes after UV irradiation, that IL6 is also shown as upregulated (by 1.21 and 2.88 fold for different variants) on the list above. However the large number of downregulated genes compared to upregulated genes is contrary to what could be expected after UV irradiation, as the keratinocytes should activate multiple signalling, transcriptional, repair and apoptotic pathways (Li et al., 2001a). This implies that the 30 mJ/cm^2 UV dose used here was cytotoxic, or the 16 hr time point was too late to identify many upregulated genes, and instead the majority of cells may be in the later stages of apoptosis and shutting down transcription on a global level. Hence the only upregulated genes are a relatively low number of inflammatory proteins, and some structural proteins. For example, the list of downregulated genes includes several apoptotic proteins, including both pro- and anti-apoptotic regulators such as caspase 3, Apaf1, caspase 8, Bak, Fas; and Bcl-x (BCL2L1) and survivin (BIRC5), implying that this pathway is not being specifically regulated but undergoing overall downregulation.

The list of differentially regulated genes between pLXSN keratinocytes with 0 and 30 mJ/cm^2 was then uploaded to IPA. A summary of the analysis is shown in Table 5-5. In addition, the 19 Function groups with the most significant differential expression (and the number of molecules involved) between 0 and 30 mJ/cm^2 UV pLXSN keratinocytes is shown in Figure 5-7.

Table 5-5 Summary of IPA of genes differentially expressed in pLXSN keratinocytes after 0 and 30 mJ/cm^2 UV.

Top Networks:	*Molecule Score:*
Gene Expression, Lipid Metabolism, Small Molecule Biochemistry	39
Amino Acid Metabolism, Molecular Transport, Small Molecule Biochemistry	37
Cancer, Gastrointestinal Disease, Cell Death	33
Carbohydrate Metabolism, Small Molecule Biochemistry, Post-Translational Modification	33
Post-Translational Modification, Cell Cycle, Tumour Morphology	31
Top Bio Functions:	
Diseases and Disorders:	
Cancer	274
Organismal injury and abnormalities	25
Infection mechanism	113
Infectious Disease	109
Immunological Disease	14
Molecular and Cellular Functions:	
Gene expression	280
Cell cycle	187
Cell death	323
Amino acid metabolism	90
Post-translational modification	158
Physiological system development and function:	
Organismal development	175
Organismal survival	141
Embryonic development	141
Connective tissue development and function	119
Hematological system development and function	115
Top Canonical Pathways:	
Molecular mechanisms of cancer	
p53 Signalling	
Chronic myeloid leukemia signalling	
ERK/MAPK signalling	
Role of BRCA1 in DNA damage response	

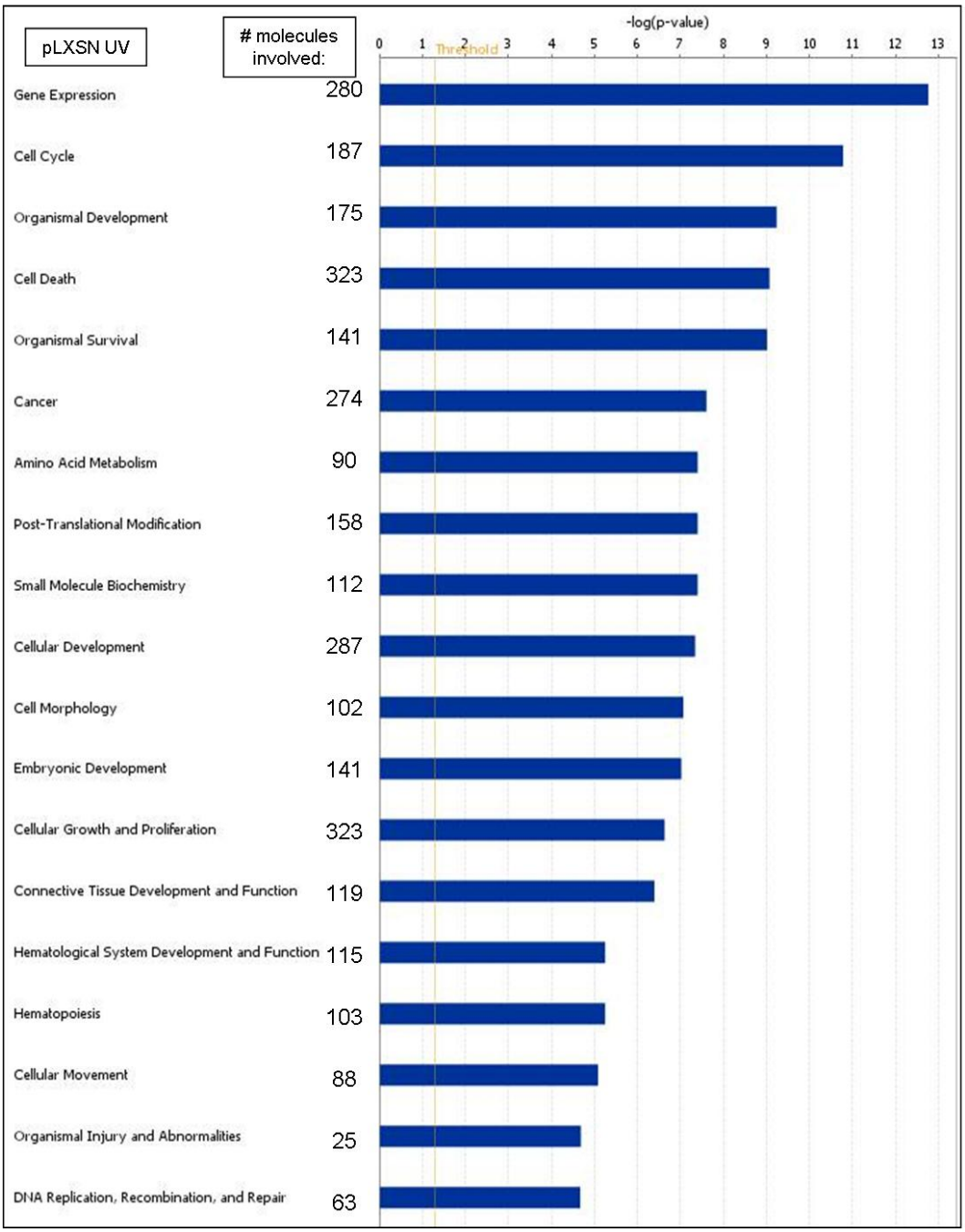

Figure 5-7 Function groups with the most significant differential expression between pLXSN keratinocytes with 0 or 30 mJ/cm^2 UV.

The summary table concurs with the hypothesis that the cells are in the later stages of apoptosis, which is shown by the most significant differentially regulated functions and networks containing genes involved in gene expression, metabolism, cell cycle, organismal survival and cell death.

Analysis focusing only on upregulated genes gives the most significant network as Cell to cell signalling and interaction, cellular movement and immune cell trafficking, with a score of 27. This is consistent with release of inflammatory signalling molecules by UV irradiated keratinocytes (Li et al., 2001a), and it can be seen in Figure 5-8 how many of the upregulated genes are in this network.

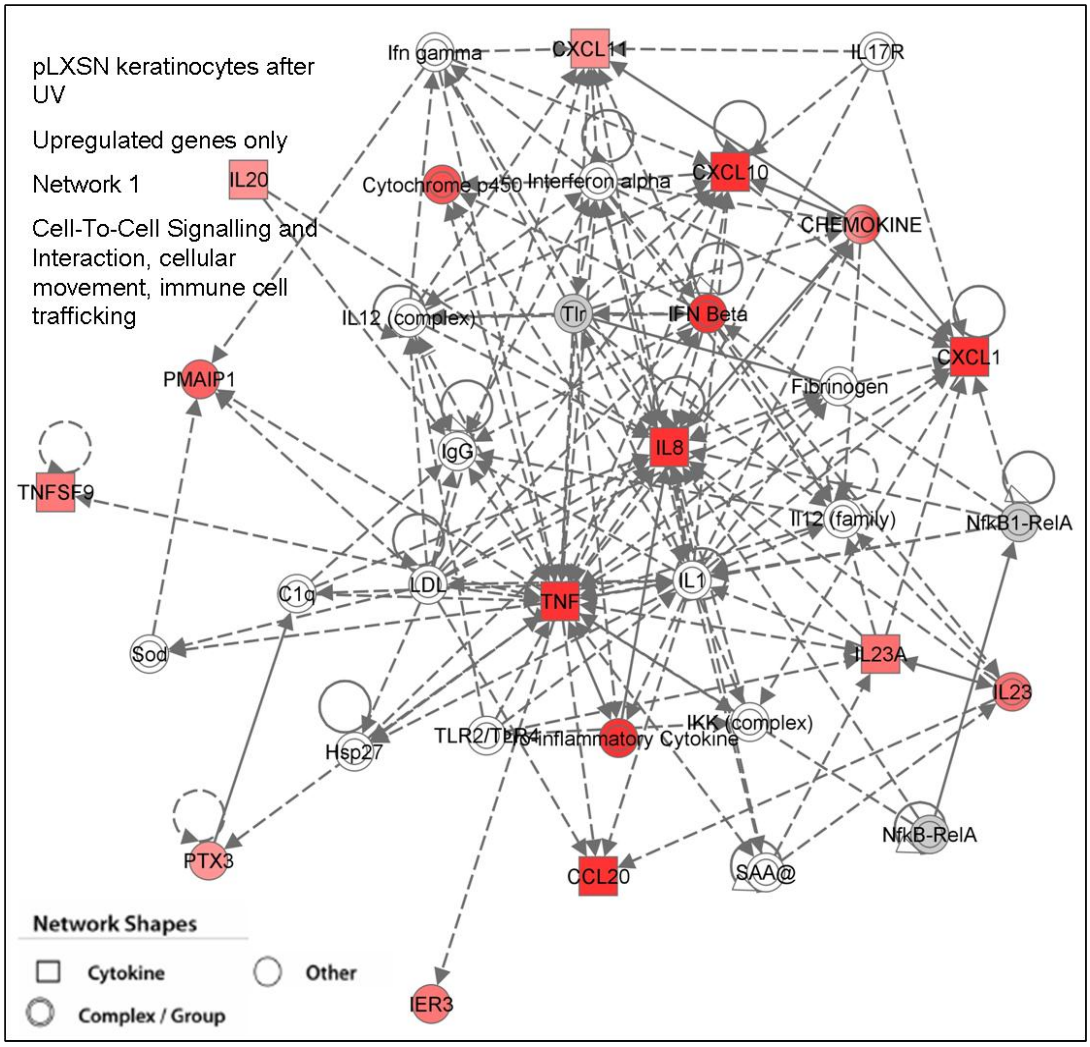

Figure 5-8 The network containing the most significantly upregulated genes in pLXSN keratinocytes after 30 mJ/cm^2 UV.

Upregulated genes are shown in red. A dotted line indicates an indirect interaction.

Several of the genes that were found to be upregulated by UV irradiation in both pLXSN and HPV5E6 (shown presently) keratinocytes are related to proinflammatory signalling and known to be involved in UV-induced signalling. For example, CCL20 (chemokine (c-c motif) ligand 20, also called MIP3A [macrophage

inflammatory protein 3A]) is a proinflammatory cytokine expressed by keratinocytes at low levels, and is upregulated upon TNFα, NF-κB, p38 and IL17 stimulation. It displays some direct antimicrobial activity and also mediates Langerhans cell migration (Tohyama et al., 2001). CXC chemokines are inflammatory, chemotactic and can regulate angiogenesis. For example CXCL1 (also called melanoma growth stimulating activity, and GROα) is expressed at low levels in keratinocytes but can be induced by NF-κB, and is also associated with malignant melanoma (Dhawan and Richmond, 2002). CXCL1/GRO was also found to be upregulated in HPV8E6 conditioned media from keratinocytes, and conditioned media from HPV5 and 8E6 HT1080s, shown in Figure 4-5 C. CXCL2 is also called GROβ/MIP2, and CXCL3 GROγ/MIP2b, and are also involved in the inflammatory response of keratinocytes (Farley et al., 2006; Geiser et al., 1993). Interleukin (IL) 8 is also called CXCL8, and is also known to be secreted by keratinocytes, is induced by NF-κB and has been shown to be upregulated following UV irradiation (Sesto et al., 2002). Similarly, TNF (tumour necrosis factor) is a major mediator of inflammation and along with its role in innate immunity, is known to be upregulated by UV irradiation (Bashir et al., 2009).

5.2.5 Expression changes in keratinocytes with HPV5E6 and after UV

The expression levels in HPV5E6 keratinocytes after 0 and 30 mJ/cm^2 UV irradiation for 16 hrs were then compared. Figure 5-9 summarises the results, and it can be seen again that there is a large number of downregulated genes. The details of the 200 most significant changes (out of 2565 where $P<0.05$) are shown in Table 5-12 with the upregulated genes highlighted in red.

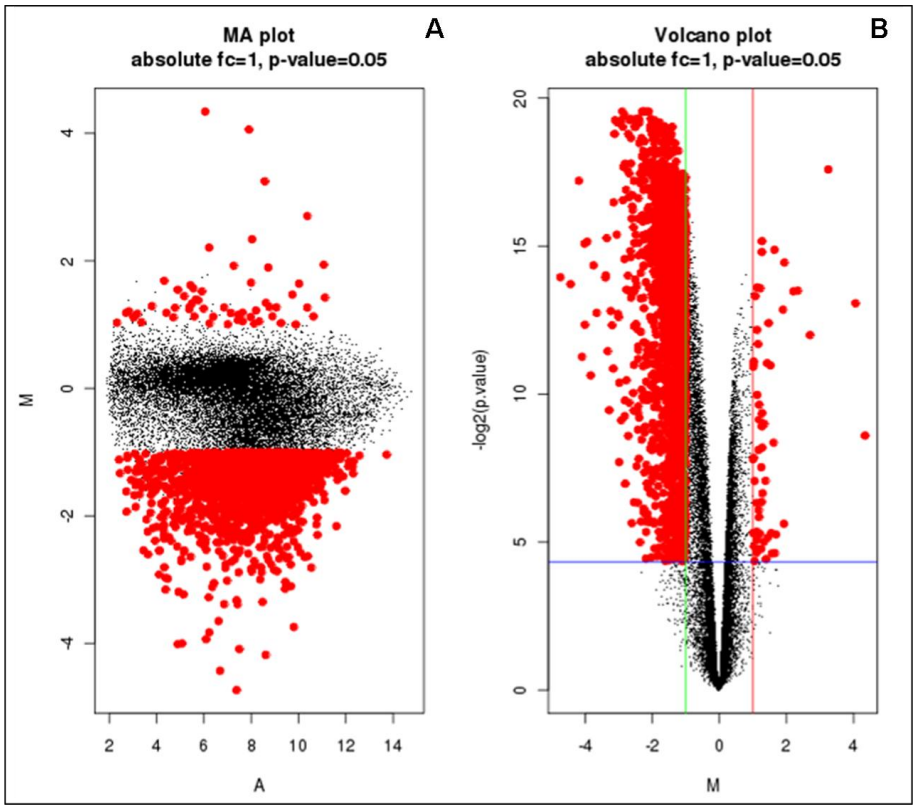

Figure 5-9 Graphical representation of expression changes in primary keratinocytes expressing HPV5E6 16 hrs after 30 mJ/cm^2 UV

A The MA plot shows significantly upregulated and downregulated genes in red, comparing the log ratios (M) and log intensities (A).

B The volcano plot shows the significantly upregulated (right) and downregulated (left) genes in red.

For ease of comparison, the most significantly upregulated genes in HPV5E6 keratinocytes after UV irradiation are shown in Table 5-6. Again, the large number of downregulated genes suggests that the keratinocytes are in the later stages of apoptosis and undergoing global transcription downregulation. Of the relatively few upregulated genes, many are proinflammatory and are the same as those shown in Table 5-4, the upregulated genes in pLXSN keratinocytes after UV. This includes CCL20, C12orf57, Histone2H2BE, TNF, IL8, CXCL1, CXCL2, and CXCL3; chiefly members of the inflammatory pathway discussed previously in section 5.2.4, and involved in signalling UV-damage to neighbouring tissues and stimulating migration of immune cells.

Table 5-6 Significantly upregulated genes in HPV5E6 keratinocytes post UV

The gene is shown by GenBank symbol and description. The table is ordered according to descending B statistic, which incorporates P and M (= absolute fold change).

SYMBOL	DESCRIPTION	M	P Value	B
CCL20	chemokine (C-C motif) ligand 20	3.24	0.0000	9.61
TNFSF9	tumor necrosis factor (ligand) superfamily, member 9	1.27	0.0000	6.27
C12orf57	chromosome 12 open reading frame 57	1.27	0.0000	5.85
HIST2H2BE	histone cluster 2, H2be	1.94	0.0000	5.43
CHAC1	ChaC, cation transport regulator homolog 1 (E. coli)	1.22	0.0001	4.43
TNF	tumor necrosis factor (TNF superfamily, member 2)	2.34	0.0001	4.34
ARL14	ADP-ribosylation factor-like 14	2.21	0.0001	4.32
H2AFJ	H2A histone family, member J	1.07	0.0001	4.14
CXCL2	chemokine (C-X-C motif) ligand 2	4.06	0.0001	3.89
CXCL3	chemokine (C-X-C motif) ligand 3	1.89	0.0001	3.67
PMAIP1	phorbol-12-myristate-13-acetate-induced protein 1	1.47	0.0002	3.22
PHLDA2	pleckstrin homology-like domain, family A, member 2	1.13	0.0002	2.97
IL8	interleukin 8	2.70	0.0002	2.79
HCST	hematopoietic cell signal transducer	1.15	0.0003	2.49
CXCL1	chemokine (C-X-C motif) ligand 1 (melanoma growth stimulating activity, alpha)	1.42	0.0005	1.87
KRTAP4-9	keratin associated protein 4-9	1.52	0.0005	1.80
FLJ16171	FLJ16171 protein	1.01	0.0005	1.76
TRA2A	transformer 2 alpha homolog (Drosophila)	1.19	0.0013	0.55
HCP5	HLA complex P5	1.34	0.0020	-0.05
MT1X	metallothionein 1X	1.27	0.0021	-0.13
KRTAP19-1	keratin associated protein 19-1	4.34	0.0026	-0.42
CLDN6	claudin 6	1.62	0.0030	-0.65
OR10H4	olfactory receptor, family 10, subfamily H, member 4	1.28	0.0034	-0.81
INSL4	insulin-like 4 (placenta)	1.25	0.0054	-1.42
CSF2	colony stimulating factor 2 (granulocyte-macrophage)	1.18	0.0148	-2.74
KRTAP4-12	keratin associated protein 4-12	1.69	0.0262	-3.46
PRB4	proline-rich protein BstNI subfamily 4	1.11	0.0401	-4.00
CYP1A1	cytochrome P450, family 1, subfamily A, polypeptide 1	1.66	0.0405	-4.01
LCE1D	late cornified envelope 1D	1.05	0.0487	-4.24

The list of differentially regulated genes in HPV5E6 expressing keratinocytes with 0 or 30 mJ/cm^2 UV was also analysed with IPA, and the summary of the analysis shown in Table 5-7. In addition, the 19 Function groups with the most significant differential expression (and the number of molecules involved) between 0 and 30 mJ/cm^2 UV HPV5E6 keratinocytes is shown in Figure 5-10.

Table 5-7 Summary of IPA of genes differentially expressed in HPV5E6 keratinocytes after 0 and 30 mJ/cm^2 UV.

Top Networks:	*Molecule Score:*
Cell Death, Lipid Metabolism, Small Molecule Biochemistry	34
Cellular assembly and organization, nucleic acid metabolism, small molecule biochemistry	34
Behaviour, nervous system development and function, RNA post-transcriptional modification	34
Amino acid metabolism, small molecule biochemistry, cell death	34
Cellular assembly and organization, cell cycle, cell death	34
Top Bio Functions:	
Diseases and Disorders:	
Cancer	326
Neurological disease	15
Infection mechanism	149
Infectious Disease	126
Genetic disorder	29
Molecular and Cellular Functions:	
Cell cycle	270
Gene expression	340
DNA replication, recombination, and repair	187
Cell death	384
Post-translational modification	186
Physiological system development and function:	
Organismal survival	170
Organismal developement	172
Connective tissue development and function	120
Embryonic development	143
Tumour morphology	40
Top Canonical Pathways:	
Molecular mechanisms of cancer Role of BRCA1 in DNA damage response Mitotic roles of polo-like kinase p53 signalling ATM signalling	

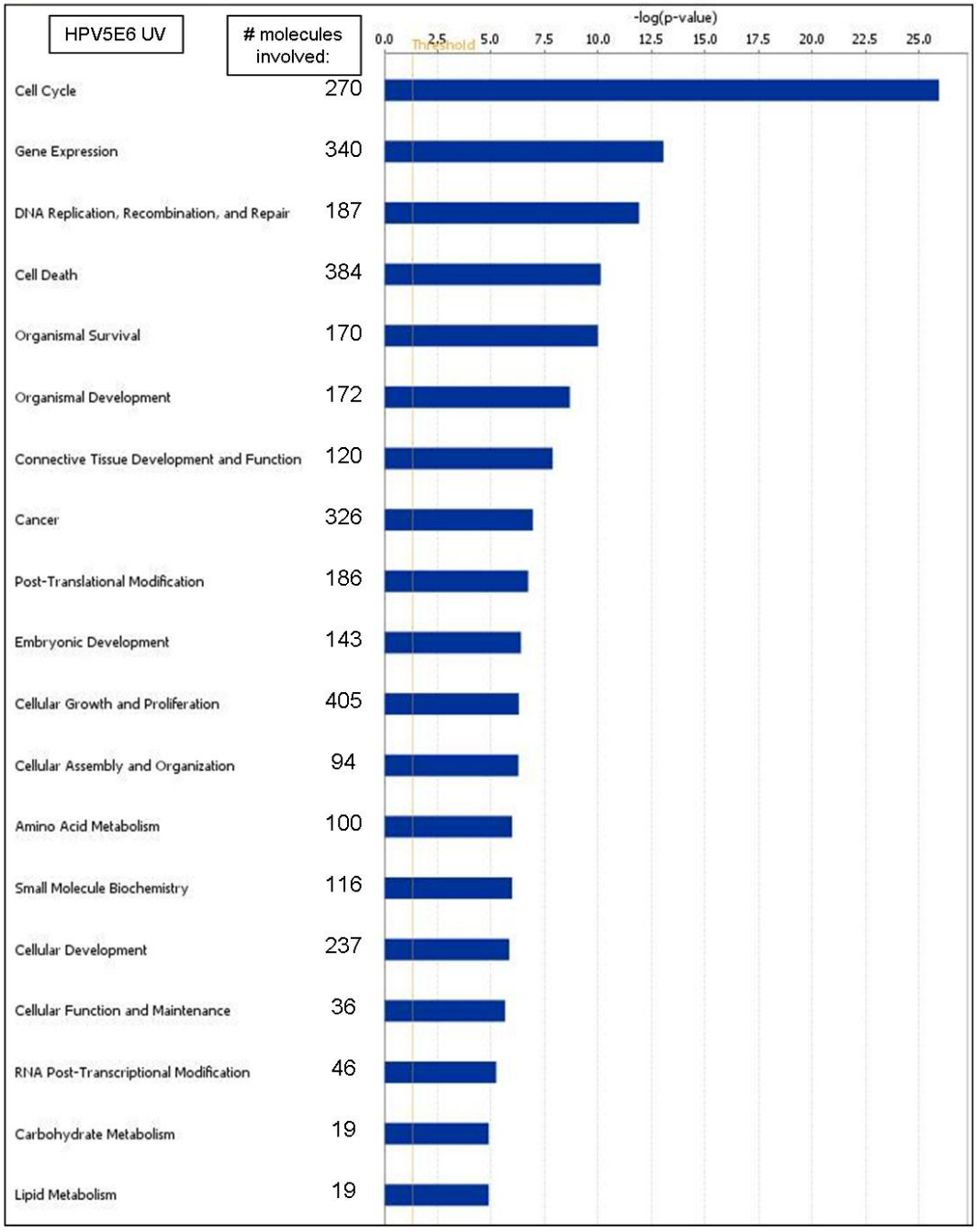

Figure 5-10 Function groups with the most significant differential expression between HPV5E6 keratinocytes with 0 or 30 mJ/cm^2 UV.

Both the summary Table 5-11 and the representative Figure 5-7 show that similar functions and pathways are differentially regulated in HPV5E6 expressing keratinocytes as in the pLXSN keratinocytes after UV irradiation, with metabolism, cell death, cell cycle and gene expression all being significant. However there are some differences which could shed light on the activities of HPV5E6 in the cell. In

Figure 5-10, cell cycle function has moved to the top of the list of most significant differentially regulated genes, and DNA replication, recombination and replication function is also much more significant than in pLXSN keratinocytes after UV. This could be linked to the disruption of cell cycle checkpoints and inhibition of DNA repair mediated by HPV5E6, which has previously been observed in HT1080 cells (Giampieri and Storey, 2004). Further analysis of the differences between pLXSN and HPV5E6 keratinocytes after UV irradiation is described below.

5.2.6 Differences in expression changes after UV

A comparison was then performed between the pLXSN and HPV5E6 expressing keratinocytes, both after 30 mJ/cm^2 UV irradiation. A summary of the results is shown in Figure 5-11. It can be observed that there is a relatively small number of significantly differentially regulated genes. These are detailed at the end of the chapter in Table 5-13.

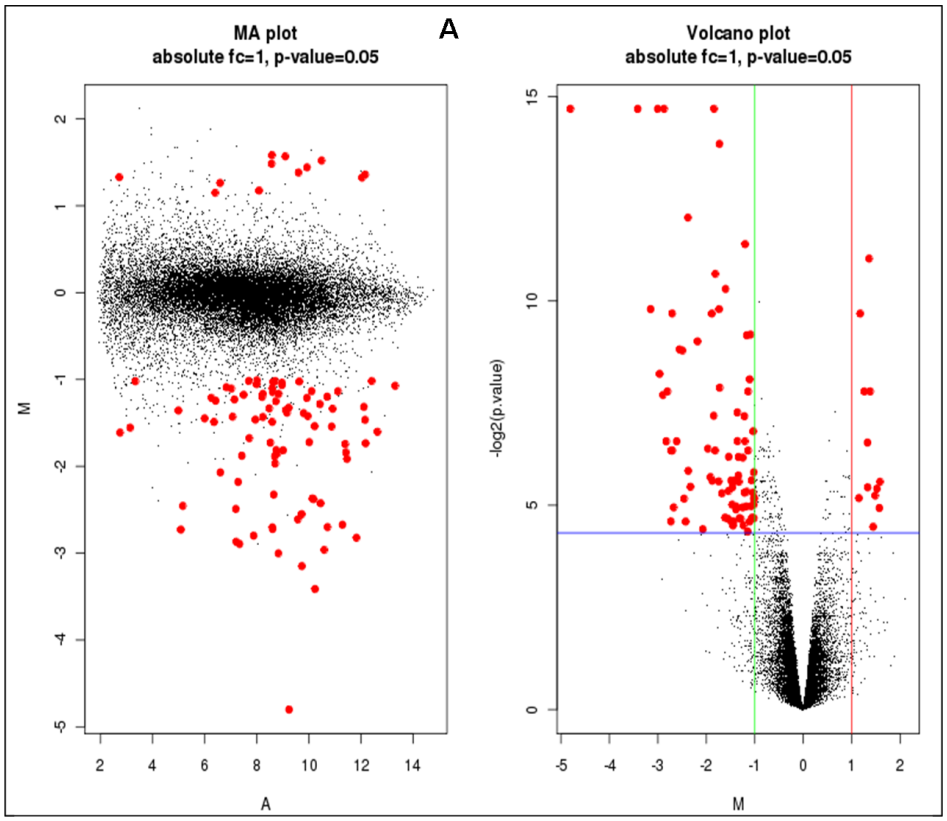

Figure 5-11 Graphical representation of expression changes in HPV5E6 expressing primary keratinocytes compared to pLXSN controls, after 30 mJ/cm^2 UV

A The MA plot shows significantly upregulated and downregulated genes in red, comparing the log ratios (M) and log intensities (A).

B The volcano plot shows the significantly upregulated (right) and downregulated (left) genes in red.

More genes are downregulated in HPV5E6 expressing keratinocytes than in control pLXSN cells after 30 mJ/cm^2 UV. Similarly to the changes seen without UV irradiation in Table 5-1, the list includes several which are involved in regulation and formation of the cornified envelope of the skin, which have been collected and shown in Table 5-8. The continued deregulation of differentiation and cornified envelope formation possibly induced by HPV5E6 expression could have additional effects after UV irradiation, for example, epidermal thickening is a cutaneous response to protect against UV damage, which could be affected by HPV5E6 differentiation deregulation and therefore lead to increased UV-induced damage.

Table 5-8 Genes downregulated in HPV5E6 expressing keratinocytes compared to pLXSN controls, after UV.

The gene is shown by GenBank symbol and description. The table is ordered according to descending B statistic, which incorporates P and M (= absolute fold change).

SYMBOL	DESCRIPTION	M	P Value	B
SPRR3	small proline-rich protein 3	-3.41	0.0000	9.92
ECM1	extracellular matrix protein 1	-1.84	0.0000	9.85
SPRR2A	small proline-rich protein 2A	-1.60	0.0008	6.64
SPRR2D	small proline-rich protein 2D	-1.74	0.0011	6.20
KRT4	keratin 4	-3.15	0.0011	6.17
KRT24	keratin 24	-1.10	0.0037	4.69
SPRR1A	small proline-rich protein 1A	-2.82	0.0106	3.17
CLDN4	claudin 4	-1.34	0.0189	2.10
LCN2	lipocalin 2	-1.91	0.0194	1.98
SPRR4	small proline-rich protein 4	-1.43	0.0209	1.70
FN1	fibronectin 1	1.48	0.0265	1.21
IVL	involucrin	-1.46	0.0309	0.93

The possible global downregulation in keratinocytes due to the late time point and relatively high UV dose which has been discussed could mean that HPV5E6-mediated changes in expression are being masked. However for ease of comparison, the genes upregulated in keratinocytes expressing HPV5E6 compared to pLXSN controls after 30 mJ/cm^2 UV are shown separately in Table 5-9.

Table 5-9 Significantly upregulated genes in HPV5E6 expressing keratinocytes after 30 mJ/cm^2 UV

SYMBOL	DESCRIPTION	M	P Value	B
NDRG1	N-myc downstream regulated 1	1.36	0.0005	7.21
SMARCA1	SWI/SNF related, matrix associated, actin dependent regulator of chromatin, subfamily a, member 1	1.18	0.0012	5.98
SERPINE2	serpin peptidase inhibitor, clade E (nexin, plasminogen activator inhibitor type 1), member 2	1.38	0.0045	4.41
SERPINE1	serpin peptidase inhibitor, clade E (nexin, plasminogen activator inhibitor type 1), member 1	1.33	0.0108	3.13
SLCO2A1	solute carrier organic anion transporter family, member 2A1	1.58	0.0210	1.68
BNIP3	BCL2/adenovirus E1B 19kDa interacting protein 3	1.52	0.0236	1.47
FN1	fibronectin 1	1.48	0.0265	1.21
CSH1	chorionic somatomammotropin hormone 1 (placental lactogen)	1.15	0.0277	1.12
FAP	fibroblast activation protein, alpha	1.57	0.0328	0.82
IVNS1ABP	influenza virus NS1A binding protein	1.44	0.0450	0.25

Several of these upregulated genes were also upregulated in HPV5E6 keratinocytes prior to UV irradiation, including BNIP3, SLCO2A1, FAP and IVNS1ABP. However two Serpin variants are also upregulated. Serpins are are large family of serine peptidase inhibitors, clade E members 1 and 2 are both extracellular and can inhibit thrombin. SerpinE1 is also called plasminogen activator inhibitor 1 (PAI 1) and has a role in wound repair. It has also been shown to have several roles in tumourigenesis, promoting invasion and angiogenesis (Bajou et al., 2004), and inhibiting FasL induced apoptosis of endothelial cells (Bajou et al., 2008). It also induces an invasive phenotype of cutaneous SCCs (Wilkins-Port et al., 2007). This suggests upregulation of PAI 1 by HPV5E6 also contributes to the disruption of keratinocyte differentiation, and could also augment UV-induced epidermal damage, and have a role in tumourigenesis.

IPA comparison between analyses was performed on the results for pLXSN and HPV5E6 keratinocytes after 30 mJ/cm^2 UV. A summary of the results is shown in Figure 5-12, which shows the canonical pathways that are most significantly

differentially regulated after UV irradiation in both pLXSN and HPV5E6 keratinocytes. In agreement with the results discussed above, the main differences are in functions related to cell cycle control and DNA repair which are more significantly differentially regulated in HPV5E6 keratinocytes, namely 'role of BRCA1 in DNA damage repair' and 'cell cycle G1/S checkpoint regulation'. In addition to the functions shown in Figure 5-12, several functions which were not in the top 22 nevertheless showed significant differences between pLXSN and HPV5E6 keratinocytes. These include 'role of CHK proteins in cell cycle checkpoint control', 'mitotic roles of polo-like kinase', 'cell cycle, G2/M DNA damage checkpoint regulation' and 'ATM signalling'. In summary, these functions contain selections of a group of genes that were found to be downregulated in HPV5E6 but not pLXSN keratinocytes after UV irradiation, including BRCA1 (1.3 fold), CDC2 (2.4 fold), CDK2 (1.1), cyclin B2 (2.0), CDC7 (1.33), CDC20 (2.0), and PLK1 (1.9). Control of the cell cycle is closely linked to detection of DNA damage at checkpoints, which results in cell cycle arrest to allow DNA repair and prevent transmission of mutations to daughter cells. The CDK (cyclin dependent kinase) group are the catalytic subunits which together with different cyclins form the kinase complexes which are essential for regulation of all stages of cell cycle progression, and deregulation of which is often linked to cancer (Malumbres and Barbacid, 2009). For example, the CDC (cell division cycle) 2 (also called CDK [cyclin dependent kinase] 1) association with cyclins A or B is essential for progression to mitosis. CDK2 is essential for G1/S progression, and CDC7 is also involved in this transition. CDC20 (also called Fizzy) and PLK1 (polo-like kinase 1) are also involved in cell cycle regulation. The tumour suppressor BRCA1 (breast cancer susceptibility 1) has been called a master regulator of genome integrity as it is involved in checkpoint control at different stages of the cell cycle, and is involved in several aspects of DNA repair, including localisation to sites of damage and recruitment of signalling molecules (Huen et al., 2010).

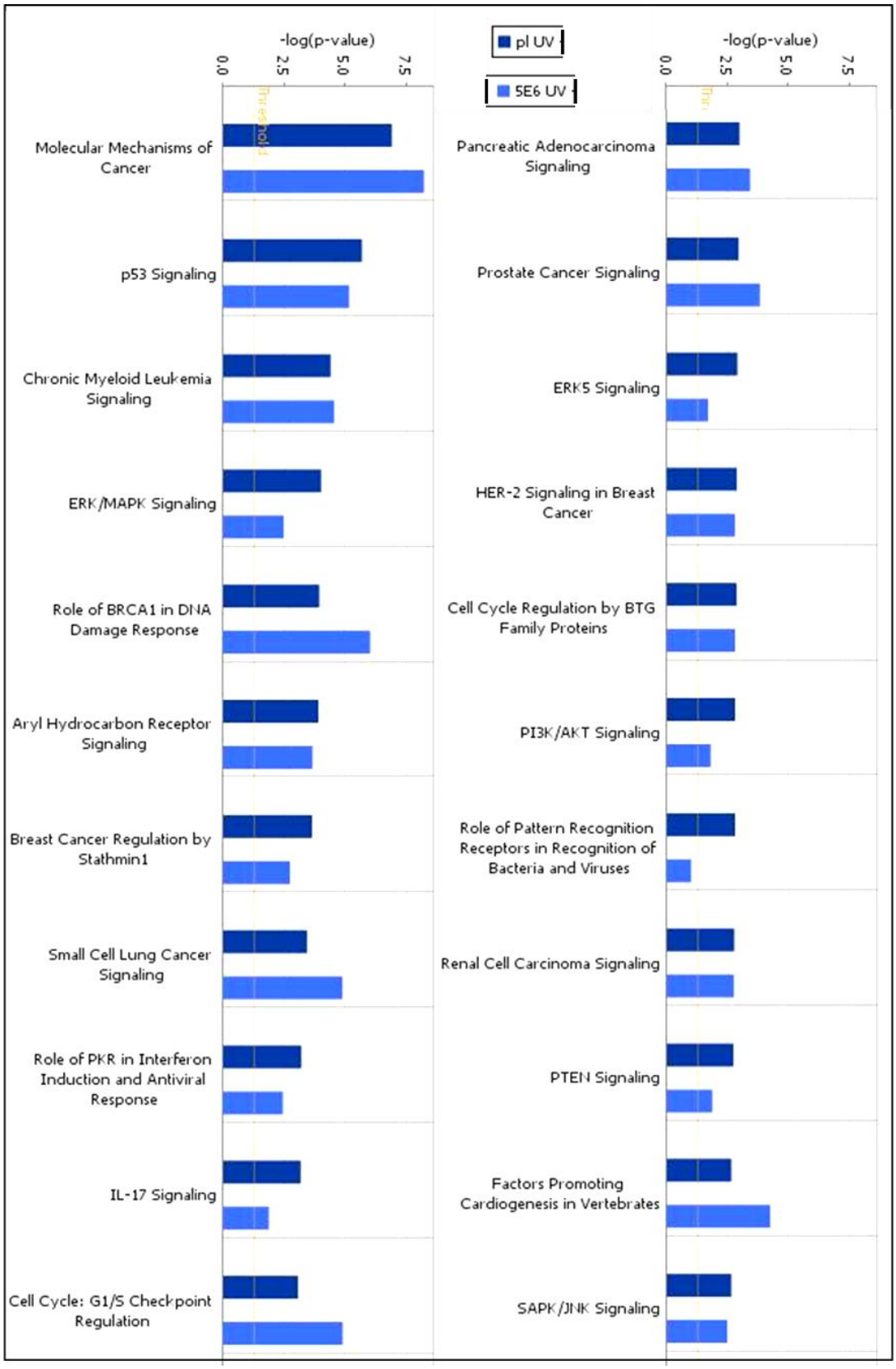

Figure 5-12 The 22 canonical pathways with the most significant differential regulation after UV irradiation, pLXSN in dark and HPV5E6 in lighter blue.

5.2.7 Decrease in Mcl1 upon UV irradiation

It was interesting to note that several anti-apoptotic genes were downregulated in both pLXSN and HPV5E6 expressing keratinocytes upon UV, including BIRC5 (the IAP survivin), BCL2L1 (Bcl-x) and MCL1. This corresponds to the idea that the UV dose and time point measured here meant that the majority of cells are in the later stages of apoptosis, and so down-regulate survival genes to allow apoptosis to progress. The downregulation of Mcl1 has been shown to be essential in allowing UV induced apoptosis to proceed in HeLa cells (Nijhawan et al., 2003) and it is also an essential survival protein as seen in keratinocyte organotypic models (Sitailo et al., 2009). Therefore the downregulation of Mcl1 in keratinocytes post UV was investigated by western blot. Primary keratinocytes were grown in EpiLife, when 60% confluent were induced with 0 or 15 mJ/cm^2 UV and harvested 16 hrs later with RIPA lysis buffer on ice for 5 minutes with scraping. The lysates were then separated by SDS-PAGE, transferred to membrane and probed for Mcl1, with the results shown in Figure 5-13. PARP cleavage was used to confirm apoptosis was progressing as is shown by the increase of the smaller band after UV, and it can be seen that Mcl1 does decrease after UV irradiation.

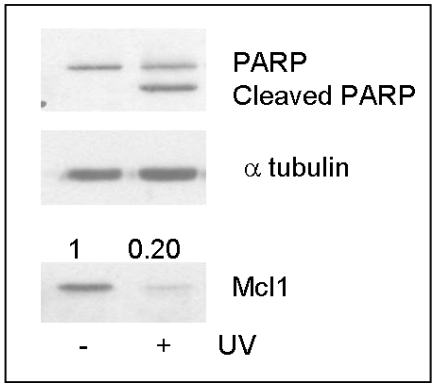

Figure 5-13 Levels of Mcl1.

α tubulin was used to ensure equal loading and the fold change relative to un-irradiated keratinocytes is shown.

5.3 Discussion and further work

5.3.1 Differences between pLXSN and HPV5E6 keratinocytes without UV

The differences in expression between pLXSN and HPV5E6 keratinocytes without UV irradiation indicated that it would be interesting to validate and further investigate changes in signalling molecules, especially the p38 MAP kinase pathway, and also MCAM, as it was the most significantly upregulated molecule. Examination of any differences in NF-κB signalling induced by HPV5E6 expression in keratinocytes would also be interesting given its important role in many skin pathways. The number of downregulated genes involved in cornified envelope formation also suggests a role for HPV5E6 in disruption of barrier formation, which could be beneficial in the viral lifecycle. These results mirror the deregulation of keratinocyte differentiation proteins which has also been seen in high-risk genus-α HPVs (Duffy et al., 2003). Further investigation into the effects on keratinocyte differentiation, for example with organotypic culture models would be useful.
HPV5E6 downregulation of several genes could be via direct or indirect mechanisms, or a combination. For example, the differentiation of keratinocytes is a sequential process, and inhibition of an early step could lead to downregulation of later differentiation markers, such as Keratin 10. Alternatively HPV5E6 could target a master regulatory molecule which therefore disrupts many cellular processes. An example of this could be the targeting of a microRNA which in turn regulates other cellular processes. The E6 proteins of HPVs 16 and 18 have recently been shown to reduce expression of the tumour suppressor miR34-a in organotypic keratinocyte culture, via p53 degradation (Wang et al., 2009b). miRNA34-a is part of the p53 transcriptional network, it regulates genes involved in cell-cycle progression and DNA repair, and its expression promotes apoptosis (Chang et al., 2007).
The absence of Interleukin 6 from the list of genes upregulated in HPV5E6 keratinocytes is unexpected given the significant upregulation seen at mRNA and

protein level in Chapter 4. It could be that the slight differences observed in the clustering of the arrays which indicated a difference in the 5E63 sample, possibly linked to reduced HPV5E6 expression in that replicate, caused some gene changes to be missed from the analysis. Re-processing of the results without this replicate may reveal more biologically relevant changes, although the statistical power would be reduced. The level of HPV5E6 expression in these samples could also be checked. Any changes seen on the arrays should be validated by investigation into the mRNA and protein levels as the first step in further research.

5.3.2 UV-induced gene expression changes

It has been hypothesised that UV activates a specific set of signalling pathways in keratinocytes, distinct from those it induces in other cell types as a consequence of the general cellular stress and DNA damage it causes (Adachi et al., 2003). Previous studies analysis of expression changes in UV irradiated keratinocytes have concluded the response occurs in waves, with early changes (0.5 to 2 hrs) related to signal transduction and transcriptional regulation, intermediate changes (4 to 8 hrs) affecting cytokine and chemokine secretion, and the third wave of changes (16 to 24 hrs) related to the structure of the cells (Li et al., 2001a). That study used lower doses of UV (8 mJ/cm^2), chosen to kill only 10% of the cells. In contrast the dose used here was based on AnnexinV/PI apoptosis assays which typically cause apoptosis in 40% of the cells, which in combination with a later time point, meant that the early changes were not seen here; rather we observed overall downregulation of genes, with upregulation primarily of inflammatory signals, as keratinocytes were progressing through apoptosis. The pattern of signalling changes observed here, the upregulation of TNF and IL8-family members, concurs with previous studies, which show upregulation of inflammatory signalling post UV (Bashir et al., 2009). The inflammatory role of TNF in signalling UV-induced damage to keratinocytes could also be important in cancer, with TNFα

inflammation known to have both positive and negative effects on cancer cells (Balkwill, 2009).

Similarly the UV-induced downregulation of Myc seen in these results concurs with previous studies (Li et al., 2001a; Sesto et al., 2002). The transcription factor Myc is important in proliferation and is often upregulated in cancers, which could mean inappropriate activity after UV irradiation contributes to tumourigenesis (Pelengaris et al., 1999). Therefore it is downregulated, and this is not significantly affected by HPV5E6 expression, shown here by 2.85 fold reduction in pLXSN and by 3.1 fold reduction in HPV5E6 keratinocytes.

5.3.3 Differences between pLXSN and HPV5E6 keratinocytes after UV

The more significant disruption of cell cycle and DNA damage repair pathways in HPV5E6 compared to pLXSN keratinocytes after UV irradiation, shown in IPA by differences in several functions and pathways, and by the increased downregulation of several genes involved in cell cycle regulation, is an interesting indication of HPV5E6 activities in keratinocytes. Further validation of this disruption and further investigation of the mechanisms would be useful and could shed light on the tumourigenic role of EV-HPV and UV in keratinocytes. Previous work on disruption of the cell cycle by HPV5E6 showed nuclear cyclin A accumulation despite the persistence of DNA damage in HT1080s cells (Giampieri and Storey, 2004). It would also be interesting to validate and investigate the upregulation of PAI 1 (serpinE1) by HPV5E6 in keratinocytes. The effect of overall deregulation of keratinocyte differentiation especially with regards to UV-induced damage of the epidermis would be of interest, and could possibly be investigated in SCC samples.

5.4 Lists of gene changes

5.4.1.1 Differences between pLXSN and HPV5E6 keratinocytes without UV

Table 5-10 Differentially expressed genes in HPV5E6 expressing primary keratinocytes compared to pLXSN controls.

The gene is shown by GenBank symbol and description. The table is ordered according to descending B statistic, which incorporates P and M (= absolute fold change).

SYMBOL	DESCRIPTION	M	P.Value	B
SPRR3	small proline-rich protein 3	-3.76	0.0000	10.75
ALPP	alkaline phosphatase, placental (Regan isozyme)	-5.34	0.0000	10.38
ECM1	extracellular matrix protein 1	-1.83	0.0000	10.08
NDRG2	NDRG family member 2	-2.91	0.0001	9.43
ANXA9	annexin A9	-1.73	0.0001	9.12
AZGP1	alpha-2-glycoprotein 1, zinc-binding	-2.56	0.0001	9.06
RAB11FIP1	RAB11 family interacting protein 1 (class I)	-1.50	0.0004	7.63
GALNT5	UDP-N-acetyl-alpha-D-galactosamine:polypeptide N-acetylgalactosaminyltransferase 5 (GalNAc-T5)	-2.11	0.0006	7.16
KRT24	keratin 24	-1.48	0.0006	7.14
SPRR2A	small proline-rich protein 2A	-1.58	0.0009	6.64
RASA1	RAS p21 protein activator (GTPase activating protein) 1	-1.06	0.0009	6.64
SPRR2D	small proline-rich protein 2D	-1.78	0.0010	6.49
KRT4	keratin 4	-3.17	0.0011	6.31
CEACAM6	carcinoembryonic antigen-related cell adhesion molecule 6 (non-specific cross reacting antigen)	-2.79	0.0014	6.05
CEACAM5	carcinoembryonic antigen-related cell adhesion molecule 5	-1.26	0.0025	5.45
HPGD	hydroxyprostaglandin dehydrogenase 15-(NAD)	-1.45	0.0026	5.29
LY6G6C	lymphocyte antigen 6 complex, locus G6C	-1.46	0.0026	5.28
ATP12A	ATPase, H+/K+ transporting, nongastric, alpha polypeptide	-2.10	0.0027	5.18
CEACAM1	carcinoembryonic antigen-related cell adhesion molecule 1 (biliary glycoprotein)	-1.02	0.0028	5.10
GCOM1	GRINL1A complex locus	-1.22	0.0031	4.90
PTPRU	protein tyrosine phosphatase, receptor type, U	-1.05	0.0036	4.73
KRT80	keratin 80	-1.21	0.0042	4.45
MCAM	melanoma cell adhesion molecule	1.28	0.0042	4.45
S100P	S100 calcium binding protein P	-1.55	0.0042	4.42
PCDH7	protocadherin 7	1.22	0.0045	4.28
SCNN1B	sodium channel, nonvoltage-gated 1, beta	-1.02	0.0047	4.20
HS3ST1	heparan sulfate (glucosamine) 3-O-sulfotransferase 1	-1.15	0.0049	4.09
KLK6	kallikrein-related peptidase 6	-2.10	0.0049	4.02
TPRG1	tumor protein p63 regulated 1	-1.49	0.0049	4.01
S100A7	S100 calcium binding protein A7	-2.66	0.0049	3.97
MUCL1	mucin-like 1	-2.77	0.0049	3.93
GPR110	G protein-coupled receptor 110	-1.59	0.0049	3.93
PLEKHA7	pleckstrin homology domain containing, family A member 7	-1.26	0.0051	3.85

SYMBOL	DESCRIPTION	M	P.Value	B
SLC39A2	solute carrier family 39 (zinc transporter), member 2	-2.63	0.0051	3.85
LPHN2	latrophilin 2	-2.02	0.0054	3.76
BCAT1	branched chain aminotransferase 1, cytosolic	-1.56	0.0055	3.71
AIM1L	absent in melanoma 1-like	-1.03	0.0060	3.55
MYEOV	myeloma overexpressed (in a subset of t(11;14) positive multiple myelomas)	-1.21	0.0060	3.55
ITGBL1	integrin, beta-like 1 (with EGF-like repeat domains)	-1.21	0.0060	3.54
HSD11B2	hydroxysteroid (11-beta) dehydrogenase 2	-1.49	0.0065	3.44
GDPD3	glycerophosphodiester phosphodiesterase domain containing 3	-1.22	0.0070	3.34
SLCO2A1	solute carrier organic anion transporter family, member 2A1	1.91	0.0074	3.22
NA	NA	1.11	0.0075	3.19
DUSP10	dual specificity phosphatase 10	-1.16	0.0075	3.16
DGAT2	diacylglycerol O-acyltransferase homolog 2 (mouse)	-1.75	0.0075	3.15
LCN2	lipocalin 2	-2.21	0.0075	3.15
CLIC5	chloride intracellular channel 5	-1.76	0.0077	3.11
LIPH	lipase, member H	-2.08	0.0082	3.01
GPR110	G protein-coupled receptor 110	-1.67	0.0082	3.01
SLC39A8	solute carrier family 39 (zinc transporter), member 8	-1.12	0.0083	2.98
ANO1	anoctamin 1, calcium activated chloride channel	-1.12	0.0085	2.94
AKR1C3	aldo-keto reductase family 1, member C3 (3-alpha hydroxysteroid dehydrogenase, type II)	-2.15	0.0087	2.89
RARRES1	retinoic acid receptor responder (tazarotene induced) 1	-2.73	0.0089	2.84
NCCRP1	non-specific cytotoxic cell receptor protein 1 homolog (zebrafish)	-1.26	0.0089	2.81
KLK8	kallikrein-related peptidase 8	-1.14	0.0090	2.77
POF1B	premature ovarian failure, 1B	-1.51	0.0091	2.75
SEMA3A	sema domain, immunoglobulin domain (Ig), short basic domain, secreted, (semaphorin) 3A	-1.90	0.0097	2.68
KRT10	keratin 10	-2.07	0.0103	2.59
PLA2G7	phospholipase A2, group VII (platelet-activating factor acetylhydrolase, plasma)	-2.65	0.0105	2.53
DHRS9	dehydrogenase/reductase (SDR family) member 9	-1.94	0.0109	2.47
GCNT3	glucosaminyl (N-acetyl) transferase 3, mucin type	-1.20	0.0109	2.46
PI3	peptidase inhibitor 3, skin-derived	-1.20	0.0110	2.43
ATAD4	ATPase family, AAA domain containing 4	-1.58	0.0112	2.39
ERP27	endoplasmic reticulum protein 27	-1.34	0.0112	2.39
PDIA6	protein disulfide isomerase family A, member 6	-1.34	0.0112	2.36
CLDN4	claudin 4	-1.38	0.0112	2.35
SLC15A1	solute carrier family 15 (oligopeptide transporter), member 1	-1.40	0.0118	2.26
SULT2B1	sulfotransferase family, cytosolic, 2B, member 1	-1.62	0.0118	2.26
WFDC12	WAP four-disulfide core domain 12	-2.31	0.0118	2.25
ARRB1	arrestin, beta 1	-1.10	0.0118	2.24
PPL	periplakin	-1.27	0.0118	2.23
SLPI	secretory leukocyte peptidase inhibitor	-1.27	0.0118	2.22
PDPN	podoplanin	1.03	0.0120	2.19

SYMBOL	DESCRIPTION	M	P.Value	B
SPINK5	serine peptidase inhibitor, Kazal type 5	-2.50	0.0124	2.13
HSPB8	heat shock 22kDa protein 8	-1.12	0.0131	2.03
MUC15	mucin 15, cell surface associated	-2.63	0.0131	2.02
ANKRD22	ankyrin repeat domain 22	-1.73	0.0138	1.92
AIF1L	allograft inflammatory factor 1-like	-1.12	0.0138	1.90
SH2D1B	SH2 domain containing 1B	-1.29	0.0138	1.90
DUSP16	dual specificity phosphatase 16	-1.50	0.0143	1.84
EHD3	EH-domain containing 3	-1.13	0.0145	1.81
BNIP3	BCL2/adenovirus E1B 19kDa interacting protein 3	1.59	0.0145	1.81
MT1G	metallothionein 1G	2.07	0.0156	1.71
MAP2	microtubule-associated protein 2	-1.12	0.0157	1.69
AS3MT	arsenic (+3 oxidation state) methyltransferase	1.13	0.0157	1.68
ACSL1	acyl-CoA synthetase long-chain family member 1	-1.38	0.0158	1.67
SCEL	sciellin	-1.58	0.0165	1.62
RPS10P7	ribosomal protein S10 pseudogene 7	1.52	0.0185	1.43
MANSC1	MANSC domain containing 1	-1.08	0.0185	1.41
ACVR2A	activin A receptor, type IIA	-1.16	0.0201	1.29
ALDH2	aldehyde dehydrogenase 2 family (mitochondrial)	1.01	0.0202	1.27
DHRS11	dehydrogenase/reductase (SDR family) member 11	-1.32	0.0205	1.24
SLC1A1	solute carrier family 1 (neuronal/epithelial high affinity glutamate transporter, system Xag), member 1	1.18	0.0210	1.20
SLC6A14	solute carrier family 6 (amino acid transporter), member 14	-1.64	0.0211	1.19
LPIN1	lipin 1	-1.07	0.0227	1.09
IVNS1ABP	influenza virus NS1A binding protein	1.62	0.0227	1.09
SPRR1A	small proline-rich protein 1A	-2.17	0.0231	1.07
IL28A	interleukin 28A (interferon, lambda 2)	2.98	0.0234	1.04
SLC5A1	solute carrier family 5 (sodium/glucose cotransporter), member 1	-1.41	0.0237	1.02
FAP	fibroblast activation protein, alpha	1.61	0.0243	0.98
TGFBI	transforming growth factor, beta-induced, 68kDa	1.10	0.0246	0.95
OR10A3	olfactory receptor, family 10, subfamily A, member 3	-1.41	0.0253	0.89
CARD18	caspase recruitment domain family, member 18	-1.46	0.0259	0.85
C12orf36	chromosome 12 open reading frame 36	-1.01	0.0272	0.75
TMPRSS11E	transmembrane protease, serine 11E	-1.70	0.0281	0.70
TMPRSS11F	transmembrane protease, serine 11F	-1.24	0.0288	0.67
SLC40A1	solute carrier family 40 (iron-regulated transporter), member 1	-1.25	0.0293	0.65
MAPRE2	microtubule-associated protein, RP/EB family, member 2	-1.21	0.0307	0.59
SPRR4	small proline-rich protein 4	-1.24	0.0307	0.58
LMO7	LIM domain 7	-1.08	0.0312	0.54
BNIPL	BCL2/adenovirus E1B 19kD interacting protein like	-1.04	0.0317	0.51
TTC39A	tetratricopeptide repeat domain 39A	-1.06	0.0338	0.40
GPR155	G protein-coupled receptor 155	1.19	0.0351	0.32
NA	NA	-1.01	0.0351	0.31
GRHL1	grainyhead-like 1 (Drosophila)	-1.40	0.0378	0.20
CXCL1	chemokine (C-X-C motif) ligand 1 (melanoma growth stimulating activity, alpha)	1.07	0.0422	0.03

SYMBOL	DESCRIPTION	M	P.Value	B
TRIM2	tripartite motif-containing 2	-1.02	0.0422	0.02
RHCG	Rh family, C glycoprotein	-2.40	0.0425	0.01
SBSN	suprabasin	-1.78	0.0429	-0.02
IVL	involucrin	-1.28	0.0456	-0.11
KRT19	keratin 19	-1.19	0.0485	-0.21
TMPRSS4	transmembrane protease, serine 4	-1.05	0.0493	-0.23

5.4.1.2 Differences in pLXSN keratinocytes upon UV.

Table 5-11 Differentially expressed genes in primary pLXSN keratinocytes after 30 mJ/cm^2 UV.

The gene is shown by GenBank symbol and description. The table is ordered according to descending B statistic, which incorporates P and M (= absolute fold change).

SYMBOL	DESCRIPTION	M	P Value	B
HMGXB4	HMG box domain containing 4	-2.05	0.0000	14.22
EFNB2	ephrin-B2	-2.25	0.0000	13.51
PAPOLG	poly(A) polymerase gamma	-2.13	0.0000	13.42
NA	NA	-2.09	0.0000	13.20
SLC38A2	solute carrier family 38, member 2	-1.87	0.0000	13.10
PLEKHF2	pleckstrin homology domain containing, family F (with FYVE domain) member 2	-2.63	0.0000	13.04
SOCS6	suppressor of cytokine signaling 6	-2.85	0.0000	12.83
DUSP6	dual specificity phosphatase 6	-3.11	0.0000	12.68
TGS1	trimethylguanosine synthase homolog (S. cerevisiae)	-2.30	0.0000	12.57
ZNF136	zinc finger protein 136	-1.51	0.0000	12.50
MAT2A	methionine adenosyltransferase II, alpha	-2.53	0.0000	12.50
ZFX	zinc finger protein, X-linked	-1.93	0.0000	12.29
SNX4	sorting nexin 4	-1.84	0.0000	12.20
SPTLC2	serine palmitoyltransferase, long chain base subunit 2	-1.68	0.0000	12.08
PLK2	polo-like kinase 2 (Drosophila)	-2.40	0.0000	12.07
MYC	v-myc myelocytomatosis viral oncogene homolog (avian)	-2.85	0.0000	11.95
E2F3	E2F transcription factor 3	-2.06	0.0000	11.93
NA	NA	-3.16	0.0000	11.64
UGCG	UDP-glucose ceramide glucosyltransferase	-1.70	0.0000	11.61
KLF6	Kruppel-like factor 6	-2.10	0.0000	11.45
ZNF644	zinc finger protein 644	-2.11	0.0000	11.44
MIER1	mesoderm induction early response 1 homolog (Xenopus laevis)	-1.68	0.0000	11.42
EPC1	enhancer of polycomb homolog 1 (Drosophila)	-1.41	0.0000	11.38
DCUN1D3	DCN1, defective in cullin neddylation 1, domain containing 3 (S. cerevisiae)	-1.98	0.0000	11.34
IREB2	iron-responsive element binding protein 2	-2.68	0.0000	11.32
JMJD1C	jumonji domain containing 1C	-2.00	0.0000	11.29
TADA1L	transcriptional adaptor 1 (HFI1 homolog, yeast)-like	-2.07	0.0000	11.26
NA	NA	-1.68	0.0000	11.26

SYMBOL	DESCRIPTION	M	P Value	B
DUSP7	dual specificity phosphatase 7	-1.67	0.0000	11.17
PALB2	partner and localizer of BRCA2	-2.29	0.0000	11.15
DCAF12	DDB1 and CUL4 associated factor 12	-1.44	0.0000	11.12
AMD1	adenosylmethionine decarboxylase 1	-2.25	0.0000	11.11
MSL2	male-specific lethal 2 homolog (Drosophila)	-2.58	0.0000	11.07
RYBP	RING1 and YY1 binding protein	-1.75	0.0000	11.06
ZNF562	zinc finger protein 562	-1.69	0.0000	10.99
HS3ST1	heparan sulfate (glucosamine) 3-O-sulfotransferase 1	-2.37	0.0000	10.96
WDR82	WD repeat domain 82	-2.23	0.0000	10.89
C7orf60	chromosome 7 open reading frame 60	-2.54	0.0000	10.86
CCL20	chemokine (C-C motif) ligand 20	3.69	0.0000	10.83
RBM5	RNA binding motif protein 5	-1.83	0.0000	10.82
PPP1R10	protein phosphatase 1, regulatory (inhibitor) subunit 10	-1.66	0.0000	10.81
CTR9	Ctr9, Paf1/RNA polymerase II complex component, homolog (S. cerevisiae)	-1.73	0.0000	10.78
C16orf70	chromosome 16 open reading frame 70	-1.96	0.0000	10.75
YTHDF1	YTH domain family, member 1	-1.52	0.0000	10.73
IRF2	interferon regulatory factor 2	-1.51	0.0000	10.66
GPBP1	GC-rich promoter binding protein 1	-1.77	0.0000	10.62
SGMS1	sphingomyelin synthase 1	-1.37	0.0000	10.62
RIPK4	receptor-interacting serine-threonine kinase 4	-2.04	0.0000	10.56
FBXL5	F-box and leucine-rich repeat protein 5	-1.37	0.0000	10.55
FBXO34	F-box protein 34	-2.27	0.0000	10.54
ZNF611	zinc finger protein 611	-1.52	0.0000	10.45
C22orf30	chromosome 22 open reading frame 30	-1.38	0.0000	10.42
B3GNT2	UDP-GlcNAc:betaGal beta-1,3-N-acetylglucosaminyltransferase 2	-2.15	0.0000	10.41
FTSJD1	FtsJ methyltransferase domain containing 1	-1.60	0.0000	10.29
RBPJ	recombination signal binding protein for immunoglobulin kappa J region	-1.16	0.0000	10.28
TMF1	TATA element modulatory factor 1	-1.41	0.0000	10.26
EPC2	enhancer of polycomb homolog 2 (Drosophila)	-1.94	0.0000	10.22
ENTPD7	ectonucleoside triphosphate diphosphohydrolase 7	-1.72	0.0000	10.18
PHLPP1	PH domain and leucine rich repeat protein phosphatase 1	-1.37	0.0000	10.12
SNRK	SNF related kinase	-1.43	0.0000	10.09
TBK1	TANK-binding kinase 1	-2.14	0.0000	10.06
MED23	mediator complex subunit 23	-1.66	0.0000	10.02
TIPARP	TCDD-inducible poly(ADP-ribose) polymerase	-2.03	0.0000	9.99
C5orf24	chromosome 5 open reading frame 24	-1.31	0.0000	9.96
CREB1	cAMP responsive element binding protein 1	-1.32	0.0000	9.90
HPS5	Hermansky-Pudlak syndrome 5	-1.26	0.0000	9.89
WAC	WW domain containing adaptor with coiled-coil	-1.52	0.0000	9.88
SHOC2	soc-2 suppressor of clear homolog (C. elegans)	-1.90	0.0000	9.82
RLIM	ring finger protein, LIM domain interacting	-1.73	0.0000	9.78
HIPK1	homeodomain interacting protein kinase 1	-1.24	0.0000	9.77

SYMBOL	DESCRIPTION	M	P Value	B
ZNF234	zinc finger protein 234	-1.58	0.0000	9.77
RAP2B	RAP2B, member of RAS oncogene family	-1.35	0.0000	9.69
WDR36	WD repeat domain 36	-1.45	0.0000	9.69
ARF6	ADP-ribosylation factor 6	-1.27	0.0000	9.62
SMNDC1	survival motor neuron domain containing 1	-1.57	0.0000	9.60
TMEM188	transmembrane protein 188	-2.51	0.0000	9.56
ZNF616	zinc finger protein 616	-1.83	0.0000	9.55
BCOR	BCL6 co-repressor	-1.31	0.0000	9.49
BAG4	BCL2-associated athanogene 4	-1.24	0.0000	9.46
GCNT4	glucosaminyl (N-acetyl) transferase 4, core 2 (beta-1,6-N-acetylglucosaminyltransferase)	-2.70	0.0000	9.46
SERTAD3	SERTA domain containing 3	-2.27	0.0000	9.41
NUP153	nucleoporin 153kDa	-1.62	0.0000	9.40
RPP14	ribonuclease P/MRP 14kDa subunit	-1.87	0.0000	9.39
RAPGEF2	Rap guanine nucleotide exchange factor (GEF) 2	-1.73	0.0000	9.38
CUGBP1	CUG triplet repeat, RNA binding protein 1	-1.47	0.0000	9.36
NR2F2	nuclear receptor subfamily 2, group F, member 2	-1.49	0.0000	9.35
CTDSP2	CTD (carboxy-terminal domain, RNA polymerase II, polypeptide A) small phosphatase 2	-1.30	0.0000	9.34
NUFIP2	nuclear fragile X mental retardation protein interacting protein 2	-2.02	0.0000	9.32
NDST2	N-deacetylase/N-sulfotransferase (heparan glucosaminyl) 2	-1.43	0.0000	9.32
ZFP91	zinc finger protein 91 homolog (mouse)	-1.01	0.0000	9.23
DUSP11	dual specificity phosphatase 11 (RNA/RNP complex 1-interacting)	-1.24	0.0000	9.20
PUM1	pumilio homolog 1 (Drosophila)	-1.80	0.0000	9.20
HEATR1	HEAT repeat containing 1	-1.48	0.0000	9.20
TMCC1	transmembrane and coiled-coil domain family 1	-1.69	0.0000	9.19
RNF34	ring finger protein 34	-1.17	0.0000	9.19
KLF3	Kruppel-like factor 3 (basic)	-1.61	0.0000	9.17
KCTD20	potassium channel tetramerisation domain containing 20	-1.85	0.0000	9.17
ZNF260	zinc finger protein 260	-1.13	0.0000	9.17
ELF1	E74-like factor 1 (ets domain transcription factor)	-1.93	0.0000	9.14
KDM6A	lysine (K)-specific demethylase 6A	-1.87	0.0000	9.12
SAMD8	sterile alpha motif domain containing 8	-1.45	0.0000	9.11
FOXJ3	forkhead box J3	-1.34	0.0000	9.09
FRS2	fibroblast growth factor receptor substrate 2	-1.71	0.0000	9.08
DBF4	DBF4 homolog (S. cerevisiae)	-1.33	0.0000	9.06
LUZP1	leucine zipper protein 1	-1.31	0.0000	9.05
MIER3	mesoderm induction early response 1, family member 3	-1.99	0.0000	9.03
ARHGAP12	Rho GTPase activating protein 12	-2.04	0.0000	9.02
RBBP6	retinoblastoma binding protein 6	-1.59	0.0000	9.01
PVRL4	poliovirus receptor-related 4	-2.03	0.0000	9.01
GTF2E1	general transcription factor IIE, polypeptide 1, alpha 56kDa	-1.94	0.0000	9.00
RNF139	ring finger protein 139	-1.54	0.0000	8.99

SYMBOL	DESCRIPTION	M	P Value	B
DCUN1D1	DCN1, defective in cullin neddylation 1, domain containing 1 (S. cerevisiae)	-1.39	0.0000	8.99
CASP3	caspase 3, apoptosis-related cysteine peptidase	-1.49	0.0000	8.98
GNA13	guanine nucleotide binding protein (G protein), alpha 13	-1.79	0.0000	8.97
FYN	FYN oncogene related to SRC, FGR, YES	-1.24	0.0000	8.96
COIL	coilin	-2.08	0.0000	8.95
TBC1D22B	TBC1 domain family, member 22B	-1.06	0.0000	8.95
NA	NA	-4.14	0.0000	8.94
ELL2	elongation factor, RNA polymerase II, 2	-1.58	0.0000	8.89
MAP4K3	mitogen-activated protein kinase kinase kinase kinase 3	-1.89	0.0000	8.89
ZBED5	zinc finger, BED-type containing 5	-1.94	0.0000	8.88
ZNF22	zinc finger protein 22 (KOX 15)	-1.48	0.0000	8.88
LMBR1	limb region 1 homolog (mouse)	-2.02	0.0000	8.87
DDX3X	DEAD (Asp-Glu-Ala-Asp) box polypeptide 3, X-linked	-1.49	0.0000	8.85
SFRS15	splicing factor, arginine/serine-rich 15	-1.43	0.0000	8.84
ARHGEF3	Rho guanine nucleotide exchange factor (GEF) 3	-1.56	0.0000	8.82
STK35	serine/threonine kinase 35	-1.65	0.0000	8.81
MCL1	myeloid cell leukemia sequence 1 (BCL2-related)	-2.32	0.0000	8.78
CUL1	cullin 1	-1.34	0.0000	8.74
RAPGEF6	Rap guanine nucleotide exchange factor (GEF) 6	-1.14	0.0000	8.73
EIF2AK3	eukaryotic translation initiation factor 2-alpha kinase 3	-1.61	0.0000	8.71
PPM1B	protein phosphatase 1B (formerly 2C), magnesium-dependent, beta isoform	-1.12	0.0000	8.71
PRDM4	PR domain containing 4	-1.45	0.0000	8.70
BNC1	basonuclin 1	-1.53	0.0000	8.70
C17orf63	chromosome 17 open reading frame 63	-1.60	0.0000	8.69
IMP3	IMP3, U3 small nucleolar ribonucleoprotein, homolog (yeast)	-1.84	0.0000	8.68
FBXO30	F-box protein 30	-1.57	0.0000	8.67
NA	NA	-1.76	0.0000	8.65
DIP2B	DIP2 disco-interacting protein 2 homolog B (Drosophila)	-1.44	0.0000	8.63
POLR1C	polymerase (RNA) I polypeptide C, 30kDa	-1.56	0.0000	8.63
ZNF134	zinc finger protein 134	-1.65	0.0000	8.61
ADNP	activity-dependent neuroprotector homeobox	-1.60	0.0000	8.60
IPPK	inositol 1,3,4,5,6-pentakisphosphate 2-kinase	-1.45	0.0000	8.60
RBBP5	retinoblastoma binding protein 5	-1.18	0.0000	8.59
CHD1	chromodomain helicase DNA binding protein 1	-1.55	0.0000	8.58
POGK	pogo transposable element with KRAB domain	-1.32	0.0000	8.57
ZNF480	zinc finger protein 480	-1.80	0.0000	8.51
MOBKL2A	MOB1, Mps One Binder kinase activator-like 2A (yeast)	-1.17	0.0000	8.49
NCK1	NCK adaptor protein 1	-1.62	0.0000	8.49
ARL5B	ADP-ribosylation factor-like 5B	-1.57	0.0000	8.48

SYMBOL	DESCRIPTION	M	P Value	B
TOR1AIP2	torsin A interacting protein 2	-1.57	0.0000	8.47
USPL1	ubiquitin specific peptidase like 1	-2.45	0.0000	8.45
DUSP18	dual specificity phosphatase 18	-1.41	0.0000	8.45
RNF19A	ring finger protein 19A	-1.84	0.0000	8.43
ZNF302	zinc finger protein 302	-1.88	0.0000	8.43
C12orf57	chromosome 12 open reading frame 57	1.64	0.0000	8.42
MFSD2	major facilitator superfamily domain containing 2	-1.23	0.0000	8.41
MFAP1	microfibrillar-associated protein 1	-1.11	0.0000	8.39
GTF3C4	general transcription factor IIIC, polypeptide 4, 90kDa	-1.34	0.0000	8.39
NA	NA	-1.36	0.0000	8.37
TNRC6A	trinucleotide repeat containing 6A	-1.33	0.0000	8.37
BCL2L1	BCL2-like 1, Bcl-x	-1.20	0.0000	8.36
MOBKL1A	MOB1, Mps One Binder kinase activator-like 1A (yeast)	-1.68	0.0000	8.36
NIPAL1	NIPA-like domain containing 1	-1.53	0.0000	8.34
WDR44	WD repeat domain 44	-1.51	0.0000	8.33
GNE	glucosamine (UDP-N-acetyl)-2-epimerase/N-acetylmannosamine kinase	-1.19	0.0000	8.33
ANKRD50	ankyrin repeat domain 50	-1.79	0.0000	8.31
NA	NA	-2.50	0.0000	8.30
LARP4	La ribonucleoprotein domain family, member 4	-1.46	0.0000	8.29
NR3C1	nuclear receptor subfamily 3, group C, member 1 (glucocorticoid receptor)	-1.65	0.0000	8.28
TTLL4	tubulin tyrosine ligase-like family, member 4	-1.20	0.0000	8.28
PPP4R2	protein phosphatase 4, regulatory subunit 2	-1.92	0.0000	8.28
NA	NA	-1.34	0.0000	8.27
RNF146	ring finger protein 146	-1.95	0.0000	8.26
SOCS4	suppressor of cytokine signaling 4	-1.62	0.0000	8.25
AKIRIN2	akirin 2	-1.25	0.0000	8.25
C1orf107	chromosome 1 open reading frame 107	-1.28	0.0000	8.20
KBTBD2	kelch repeat and BTB (POZ) domain containing 2	-1.54	0.0000	8.19
SGK196	protein kinase-like protein SgK196	-1.90	0.0000	8.17
PCF11	PCF11, cleavage and polyadenylation factor subunit, homolog (S. cerevisiae)	-2.18	0.0000	8.16
DHX8	DEAH (Asp-Glu-Ala-His) box polypeptide 8	-1.14	0.0000	8.16
MBIP	MAP3K12 binding inhibitory protein 1	-2.33	0.0000	8.15
FEM1C	fem-1 homolog c (C. elegans)	-1.39	0.0000	8.14
EEA1	early endosome antigen 1	-1.84	0.0000	8.14
KIAA0317	KIAA0317	-1.14	0.0000	8.12
HK2	hexokinase 2	-1.18	0.0000	8.11
PPM1K	protein phosphatase 1K (PP2C domain containing)	-1.03	0.0000	8.11
RTF1	Rtf1, Paf1/RNA polymerase II complex component, homolog (S. cerevisiae)	-1.31	0.0000	8.09
GOLPH3	golgi phosphoprotein 3 (coat-protein)	-1.27	0.0000	8.09
SPRED1	sprouty-related, EVH1 domain containing 1	-1.78	0.0000	8.08
GIGYF2	GRB10 interacting GYF protein 2	-1.13	0.0000	8.07
NA	NA	-1.55	0.0000	8.07
CNOT8	CCR4-NOT transcription complex, subunit 8	-1.74	0.0000	8.06

SYMBOL	DESCRIPTION	M	P Value	B
FAM175B	family with sequence similarity 175, member B	-1.34	0.0000	8.05
MOBKL2B	MOB1, Mps One Binder kinase activator-like 2B (yeast)	-1.08	0.0000	8.03
RNF219	ring finger protein 219	-1.91	0.0000	8.03
MAFB	v-maf musculoaponeurotic fibrosarcoma oncogene homolog B (avian)	1.15	0.0000	8.02
CTNNB1	catenin (cadherin-associated protein), beta 1, 88kDa	-1.06	0.0000	8.02

5.4.1.3 Differences in HPV5E6 expressing keratinocytes upon UV.

Table 5-12 Differentially expressed genes in primary keratinocytes expressing HPV5E6 after 30 mJ/cm^2 UV.

The gene is shown by GenBank symbol and description. The table is ordered according to descending B statistic, which incorporates P and M (= absolute fold change).

SYMBOL	DESCRIPTION	M	P Value	B
HMGXB4	HMG box domain containing 4	-2.10	0.0000	14.60
SLC38A2	solute carrier family 38, member 2	-2.16	0.0000	14.53
PAPOLG	poly(A) polymerase gamma	-2.27	0.0000	14.10
SNX4	sorting nexin 4	-2.23	0.0000	14.02
PLEKHF2	pleckstrin homology domain containing, family F (with FYVE domain) member 2	-2.89	0.0000	14.00
EFNB2	ephrin-B2	-2.30	0.0000	13.85
PLK2	polo-like kinase 2 (Drosophila)	-2.81	0.0000	13.63
E2F3	E2F transcription factor 3	-2.41	0.0000	13.44
KLF6	Kruppel-like factor 6	-2.49	0.0000	13.11
NA	NA	-2.04	0.0000	13.07
TGS1	trimethylguanosine synthase homolog (S. cerevisiae)	-2.40	0.0000	13.06
SOCS6	suppressor of cytokine signaling 6	-2.88	0.0000	13.03
MAT2A	methionine adenosyltransferase II, alpha	-2.65	0.0000	13.00
UGCG	UDP-glucose ceramide glucosyltransferase	-1.93	0.0000	12.86
MYC	v-myc myelocytomatosis viral oncogene homolog (avian)	-3.10	0.0000	12.82
AMD1	adenosylmethionine decarboxylase 1	-2.67	0.0000	12.78
SPTLC2	serine palmitoyltransferase, long chain base subunit 2	-1.78	0.0000	12.65
ZNF644	zinc finger protein 644	-2.38	0.0000	12.62
DUSP6	dual specificity phosphatase 6	-3.04	0.0000	12.54
ZFX	zinc finger protein, X-linked	-1.95	0.0000	12.49
RYBP	RING1 and YY1 binding protein	-2.02	0.0000	12.48
MIER1	mesoderm induction early response 1 homolog (Xenopus laevis)	-1.84	0.0000	12.30
FBXL5	F-box and leucine-rich repeat protein 5	-1.63	0.0000	12.28
WDR36	WD repeat domain 36	-1.89	0.0000	12.27
DUSP7	dual specificity phosphatase 7	-1.84	0.0000	12.18
TIPARP	TCDD-inducible poly(ADP-ribose) polymerase	-2.52	0.0000	12.09
RBPJ	recombination signal binding protein for	-1.40	0.0000	12.09

SYMBOL	DESCRIPTION	M	P Value	B
	immunoglobulin kappa J region			
ZNF22	zinc finger protein 22 (KOX 15)	-2.05	0.0000	12.08
CREB1	cAMP responsive element binding protein 1	-1.65	0.0000	12.06
IREB2	iron-responsive element binding protein 2	-2.87	0.0000	12.02
WDR82	WD repeat domain 82	-2.49	0.0000	12.00
ENTPD7	ectonucleoside triphosphate diphosphohydrolase 7	-2.06	0.0000	11.97
RAP2B	RAP2B, member of RAS oncogene family	-1.70	0.0000	11.96
ZNF562	zinc finger protein 562	-1.85	0.0000	11.91
CTR9	Ctr9, Paf1/RNA polymerase II complex component, homolog (S. cerevisiae)	-1.94	0.0000	11.89
NA	NA	-1.79	0.0000	11.87
DCAF12	DDB1 and CUL4 associated factor 12	-1.53	0.0000	11.79
DCUN1D3	DCN1, defective in cullin neddylation 1, domain containing 3 (S. cerevisiae)	-2.06	0.0000	11.78
CUGBP1	CUG triplet repeat, RNA binding protein 1	-1.85	0.0000	11.59
PPP1R10	protein phosphatase 1, regulatory (inhibitor) subunit 10	-1.78	0.0000	11.57
NA	NA	-3.12	0.0000	11.56
DUSP11	dual specificity phosphatase 11 (RNA/RNP complex 1-interacting)	-1.58	0.0000	11.54
MED23	mediator complex subunit 23	-1.93	0.0000	11.53
C7orf60	chromosome 7 open reading frame 60	-2.71	0.0000	11.53
NUP153	nucleoporin 153kDa	-2.00	0.0000	11.47
ZNF260	zinc finger protein 260	-1.42	0.0000	11.45
GPBP1	GC-rich promoter binding protein 1	-1.93	0.0000	11.44
SNRK	SNF related kinase	-1.64	0.0000	11.43
MSL2	male-specific lethal 2 homolog (Drosophila)	-2.63	0.0000	11.31
PALB2	partner and localizer of BRCA2	-2.32	0.0000	11.31
YTHDF1	YTH domain family, member 1	-1.60	0.0000	11.28
RBM5	RNA binding motif protein 5	-1.91	0.0000	11.27
JMJD1C	jumonji domain containing 1C	-1.97	0.0000	11.22
SMNDC1	survival motor neuron domain containing 1	-1.85	0.0000	11.21
RPP14	ribonuclease P/MRP 14kDa subunit	-2.23	0.0000	11.13
HIPK1	homeodomain interacting protein kinase 1	-1.42	0.0000	11.13
TBC1D22B	TBC1 domain family, member 22B	-1.32	0.0000	11.06
TMF1	TATA element modulatory factor 1	-1.53	0.0000	11.04
GTF2E1	general transcription factor IIE, polypeptide 1, alpha 56kDa	-2.38	0.0000	11.03
KLF3	Kruppel-like factor 3 (basic)	-1.94	0.0000	11.01
CUL1	cullin 1	-1.68	0.0000	11.00
RNF34	ring finger protein 34	-1.37	0.0000	10.77
C16orf70	chromosome 16 open reading frame 70	-1.96	0.0000	10.76
EPC1	enhancer of polycomb homolog 1 (Drosophila)	-1.31	0.0000	10.76
ZNF35	zinc finger protein 35	-1.92	0.0000	10.75
ETS2	v-ets erythroblastosis virus E26 oncogene homolog 2 (avian)	-2.01	0.0000	10.73
IRF2	interferon regulatory factor 2	-1.52	0.0000	10.73
ZNF611	zinc finger protein 611	-1.56	0.0000	10.71
C1orf107	chromosome 1 open reading frame 107	-1.65	0.0000	10.68
BLCAP	bladder cancer associated protein	-1.52	0.0000	10.67
WAC	WW domain containing adaptor with coiled-	-1.64	0.0000	10.65

SYMBOL	DESCRIPTION	M	P Value	B
	coil			
PHLPP1	PH domain and leucine rich repeat protein phosphatase 1	-1.45	0.0000	10.64
RIPK4	receptor-interacting serine-threonine kinase 4	-2.04	0.0000	10.63
TBK1	TANK-binding kinase 1	-2.27	0.0000	10.63
EPC2	enhancer of polycomb homolog 2 (Drosophila)	-2.02	0.0000	10.61
PRDM4	PR domain containing 4	-1.76	0.0000	10.59
LUZP1	leucine zipper protein 1	-1.53	0.0000	10.59
CHD1	chromodomain helicase DNA binding protein 1	-1.90	0.0000	10.58
RAPGEF6	Rap guanine nucleotide exchange factor (GEF) 6	-1.38	0.0000	10.55
TADA1L	transcriptional adaptor 1 (HFI1 homolog, yeast)-like	-1.92	0.0000	10.54
SGMS1	sphingomyelin synthase 1	-1.36	0.0000	10.54
SNAI2	snail homolog 2 (Drosophila)	-2.03	0.0000	10.54
ZNF136	zinc finger protein 136	-1.22	0.0000	10.53
NA	NA	-1.67	0.0000	10.51
DDX3X	DEAD (Asp-Glu-Ala-Asp) box polypeptide 3, X-linked	-1.75	0.0000	10.47
C22orf30	chromosome 22 open reading frame 30	-1.38	0.0000	10.45
C21orf91	chromosome 21 open reading frame 91	-2.11	0.0000	10.42
CTDSP2	CTD (carboxy-terminal domain, RNA polymerase II, polypeptide A) small phosphatase 2	-1.45	0.0000	10.42
POLR1C	polymerase (RNA) I polypeptide C, 30kDa	-1.87	0.0000	10.41
HAS3	hyaluronan synthase 3	-1.80	0.0000	10.39
DCUN1D1	DCN1, defective in cullin neddylation 1, domain containing 1 (S. cerevisiae)	-1.60	0.0000	10.39
FBXO34	F-box protein 34	-2.23	0.0000	10.37
NA	NA	-1.66	0.0000	10.37
ELF1	E74-like factor 1 (ets domain transcription factor)	-2.19	0.0000	10.36
RBAK	RB-associated KRAB zinc finger	-1.91	0.0000	10.32
FOXJ3	forkhead box J3	-1.51	0.0000	10.28
RND3	Rho family GTPase 3	-2.30	0.0000	10.24
ZBED5	zinc finger, BED-type containing 5	-2.22	0.0000	10.21
IPPK	inositol 1,3,4,5,6-pentakisphosphate 2-kinase	-1.69	0.0000	10.13
PPM1B	protein phosphatase 1B (formerly 2C), magnesium-dependent, beta isoform	-1.29	0.0000	10.10
PUM1	pumilio homolog 1 (Drosophila)	-1.97	0.0000	10.08
KCTD20	potassium channel tetramerisation domain containing 20	-2.03	0.0000	10.07
HEATR1	HEAT repeat containing 1	-1.61	0.0000	10.04
MCL1	myeloid cell leukemia sequence 1 (BCL2-related)	-2.63	0.0000	10.02
IMP3	IMP3, U3 small nucleolar ribonucleoprotein, homolog (yeast)	-2.10	0.0000	9.99
RLIM	ring finger protein, LIM domain interacting	-1.76	0.0000	9.99
CCNG1	cyclin G1	-2.80	0.0000	9.98
NR3C1	nuclear receptor subfamily 3, group C, member 1 (glucocorticoid receptor)	-1.96	0.0000	9.97

SYMBOL	DESCRIPTION	M	P Value	B
MIER3	mesoderm induction early response 1, family member 3	-2.19	0.0000	9.96
SMARCAD1	SWI/SNF-related, matrix-associated actin-dependent regulator of chromatin, subfamily a, containing DEAD/H box 1	-2.15	0.0000	9.92
CASP3	caspase 3, apoptosis-related cysteine peptidase	-1.64	0.0000	9.90
E2F4	E2F transcription factor 4, p107/p130-binding	-1.56	0.0000	9.87
NCK1	NCK adaptor protein 1	-1.87	0.0000	9.86
DHX8	DEAH (Asp-Glu-Ala-His) box polypeptide 8	-1.35	0.0000	9.84
RNF146	ring finger protein 146	-2.29	0.0000	9.82
TTLL4	tubulin tyrosine ligase-like family, member 4	-1.40	0.0000	9.82
CNOT8	CCR4-NOT transcription complex, subunit 8	-2.08	0.0000	9.82
RBMS1	RNA binding motif, single stranded interacting protein 1	-2.85	0.0000	9.82
GIGYF2	GRB10 interacting GYF protein 2	-1.34	0.0000	9.79
BTG2	BTG family, member 2	-1.94	0.0000	9.78
B3GNT2	UDP-GlcNAc:betaGal beta-1,3-N-acetylglucosaminyltransferase 2	-2.01	0.0000	9.75
SFRS15	splicing factor, arginine/serine-rich 15	-1.57	0.0000	9.75
C5orf51	chromosome 5 open reading frame 51	-1.80	0.0000	9.74
LTV1	LTV1 homolog (S. cerevisiae)	-1.85	0.0000	9.72
MAK16	MAK16 homolog (S. cerevisiae)	-1.86	0.0000	9.72
POLH	polymerase (DNA directed), eta	-1.58	0.0000	9.71
NA	NA	-1.55	0.0000	9.71
G2E3	G2/M-phase specific E3 ubiquitin ligase	-1.99	0.0000	9.67
NFKB1	nuclear factor of kappa light polypeptide gene enhancer in B-cells 1	-1.80	0.0000	9.65
TMCC1	transmembrane and coiled-coil domain family 1	-1.76	0.0000	9.64
GABPB1	GA binding protein transcription factor, beta subunit 1	-1.46	0.0000	9.64
FRS2	fibroblast growth factor receptor substrate 2	-1.80	0.0000	9.62
FYN	FYN oncogene related to SRC, FGR, YES	-1.33	0.0000	9.62
PPP4R2	protein phosphatase 4, regulatory subunit 2	-2.20	0.0000	9.62
CCL20	chemokine (C-C motif) ligand 20	3.24	0.0000	9.61
USPL1	ubiquitin specific peptidase like 1	-2.76	0.0000	9.61
ZNF134	zinc finger protein 134	-1.83	0.0000	9.61
APAF1	apoptotic peptidase activating factor 1	-1.94	0.0000	9.59
MAP2K4	mitogen-activated protein kinase kinase 4	-1.57	0.0000	9.57
SLC25A13	solute carrier family 25, member 13 (citrin)	-1.79	0.0000	9.57
TP63	tumor protein p63	-1.74	0.0000	9.57
MFSD2	major facilitator superfamily domain containing 2	-1.38	0.0000	9.56
TARDBP	TAR DNA binding protein	-1.69	0.0000	9.54
SERTAD3	SERTA domain containing 3	-2.29	0.0000	9.52
LMBR1	limb region 1 homolog (mouse)	-2.15	0.0000	9.49
ERCC4	excision repair cross-complementing rodent repair deficiency, complementation group 4	-1.46	0.0000	9.48
DUSP18	dual specificity phosphatase 18	-1.56	0.0000	9.48
MAP4K3	mitogen-activated protein kinase kinase kinase kinase 3	-2.00	0.0000	9.46
RNF139	ring finger protein 139	-1.61	0.0000	9.42

SYMBOL	DESCRIPTION	M	P Value	B
C17orf63	chromosome 17 open reading frame 63	-1.73	0.0000	9.41
SHOC2	soc-2 suppressor of clear homolog (C. elegans)	-1.82	0.0000	9.41
CSTF1	cleavage stimulation factor, 3' pre-RNA, subunit 1, 50kDa	-2.07	0.0000	9.41
ZNF557	zinc finger protein 557	-2.36	0.0000	9.40
GCNT4	glucosaminyl (N-acetyl) transferase 4, core 2 (beta-1,6-N-acetylglucosaminyltransferase)	-2.68	0.0000	9.39
UCK2	uridine-cytidine kinase 2	-1.09	0.0000	9.39
ARHGEF3	Rho guanine nucleotide exchange factor (GEF) 3	-1.65	0.0000	9.38
AKIRIN2	akirin 2	-1.40	0.0000	9.37
ZMYM1	zinc finger, MYM-type 1	-1.87	0.0000	9.35
ADNP	activity-dependent neuroprotector homeobox	-1.73	0.0000	9.35
POGK	pogo transposable element with KRAB domain	-1.43	0.0000	9.33
AVPI1	arginine vasopressin-induced 1	-1.22	0.0000	9.33
RBBP6	retinoblastoma binding protein 6	-1.64	0.0000	9.33
MED17	mediator complex subunit 17	-2.27	0.0000	9.32
FBXO30	F-box protein 30	-1.68	0.0000	9.29
RAPGEF2	Rap guanine nucleotide exchange factor (GEF) 2	-1.72	0.0000	9.28
NUFIP2	nuclear fragile X mental retardation protein interacting protein 2	-2.01	0.0000	9.26
ARF6	ADP-ribosylation factor 6	-1.22	0.0000	9.24
SAMD8	sterile alpha motif domain containing 8	-1.47	0.0000	9.23
HS3ST1	heparan sulfate (glucosamine) 3-O-sulfotransferase 1	-1.98	0.0000	9.23
ZNF234	zinc finger protein 234	-1.49	0.0000	9.22
TBP	TATA box binding protein	-1.36	0.0000	9.21
MOBKL2A	MOB1, Mps One Binder kinase activator-like 2A (yeast)	-1.27	0.0000	9.21
VPS33B	vacuolar protein sorting 33 homolog B (yeast)	-1.30	0.0000	9.20
DCP1A	DCP1 decapping enzyme homolog A (S. cerevisiae)	-1.72	0.0000	9.18
MIOS	missing oocyte, meiosis regulator, homolog (Drosophila)	-1.70	0.0000	9.17
ZFP91	zinc finger protein 91 homolog (mouse)	-1.01	0.0000	9.17
GPBP1L1	GC-rich promoter binding protein 1-like 1	-1.31	0.0000	9.17
RBBP5	retinoblastoma binding protein 5	-1.25	0.0000	9.16
TOP1	topoisomerase (DNA) I	-1.32	0.0000	9.13
FTSJD1	FtsJ methyltransferase domain containing 1	-1.42	0.0000	9.12
SIRT1	sirtuin (silent mating type information regulation 2 homolog) 1 (S. cerevisiae)	-1.87	0.0000	9.10
PUM2	pumilio homolog 2 (Drosophila)	-1.72	0.0000	9.07
IP6K1	inositol hexakisphosphate kinase 1	-1.35	0.0000	9.06
NA	NA	-4.18	0.0000	9.04
C5orf24	chromosome 5 open reading frame 24	-1.19	0.0000	9.04
KIAA0040	KIAA0040	-1.54	0.0000	9.03
ZBTB1	zinc finger and BTB domain containing 1	-1.75	0.0000	9.03
TMEM188	transmembrane protein 188	-2.37	0.0000	9.03
TSC22D2	TSC22 domain family, member 2	-1.04	0.0000	9.02
CXorf26	chromosome X open reading frame 26	-1.41	0.0000	9.01

SYMBOL	DESCRIPTION	M	P Value	B
CNOT2	CCR4-NOT transcription complex, subunit 2	-1.92	0.0000	9.00
CAND1	cullin-associated and neddylation-dissociated 1	-1.56	0.0000	8.99
GNE	glucosamine (UDP-N-acetyl)-2-epimerase/N-acetylmannosamine kinase	-1.28	0.0000	8.99
MBIP	MAP3K12 binding inhibitory protein 1	-2.54	0.0000	8.99
NA	NA	-2.22	0.0000	8.98
KIAA0317	KIAA0317	-1.25	0.0000	8.97
ARL5B	ADP-ribosylation factor-like 5B	-1.65	0.0000	8.97
KDM6A	lysine (K)-specific demethylase 6A	-1.84	0.0000	8.96
PIKFYVE	phosphoinositide kinase, FYVE finger containing	-1.32	0.0000	8.96

5.4.1.4 Differences between pLXSN and HPV5E6 keratinocytes upon UV

Table 5-13 Differentially expressed genes in HPV5E6 expressing primary keratinocytes compared to pLXSN controls, after 30 mJ/cm^2 UV.

The gene is shown by GenBank symbol and description. The table is ordered according to descending B statistic, which incorporates P and M (= absolute fold change).

SYMBOL	DESCRIPTION	M	P Value	B
SPRR3	small proline-rich protein 3	-3.41	0.0000	9.92
ECM1	extracellular matrix protein 1	-1.84	0.0000	9.85
AZGP1	alpha-2-glycoprotein 1, zinc-binding	-2.87	0.0000	9.60
ALPP	alkaline phosphatase, placental (Regan isozyme)	-4.80	0.0000	9.48
NDRG2	NDRG family member 2	-3.00	0.0000	9.40
ANXA9	annexin A9	-1.73	0.0001	8.90
GALNT5	UDP-N-acetyl-alpha-D-galactosamine:polypeptide N-acetylgalactosaminyltransferase 5 (GalNAc-T5)	-2.38	0.0002	7.92
RASA1	RAS p21 protein activator (GTPase activating protein) 1	-1.20	0.0004	7.49
NDRG1	N-myc downstream regulated 1	1.36	0.0005	7.21
LY6G6C	lymphocyte antigen 6 complex, locus G6C	-1.81	0.0006	6.92
SPRR2A	small proline-rich protein 2A	-1.60	0.0008	6.64
SPRR2D	small proline-rich protein 2D	-1.74	0.0011	6.20
KRT4	keratin 4	-3.15	0.0011	6.17
KLK6	kallikrein-related peptidase 6	-2.70	0.0012	6.03
SMARCA1	SWI/SNF related, matrix associated, actin dependent regulator of chromatin, subfamily a, member 1	1.18	0.0012	5.98
S100P	S100 calcium binding protein P	-1.88	0.0012	5.94
CEACAM1	carcinoembryonic antigen-related cell adhesion molecule 1 (biliary glycoprotein)	-1.09	0.0017	5.60
RAB11FIP1	RAB11 family interacting protein 1 (class I)	-1.16	0.0017	5.54
ATP12A	ATPase, H+/K+ transporting, nongastric, alpha polypeptide	-2.18	0.0019	5.41

SYMBOL	DESCRIPTION	M	P Value	B
CEACAM6	carcinoembryonic antigen-related cell adhesion molecule 6 (non-specific cross reacting antigen)	-2.55	0.0022	5.25
CARD18	caspase recruitment domain family, member 18	-2.49	0.0023	5.19
S100A7	S100 calcium binding protein A7	-2.96	0.0034	4.81
KRT24	keratin 24	-1.10	0.0037	4.69
GPR110	G protein-coupled receptor 110	-1.72	0.0043	4.53
SERPINE2	serpin peptidase inhibitor, clade E (nexin, plasminogen activator inhibitor type 1), member 2	1.38	0.0045	4.41
PLBD1	phospholipase B domain containing 1	-1.13	0.0045	4.35
SLC39A2	solute carrier family 39 (zinc transporter), member 2	-2.80	0.0045	4.34
NA	NA	1.26	0.0045	4.34
MUCL1	mucin-like 1	-2.89	0.0048	4.25
GK3P	glycerol kinase 3 pseudogene	-1.36	0.0065	3.89
GPR110	G protein-coupled receptor 110	-1.85	0.0068	3.80
HPGD	hydroxyprostaglandin dehydrogenase 15-(NAD)	-1.21	0.0069	3.76
NAMPT	nicotinamide phosphoribosyltransferase	-1.03	0.0089	3.48
EHD3	EH-domain containing 3	-1.36	0.0105	3.26
WFDC12	WAP four-disulfide core domain 12	-2.61	0.0106	3.23
GDPD3	glycerophosphodiester phosphodiesterase domain containing 3	-1.20	0.0106	3.18
SPRR1A	small proline-rich protein 1A	-2.82	0.0106	3.17
SERPINE1	serpin peptidase inhibitor, clade E (nexin, plasminogen activator inhibitor type 1), member 1	1.33	0.0108	3.13
ANKRD22	ankyrin repeat domain 22	-1.97	0.0120	2.95
LPHN2	latrophilin 2	-1.82	0.0123	2.85
SPINK5	serine peptidase inhibitor, Kazal type 5	-2.70	0.0123	2.76
PLA2G7	phospholipase A2, group VII (platelet-activating factor acetylhydrolase, plasma)	-2.72	0.0123	2.73
KLK8	kallikrein-related peptidase 8	-1.14	0.0123	2.73
ACSL1	acyl-CoA synthetase long-chain family member 1	-1.54	0.0137	2.54
HSD11B2	hydroxysteroid (11-beta) dehydrogenase 2	-1.33	0.0138	2.51
TPRG1	tumor protein p63 regulated 1	-1.24	0.0139	2.48
SBSN	suprabasin	-2.37	0.0174	2.23
NA	NA	-1.02	0.0178	2.19
CLDN4	claudin 4	-1.34	0.0189	2.10
LCN2	lipocalin 2	-1.91	0.0194	1.98
OBFC1	oligonucleotide/oligosaccharide-binding fold containing 1	-1.06	0.0205	1.90
DHRS11	dehydrogenase/reductase (SDR family) member 11	-1.42	0.0206	1.84
DGAT2	diacylglycerol O-acyltransferase homolog 2 (mouse)	-1.49	0.0206	1.83
AKR1C3	aldo-keto reductase family 1, member C3 (3-alpha hydroxysteroid dehydrogenase, type II)	-1.88	0.0206	1.78
SLC6A14	solute carrier family 6 (amino acid transporter), member 14	-1.74	0.0209	1.71
SPRR4	small proline-rich protein 4	-1.43	0.0209	1.70
SLCO2A1	solute carrier organic anion transporter	1.58	0.0210	1.68

SYMBOL	DESCRIPTION	M	P Value	B
	family, member 2A1			
POF1B	premature ovarian failure, 1B	-1.32	0.0210	1.67
RARRES1	retinoic acid receptor responder (tazarotene induced) 1	-2.33	0.0229	1.55
NA	NA	1.33	0.0231	1.52
ALDH3B2	aldehyde dehydrogenase 3 family, member B2	-1.46	0.0231	1.52
BNIP3	BCL2/adenovirus E1B 19kDa interacting protein 3	1.52	0.0236	1.47
SCEL	sciellin	-1.54	0.0246	1.42
BCAT1	branched chain aminotransferase 1, cytosolic	-1.17	0.0248	1.36
RNF144B	ring finger protein 144B	-1.21	0.0252	1.31
AIF1L	allograft inflammatory factor 1-like	-1.04	0.0252	1.29
LIPH	lipase, member H	-1.68	0.0255	1.28
FN1	fibronectin 1	1.48	0.0265	1.21
PI3	peptidase inhibitor 3, skin-derived	-1.02	0.0273	1.15
CSH1	chorionic somatomammotropin hormone 1 (placental lactogen)	1.15	0.0277	1.12
FCHO2	FCH domain only 2	-1.01	0.0280	1.10
NA	NA	-1.02	0.0280	1.09
NA	NA	-2.46	0.0280	1.08
MANSC1	MANSC domain containing 1	-1.02	0.0309	0.93
IVL	involucrin	-1.46	0.0309	0.93
SLPI	secretory leukocyte peptidase inhibitor	-1.07	0.0318	0.89
ATP1B1	ATPase, Na+/K+ transporting, beta 1 polypeptide	-1.38	0.0319	0.87
SLC15A1	solute carrier family 15 (oligopeptide transporter), member 1	-1.18	0.0319	0.87
RHCG	Rh family, C glycoprotein	-2.67	0.0324	0.85
MAPRE2	microtubule-associated protein, RP/EB family, member 2	-1.25	0.0324	0.85
FAP	fibroblast activation protein, alpha	1.57	0.0328	0.82
OR10A3	olfactory receptor, family 10, subfamily A, member 3	-1.39	0.0335	0.79
ACVR2A	activin A receptor, type IIA	-1.05	0.0385	0.54
NA	NA	-1.61	0.0385	0.54
EMP1	epithelial membrane protein 1	-1.32	0.0389	0.50
TAF11	TAF11 RNA polymerase II, TATA box binding protein (TBP)-associated factor, 28kDa	-1.02	0.0389	0.49
NA	NA	-1.56	0.0393	0.46
SULT2B1	sulfotransferase family, cytosolic, 2B, member 1	-1.28	0.0396	0.44
DHRS9	dehydrogenase/reductase (SDR family) member 9	-1.49	0.0410	0.40
NA	NA	-2.73	0.0411	0.39
PGLYRP4	peptidoglycan recognition protein 4	-1.10	0.0411	0.38
NEBL	nebulette	-2.42	0.0411	0.37
GRHL1	grainyhead-like 1 (Drosophila)	-1.43	0.0411	0.37
CLIC5	chloride intracellular channel 5	-1.23	0.0440	0.29
INSL4	insulin-like 4 (placenta)	-1.45	0.0440	0.29
IVNS1ABP	influenza virus NS1A binding protein	1.44	0.0450	0.25
MUC15	mucin 15, cell surface associated	-2.07	0.0470	0.18

SYMBOL	DESCRIPTION	M	P Value	B
STEAP4	STEAP family member 4	-1.15	0.0488	0.13

General Discussion

SCC is a very common cancer with increasing worldwide incidence, causing a significant healthcare burden. The association between a subset of cutaneous HPVs and development of SCC, in combination with UV, is supported by several lines of evidence, including the cases of Epidermodysplasia verruciformis and immunosuppressed transplant patients, epidemiological studies, and investigations into viral activities. However the mechanisms of viral tumourigenesis have not been fully described, in contrast to the more well-studied association between cervical cancer and high-risk mucosal HPVs.

The results shown here contribute to the hypothesis that the E6 protein of several cutaneous HPVs can play a role in tumourigenesis. Investigation into expression of proteins regulating apoptosis revealed upregulation of several anti-apoptotic proteins in keratinocytes expressing HPV5E6, which could play important roles in the apoptotic response to UV. Additional studies on the inhibition of death-receptor and UV-induced apoptosis by E6 of several cutaneous HPV types, namely 5, 8, 10 and 77E6, demonstrated how the presence of HPV could be relevant in SCC formation. Prevention of the removal of damaged cells from the epidermis by HPVE6 inhibition of apoptosis could contribute to the accumulation of mutations and progression to cancer. Using primary keratinocytes is important not only because they are the natural host cell of HPVs, but also due to their specific response to UV. However further studies of the role of HPV in the epidermis are hampered by the difficulty of generating E6-expressing organotypic cultures.

One of the major differences between HPV-associated tumourigenesis of the cervix and the epidermis is that HPV proteins are expressed in every cervical cancer cell, whereas HPV presence in SCC is low. This suggests a role for cutaneous HPVs early in tumourigenesis. Additionally, the observation that HPV positive SCC

display lower apoptotic rates than HPV negative SCC, despite the low HPV copy number, suggests that HPV-infected cells can influence the tumour overall, through a bystander effect. The results presented here provide support for the bystander effect, showing that HPVE6 expressing cells secrete survival factors which can inhibit apoptosis of neighbouring cells. This could be important in allowing further accumulation of UV-damaged cells. The factors OPG and IL6 were found to play a role in this, via their inhibition of the extrinsic and intrinsic apoptotic pathways that are important in UV irradiated keratinocytes. Moreover, IL6 upregulation has been shown in HPV positive SCCs, further indicating that it could be involved in tumourigenesis. The activation of signalling by IL6 could be important in several survival pathways.

The microarray analysis of keratinocytes expressing HPV5E6, and the effect of UV irradiation, provides further evidence that the activities of the viral gene could promote tumourigenesis. In particular, the implied disruption of keratinocyte differentiation and cornified envelope formation, and of the cell cycle, concurs with previous findings that HPV5E6 plays a role in these pathways, however further work is required to see what effect this would have on epidermal function and the response to UV. The role of survival signalling pathways and their modulation by HPV5E6 is also of relevance to SCC formation.

The work presented here is also applicable to characterising the differences between cutaneous and mucosal HPVs and their roles in tumourigenesis. Differences in the lifecycle, infection sites and viral proteins all contribute to differences in tumourigenesis, and it is now clear that different models for cancer formation are applicable. For example, the persistent presence of HPV in the epidermis is believed to contribute to early steps in tumourigenesis by potentially promoting the accumulation of deleterious mutations. Additionally the bystander effect could contribute at several stages of tumourigenesis by activating survival signalling in non-infected cells, meaning that HPV is not detected in every tumour

cell, in contrast to cervical cancer where expression of the high-risk proteins is essential for cancer cell survival. Further work defining the role of cutaneous HPVs in SCC formation will be of relevance not only to skin cancer, but could also contribute to the understanding of viral-associated neoplasias.

Appendices

Appendix 1 Complete map of the Proteome Profiler array.

Coordinate	Target/Control	Coordinate	Target/Control
A1, A2	Positive Control	C13, C14	HO-2/HMOX2
A23, A24	Positive Control	C15, C16	HSP27
B1, B2	Bad	C17, C18	HSP60
B3, B4	Bax	C19, C20	HSP70
B5, B6	Bcl-2	C21, C22	HTRA2/Omi
B7, B8	Bcl-x	C23, C24	Livin
B9, B10	Pro-Caspase-3	D1, D2	PON2
B11, B12	Cleaved Caspase-3	D3, D4	p21/CIP1/CDNK1A
B13, B14	Catalase	D5, D6	p27/Kip1
B15, B16	cIAP-1	D7, D8	Phospho-p53 (S15)
B17, B18	cIAP-2	D9, D10	Phospho-p53 (S46)
B19, B20	Claspin	D11, D12	Phospho-p53 (S392)
B21, B22	Clusterin	D13, D14	Phospho-Rad17 (S635)
B23, B24	Cytochrome c	D15, D16	SMAC/Diablo
C1, C2	TRAIL R1/DR4	D17, D18	Survivin
C3, C4	TRAIL R2/DR5	D19, D20	TNF RI/TNFRSF1A
C5, C6	FADD	D21, D22	XIAP
C7, C8	Fas/TNFSF6	D23, D24	PBS (Negative Control)
C9, C10	HIF-1α	E1, E2	Positive Control
C11, C12	HO-1/HMOX1/HSP32		

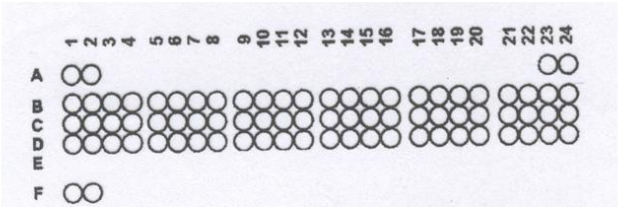

Appendix 2 A full list of the fold changes seen on the Proteome profiler arrays.

Protein	Without UV		Change upon UV			
	HPV5E6 compared to empty vector		HT1080		Keratinocytes	
	HT1080s	Keratinocytes	Empty vector	HPV5E6	Empty vector	HPV5E6
Bad	1.09	1.08	0.19	0.31	1.42	0.77
Bax	1.19	1.60	0.44	0.66	1.20	0.75
Bcl-2	1.89	2.33	0.67	0.56	1.67	1.14
Bcl-x	1.67	6.89	0.44	0.30	1.44	0.48
Pro-Caspase-3	1.01	1.24	0.96	0.89	0.92	0.92
Cleaved Caspase-3	0.50	2.00	7.50	13.00	1.00	9.50
Catalase	1.00	1.00	1.33	1.33	0.50	1.50
cIAP-1	1.15	6.00	0.69	0.80	1.50	0.33
cIAP-2	1.58	2.00	1.00	1.00	1.50	1.00
Claspin	1.50	3.50	0.70	0.60	1.50	0.57
Clusterin	1.53	1.50	1.16	0.76	0.75	1.17
Cytochrome c	1.00	1.30	0.99	1.00	0.84	0.94
TRAIL R1/DR4	1.21	4.33	0.47	0.57	1.00	1.00
TRAIL R2/DR5	0.99	7.33	0.88	0.79	1.00	0.50
FADD	1.11	4.88	0.80	0.74	1.13	0.54
Fas/TNFSF6	1.03	7.33	0.88	0.81	0.67	0.55
HIF-1	1.12	2.33	0.53	0.42	1.00	0.14
HO-1/HMOX1/HSP32	1.07	2.50	0.71	0.73	2.50	0.60
HO-2/HMOX2	1.09	2.00	0.85	0.86	1.23	0.73
HSP27	1.40	1.17	1.40	0.86	0.83	0.71
HSP60	1.04	1.29	1.02	1.00	1.00	2.00
HSP70	1.09	2.44	1.07	0.99	1.33	0.91
HTRA2/Omi	1.40	5.25	1.00	0.76	2.00	0.81
Livin	1.56	1.00	1.11	1.00	2.00	1.00
PON2	1.00	2.33	0.40	0.70	0.67	1.14
p21/CIP1/CDNK1A	1.38	1.00	0.46	0.56	0.75	0.75
p27/Kip1	1.25	1.67	0.75	0.60	0.33	0.60
Phospho-p53 (S15)	1.26	0.86	1.95	1.71	0.71	1.83
Phospho-p53 (S46)	2.00	2.00	7.33	3.67	0.50	0.50
Phospho-p53 (S392)	1.17	5.00	7.00	5.71	2.00	0.80
Phospho-Rad17 (S635)	1.11	2.00	1.00	0.90	1.00	1.00
SMAC/Diablo	1.13	3.80	0.80	0.61	1.20	0.58
Survivin	1.14	4.00	0.81	0.88	1.00	1.00
TNF RI/TNFRSF1A	1.50	5.00	0.40	0.40	2.00	0.60
XIAP	1.34	3.60	1.07	0.81	1.00	0.94

Adachi M., Gazel A., Pintucci G., Shuck A., Shifteh S., Ginsburg D., Rao L. S., Kaneko T., Freedberg I. M., Tamaki K. and Blumenberg M. (2003) Specificity in stress response: epidermal keratinocytes exhibit specialized UV-responsive signal transduction pathways. *DNA Cell Biol* **22**, 665-77.

Advani A. S. (2005) FLT3 and acute myelogenous leukemia: biology, clinical significance and therapeutic applications. *Curr Pharm Des* **11**, 3449-57.

Ahmad N. and Mukhtar H. (2004) Cytochrome p450: a target for drug development for skin diseases. *J Invest Dermatol* **123**, 417-25.

Akgul B., Bostanci N., Westphal K., Nindl I., Navsaria H., Storey A. and Pfister H. (2010) Human papillomavirus 5 and 8 E6 downregulate interleukin-8 secretion in primary human keratinocytes. *J Gen Virol* **91**, 888-92.

Akgul B., Cooke J. C. and Storey A. (2006a) HPV-associated skin disease. *J Pathol* **208**, 165-75.

Akgul B., Garcia-Escudero R., Ghali L., Pfister H. J., Fuchs P. G., Navsaria H. and Storey A. (2005a) The E7 protein of cutaneous human papillomavirus type 8 causes invasion of human keratinocytes into the dermis in organotypic cultures of skin. *Cancer Res* **65**, 2216-23.

Akgul B., Ghali L., Davies D., Pfister H., Leigh I. M. and Storey A. (2007a) HPV8 early genes modulate differentiation and cell cycle of primary human adult keratinocytes. *Exp Dermatol* **16**, 590-9.

Akgul B., Kose O., Safali M., Purdie K., Cerio R., Proby C. and Storey A. (2007b) A distinct variant of Epidermodysplasia verruciformis in a Turkish family lacking EVER1 and EVER2 mutations. *J Dermatol Sci* **46**, 214-6.

Akgul B., Lemme W., Garcia-Escudero R., Storey A. and Pfister H. J. (2005b) UV-B irradiation stimulates the promoter activity of the high-risk, cutaneous human papillomavirus 5 and 8 in primary keratinocytes. *Arch Virol* **150**, 145-51.

Akgul B., Pfefferle R., Marcuzzi G. P., Zigrino P., Krieg T., Pfister H. and Mauch C. (2006b) Expression of matrix metalloproteinase (MMP)-2, MMP-9, MMP-13, and MT1-MMP in skin tumors of human papillomavirus type 8 transgenic mice. *Exp Dermatol* **15**, 35-42.

Ali N. A., Gaughan A. A., Orosz C. G., Baran C. P., McMaken S., Wang Y., Eubank T. D., Hunter M., Lichtenberger F. J., Flavahan N. A., Lawler J. and Marsh C. B. (2008) Latency associated peptide has in vitro and in vivo immune effects independent of TGF-beta1. *PLoS One* **3**, e1914.

Alotaibi L., Provost N., Gagnon S., Franco E. L. and Coutlee F. (2006) Diversity of cutaneous human papillomavirus types in individuals with and without skin lesion. *J Clin Virol*.

Amin A. A., Titolo S., Pelletier A., Fink D., Cordingley M. G. and Archambault J. (2000) Identification of domains of the HPV11 E1 protein required for DNA replication in vitro. *Virology* **272**, 137-50.

Antignani A. and Youle R. J. (2006) How do Bax and Bak lead to permeabilization of the outer mitochondrial membrane? *Curr Opin Cell Biol* **18**, 685-9.

Antonsson A., Erfurt C., Hazard K., Holmgren V., Simon M., Kataoka A., Hossain S., Hakangard C. and Hansson B. G. (2003) Prevalence and type spectrum of human papillomaviruses in healthy skin samples collected in three continents. *J Gen Virol* **84**, 1881-6.

Aragane Y., Kulms D., Metze D., Wilkes G., Poppelmann B., Luger T. A. and Schwarz T. (1998) Ultraviolet light induces apoptosis via direct activation of CD95 (Fas/APO-1) independently of its ligand CD95L. *J Cell Biol* **140**, 171-82.

Asgari M. M., Kiviat N. B., Critchlow C. W., Stern J. E., Argenyi Z. B., Raugi G. J., Berg D., Odland P. B., Hawes S. E. and de Villiers E. M. (2008) Detection of human papillomavirus DNA in cutaneous squamous cell carcinoma among immunocompetent individuals. *J Invest Dermatol* **128**, 1409-17.

Ashrafi G. H., Brown D. R., Fife K. H. and Campo M. S. (2006) Down-regulation of MHC class I is a property common to papillomavirus E5 proteins. *Virus Res* **120**, 208-11.

Assefa Z., Garmyn M., Vantieghem A., Declercq W., Vandenabeele P., Vandenheede J. R. and Agostinis P. (2003) Ultraviolet B radiation-induced apoptosis in human keratinocytes: cytosolic activation of procaspase-8 and the role of Bcl-2. *FEBS Lett* **540**, 125-32.

Assefa Z., Vantieghem A., Garmyn M., Declercq W., Vandenabeele P., Vandenheede J. R., Bouillon R., Merlevede W. and Agostinis P. (2000) p38 mitogen-activated protein kinase regulates a novel, caspase-independent pathway for the mitochondrial cytochrome c release in ultraviolet B radiation-induced apoptosis. *J Biol Chem* **275**, 21416-21.

Azzimonti B., Dell'oste V., Borgogna C., Mondini M., Gugliesi F., De Andrea M., Chiorino G., Scatolini M., Ghimenti C., Landolfo S. and Gariglio M. (2009) The epithelial-mesenchymal transition induced by keratinocyte growth conditions is overcome by E6 and E7 from HPV16, but not HPV8 and HPV38: characterization of global transcription profiles. *Virology* **388**, 260-9.

Bachmann F., Buechner S. A., Wernli M., Strebel S. and Erb P. (2001) Ultraviolet light downregulates CD95 ligand and TRAIL receptor expression facilitating actinic keratosis and squamous cell carcinoma formation. *J Invest Dermatol* **117**, 59-66.

Bajou K., Maillard C., Jost M., Lijnen R. H., Gils A., Declerck P., Carmeliet P., Foidart J. M. and Noel A. (2004) Host-derived plasminogen activator inhibitor-1 (PAI-1) concentration is critical for in vivo tumoral angiogenesis and growth. *Oncogene* **23**, 6986-90.

Bajou K., Peng H., Laug W. E., Maillard C., Noel A., Foidart J. M., Martial J. A. and DeClerck Y. A. (2008) Plasminogen activator inhibitor-1 protects endothelial cells from FasL-mediated apoptosis. *Cancer Cell* **14**, 324-34.

Balkwill F. (2009) Tumour necrosis factor and cancer. *Nat Rev Cancer* **9**, 361-71.

Barnhart B. C., Legembre P., Pietras E., Bubici C., Franzoso G. and Peter M. E. (2004) CD95 ligand induces motility and invasiveness of apoptosis-resistant tumor cells. *EMBO J* **23**, 3175-85.

Barr E. and Tamms G. (2007) Quadrivalent human papillomavirus vaccine. *Clin Infect Dis* **45**, 609-7.

Bashir M. M., Sharma M. R. and Werth V. P. (2009) UVB and proinflammatory cytokines synergistically activate TNF-alpha production in keratinocytes through enhanced gene transcription. *J Invest Dermatol* **129**, 994-1001.

Basuroy S., Bhattacharya S., Tcheranova D., Qu Y., Regan R. F., Leffler C. W. and Parfenova H. (2006) HO-2 provides endogenous protection against oxidative stress and apoptosis caused by TNF-alpha in cerebral vascular endothelial cells. *Am J Physiol Cell Physiol* **291**, C897-908.

Bedard K. M., Underbrink M. P., Howie H. L. and Galloway D. A. (2008) The E6 oncoproteins from human betapapillomaviruses differentially activate telomerase through an E6AP-dependent mechanism and prolong the lifespan of primary keratinocytes. *J Virol* **82**, 3894-902.

Bell I., Martin A. and Roberts S. (2007) The E1circumflexE4 protein of human papillomavirus interacts with the serine-arginine-specific protein kinase SRPK1. *J Virol* **81**, 5437-48.

Berkhout R. J., Bouwes Bavinck J. N. and ter Schegget J. (2000) Persistence of human papillomavirus DNA in benign and (pre)malignant skin lesions from renal transplant recipients. *J Clin Microbiol* **38**, 2087-96.

Bernard H. U. (2005) The clinical importance of the nomenclature, evolution and taxonomy of human papillomaviruses. *J Clin Virol* **32 Suppl 1**, S1-6.

Bertrand M. J., Milutinovic S., Dickson K. M., Ho W. C., Boudreault A., Durkin J., Gillard J. W., Jaquith J. B., Morris S. J. and Barker P. A. (2008) cIAP1 and cIAP2 facilitate cancer cell survival by functioning as E3 ligases that promote RIP1 ubiquitination. *Mol Cell* **30**, 689-700.

Boatright K. M., Renatus M., Scott F. L., Sperandio S., Shin H., Pedersen I. M., Ricci J. E., Edris W. A., Sutherlin D. P., Green D. R. and Salvesen G. S. (2003) A unified model for apical caspase activation. *Mol Cell* **11**, 529-41.

Boczonadi V., McInroy L. and Maatta A. (2007) Cytolinker cross-talk: periplakin N-terminus interacts with plectin to regulate keratin organisation and epithelial migration. *Exp Cell Res* **313**, 3579-91.

Borbely A. A., Murvai M., Konya J., Beck Z., Gergely L., Li F. and Veress G. (2006) Effects of human papillomavirus type 16 oncoproteins on survivin gene expression. *Journal of General Virology* **87**, 287-294.

Bossis I., Roden R. B., Gambhira R., Yang R., Tagaya M., Howley P. M. and Meneses P. I. (2005) Interaction of tSNARE syntaxin 18 with the papillomavirus minor capsid protein mediates infection. *J Virol* **79**, 6723-31.

Boukamp P. (2005) Non-melanoma skin cancer: what drives tumor development and progression? *Carcinogenesis* **26**, 1657-67.

Boukamp P., Petrussevska R. T., Breitkreutz D., Hornung J., Markham A. and Fusenig N. E. (1988) Normal keratinization in a spontaneously immortalized aneuploid human keratinocyte cell line. *J Cell Biol* **106**, 761-71.

Bowen A. R., Hanks A. N., Allen S. M., Alexander A., Diedrich M. J. and Grossman D. (2003) Apoptosis regulators and responses in human melanocytic and keratinocytic cells. *J Invest Dermatol* **120**, 48-55.

Boxman I. L., Berkhout R. J., Mulder L. H., Wolkers M. C., Bouwes Bavinck J. N., Vermeer B. J. and ter Schegget J. (1997) Detection of human papillomavirus DNA in plucked hairs from renal transplant recipients and healthy volunteers. *J Invest Dermatol* **108**, 712-5.

Boxman I. L., Mulder L. H., Noya F., de Waard V., Gibbs S., Broker T. R., ten Kate F., Chow L. T. and ter Schegget J. (2001) Transduction of the E6 and E7 genes of epidermodysplasia-verruciformis-associated human papillomaviruses alters human keratinocyte growth and differentiation in organotypic cultures. *J Invest Dermatol* **117**, 1397-404.

Brash D. E. and Haseltine W. A. (1982) UV-induced mutation hotspots occur at DNA damage hotspots. *Nature* **298**, 189-92.

Brenner D. and Mak T. W. (2009) Mitochondrial cell death effectors. *Curr Opin Cell Biol* **21**, 871-7.

Cabral A., Voskamp P., Cleton-Jansen A. M., South A., Nizetic D. and Backendorf C. (2001) Structural organization and regulation of the small proline-rich family of cornified envelope precursors suggest a role in adaptive barrier function. *J Biol Chem* **276**, 19231-7.

Caldeira S., de Villiers E. M. and Tommasino M. (2000) Human papillomavirus E7 proteins stimulate proliferation independently of their ability to associate with retinoblastoma protein. *Oncogene* **19**, 821-6.

Caldeira S., Zehbe I., Accardi R., Malanchi I., Dong W., Giarre M., de Villiers E. M., Filotico R., Boukamp P. and Tommasino M. (2003) The E6 and E7 proteins of the cutaneous human papillomavirus type 38 display transforming properties. *J Virol* **77**, 2195-206.

Castello G., Scala S., Palmieri G., Curley S. A. and Izzo F. (2009) HCV-related hepatocellular carcinoma: From chronic inflammation to cancer. *Clin Immunol*.

Cavarretta I. T., Neuwirt H., Untergasser G., Moser P. L., Zaki M. H., Steiner H., Rumpold H., Fuchs D., Hobisch A., Nemeth J. A. and Culig Z. (2007) The antiapoptotic effect of IL-6 autocrine loop in a cellular model of advanced prostate cancer is mediated by Mcl-1. *Oncogene* **26**, 2822-32.

Chai J., Wu Q., Shiozaki E., Srinivasula S. M., Alnemri E. S. and Shi Y. (2001) Crystal structure of a procaspase-7 zymogen: mechanisms of activation and substrate binding. *Cell* **107**, 399-407.

Chamoux E., Houde N., L'Eriger K. and Roux S. (2008) Osteoprotegerin decreases human osteoclast apoptosis by inhibiting the TRAIL pathway. *J Cell Physiol* **216**, 536-42.

Chamulitrat W., Sattayakhom A., Herold-Mended C. and Stremmel W. (2009) Human papillomavirus 16 E6/E7-immortalized human gingival keratinocytes with epithelial mesenchymal transition acquire increased expression of cIAP-1, Bclx and p27(Kip1). *Exp Dermatol* **18**, 1067-9.

Chan F. K., Chun H. J., Zheng L., Siegel R. M., Bui K. L. and Lenardo M. J. (2000) A domain in TNF receptors that mediates ligand-independent receptor assembly and signaling. *Science* **288**, 2351-4.

Chan I. (2004) The role of extracellular matrix protein 1 in human skin. *Clin Exp Dermatol* **29**, 52-6.

Chang D. W., Xing Z., Pan Y., Algeciras-Schimnich A., Barnhart B. C., Yaish-Ohad S., Peter M. E. and Yang X. (2002) c-FLIP(L) is a dual function regulator for caspase-8 activation and CD95-mediated apoptosis. *EMBO J* **21**, 3704-14.

Chang T. C., Wentzel E. A., Kent O. A., Ramachandran K., Mullendore M., Lee K. H., Feldmann G., Yamakuchi M., Ferlito M., Lowenstein C. J., Arking D. E., Beer M. A., Maitra A. and Mendell J. T. (2007) Transactivation of miR-34a by p53 broadly influences gene expression and promotes apoptosis. *Mol Cell* **26**, 745-52.

Chauhan D., Kharbanda S., Ogata A., Urashima M., Teoh G., Robertson M., Kufe D. W. and Anderson K. C. (1997) Interleukin-6 inhibits Fas-induced apoptosis and stress-activated protein kinase activation in multiple myeloma cells. *Blood* **89**, 227-34.

Chen L., Willis S. N., Wei A., Smith B. J., Fletcher J. I., Hinds M. G., Colman P. M., Day C. L., Adams J. M. and Huang D. C. (2005) Differential targeting of prosurvival Bcl-2 proteins by their BH3-only ligands allows complementary apoptotic function. *Mol Cell* **17**, 393-403.

Clark R. A. (2010) Skin-resident T cells: the ups and downs of on site immunity. *J Invest Dermatol* **130**, 362-70.

Clem R. J. and Miller L. K. (1994) Control of programmed cell death by the baculovirus genes p35 and iap. *Mol Cell Biol* **14**, 5212-22.

Conrad M., Bubb V. J. and Schlegel R. (1993) The human papillomavirus type 6 and 16 E5 proteins are membrane-associated proteins which associate with the 16-kilodalton pore-forming protein. *J Virol* **67**, 6170-8.

Cordano P., Gillan V., Bratlie S., Bouvard V., Banks L., Tommasino M. and Campo M. S. (2008) The E6E7 oncoproteins of cutaneous human papillomavirus type 38 interfere with the interferon pathway. *Virology* **377**, 408-18.

Crusius K., Auvinen E. and Alonso A. (1997) Enhancement of EGF- and PMA-mediated MAP kinase activation in cells expressing the human papillomavirus type 16 E5 protein. *Oncogene* **15**, 1437-44.

Culp T. D., Budgeon L. R., Marinkovich M. P., Meneguzzi G. and Christensen N. D. (2006) Keratinocyte-secreted laminin 5 can function as a transient receptor for human papillomaviruses by binding virions and transferring them to adjacent cells. *J Virol* **80**, 8940-50.

Czegledy J., Evander M., Hernadi Z., Gergely L. and Wadell G. (1994) Human papillomavirus type 18 E6* mRNA in primary tumors and pelvic lymph nodes of Hungarian patients with squamous cervical cancer. *Int J Cancer* **56**, 182-6.

Daehn I. S., Varelias A. and Rayner T. E. (2009) T-lymphocyte-induced, fas-mediated apoptosis is associated with early keratinocyte differentiation. *Exp Dermatol*.

Daher A., Simbulan-Rosenthal C. M. and Rosenthal D. S. (2006) Apoptosis induced by ultraviolet B in HPV-immortalized human keratinocytes requires caspase-9 and is death receptor independent. *Exp Dermatol* **15**, 23-34.

Dang C., Koehler A., Forschner T., Sehr P., Michael K., Pawlita M., Stockfleth E. and Nindl I. (2006) E6/E7 expression of human papillomavirus types in cutaneous squamous cell dysplasia and carcinoma in immunosuppressed organ transplant recipients. *Br J Dermatol* **155**, 129-36.

Davy C. E., Jackson D. J., Raj K., Peh W. L., Southern S. A., Das P., Sorathia R., Laskey P., Middleton K., Nakahara T., Wang Q., Masterson P. J., Lambert P. F., Cuthill S., Millar J. B. and Doorbar J. (2005) Human papillomavirus type 16 E1 E4-induced G2 arrest is associated with cytoplasmic retention of active Cdk1/cyclin B1 complexes. *J Virol* **79**, 3998-4011.

Day P. M., Lowy D. R. and Schiller J. T. (2003) Papillomaviruses infect cells via a clathrin-dependent pathway. *Virology* **307**, 1-11.

De Andrea M., Mondini M., Azzimonti B., Dell'Oste V., Germano S., Gaudino G., Musso T., Landolfo S. and Gariglio M. (2007) Alpha- and betapapillomavirus E6/E7 genes differentially modulate pro-inflammatory gene expression. *Virus Res* **124**, 220-5.

de Gruijl F. R. and Rebel H. (2008) Early events in UV carcinogenesis--DNA damage, target cells and mutant p53 foci. *Photochem Photobiol* **84**, 382-7.

de Koning M., Quint W., Struijk L., Kleter B., Wanningen P., van Doorn L. J., Weissenborn S. J., Feltkamp M. and ter Schegget J. (2006) Evaluation of a novel highly sensitive, broad-spectrum PCR-reverse hybridization assay for detection and identification of beta-papillomavirus DNA. *J Clin Microbiol* **44**, 1792-800.

de Koning M. N., Struijk L., Bavinck J. N., Kleter B., ter Schegget J., Quint W. G. and Feltkamp M. C. (2007) Betapapillomaviruses frequently persist in the skin of healthy individuals. *J Gen Virol* **88**, 1489-95.

de Villiers E. M., Fauquet C., Broker T. R., Bernard H. U. and zur Hausen H. (2004) Classification of papillomaviruses. *Virology* **324**, 17-27.

de Villiers E. M., Lavergne D., McLaren K. and Benton E. C. (1997) Prevailing papillomavirus types in non-melanoma carcinomas of the skin in renal allograft recipients. *Int J Cancer* **73**, 356-61.

Degterev A., Boyce M. and Yuan J. (2003) A decade of caspases. *Oncogene* **22**, 8543-67.

Dell'Oste V., Azzimonti B., De Andrea M., Mondini M., Zavattaro E., Leigheb G., Weissenborn S. J., Pfister H., Michael K. M., Waterboer T., Pawlita M., Amantea A., Landolfo S. and Gariglio M. (2009) High beta-HPV DNA loads and strong seroreactivity are present in epidermodysplasia verruciformis. *J Invest Dermatol* **129**, 1026-34.

Dell'oste V., Azzimonti B., Mondini M., De Andrea M., Borgogna C., Mesturini R., Accardi R., Tommasino M., Landolfo S., Dianzani U. and Gariglio M. (2008) Altered expression of UVB-induced cytokines in human papillomavirus-immortalized epithelial cells. *J Gen Virol* **89**, 2461-6.

Deng W., Lin B. Y., Jin G., Wheeler C. G., Ma T., Harper J. W., Broker T. R. and Chow L. T. (2004) Cyclin/CDK regulates the nucleocytoplasmic localization of the human papillomavirus E1 DNA helicase. *J Virol* **78**, 13954-65.

Derocq J. M., Segui M., Poinot-Chazel C., Minty A., Caput D., Ferrara P. and Casellas P. (1994) Interleukin-13 stimulates interleukin-6 production by human keratinocytes. Similarity with interleukin-4. *FEBS Lett* **343**, 32-6.

Deveraux Q. L., Leo E., Stennicke H. R., Welsh K., Salvesen G. S. and Reed J. C. (1999) Cleavage of human inhibitor of apoptosis protein XIAP results in fragments with distinct specificities for caspases. *Embo J* **18**, 5242-51.

Dhawan P. and Richmond A. (2002) Role of CXCL1 in tumorigenesis of melanoma. *J Leukoc Biol* **72**, 9-18.

Dickson M. A., Hahn W. C., Ino Y., Ronfard V., Wu J. Y., Weinberg R. A., Louis D. N., Li F. P. and Rheinwald J. G. (2000) Human keratinocytes that express hTERT and also bypass a p16(INK4a)-enforced mechanism that limits life span become immortal yet retain normal growth and differentiation characteristics. *Mol Cell Biol* **20**, 1436-47.

Dieriks B., De Vos W. H., Derradji H., Baatout S. and Van Oostveldt P. (2010) Medium-mediated DNA repair response after ionizing radiation is correlated with the increase of specific cytokines in human fibroblasts. *Mutat Res*.

Domaszewska-Szostek A., Zaleska M. and Olszewski W. L. (2009) The influence of tissue fluid/lymph cytokines and growth factors on human keratinocyte proliferation and differentiation. *Transplant Proc* **41**, 3269-71.

Dong W., Arpin C., Accardi R., Gissmann L., Sylla B. S., Marvel J. and Tommasino M. (2008) Loss of p53 or p73 in human papillomavirus type 38 E6 and E7 transgenic

mice partially restores the UV-activated cell cycle checkpoints. *Oncogene* **27**, 2923-8.

Dong W., Kloz U., Accardi R., Caldeira S., Tong W. M., Wang Z. Q., Jansen L., Durst M., Sylla B. S., Gissmann L. and Tommasino M. (2005) Skin hyperproliferation and susceptibility to chemical carcinogenesis in transgenic mice expressing E6 and E7 of human papillomavirus type 38. *J Virol* **79**, 14899-908.

Doorbar J. (2006) Molecular biology of human papillomavirus infection and cervical cancer. *Clin Sci (Lond)* **110**, 525-41.

Doorbar J., Elston R. C., Napthine S., Raj K., Medcalf E., Jackson D., Coleman N., Griffin H. M., Masterson P., Stacey S., Mengistu Y. and Dunlop J. (2000) The E1E4 protein of human papillomavirus type 16 associates with a putative RNA helicase through sequences in its C terminus. *J Virol* **74**, 10081-95.

Doorbar J., Foo C., Coleman N., Medcalf L., Hartley O., Prospero T., Napthine S., Sterling J., Winter G. and Griffin H. (1997) Characterization of events during the late stages of HPV16 infection in vivo using high-affinity synthetic Fabs to E4. *Virology* **238**, 40-52.

Du C., Fang M., Li Y., Li L. and Wang X. (2000) Smac, a mitochondrial protein that promotes cytochrome c-dependent caspase activation by eliminating IAP inhibition. *Cell* **102**, 33-42.

Du J., Chen G. G., Vlantis A. C., Chan P. K., Tsang R. K. and van Hasselt C. A. (2004) Resistance to apoptosis of HPV 16-infected laryngeal cancer cells is associated with decreased Bak and increased Bcl-2 expression. *Cancer Lett* **205**, 81-8.

Duensing S., Lee L. Y., Duensing A., Basile J., Piboonniyom S., Gonzalez S., Crum C. P. and Munger K. (2000) The human papillomavirus type 16 E6 and E7 oncoproteins cooperate to induce mitotic defects and genomic instability by uncoupling centrosome duplication from the cell division cycle. *Proc Natl Acad Sci U S A* **97**, 10002-7.

Duffy C. L., Phillips S. L. and Klingelhutz A. J. (2003) Microarray analysis identifies differentiation-associated genes regulated by human papillomavirus type 16 E6. *Virology* **314**, 196-205.

Durai R., Davies M., Yang W., Yang S. Y., Seifalian A., Goldspink G. and Winslet M. (2006) Biology of insulin-like growth factor binding protein-4 and its role in cancer (review). *Int J Oncol* **28**, 1317-25.

Ea C. K., Deng L., Xia Z. P., Pineda G. and Chen Z. J. (2006) Activation of IKK by TNFalpha requires site-specific ubiquitination of RIP1 and polyubiquitin binding by NEMO. *Mol Cell* **22**, 245-57.

Eberstadt M., Huang B., Chen Z., Meadows R. P., Ng S. C., Zheng L., Lenardo M. J. and Fesik S. W. (1998) NMR structure and mutagenesis of the FADD (Mort1) death-effector domain. *Nature* **392**, 941-5.

Eckelman B. P. and Salvesen G. S. (2006) The human anti-apoptotic proteins cIAP1 and cIAP2 bind but do not inhibit caspases. *J Biol Chem* **281**, 3254-60.

Edinger A. L. and Thompson C. B. (2004) Death by design: apoptosis, necrosis and autophagy. *Curr Opin Cell Biol* **16**, 663-9.

Egawa K. (2003) Do human papillomaviruses target epidermal stem cells? *Dermatology* **207**, 251-4.

Elias P. M. (1983) Epidermal lipids, barrier function, and desquamation. *J Invest Dermatol* **80 Suppl**, 44s-49s.

Elias P. M. (2005) Stratum corneum defensive functions: an integrated view. *J Invest Dermatol* **125**, 183-200.

Erb P., Ji J., Kump E., Mielgo A. and Wernli M. (2008) Apoptosis and pathogenesis of melanoma and nonmelanoma skin cancer. *Adv Exp Med Biol* **624**, 283-95.

Evander M., Frazer I. H., Payne E., Qi Y. M., Hengst K. and McMillan N. A. (1997) Identification of the alpha6 integrin as a candidate receptor for papillomaviruses. *J Virol* **71**, 2449-56.

Fadeel B. and Orrenius S. (2005) Apoptosis: a basic biological phenomenon with wide-ranging implications in human disease. *J Intern Med* **258**, 479-517.

Falschlehner C., Emmerich C. H., Gerlach B. and Walczak H. (2007) TRAIL signalling: decisions between life and death. *Int J Biochem Cell Biol* **39**, 1462-75.

Farley S. M., Dotson A. D., Purdy D. E., Sundholm A. J., Schneider P., Magun B. E. and Iordanov M. S. (2006) Fas ligand elicits a caspase-independent proinflammatory response in human keratinocytes: implications for dermatitis. *J Invest Dermatol* **126**, 2438-51.

Fehrmann F., Klumpp D. J. and Laimins L. A. (2003) Human papillomavirus type 31 E5 protein supports cell cycle progression and activates late viral functions upon epithelial differentiation. *J Virol* **77**, 2819-31.

Filipowicz E., Adegboyega P., Sanchez R. L. and Gatalica Z. (2002) Expression of CD95 (Fas) in sun-exposed human skin and cutaneous carcinomas. *Cancer* **94**, 814-9.

Filippova M., Johnson M. M., Bautista M., Filippov V., Fodor N., Tungteakkhun S. S., Williams K. and Duerksen-Hughes P. J. (2007) The Large And Small Isoforms Of Hpv 16 E6 Bind To And Differentially Affect Procaspase 8 Stability And Activity. *J Virol*.

Filippova M., Parkhurst L. and Duerksen-Hughes P. J. (2004) The human papillomavirus 16 E6 protein binds to Fas-associated death domain and protects cells from Fas-triggered apoptosis. *J Biol Chem* **279**, 25729-44.

Filippova M., Song H., Connolly J. L., Dermody T. S. and Duerksen-Hughes P. J. (2002) The human papillomavirus 16 E6 protein binds to tumor necrosis factor (TNF) R1 and protects cells from TNF-induced apoptosis. *J Biol Chem* **277**, 21730-9.

Florin L., Sapp C., Streeck R. E. and Sapp M. (2002) Assembly and translocation of papillomavirus capsid proteins. *J Virol* **76**, 10009-14.

Forslund O., Iftner T., Andersson K., Lindelof B., Hradil E., Nordin P., Stenquist B., Kirnbauer R., Dillner J. and de Villiers E. M. (2007) Cutaneous human papillomaviruses found in sun-exposed skin: Beta-papillomavirus species 2 predominates in squamous cell carcinoma. *J Infect Dis* **196**, 876-83.

Fuchs B. C. and Bode B. P. (2006) Stressing out over survival: glutamine as an apoptotic modulator. *J Surg Res* **131**, 26-40.

Fujii T., Masumoto N., Saito M., Hirao N., Niimi S., Mukai M., Ono A., Hayashi S., Kubushiro K., Sakai E., Tsukazaki K. and Nozawa S. (2005) Comparison between in situ hybridization and real-time PCR technique as a means of detecting the integrated form of human papillomavirus 16 in cervical neoplasia. *Diagn Mol Pathol* **14**, 103-8.

Fujita K. and Srinivasula S. M. (2009) Ubiquitination and TNFR1 signaling. *Results Probl Cell Differ* **49**, 87-114.

Funk J. O., Waga S., Harry J. B., Espling E., Stillman B. and Galloway D. A. (1997) Inhibition of CDK activity and PCNA-dependent DNA replication by p21 is blocked by interaction with the HPV-16 E7 oncoprotein. *Genes Dev* **11**, 2090-100.

Furniss C. S., McClean M. D., Smith J. F., Bryan J., Nelson H. H., Peters E. S., Posner M. R., Clark J. R., Eisen E. A. and Kelsey K. T. (2007) Human papillomavirus 16 and head and neck squamous cell carcinoma. *Int J Cancer* **120**, 2386-92.

Gailani M. R., Stahle-Backdahl M., Leffell D. J., Glynn M., Zaphiropoulos P. G., Pressman C., Unden A. B., Dean M., Brash D. E., Bale A. E. and Toftgard R. (1996) The role of the human homologue of Drosophila patched in sporadic basal cell carcinomas. *Nat Genet* **14**, 78-81.

Garinis G. A., Mitchell J. R., Moorhouse M. J., Hanada K., de Waard H., Vandeputte D., Jans J., Brand K., Smid M., van der Spek P. J., Hoeijmakers J. H., Kanaar R. and van der Horst G. T. (2005) Transcriptome analysis reveals cyclobutane pyrimidine dimers as a major source of UV-induced DNA breaks. *EMBO J* **24**, 3952-62.

Garner-Hamrick P. A., Fostel J. M., Chien W. M., Banerjee N. S., Chow L. T., Broker T. R. and Fisher C. (2004) Global effects of human papillomavirus type 18 E6/E7 in an organotypic keratinocyte culture system. *J Virol* **78**, 9041-50.

Garnett T. O., Filippova M. and Duerksen-Hughes P. J. (2006) Accelerated degradation of FADD and procaspase 8 in cells expressing human papilloma virus 16 E6 impairs TRAIL-mediated apoptosis. *Cell Death Differ* **13**, 1915-26.

Geiser T., Dewald B., Ehrengruber M. U., Clark-Lewis I. and Baggiolini M. (1993) The interleukin-8-related chemotactic cytokines GRO alpha, GRO beta, and GRO gamma activate human neutrophil and basophil leukocytes. *J Biol Chem* **268**, 15419-24.

Ghittoni R., Accardi R., Hasan U., Gheit T., Sylla B. and Tommasino M. (2010) The biological properties of E6 and E7 oncoproteins from human papillomaviruses. *Virus Genes* **40**, 1-13.

Ghoreishi M. and Dutz J. P. (2006) Tolerance induction by transcutaneous immunization through ultraviolet-irradiated skin is transferable through CD4+CD25+ T regulatory cells and is dependent on host-derived IL-10. *J Immunol* **176**, 2635-44.

Giampieri S., Garcia-Escudero R., Green J. and Storey A. (2004) Human papillomavirus type 77 E6 protein selectively inhibits p53-dependent transcription of proapoptotic genes following UV-B irradiation. *Oncogene* **23**, 5864-70.

Giampieri S. and Storey A. (2004) Repair of UV-induced thymine dimers is compromised in cells expressing the E6 protein from human papillomaviruses types 5 and 18. *Br J Cancer* **90**, 2203-9.

Giglia-Mari G. and Sarasin A. (2003) TP53 mutations in human skin cancers. *Hum Mutat* **21**, 217-28.

Girardi M. (2007) Cutaneous perspectives on adaptive immunity. *Clin Rev Allergy Immunol* **33**, 4-14.

Gissmann L., Boshart M., Durst M., Ikenberg H., Wagner D. and zur Hausen H. (1984) Presence of human papillomavirus in genital tumors. *J Invest Dermatol* **83**, 26s-28s.

Goodwin E. C. and DiMaio D. (2000) Repression of human papillomavirus oncogenes in HeLa cervical carcinoma cells causes the orderly reactivation of dormant tumor suppressor pathways. *Proc Natl Acad Sci U S A* **97**, 12513-8.

Griffiths A., Miller J., Suzuki D., Lewontin R. and Gelbart W. (2000) Mechanisms of gene mutation. *In 'An Introduction to Genetic Analysis', WH Freeman, New York* **Chapter 16**.

Griffiths G. J., Dubrez L., Morgan C. P., Jones N. A., Whitehouse J., Corfe B. M., Dive C. and Hickman J. A. (1999) Cell damage-induced conformational changes of the pro-apoptotic protein Bak in vivo precede the onset of apoptosis. *J Cell Biol* **144**, 903-14.

Grone A. (2002) Keratinocytes and cytokines. *Vet Immunol Immunopathol* **88**, 1-12.

Grossman R. M., Krueger J., Yourish D., Granelli-Piperno A., Murphy D. P., May L. T., Kupper T. S., Sehgal P. B. and Gottlieb A. B. (1989) Interleukin 6 is expressed in high levels in psoriatic skin and stimulates proliferation of cultured human keratinocytes. *Proc Natl Acad Sci U S A* **86**, 6367-71.

Guicciardi M. E. and Gores G. J. (2009) Life and death by death receptors. *FASEB J* **23**, 1625-37.

Hadaschik D., Hinterkeuser K., Oldak M., Pfister H. J. and Smola-Hess S. (2003) The Papillomavirus E2 protein binds to and synergizes with C/EBP factors involved in keratinocyte differentiation. *J Virol* **77**, 5253-65.

Hamid N. A., Brown C. and Gaston K. (2009) The regulation of cell proliferation by the papillomavirus early proteins. *Cell Mol Life Sci* **66**, 1700-17.

Han G. W., Iwatsuki K., Inoue M., Matsui T., Nishibu A., Akiba H. and Kaneko F. (1999) Interleukin-15 is not a constitutive cytokine in the epidermis, but is inducible in culture or inflammatory conditions. *Acta Derm Venereol* **79**, 37-40.

Harwood C. A., Spink P. J., Surentheran T., Leigh I. M., de Villiers E. M., McGregor J. M., Proby C. M. and Breuer J. (1999) Degenerate and nested PCR: a highly sensitive and specific method for detection of human papillomavirus infection in cutaneous warts. *J Clin Microbiol* **37**, 3545-55.

Harwood C. A., Surentheran T., McGregor J. M., Spink P. J., Leigh I. M., Breuer J. and Proby C. M. (2000) Human papillomavirus infection and non-melanoma skin cancer in immunosuppressed and immunocompetent individuals. *J Med Virol* **61**, 289-97.

Harwood C. A., Surentheran T., Sasieni P., Proby C. M., Bordea C., Leigh I. M., Wojnarowska F., Breuer J. and McGregor J. M. (2004) Increased risk of skin cancer associated with the presence of epidermodysplasia verruciformis human papillomavirus types in normal skin. *Br J Dermatol* **150**, 949-57.

Hasan U. A., Bates E., Takeshita F., Biliato A., Accardi R., Bouvard V., Mansour M., Vincent I., Gissmann L., Iftner T., Sideri M., Stubenrauch F. and Tommasino M. (2007) TLR9 expression and function is abolished by the cervical cancer-associated human papillomavirus type 16. *J Immunol* **178**, 3186-97.

Hatzivassiliou G., Zhao F., Bauer D. E., Andreadis C., Shaw A. N., Dhanak D., Hingorani S. R., Tuveson D. A. and Thompson C. B. (2005) ATP citrate lyase inhibition can suppress tumor cell growth. *Cancer Cell* **8**, 311-21.

Hazard K., Karlsson A., Andersson K., Ekberg H., Dillner J. and Forslund O. (2007) Cutaneous human papillomaviruses persist on healthy skin. *J Invest Dermatol* **127**, 116-9.

Hebner C. M. and Laimins L. A. (2006) Human papillomaviruses: basic mechanisms of pathogenesis and oncogenicity. *Rev Med Virol* **16**, 83-97.

Hengge U. R. (2008) Role of viruses in the development of squamous cell cancer and melanoma. *Adv Exp Med Biol* **624**, 179-86.

Hill L. L., Ouhtit A., Loughlin S. M., Kripke M. L., Ananthaswamy H. N. and Owen-Schaub L. B. (1999) Fas ligand: a sensor for DNA damage critical in skin cancer etiology. *Science* **285**, 898-900.

Hodge D. R., Hurt E. M. and Farrar W. L. (2005) The role of IL-6 and STAT3 in inflammation and cancer. *Eur J Cancer* **41**, 2502-12.

Holmgren S. C., Patterson N. A., Ozbun M. A. and Lambert P. F. (2005) The minor capsid protein L2 contributes to two steps in the human papillomavirus type 31 life cycle. *J Virol* **79**, 3938-48.

Hopfl R., Heim K., Christensen N., Zumbach K., Wieland U., Volgger B., Widschwendter A., Haimbuchner S., Muller-Holzner E., Pawlita M., Pfister H. and Fritsch P. (2000) Spontaneous regression of CIN and delayed-type hypersensitivity to HPV-16 oncoprotein E7. *Lancet* **356**, 1985-6.

Hougardy B. M., van der Zee A. G., van den Heuvel F. A., Timmer T., de Vries E. G. and de Jong S. (2005) Sensitivity to Fas-mediated apoptosis in high-risk HPV-positive human cervical cancer cells: relationship with Fas, caspase-8, and Bid. *Gynecol Oncol* **97**, 353-64.

Howie H. L., Katzenellenbogen R. A. and Galloway D. A. (2009) Papillomavirus E6 proteins. *Virology* **384**, 324-34.

Hsu H., Xiong J. and Goeddel D. V. (1995) The TNF receptor 1-associated protein TRADD signals cell death and NF-kappa B activation. *Cell* **81**, 495-504.

Huang H., Joazeiro C. A., Bonfoco E., Kamada S., Leverson J. D. and Hunter T. (2000) The inhibitor of apoptosis, cIAP2, functions as a ubiquitin-protein ligase and promotes in vitro monoubiquitination of caspases 3 and 7. *J Biol Chem* **275**, 26661-4.

Hubbert N. L., Sedman S. A. and Schiller J. T. (1992) Human papillomavirus type 16 E6 increases the degradation rate of p53 in human keratinocytes. *J Virol* **66**, 6237-41.

Huen M. S., Sy S. M. and Chen J. (2010) BRCA1 and its toolbox for the maintenance of genome integrity. *Nat Rev Mol Cell Biol* **11**, 138-48.

Hughes F. J. and Romanos M. A. (1993) E1 protein of human papillomavirus is a DNA helicase/ATPase. *Nucleic Acids Res* **21**, 5817-23.

Huibregtse J. M., Scheffner M. and Howley P. M. (1993) Cloning and expression of the cDNA for E6-AP, a protein that mediates the interaction of the human papillomavirus E6 oncoprotein with p53. *Mol Cell Biol* **13**, 775-84.

Hussein M. R. (2005) Ultraviolet radiation and skin cancer: molecular mechanisms. *J Cutan Pathol* **32**, 191-205.

Iftner T., Elbel M., Schopp B., Hiller T., Loizou J. I., Caldecott K. W. and Stubenrauch F. (2002) Interference of papillomavirus E6 protein with single-strand break repair by interaction with XRCC1. *Embo J* **21**, 4741-8.

Irmler M., Thome M., Hahne M., Schneider P., Hofmann K., Steiner V., Bodmer J. L., Schroter M., Burns K., Mattmann C., Rimoldi D., French L. E. and Tschopp J. (1997) Inhibition of death receptor signals by cellular FLIP. *Nature* **388**, 190-5.

Itoh N. and Nagata S. (1993) A novel protein domain required for apoptosis. Mutational analysis of human Fas antigen. *J Biol Chem* **268**, 10932-7.

Jaattela M., Wissing D., Kokholm K., Kallunki T. and Egeblad M. (1998) Hsp70 exerts its anti-apoptotic function downstream of caspase-3-like proteases. *Embo J* **17**, 6124-34.

Jackson S., Ghali L., Harwood C. and Storey A. (2002) Reduced apoptotic levels in squamous but not basal cell carcinomas correlates with detection of cutaneous human papillomavirus. *Br J Cancer* **87**, 319-23.

Jackson S., Harwood C., Thomas M., Banks L. and Storey A. (2000) Role of Bak in UV-induced apoptosis in skin cancer and abrogation by HPV E6 proteins. *Genes Dev* **14**, 3065-73.

Jackson S. and Storey A. (2000) E6 proteins from diverse cutaneous HPV types inhibit apoptosis in response to UV damage. *Oncogene* **19**, 592-8.

James M. A., Lee J. H. and Klingelhutz A. J. (2006) Human papillomavirus type 16 E6 activates NF-kappaB, induces cIAP-2 expression, and protects against apoptosis in a PDZ binding motif-dependent manner. *J Virol* **80**, 5301-7.

Jans J., Garinis G. A., Schul W., van Oudenaren A., Moorhouse M., Smid M., Sert Y. G., van der Velde A., Rijksen Y., de Gruijl F. R., van der Spek P. J., Yasui A., Hoeijmakers J. H., Leenen P. J. and van der Horst G. T. (2006) Differential role of basal keratinocytes in UV-induced immunosuppression and skin cancer. *Mol Cell Biol* **26**, 8515-26.

Jin Z. and El-Deiry W. S. (2005) Overview of cell death signaling pathways. *Cancer Biol Ther* **4**, 139-63.

Jonak C., Klosner G. and Trautinger F. (2006) Heat shock proteins in the skin. *Int J Cosmet Sci* **28**, 233-41.

Jonason A. S., Kunala S., Price G. J., Restifo R. J., Spinelli H. M., Persing J. A., Leffell D. J., Tarone R. E. and Brash D. E. (1996) Frequent clones of p53-mutated keratinocytes in normal human skin. *Proc Natl Acad Sci U S A* **93**, 14025-9.

Jonsson M., Engstrom M. and Jonsson J. I. (2004) FLT3 ligand regulates apoptosis through AKT-dependent inactivation of transcription factor FoxO3. *Biochem Biophys Res Commun* **318**, 899-903.

Kabsch K. and Alonso A. (2002) The human papillomavirus type 16 E5 protein impairs TRAIL- and FasL-mediated apoptosis in HaCaT cells by different mechanisms. *J Virol* **76**, 12162-72.

Kabsch K., Mossadegh N., Kohl A., Komposch G., Schenkel J., Alonso A. and Tomakidi P. (2004) The HPV-16 E5 protein inhibits TRAIL- and FasL-mediated apoptosis in human keratinocyte raft cultures. *Intervirology* **47**, 48-56.

Kanda M., Nomoto S., Okamura Y., Nishikawa Y., Sugimoto H., Kanazumi N., Takeda S. and Nakao A. (2009) Detection of metallothionein 1G as a methylated tumor suppressor gene in human hepatocellular carcinoma using a novel method of double combination array analysis. *Int J Oncol* **35**, 477-83.

Karagas M. R., Nelson H. H., Sehr P., Waterboer T., Stukel T. A., Andrew A., Green A. C., Bavinck J. N., Perry A., Spencer S., Rees J. R., Mott L. A. and Pawlita M. (2006) Human papillomavirus infection and incidence of squamous cell and basal cell carcinomas of the skin. *J Natl Cancer Inst* **98**, 389-95.

Katzenellenbogen R. A., Egelkrout E. M., Vliet-Gregg P., Gewin L. C., Gafken P. R. and Galloway D. A. (2007) NFX1-123 and poly(A) binding proteins synergistically augment activation of telomerase in human papillomavirus type 16 E6-expressing cells. *J Virol* **81**, 3786-96.

Kerr J. F., Wyllie A. H. and Currie A. R. (1972) Apoptosis: a basic biological phenomenon with wide-ranging implications in tissue kinetics. *Br J Cancer* **26**, 239-57.

Kim D. J., Kataoka K., Sano S., Connolly K., Kiguchi K. and DiGiovanni J. (2009) Targeted disruption of Bcl-xL in mouse keratinocytes inhibits both UVB- and chemically induced skin carcinogenesis. *Mol Carcinog* **48**, 873-85.

Kischkel F. C., Hellbardt S., Behrmann I., Germer M., Pawlita M., Krammer P. H. and Peter M. E. (1995) Cytotoxicity-dependent APO-1 (Fas/CD95)-associated proteins form a death-inducing signaling complex (DISC) with the receptor. *EMBO J* **14**, 5579-88.

Klumpp D. J. and Laimins L. A. (1999) Differentiation-induced changes in promoter usage for transcripts encoding the human papillomavirus type 31 replication protein E1. *Virology* **257**, 239-46.

Knight G. L., Grainger J. R., Gallimore P. H. and Roberts S. (2004) Cooperation between different forms of the human papillomavirus type 1 E4 protein to block cell cycle progression and cellular DNA synthesis. *J Virol* **78**, 13920-33.

Konur A., Schulz U., Eissner G., Andreesen R. and Holler E. (2005) Interferon (IFN)-γ is a main mediator of keratinocyte (HaCaT) apoptosis and contributes to autocrine IFN-γ and tumour necrosis factor-α production. *British Journal of Dermatology* **152**, 1134-1142.

Kothakota S., Azuma T., Reinhard C., Klippel A., Tang J., Chu K., McGarry T. J., Kirschner M. W., Koths K., Kwiatkowski D. J. and Williams L. T. (1997) Caspase-3-generated fragment of gelsolin: effector of morphological change in apoptosis. *Science* **278**, 294-8.

Kothny-Wilkes G., Kulms D., Poppelmann B., Luger T. A., Kubin M. and Schwarz T. (1998) Interleukin-1 protects transformed keratinocytes from tumor necrosis factor-related apoptosis-inducing ligand. *J Biol Chem* **273**, 29247-53.

Koutsky L. (1997) Epidemiology of genital human papillomavirus infection. *Am J Med* **102**, 3-8.

Krammer P. H. (2000) CD95's deadly mission in the immune system. *Nature* **407**, 789-95.

Kreuz S., Siegmund D., Rumpf J. J., Samel D., Leverkus M., Janssen O., Hacker G., Dittrich-Breiholz O., Kracht M., Scheurich P. and Wajant H. (2004) NFkappaB activation by Fas is mediated through FADD, caspase-8, and RIP and is inhibited by FLIP. *J Cell Biol* **166**, 369-80.

Kuchel J. M., Barnetson R. S. and Halliday G. M. (2005) Cyclobutane pyrimidine dimer formation is a molecular trigger for solar-simulated ultraviolet radiation-induced suppression of memory immunity in humans. *Photochem Photobiol Sci* **4**, 577-82.

Kupper T. S., Chua A. O., Flood P., McGuire J. and Gubler U. (1987) Interleukin 1 gene expression in cultured human keratinocytes is augmented by ultraviolet irradiation. *J Clin Invest* **80**, 430-6.

Kuribayashi K., Krigsfeld G., Wang W., Xu J., Mayes P. A., Dicker D. T., Wu G. S. and El-Deiry W. S. (2008) TNFSF10 (TRAIL), a p53 target gene that mediates p53-dependent cell death. *Cancer Biol Ther* **7**, 2034-8.

Laffort C., Le Deist F., Favre M., Caillat-Zucman S., Radford-Weiss I., Debre M., Fraitag S., Blanche S., Cavazzana-Calvo M., de Saint Basile G., de Villartay J. P., Giliani S., Orth G., Casanova J. L., Bodemer C. and Fischer A. (2004) Severe cutaneous papillomavirus disease after haemopoietic stem-cell transplantation in patients with severe combined immune deficiency caused by common gammac cytokine receptor subunit or JAK-3 deficiency. *Lancet* **363**, 2051-4.

Latonen L. and Laiho M. (2005) Cellular UV damage responses--functions of tumor suppressor p53. *Biochim Biophys Acta* **1755**, 71-89.

Lautrette C., Loum-Ribot E., Petit D., Vermot-Desroches C., Wijdenes J. and Jauberteau M. O. (2006) Increase of Fas-induced apoptosis by inhibition of extracellular phosphorylation of Fas receptor in Jurkat cell line. *Apoptosis* **11**, 1195-204.

Lavin M. F. and Gueven N. (2006) The complexity of p53 stabilization and activation. *Cell Death Differ* **13**, 941-50.

Lazarczyk M., Cassonnet P., Pons C., Jacob Y. and Favre M. (2009) The EVER proteins as a natural barrier against papillomaviruses: a new insight into the pathogenesis of human papillomavirus infections. *Microbiol Mol Biol Rev* **73**, 348-70.

Lazarczyk M., Pons C., Mendoza J. A., Cassonnet P., Jacob Y. and Favre M. (2008) Regulation of cellular zinc balance as a potential mechanism of EVER-mediated protection against pathogenesis by cutaneous oncogenic human papillomaviruses. *J Exp Med* **205**, 35-42.

Lazebnik Y. A., Kaufmann S. H., Desnoyers S., Poirier G. G. and Earnshaw W. C. (1994) Cleavage of poly(ADP-ribose) polymerase by a proteinase with properties like ICE. *Nature* **371**, 346-7.

Lechner M. S. and Laimins L. A. (1994) Inhibition of p53 DNA binding by human papillomavirus E6 proteins. *J Virol* **68**, 4262-73.

Lee J. H., Kye K. C., Seo E. Y., Lee K., Lee S. K., Lim J. S., Seo Y. J., Kim C. D. and Park J. K. (2008) Expression of neutrophil gelatinase-associated lipocalin in calcium-induced keratinocyte differentiation. *J Korean Med Sci* **23**, 302-6.

Lee K. H., Feig C., Tchikov V., Schickel R., Hallas C., Schutze S., Peter M. E. and Chan A. C. (2006) The role of receptor internalization in CD95 signaling. *EMBO J* **25**, 1009-23.

Lessene G., Czabotar P. E. and Colman P. M. (2008) BCL-2 family antagonists for cancer therapy. *Nat Rev Drug Discov* **7**, 989-1000.

Letai A., Bassik M. C., Walensky L. D., Sorcinelli M. D., Weiler S. and Korsmeyer S. J. (2002) Distinct BH3 domains either sensitize or activate mitochondrial apoptosis, serving as prototype cancer therapeutics. *Cancer Cell* **2**, 183-92.

Leu J. I., Dumont P., Hafey M., Murphy M. E. and George D. L. (2004) Mitochondrial p53 activates Bak and causes disruption of a Bak-Mcl1 complex. *Nat Cell Biol* **6**, 443-50.

Leverkus M., Sprick M. R., Wachter T., Mengling T., Baumann B., Serfling E., Brocker E. B., Goebeler M., Neumann M. and Walczak H. (2003) Proteasome inhibition results in TRAIL sensitization of primary keratinocytes by removing the resistance-mediating block of effector caspase maturation. *Mol Cell Biol* **23**, 777-90.

Leverkus M., Yaar M. and Gilchrest B. A. (1997) Fas/Fas ligand interaction contributes to UV-induced apoptosis in human keratinocytes. *Exp Cell Res* **232**, 255-62.

Leverrier S., Bergamaschi D., Ghali L., Ola A., Warnes G., Akgul B., Blight K., Garcia-Escudero R., Penna A., Eddaoudi A. and Storey A. (2007) Role of HPV E6 proteins in preventing UVB-induced release of pro-apoptotic factors from the mitochondria. *Apoptosis* **12**, 549-60.

Li D., Turi T. G., Schuck A., Freedberg I. M., Khitrov G. and Blumenberg M. (2001a) Rays and arrays: the transcriptional program in the response of human epidermal keratinocytes to UVB illumination. *Faseb J* **15**, 2533-5.

Li H., Zhu H., Xu C. J. and Yuan J. (1998) Cleavage of BID by caspase 8 mediates the mitochondrial damage in the Fas pathway of apoptosis. *Cell* **94**, 491-501.

Li L. Y., Luo X. and Wang X. (2001b) Endonuclease G is an apoptotic DNase when released from mitochondria. *Nature* **412**, 95-9.

Li P., Nijhawan D., Budihardjo I., Srinivasula S. M., Ahmad M., Alnemri E. S. and Wang X. (1997) Cytochrome c and dATP-dependent formation of Apaf-1/caspase-9 complex initiates an apoptotic protease cascade. *Cell* **91**, 479-89.

Lin Y., Devin A., Rodriguez Y. and Liu Z. G. (1999) Cleavage of the death domain kinase RIP by caspase-8 prompts TNF-induced apoptosis. *Genes Dev* **13**, 2514-26.

Lippens S., Denecker G., Ovaere P., Vandenabeele P. and Declercq W. (2005) Death penalty for keratinocytes: apoptosis versus cornification. *Cell Death Differ* **12 Suppl 2**, 1497-508.

Liu X., Dakic A., Zhang Y., Dai Y., Chen R. and Schlegel R. (2009) HPV E6 protein interacts physically and functionally with the cellular telomerase complex. *Proc Natl Acad Sci U S A* **106**, 18780-5.

Liu X., Kim C. N., Yang J., Jemmerson R. and Wang X. (1996) Induction of apoptotic program in cell-free extracts: requirement for dATP and cytochrome c. *Cell* **86**, 147-57.

Liu X., Yuan H., Fu B., Disbrow G. L., Apolinario T., Tomaic V., Kelley M. L., Baker C. C., Huibregtse J. and Schlegel R. (2005) The E6AP ubiquitin ligase is required for transactivation of the hTERT promoter by the human papillomavirus E6 oncoprotein. *J Biol Chem* **280**, 10807-16.

Longworth M. S. and Laimins L. A. (2004a) The binding of histone deacetylases and the integrity of zinc finger-like motifs of the E7 protein are essential for the life cycle of human papillomavirus type 31. *J Virol* **78**, 3533-41.

Longworth M. S. and Laimins L. A. (2004b) Pathogenesis of human papillomaviruses in differentiating epithelia. *Microbiol Mol Biol Rev* **68**, 362-72.

Lorenz K., Rupf T., Salvetter J. and Bader A. (2009) Enrichment of human beta 1 bri/alpha 6 bri/CD71 dim keratinocytes after culture in defined media. *Cells Tissues Organs* **189**, 382-90.

Mace P. D., Shirley S. and Day C. L. (2010) Assembling the building blocks: structure and function of inhibitor of apoptosis proteins. *Cell Death Differ* **17**, 46-53.

Mackenzie I. C. (1997) Retroviral transduction of murine epidermal stem cells demonstrates clonal units of epidermal structure. *J Invest Dermatol* **109**, 377-83.

Majewski S. and Jablonska S. (1995) Epidermodysplasia verruciformis as a model of human papillomavirus-induced genetic cancer of the skin. *Arch Dermatol* **131**, 1312-8.

Malkin D., Li F. P., Strong L. C., Fraumeni J. F., Jr., Nelson C. E., Kim D. H., Kassel J., Gryka M. A., Bischoff F. Z., Tainsky M. A. and et al. (1990) Germ line p53 mutations in a familial syndrome of breast cancer, sarcomas, and other neoplasms. *Science* **250**, 1233-8.

Malumbres M. and Barbacid M. (2009) Cell cycle, CDKs and cancer: a changing paradigm. *Nat Rev Cancer* **9**, 153-66.

Mandery K., Bujok K., Schmidt I., Wex T., Treiber G., Malfertheiner P., Rau T. T., Amann K. U., Brune K., Fromm M. F. and Glaeser H. (2010) Influence of cyclooxygenase inhibitors on the function of the prostaglandin transporter organic anion-transporting polypeptide 2A1 expressed in human gastroduodenal mucosa. *J Pharmacol Exp Ther* **332**, 345-51.

Mansour M., Touka M., Malena A., Indiveri C., Dong W., Gionfriddo I., Accardi R., Paradiso A., Sylla B. S., Gabet A. S. and Tommasino M. (2006) Human papillomavirus type 77 E7 protein is a weak deregulator of cell cycle. *Cancer Lett*.

Mantovani F. and Banks L. (2001) The human papillomavirus E6 protein and its contribution to malignant progression. *Oncogene* **20**, 7874-87.

Marconi A., Dallaglio K., Lotti R., Vaschieri C., Truzzi F., Fantini F. and Pincelli C. (2007) Survivin identifies keratinocyte stem cells and is downregulated by anti-beta1 integrin during anoikis. *Stem Cells* **25**, 149-55.

Masini C., Fuchs P. G., Gabrielli F., Stark S., Sera F., Ploner M., Melchi C. F., Primavera G., Pirchio G., Picconi O., Petasecca P., Cattaruzza M. S., Pfister H. J. and Abeni D. (2003) Evidence for the association of human papillomavirus infection and cutaneous squamous cell carcinoma in immunocompetent individuals. *Arch Dermatol* **139**, 890-4.

Massimi P., Shai A., Lambert P. and Banks L. (2008a) HPV E6 degradation of p53 and PDZ containing substrates in an E6AP null background. *Oncogene* **27**, 1800-4.

Massimi P., Thomas M., Bouvard V., Ruberto I., Campo M. S., Tommasino M. and Banks L. (2008b) Comparative transforming potential of different human papillomaviruses associated with non-melanoma skin cancer. *Virology* **371**, 374-9.

Matsuda M., Hoshino T., Yamashita Y., Tanaka K. I., Maji D., Sato K., Adachi H., Sobue G., Ihn H., Funasaka Y. and Mizushima T. (2009) Prevention of ultraviolet B radiation-induced epidermal damage by expression of heat shock protein 70. *J Biol Chem*.

Matsue H., Kobayashi H., Hosokawa T. and Akitaya T. (1995) Keratinocytes constitutively express the Fas antigen that mediates apoptosis in IFNγ treated cultured keratinocytes. *Archives Dermatological Research* **287**, 315-320.

McLaughlin-Drubin M. E. and Munger K. (2009) The human papillomavirus E7 oncoprotein. *Virology* **384**, 335-44.

McLoone P., Simics E., Barton A., Norval M. and Gibbs N. K. (2005) An action spectrum for the production of cis-urocanic acid in human skin in vivo. *J Invest Dermatol* **124**, 1071-4.

Meager A., Visvalingam K., Dilger P., Bryan D. and Wadhwa M. (2005) Biological activity of interleukins-28 and -29: comparison with type I interferons. *Cytokine* **31**, 109-18.

Meier P., Finch A. and Evan G. (2000) Apoptosis in development. *Nature* **407**, 796-801.

Menendez D., Inga A. and Resnick M. A. (2009) The expanding universe of p53 targets. *Nat Rev Cancer* **9**, 724-37.

Merkley M. A., Hildebrandt E., Podolsky R. H., Arnouk H., Ferris D. G., Dynan W. S. and Stoppler H. (2009) Large-scale analysis of protein expression changes in human keratinocytes immortalized by human papilloma virus type 16 E6 and E7 oncogenes. *Proteome Sci* **7**, 29.

Metz M. and Maurer M. (2009) Innate immunity and allergy in the skin. *Curr Opin Immunol* **21**, 687-93.

Meylan E. and Tschopp J. (2005) The RIP kinases: crucial integrators of cellular stress. *Trends Biochem Sci* **30**, 151-9.

Micheau O. and Tschopp J. (2003) Induction of TNF receptor I-mediated apoptosis via two sequential signaling complexes. *Cell* **114**, 181-90.

Michel A., Kopp-Schneider A., Zentgraf H., Gruber A. D. and de Villiers E. M. (2006) E6/E7 expression of human papillomavirus type 20 (HPV-20) and HPV-27 influences proliferation and differentiation of the skin in UV-irradiated SKH-hr1 transgenic mice. *J Virol* **80**, 11153-64.

Mikhailov V., Mikhailova M., Degenhardt K., Venkatachalam M. A., White E. and Saikumar P. (2003) Association of Bax and Bak homo-oligomers in mitochondria. Bax requirement for Bak reorganization and cytochrome c release. *J Biol Chem* **278**, 5367-76.

Minn A. J., Boise L. H. and Thompson C. B. (1996) Bcl-x(S) anatagonizes the protective effects of Bcl-x(L). *J Biol Chem* **271**, 6306-12.

Miura M., Zhu H., Rotello R., Hartwieg E. A. and Yuan J. (1993) Induction of apoptosis in fibroblasts by IL-1 beta-converting enzyme, a mammalian homolog of the C. elegans cell death gene ced-3. *Cell* **75**, 653-60.

Modis Y., Trus B. L. and Harrison S. C. (2002) Atomic model of the papillomavirus capsid. *EMBO J* **21**, 4754-62.

Moll R., Divo M. and Langbein L. (2008) The human keratins: biology and pathology. *Histochem Cell Biol* **129**, 705-33.

Moloney F. J., Comber H., O'Lorcain P., O'Kelly P., Conlon P. J. and Murphy G. M. (2006) A population-based study of skin cancer incidence and prevalence in renal transplant recipients. *Br J Dermatol* **154**, 498-504.

Muller-Schiffmann A., Beckmann J. and Steger G. (2006) The E6 protein of the cutaneous human papillomavirus type 8 can stimulate the viral early and late promoters by distinct mechanisms. *J Virol* **80**, 8718-28.

Muller M., Wilder S., Bannasch D., Israeli D., Lehlbach K., Li-Weber M., Friedman S. L., Galle P. R., Stremmel W., Oren M. and Krammer P. H. (1998) p53 activates the CD95 (APO-1/Fas) gene in response to DNA damage by anticancer drugs. *J Exp Med* **188**, 2033-45.

Munger K., Phelps W. C., Bubb V., Howley P. M. and Schlegel R. (1989) The E6 and E7 genes of the human papillomavirus type 16 together are necessary and sufficient for transformation of primary human keratinocytes. *J Virol* **63**, 4417-21.

Munoz N. (2000) Human papillomavirus and cancer: the epidemiological evidence. *J Clin Virol* **19**, 1-5.

Munoz N., Bosch F. X., de Sanjose S., Herrero R., Castellsague X., Shah K. V., Snijders P. J. and Meijer C. J. (2003) Epidemiologic classification of human papillomavirus types associated with cervical cancer. *N Engl J Med* **348**, 518-27.

Murphy G. M. (2009) Ultraviolet radiation and immunosuppression. *Br J Dermatol* **161 Suppl 3**, 90-5.

Murphy G. M., Norris P. G., Young A. R., Corbett M. F. and Hawk J. L. (1993) Low-dose ultraviolet-B irradiation depletes human epidermal Langerhans cells. *Br J Dermatol* **129**, 674-7.

Naik E., Michalak E. M., Villunger A., Adams J. M. and Strasser A. (2007) Ultraviolet radiation triggers apoptosis of fibroblasts and skin keratinocytes mainly via the BH3-only protein Noxa. *J Cell Biol* **176**, 415-24.

Nakahara T., Peh W. L., Doorbar J., Lee D. and Lambert P. F. (2005) Human papillomavirus type 16 E1circumflexE4 contributes to multiple facets of the papillomavirus life cycle. *J Virol* **79**, 13150-65.

Nakano K. and Vousden K. H. (2001) PUMA, a novel proapoptotic gene, is induced by p53. *Mol Cell* **7**, 683-94.

Nees M., Geoghegan J. M., Hyman T., Frank S., Miller L. and Woodworth C. D. (2001) Papillomavirus type 16 oncogenes downregulate expression of interferon-responsive genes and upregulate proliferation-associated and NF-kappaB-responsive genes in cervical keratinocytes. *J Virol* **75**, 4283-96.

Neville-Webbe H. L., Cross N. A., Eaton C. L., Nyambo R., Evans C. A., Coleman R. E. and Holen I. (2004) Osteoprotegerin (OPG) produced by bone marrow stromal cells protects breast cancer cells from TRAIL-induced apoptosis. *Breast Cancer Res Treat* **86**, 269-79.

Nguyen M. L., Nguyen M. M., Lee D., Griep A. E. and Lambert P. F. (2003) The PDZ ligand domain of the human papillomavirus type 16 E6 protein is required for E6's induction of epithelial hyperplasia in vivo. *J Virol* **77**, 6957-64.

Nijhawan D., Fang M., Traer E., Zhong Q., Gao W., Du F. and Wang X. (2003) Elimination of Mcl-1 is required for the initiation of apoptosis following ultraviolet irradiation. *Genes Dev* **17**, 1475-86.

Nkhata K. J., Ray A., Schuster T. F., Grossmann M. E. and Cleary M. P. (2009) Effects of adiponectin and leptin co-treatment on human breast cancer cell growth. *Oncol Rep* **21**, 1611-9.

Nomine Y., Masson M., Charbonnier S., Zanier K., Ristriani T., Deryckere F., Sibler A. P., Desplancq D., Atkinson R. A., Weiss E., Orfanoudakis G., Kieffer B. and Trave G. (2006) Structural and functional analysis of E6 oncoprotein: insights in the molecular pathways of human papillomavirus-mediated pathogenesis. *Mol Cell* **21**, 665-78.

Norris D. A., Middleton M. H., Whang K., Schleichler M., McGovern T., Bennion S. D., David-Bajar K., Davis D. and Duke R. C. (1997) Human keratinocytes maintain reversible anti-apoptotic defenses *in vivo* and *in vitro*. *Apoptosis* **2**, 136-148.

Norval M. (2006) The Effect of Ultraviolet Radiation on Human Viral Infections. *Photochem Photobiol*.

O'Donnell M. A., Legarda-Addison D., Skountzos P., Yeh W. C. and Ting A. T. (2007) Ubiquitination of RIP1 regulates an NF-kappaB-independent cell-death switch in TNF signaling. *Curr Biol* **17**, 418-24.

Ofori-Acquah S. F. and King J. A. (2008) Activated leukocyte cell adhesion molecule: a new paradox in cancer. *Transl Res* **151**, 122-8.

Ogata A., Chauhan D., Teoh G., Treon S. P., Urashima M., Schlossman R. L. and Anderson K. C. (1997) IL-6 triggers cell growth via the Ras-dependent mitogen-activated protein kinase cascade. *J Immunol* **159**, 2212-21.

Oh S. T., Longworth M. S. and Laimins L. A. (2004) Roles of the E6 and E7 proteins in the life cycle of low-risk human papillomavirus type 11. *J Virol* **78**, 2620-6.

Ohyama M., Terunuma A., Tock C. L., Radonovich M. F., Pise-Masison C. A., Hopping S. B., Brady J. N., Udey M. C. and Vogel J. C. (2006) Characterization and isolation of stem cell-enriched human hair follicle bulge cells. *J Clin Invest* **116**, 249-60.

Oldak M., Smola H., Aumailley M., Rivero F., Pfister H. and Smola-Hess S. (2004) The human papillomavirus type 8 E2 protein suppresses beta4-integrin expression in primary human keratinocytes. *J Virol* **78**, 10738-46.

Orth G. (2006) Genetics of epidermodysplasia verruciformis: Insights into host defense against papillomaviruses. *Semin Immunol* **18**, 362-74.

Orth G., Jablonska S., Jarzabek-Chorzelska M., Obalek S., Rzesa G., Favre M. and Croissant O. (1979) Characteristics of the lesions and risk of malignant conversion associated with the type of human papillomavirus involved in epidermodysplasia verruciformis. *Cancer Res* **39**, 1074-82.

Ossina N. K., Cannas A., Powers V. C., Fitzpatrick P. A., Knight J. D., Gilbert J. R., Shekhtman E. M., Tomei L. D., Umansky S. R. and Kiefer M. C. (1997) Interferon-gamma modulates a p53-independent apoptotic pathway and apoptosis-related gene expression. *J Biol Chem* **272**, 16351-7.

Ostor A. G. (1993) Natural history of cervical intraepithelial neoplasia: a critical review. *Int J Gynecol Pathol* **12**, 186-92.

Ouhtit A., Gaur R. L., Abd Elmageed Z. Y., Fernando A., Thouta R., Trappey A. K., Abdraboh M. E., El-Sayyad H. I., Rao P. and Raj M. G. (2009) Towards understanding the mode of action of the multifaceted cell adhesion receptor CD146. *Biochim Biophys Acta* **1795**, 130-6.

Overwijk W. W. and Schluns K. S. (2009) Functions of gammaC cytokines in immune homeostasis: current and potential clinical applications. *Clin Immunol* **132**, 153-65.

Owczarek W., Paplinska M., Targowski T., Jahnz-Rozyk K., Paluchowska E., Kucharczyk A. and Kasztalewicz B. (2010) Analysis of eotaxin 1/CCL11, eotaxin 2/CCL24 and eotaxin 3/CCL26 expression in lesional and non-lesional skin of patients with atopic dermatitis. *Cytokine*.

Park H. Y., Kosmadaki M., Yaar M. and Gilchrest B. A. (2009) Cellular mechanisms regulating human melanogenesis. *Cell Mol Life Sci* **66**, 1493-506.

Park J. S., Kim E. J., Kwon H. J., Hwang E. S., Namkoong S. E. and Um S. J. (2000) Inactivation of interferon regulatory factor-1 tumor suppressor protein by HPV E7

oncoprotein. Implication for the E7-mediated immune evasion mechanism in cervical carcinogenesis. *J Biol Chem* **275**, 6764-9.

Park S. M., Schickel R. and Peter M. E. (2005) Nonapoptotic functions of FADD-binding death receptors and their signaling molecules. *Curr Opin Cell Biol* **17**, 610-6.

Patrick D. R., Oliff A. and Heimbrook D. C. (1994) Identification of a novel retinoblastoma gene product binding site on human papillomavirus type 16 E7 protein. *J Biol Chem* **269**, 6842-50.

Pelengaris S., Littlewood T., Khan M., Elia G. and Evan G. (1999) Reversible activation of c-Myc in skin: induction of a complex neoplastic phenotype by a single oncogenic lesion. *Mol Cell* **3**, 565-77.

Pena J. C., Fuchs E. and Thompson C. B. (1997) Bcl-x expression influences keratinocyte cell survival but not terminal differentiation. *Cell Growth Differ* **8**, 619-29.

Peter M. E. (2005) The flip side of FLIP. *Biochemical Journal* **382**, e1-3.

Peus D., Vasa R. A., Beyerle A., Meves A., Krautmacher C. and Pittelkow M. R. (1999) UVB activates ERK1/2 and p38 signaling pathways via reactive oxygen species in cultured keratinocytes. *J Invest Dermatol* **112**, 751-6.

Pfefferle R., Marcuzzi G. P., Akgul B., Kasper H. U., Schulze F., Haase I., Wickenhauser C. and Pfister H. (2008) The human papillomavirus type 8 E2 protein induces skin tumors in transgenic mice. *J Invest Dermatol* **128**, 2310-5.

Pfister H. (2003) Chapter 8: Human papillomavirus and skin cancer. *J Natl Cancer Inst Monogr*, 52-6.

Pim D. and Banks L. (1999) HPV-18 E6*I protein modulates the E6-directed degradation of p53 by binding to full-length HPV-18 E6. *Oncogene* **18**, 7403-8.

Pisani P., Bray F. and Parkin D. M. (2002) Estimates of the world-wide prevalence of cancer for 25 sites in the adult population. *Int J Cancer* **97**, 72-81.

Poruchynsky M. S., Wang E. E., Rudin C. M., Blagosklonny M. V. and Fojo T. (1998) Bcl-xL is phosphorylated in malignant cells following microtubule disruption. *Cancer Res* **58**, 3331-8.

Purdie K. J., Pennington J., Proby C. M., Khalaf S., de Villiers E. M., Leigh I. M. and Storey A. (1999) The promoter of a novel human papillomavirus (HPV77) associated with skin cancer displays UV responsiveness, which is mediated through a consensus p53 binding sequence. *Embo J* **18**, 5359-69.

Purdie K. J., Surentheran T., Sterling J. C., Bell L., McGregor J. M., Proby C. M., Harwood C. A. and Breuer J. (2005) Human papillomavirus gene expression in cutaneous squamous cell carcinomas from immunosuppressed and immunocompetent individuals. *J Invest Dermatol* **125**, 98-107.

Qin J. Z., Bacon P. E., Chaturvedi V., Bonish B. and Nickoloff B. J. (2002) Pathways involved in proliferating, senescent and immortalized keratinocyte cell death mediated by two different TRAIL preparations. *Exp Dermatol* **11**, 573-83.

Ramoz N., Rueda L. A., Bouadjar B., Montoya L. S., Orth G. and Favre M. (2002) Mutations in two adjacent novel genes are associated with epidermodysplasia verruciformis. *Nat Genet* **32**, 579-81.

Rao L., Perez D. and White E. (1996) Lamin proteolysis facilitates nuclear events during apoptosis. *J Cell Biol* **135**, 1441-55.

Rasheed S., Nelson-Rees W. A., Toth E. M., Arnstein P. and Gardner M. B. (1974) Characterization of a newly derived human sarcoma cell line (HT-1080). *Cancer* **33**, 1027-33.

Reichelt J., Furstenberger G. and Magin T. M. (2004) Loss of keratin 10 leads to mitogen-activated protein kinase (MAPK) activation, increased keratinocyte turnover, and decreased tumor formation in mice. *J Invest Dermatol* **123**, 973-81.

Ren Z. P., Hedrum A., Ponten F., Nister M., Ahmadian A., Lundeberg J., Uhlen M. and Ponten J. (1996) Human epidermal cancer and accompanying precursors have identical p53 mutations different from p53 mutations in adjacent areas of clonally expanded non-neoplastic keratinocytes. *Oncogene* **12**, 765-73.

Renatus M., Stennicke H. R., Scott F. L., Liddington R. C. and Salvesen G. S. (2001) Dimer formation drives the activation of the cell death protease caspase 9. *Proc Natl Acad Sci U S A* **98**, 14250-5.

Riethdorf S., Riethdorf L., Richter N. and Loning T. (1998) Expression of the MCP-1 gene and the HPV 16 E6/E7 oncogenes in squamous cell carcinomas of the cervix uteri and metastases. *Pathobiology* **66**, 260-7.

Rigel D. S. (2008) Cutaneous ultraviolet exposure and its relationship to the development of skin cancer. *J Am Acad Dermatol* **58**, S129-32.

Rincon-Orozco B., Halec G., Rosenberger S., Muschik D., Nindl I., Bachmann A., Ritter T. M., Dondog B., Ly R., Bosch F. X., Zawatzky R. and Rosl F. (2009) Epigenetic silencing of interferon-kappa in human papillomavirus type 16-positive cells. *Cancer Res* **69**, 8718-25.

Ringner M. (2008) What is principal component analysis? *Nat Biotechnol* **26**, 303-4.

Ristriani T., Nomine Y., Masson M., Weiss E. and Trave G. (2001) Specific recognition of four-way DNA junctions by the C-terminal zinc-binding domain of HPV oncoprotein E6. *J Mol Biol* **305**, 729-39.

Roberts S., Ashmole I., Gibson L. J., Rookes S. M., Barton G. J. and Gallimore P. H. (1994) Mutational analysis of human papillomavirus E4 proteins: identification of structural features important in the formation of cytoplasmic E4/cytokeratin networks in epithelial cells. *J Virol* **68**, 6432-45.

Roberts S., Hillman M. L., Knight G. L. and Gallimore P. H. (2003) The ND10 component promyelocytic leukemia protein relocates to human papillomavirus type 1 E4 intranuclear inclusion bodies in cultured keratinocytes and in warts. *J Virol* **77**, 673-84.

Roberts S., Kingsbury S. R., Stoeber K., Knight G. L., Gallimore P. H. and Williams G. H. (2008) Identification of an arginine-rich motif in human papillomavirus type 1 E1;E4 protein necessary for E4-mediated inhibition of cellular DNA synthesis in vitro and in cells. *J Virol* **82**, 9056-64.

Rodier F., Coppe J. P., Patil C. K., Hoeijmakers W. A., Munoz D. P., Raza S. R., Freund A., Campeau E., Davalos A. R. and Campisi J. (2009) Persistent DNA damage signalling triggers senescence-associated inflammatory cytokine secretion. *Nat Cell Biol* **11**, 973-9.

Rodriguez A. C., Schiffman M., Herrero R., Wacholder S., Hildesheim A., Castle P. E., Solomon D. and Burk R. (2008) Rapid clearance of human papillomavirus and implications for clinical focus on persistent infections. *J Natl Cancer Inst* **100**, 513-7.

Rodust P. M., Stockfleth E., Ulrich C., Leverkus M. and Eberle J. (2009) UV-induced squamous cell carcinoma--a role for antiapoptotic signalling pathways. *Br J Dermatol* **161 Suppl 3**, 107-15.

Roy N., Deveraux Q. L., Takahashi R., Salvesen G. S. and Reed J. C. (1997) The c-IAP-1 and c-IAP-2 proteins are direct inhibitors of specific caspases. *EMBO J* **16**, 6914-25.

Rudel T. and Bokoch G. M. (1997) Membrane and morphological changes in apoptotic cells regulated by caspase-mediated activation of PAK2. *Science* **276**, 1571-4.

Ruhland A. and de Villiers E. M. (2001) Opposite regulation of the HPV 20-URR and HPV 27-URR promoters by ultraviolet irradiation and cytokines. *Int J Cancer* **91**, 828-34.

Salvesen G. S. and Dixit V. M. (1999) Caspase activation: the induced-proximity model. *Proc Natl Acad Sci U S A* **96**, 10964-7.

Sanges R., Cordero F. and Calogero R. A. (2007) oneChannelGUI: a graphical interface to Bioconductor tools, designed for life scientists who are not familiar with R language. *Bioinformatics* **23**, 3406-8.

Satchell A. C., Barnetson R. S. and Halliday G. M. (2004) Increased Fas ligand expression by T cells and tumour cells in the progression of actinic keratosis to squamous cell carcinoma. *Br J Dermatol* **151**, 42-9.

Sayama K., Yonehara S., Watanabe Y. and Miki Y. (1994) Expression of Fas antigen on keratinocytes *in vivo* and induction of apoptosis in cultured keratinocytes. *J Invest Dermatol* **103**, 330-334.

Schaper I. D., Marcuzzi G. P., Weissenborn S. J., Kasper H. U., Dries V., Smyth N., Fuchs P. and Pfister H. (2005) Development of skin tumors in mice transgenic for early genes of human papillomavirus type 8. *Cancer Res* **65**, 1394-400.

Schauber J. and Gallo R. L. (2008) Antimicrobial peptides and the skin immune defense system. *J Allergy Clin Immunol* **122**, 261-6.

Scheffner M., Werness B. A., Huibregtse J. M., Levine A. J. and Howley P. M. (1990) The E6 oncoprotein encoded by human papillomavirus types 16 and 18 promotes the degradation of p53. *Cell* **63**, 1129-36.

Schmitt A., Harry J. B., Rapp B., Wettstein F. O. and Iftner T. (1994) Comparison of the properties of the E6 and E7 genes of low- and high-risk cutaneous papillomaviruses reveals strongly transforming and high Rb-binding activity for the E7 protein of the low-risk human papillomavirus type 1. *J Virol* **68**, 7051-9.

Schmitt D. A., Walterscheid J. P. and Ullrich S. E. (2000) Reversal of ultraviolet radiation-induced immune suppression by recombinant interleukin-12: suppression of cytokine production. *Immunology* **101**, 90-6.

Schneider-Gadicke A. and Schwarz E. (1986) Different human cervical carcinoma cell lines show similar transcription patterns of human papillomavirus type 18 early genes. *EMBO J* **5**, 2285-92.

Schneider P., Holler N., Bodmer J. L., Hahne M., Frei K., Fontana A. and Tschopp J. (1998) Conversion of membrane-bound Fas(CD95) ligand to its soluble form is associated

with downregulation of its proapoptotic activity and loss of liver toxicity. *J Exp Med* **187**, 1205-13.

Schroder K. and Tschopp J. (2010) The inflammasomes. *Cell* **140**, 821-32.

Semple J. I., Smits V. A., Fernaud J. R., Mamely I. and Freire R. (2007) Cleavage and degradation of Claspin during apoptosis by caspases and the proteasome. *Cell Death Differ* **14**, 1433-42.

Sen E., Alam S. and Meyers C. (2004) Genetic and biochemical analysis of cis regulatory elements within the keratinocyte enhancer region of the human papillomavirus type 31 upstream regulatory region during different stages of the viral life cycle. *J Virol* **78**, 612-29.

Sesto A., Navarro M., Burslem F. and Jorcano J. L. (2002) Analysis of the ultraviolet B response in primary human keratinocytes using oligonucleotide microarrays. *Proc Natl Acad Sci U S A* **99**, 2965-70.

Shafti-Keramat S., Handisurya A., Kriehuber E., Meneguzzi G., Slupetzky K. and Kirnbauer R. (2003) Different heparan sulfate proteoglycans serve as cellular receptors for human papillomaviruses. *J Virol* **77**, 13125-35.

Sheikh M. S., Antinore M. J., Huang Y. and Fornace A. J., Jr. (1998) Ultraviolet-irradiation-induced apoptosis is mediated via ligand independent activation of tumor necrosis factor receptor 1. *Oncogene* **17**, 2555-63.

Shibasaki M., Wilson T. E. and Crandall C. G. (2006) Neural control and mechanisms of eccrine sweating during heat stress and exercise. *J Appl Physiol* **100**, 1692-701.

Simmonds M. and Storey A. (2008) Identification of the regions of the HPV 5 E6 protein involved in Bak degradation and inhibition of apoptosis. *Int J Cancer* **123**, 2260-6.

Singer A. (1995) Cervical cancer screening: state of the art. *Baillieres Clin Obstet Gynaecol* **9**, 39-64.

Sitailo L. A., Jerome-Morais A. and Denning M. F. (2009) Mcl-1 functions as major epidermal survival protein required for proper keratinocyte differentiation. *J Invest Dermatol* **129**, 1351-60.

Slominski A. (2005) Neuroendocrine system of the skin. *Dermatology* **211**, 199-208.

Smith J. S., Lindsay L., Hoots B., Keys J., Franceschi S., Winer R. and Clifford G. M. (2007) Human papillomavirus type distribution in invasive cervical cancer and high-grade cervical lesions: a meta-analysis update. *Int J Cancer* **121**, 621-32.

Smyth G. K. (2004) Linear models and empirical bayes methods for assessing differential expression in microarray experiments. *Stat Appl Genet Mol Biol* **3**, Article3.

Sonnenberg A., Calafat J., Janssen H., Daams H., van der Raaij-Helmer L. M., Falcioni R., Kennel S. J., Aplin J. D., Baker J., Loizidou M. and et al. (1991) Integrin alpha 6/beta 4 complex is located in hemidesmosomes, suggesting a major role in epidermal cell-basement membrane adhesion. *J Cell Biol* **113**, 907-17.

Spets H., Stromberg T., Georgii-Hemming P., Siljason J., Nilsson K. and Jernberg-Wiklund H. (2002) Expression of the bcl-2 family of pro- and anti-apoptotic genes in multiple myeloma and normal plasma cells: regulation during interleukin-6(IL-6)-induced growth and survival. *Eur J Haematol* **69**, 76-89.

Spink K. M. and Laimins L. A. (2005) Induction of the human papillomavirus type 31 late promoter requires differentiation but not DNA amplification. *J Virol* **79**, 4918-26.

Stanger B. Z., Leder P., Lee T. H., Kim E. and Seed B. (1995) RIP: a novel protein containing a death domain that interacts with Fas/APO-1 (CD95) in yeast and causes cell death. *Cell* **81**, 513-23.

Stanley M. (2006) Immune responses to human papillomavirus. *Vaccine* **24 Suppl 1**, S16-22.

Steger G. and Corbach S. (1997) Dose-dependent regulation of the early promoter of human papillomavirus type 18 by the viral E2 protein. *J Virol* **71**, 50-8.

Steller M. A., Zou Z., Schiller J. T. and Baserga R. (1996) Transformation by human papillomavirus 16 E6 and E7: role of the insulin-like growth factor 1 receptor. *Cancer Res* **56**, 5087-91.

Stockfleth E., Nindl I., Sterry W., Ulrich C., Schmook T. and Meyer T. (2004) Human papillomaviruses in transplant-associated skin cancers. *Dermatol Surg* **30**, 604-9.

Storey A. (2002) Papillomaviruses: death-defying acts in skin cancer. *Trends Mol Med* **8**, 417-21.

Struijk L., Hall L., van der Meijden E., Wanningen P., Bavinck J. N., Neale R., Green A. C., Ter Schegget J. and Feltkamp M. C. (2006) Markers of cutaneous human papillomavirus infection in individuals with tumor-free skin, actinic keratoses, and squamous cell carcinoma. *Cancer Epidemiol Biomarkers Prev* **15**, 529-35.

Struijk L., van der Meijden E., Kazem S., ter Schegget J., de Gruijl F. R., Steenbergen R. D. and Feltkamp M. C. (2008) Specific betapapillomaviruses associated with squamous cell carcinoma of the skin inhibit UVB-induced apoptosis of primary human keratinocytes. *J Gen Virol* **89**, 2303-14.

Sung K. J., Paik E. M., Jang K. A., Suh H. S. and Choi J. H. (1997) Apoptosis is induced by anti-Fas antibody alone in cultured human keratinocytes. *The Journal of Dermatology* **24**, 427-434.

Sur I., Ulvmar M. and Toftgard R. (2008) The two-faced NF-kappaB in the skin. *Int Rev Immunol* **27**, 205-23.

Sverdrup F. and Khan S. A. (1994) Replication of human papillomavirus (HPV) DNAs supported by the HPV type 18 E1 and E2 proteins. *J Virol* **68**, 505-9.

Takahashi H., Honma M., Ishida-Yamamoto A., Namikawa K., Miwa A., Okado H., Kiyama H. and Iizuka H. (2001) In vitro and in vivo transfer of bcl-2 gene into keratinocytes suppresses UVB-induced apoptosis. *Photochem Photobiol* **74**, 579-86.

Takahashi R., Deveraux Q., Tamm I., Welsh K., Assa-Munt N., Salvesen G. S. and Reed J. C. (1998) A single BIR domain of XIAP sufficient for inhibiting caspases. *J Biol Chem* **273**, 7787-90.

Tavalai N. and Stamminger T. (2008) New insights into the role of the subnuclear structure ND10 for viral infection. *Biochim Biophys Acta* **1783**, 2207-21.

Terrano D. T., Upreti M. and Chambers T. C. (2010) Cyclin-dependent kinase 1-mediated Bcl-xL/Bcl-2 phosphorylation acts as a functional link coupling mitotic arrest and apoptosis. *Mol Cell Biol* **30**, 640-56.

Terunuma A., Kapoor V., Yee C., Telford W. G., Udey M. C. and Vogel J. C. (2007) Stem cell activity of human side population and alpha6 integrin-bright keratinocytes defined by a quantitative in vivo assay. *Stem Cells* **25**, 664-9.

Thomas M., Laura R., Hepner K., Guccione E., Sawyers C., Lasky L. and Banks L. (2002) Oncogenic human papillomavirus E6 proteins target the MAGI-2 and MAGI-3 proteins for degradation. *Oncogene* **21**, 5088-96.

Tiberio R., Marconi A., Fila C., Fumelli C., Pignatti M., Krajewski S., Giannetti A., Reed J. C. and Pincelli C. (2002) Keratinocytes enriched for stem cells are protected from anoikis via an integrin signaling pathway in a Bcl-2 dependent manner. *FEBS Lett* **524**, 139-44.

Tobin D. J. (2006) Biochemistry of human skin--our brain on the outside. *Chem Soc Rev* **35**, 52-67.

Tohyama M., Shirakara Y., Yamasaki K., Sayama K. and Hashimoto K. (2001) Differentiated keratinocytes are responsible for TNF-alpha regulated production of macrophage inflammatory protein 3alpha/CCL20, a potent chemokine for Langerhans cells. *J Dermatol Sci* **27**, 130-9.

Trautmann A., Akdis M., Kleemann D., Altznauer F., Simon H. U., Graeve T., Noll M., Brocker E. B., Blaser K. and Akdis C. A. (2000) T cell-mediated Fas-induced keratinocyte apoptosis plays a key pathogenetic role in eczematous dermatitis. *J Clin Invest* **106**, 25-35.

Trougakos I. P. and Gonos E. S. (2009) Chapter 9: Oxidative stress in malignant progression: The role of Clusterin, a sensitive cellular biosensor of free radicals. *Adv Cancer Res* **104**, 171-210.

Tsao H. (2001) Genetics of nonmelanoma skin cancer. *Arch Dermatol* **137**, 1486-92.

Tungteakkhun S. S., Filippova M., Neidigh J. W., Fodor N. and Duerksen-Hughes P. J. (2008) The interaction between human papillomavirus type 16 and FADD is mediated by a novel E6 binding domain. *J Virol* **82**, 9600-14.

Turner N. and Grose R. (2010) Fibroblast growth factor signalling: from development to cancer. *Nat Rev Cancer* **10**, 116-29.

Underbrink M. P., Howie H. L., Bedard K. M., Koop J. I. and Galloway D. A. (2008) E6 proteins from multiple human betapapillomavirus types degrade Bak and protect keratinocytes from apoptosis after UVB irradiation. *J Virol* **82**, 10408-17.

Van Laethem A., Garmyn M. and Agostinis P. (2009) Starting and propagating apoptotic signals in UVB irradiated keratinocytes. *Photochem Photobiol Sci* **8**, 299-308.

Van Laethem A., Van Kelst S., Lippens S., Declercq W., Vandenabeele P., Janssens S., Vandenheede J. R., Garmyn M. and Agostinis P. (2004) Activation of p38 MAPK is required for Bax translocation to mitochondria, cytochrome c release and apoptosis induced by UVB irradiation in human keratinocytes. *Faseb J* **18**, 1946-8.

Vande Walle L., Lamkanfi M. and Vandenabeele P. (2008) The mitochondrial serine protease HtrA2/Omi: an overview. *Cell Death Differ* **15**, 453-60.

Vasiljevic N., Andersson K., Bjelkenkrantz K., Kjellstrom C., Mansson H., Nilsson E., Landberg G., Dillner J. and Forslund O. (2009) The Bcl-xL inhibitor of apoptosis is preferentially expressed in cutaneous squamous cell carcinoma compared with that in keratoacanthoma. *Int J Cancer* **124**, 2361-6.

Vaux D. L., Cory S. and Adams J. M. (1988) Bcl-2 gene promotes haemopoietic cell survival and cooperates with c-myc to immortalize pre-B cells. *Nature* **335**, 440-2.

Veldman T., Liu X., Yuan H. and Schlegel R. (2003) Human papillomavirus E6 and Myc proteins associate in vivo and bind to and cooperatively activate the telomerase reverse transcriptase promoter. *Proc Natl Acad Sci U S A* **100**, 8211-6.

Verhagen A. M., Ekert P. G., Pakusch M., Silke J., Connolly L. M., Reid G. E., Moritz R. L., Simpson R. J. and Vaux D. L. (2000) Identification of DIABLO, a mammalian protein that promotes apoptosis by binding to and antagonizing IAP proteins. *Cell* **102**, 43-53.

Verhagen A. M., Silke J., Ekert P. G., Pakusch M., Kaufmann H., Connolly L. M., Day C. L., Tikoo A., Burke R., Wrobel C., Moritz R. L., Simpson R. J. and Vaux D. L. (2002) HtrA2 promotes cell death through its serine protease activity and its ability to antagonize inhibitor of apoptosis proteins. *J Biol Chem* **277**, 445-54.

von Bubnoff D., Andres E., Hentges F., Bieber T., Michel T. and Zimmer J. (2010) Natural killer cells in atopic and autoimmune diseases of the skin. *J Allergy Clin Immunol* **125**, 60-8.

Wachter T., Sprick M., Hausmann D., Kerstan A., McPherson K., Stassi G., Brocker E. B., Walczak H. and Leverkus M. (2004) cFLIPL inhibits tumor necrosis factor-related apoptosis-inducing ligand-mediated NF-kappaB activation at the death-inducing signaling complex in human keratinocytes. *J Biol Chem* **279**, 52824-34.

Wagner L. A., Brown T., Gil S., Frank I., Carter W., Tamura R. and Wayner E. A. (1999) The keratinocyte-derived cytokine IL-7 increases adhesion of the epidermal T cell subset to the skin basement membrane protein laminin-5. *Eur J Immunol* **29**, 2530-8.

Walboomers J. M., Jacobs M. V., Manos M. M., Bosch F. X., Kummer J. A., Shah K. V., Snijders P. J., Peto J., Meijer C. J. and Munoz N. (1999) Human papillomavirus is a necessary cause of invasive cervical cancer worldwide. *J Pathol* **189**, 12-9.

Wang C. and Youle R. J. (2009) The role of mitochondria in apoptosis*. *Annu Rev Genet* **43**, 95-118.

Wang H. K., Duffy A. A., Broker T. R. and Chow L. T. (2009a) Robust production and passaging of infectious HPV in squamous epithelium of primary human keratinocytes. *Genes Dev* **23**, 181-94.

Wang J., Sampath A., Raychaudhuri P. and Bagchi S. (2001) Both Rb and E7 are regulated by the ubiquitin proteasome pathway in HPV-containing cervical tumor cells. *Oncogene* **20**, 4740-9.

Wang X., Bregegere F., Soroka Y., Kayat A., Redziniak G. and Milner Y. (2004a) Enhancement of Fas-mediated apoptosis in ageing human keratinocytes. *Mech Ageing Dev* **125**, 237-49.

Wang X., Wang H. K., McCoy J. P., Banerjee N. S., Rader J. S., Broker T. R., Meyers C., Chow L. T. and Zheng Z. M. (2009b) Oncogenic HPV infection interrupts the expression of tumor-suppressive miR-34a through viral oncoprotein E6. *RNA* **15**, 637-47.

Wang X. P., Schunck M., Kallen K. J., Neumann C., Trautwein C., Rose-John S. and Proksch E. (2004b) The interleukin-6 cytokine system regulates epidermal permeability barrier homeostasis. *J Invest Dermatol* **123**, 124-31.

Watson R. A., Thomas M., Banks L. and Roberts S. (2003) Activity of the human papillomavirus E6 PDZ-binding motif correlates with an enhanced morphological transformation of immortalized human keratinocytes. *J Cell Sci* **116**, 4925-34.

Waxman A. B. and Kolliputi N. (2009) IL-6 protects against hyperoxia-induced mitochondrial damage via Bcl-2-induced Bak interactions with mitofusins. *Am J Respir Cell Mol Biol* **41**, 385-96.

Webb A., Li A. and Kaur P. (2004) Location and phenotype of human adult keratinocyte stem cells of the skin. *Differentiation* **72**, 387-95.

Webb A. R. (2006) Who, what, where and when-influences on cutaneous vitamin D synthesis. *Prog Biophys Mol Biol* **92**, 17-25.

Wei M. C., Zong W. X., Cheng E. H., Lindsten T., Panoutsakopoulou V., Ross A. J., Roth K. A., MacGregor G. R., Thompson C. B. and Korsmeyer S. J. (2001) Proapoptotic BAX and BAK: a requisite gateway to mitochondrial dysfunction and death. *Science* **292**, 727-30.

Weissenborn S. J., Nindl I., Purdie K., Harwood C., Proby C., Breuer J., Majewski S., Pfister H. and Wieland U. (2005) Human papillomavirus-DNA loads in actinic keratoses exceed those in non-melanoma skin cancers. *J Invest Dermatol* **125**, 93-7.

Wen L. P., Fahrni J. A., Troie S., Guan J. L., Orth K. and Rosen G. D. (1997) Cleavage of focal adhesion kinase by caspases during apoptosis. *J Biol Chem* **272**, 26056-61.

Weninger W., Rendl M., Mildner M., Mayer C., Ban J., Geusau A., Bayer G., Tanew A., Majdic O. and Tschachler E. (2000) Keratinocytes express the CD146 (Muc18/S-endo) antigen in tissue culture and during inflammatory skin diseases. *J Invest Dermatol* **115**, 219-24.

Westphal K., Akgul B., Storey A. and Nindl I. (2009) Cutaneous human papillomavirus E7 type-specific effects on differentiation and proliferation of organotypic skin cultures. *Cell Oncol* **31**, 213-26.

Widlak P. and Garrard W. T. (2005) Discovery, regulation, and action of the major apoptotic nucleases DFF40/CAD and endonuclease G. *J Cell Biochem* **94**, 1078-87.

Wilkins-Port C. E., Higgins C. E., Freytag J., Higgins S. P., Carlson J. A. and Higgins P. J. (2007) PAI-1 is a Critical Upstream Regulator of the TGF-beta1/EGF-Induced Invasive Phenotype in Mutant p53 Human Cutaneous Squamous Cell Carcinoma. *J Biomed Biotechnol* **2007**, 85208.

Willis S. N., Fletcher J. I., Kaufmann T., van Delft M. F., Chen L., Czabotar P. E., Ierino H., Lee E. F., Fairlie W. D., Bouillet P., Strasser A., Kluck R. M., Adams J. M. and Huang D. C. (2007) Apoptosis initiated when BH3 ligands engage multiple Bcl-2 homologs, not Bax or Bak. *Science* **315**, 856-9.

Wilson V. G., West M., Woytek K. and Rangasamy D. (2002) Papillomavirus E1 proteins: form, function, and features. *Virus Genes* **24**, 275-90.

Wolff S., Erster S., Palacios G. and Moll U. M. (2008) p53's mitochondrial translocation and MOMP action is independent of Puma and Bax and severely disrupts mitochondrial membrane integrity. *Cell Res* **18**, 733-44.

Wolter K. G., Hsu Y. T., Smith C. L., Nechushtan A., Xi X. G. and Youle R. J. (1997) Movement of Bax from the cytosol to mitochondria during apoptosis. *J Cell Biol* **139**, 1281-92.

Wu S., Loke H. N. and Rehemtulla A. (2002) Ultraviolet radiation-induced apoptosis is mediated by Daxx. *Neoplasia* **4**, 486-92.

Yamashita T., Segawa K., Fujinaga Y., Nishikawa T. and Fujinaga K. (1993) Biological and biochemical activity of E7 genes of the cutaneous human papillomavirus type 5 and 8. *Oncogene* **8**, 2433-41.

Yang X., Khosravi-Far R., Chang H. Y. and Baltimore D. (1997) Daxx, a novel Fas-binding protein that activates JNK and apoptosis. *Cell* **89**, 1067-76.

Ye H., Cande C., Stephanou N. C., Jiang S., Gurbuxani S., Larochette N., Daugas E., Garrido C., Kroemer G. and Wu H. (2002) DNA binding is required for the apoptogenic action of apoptosis inducing factor. *Nat Struct Biol* **9**, 680-4.

Yoshida K. and Miki Y. (2010) The cell death machinery governed by the p53 tumor suppressor in response to DNA damage. *Cancer Sci*.

Yoshizaki K., Nishimoto N., Matsumoto K., Tagoh H., Taga T., Deguchi Y., Kuritani T., Hirano T., Hashimoto K., Okada N. and et al. (1990) Interleukin 6 and expression of its receptor on epidermal keratinocytes. *Cytokine* **2**, 381-7.

You J., Croyle J. L., Nishimura A., Ozato K. and Howley P. M. (2004) Interaction of the bovine papillomavirus E2 protein with Brd4 tethers the viral DNA to host mitotic chromosomes. *Cell* **117**, 349-60.

Young A. R. (1987) The sunburn cell. *Photodermatol* **4**, 127-34.

Yuan H., Fu F., Zhuo J., Wang W., Nishitani J., An D. S., Chen I. S. and Liu X. (2005) Human papillomavirus type 16 E6 and E7 oncoproteins upregulate c-IAP2 gene expression and confer resistance to apoptosis. *Oncogene* **24**, 5069-78.

Yuan J. (2006) Divergence from a dedicated cellular suicide mechanism: exploring the evolution of cell death. *Mol Cell* **23**, 1-12.

Yuki T., Haratake A., Koishikawa H., Morita K., Miyachi Y. and Inoue S. (2007) Tight junction proteins in keratinocytes: localization and contribution to barrier function. *Exp Dermatol* **16**, 324-30.

Zahir N. and Weaver V. M. (2004) Death in the third dimension: apoptosis regulation and tissue architecture. *Curr Opin Genet Dev* **14**, 71-80.

Zakeri Z. and Lockshin R. A. (2002) Cell death during development. *J Immunol Methods* **265**, 3-20.

Zambell K. L., Fitch M. D. and Fleming S. E. (2003) Acetate and butyrate are the major substrates for de novo lipogenesis in rat colonic epithelial cells. *J Nutr* **133**, 3509-15.

Zarnegar B. J., Wang Y., Mahoney D. J., Dempsey P. W., Cheung H. H., He J., Shiba T., Yang X., Yeh W. C., Mak T. W., Korneluk R. G. and Cheng G. (2008) Noncanonical NF-kappaB activation requires coordinated assembly of a regulatory complex of the adaptors cIAP1, cIAP2, TRAF2 and TRAF3 and the kinase NIK. *Nat Immunol* **9**, 1371-8.

Zauli G., Melloni E., Capitani S. and Secchiero P. (2009) Role of full-length osteoprotegerin in tumor cell biology. *Cell Mol Life Sci* **66**, 841-51.

Zhang J. and Ney P. A. (2009) Role of BNIP3 and NIX in cell death, autophagy, and mitophagy. *Cell Death Differ* **16**, 939-46.

Zheng Z. M. and Baker C. C. (2006) Papillomavirus genome structure, expression, and post-transcriptional regulation. *Front Biosci* **11**, 2286-302.

Zimmermann H., Koh C. H., Degenkolbe R., O'Connor M. J., Muller A., Steger G., Chen J. J., Lui Y., Androphy E. and Bernard H. U. (2000) Interaction with CBP/p300 enables the bovine papillomavirus type 1 E6 oncoprotein to downregulate CBP/p300-mediated transactivation by p53. *J Gen Virol* **81**, 2617-23.